



This is to certify that the

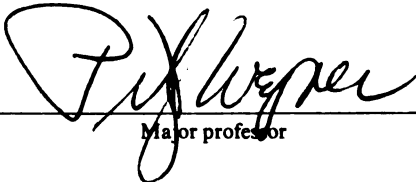
dissertation entitled

Effect of Temperature on the
Behavior of Biradical Intermediates:
Conformational Control of Product Ratios
in Photocyclization Reactions
presented by

Ali Reza Zand

has been accepted towards fulfillment
of the requirements for

Ph.D. degree in Chemistry


Major professor

Date Nov. 15, 1996

**PLACE IN RETURN BOX to remove this checkout from your record.
TO AVOID FINES return on or before date due.**

DATE DUE	DATE DUE	DATE DUE
_____	_____	_____
_____	_____	_____
_____	_____	_____
_____	_____	_____
_____	_____	_____
_____	_____	_____
_____	_____	_____

MSU is An Affirmative Action/Equal Opportunity Institution

c:\circ\d\date.due.pm3-p.1

Effect of Temperature on the Behavior of Biradical Intermediates:
Conformational Control of Product Ratios in Photocyclization Reactions

by

Ali Reza Zand

A DISSERTATION

Submitted to
Michigan State University
In partial fulfillment of the requirements
for the degree of

DOCTOR OF PHILOSOPHY

Department of Chemistry

1996

Abstract

Effect of Temperature on the Behavior of Biradical Intermediates:

Conformational Control of Product Ratios in Photocyclization

Reactions

by

Ali Reza Zand

The photochemistry of several ketones at various temperatures was investigated. Intramolecular δ -hydrogen abstraction by excited carbonyl groups results in formation of 1,5-biradicals which upon cyclization yield indanols as photoproducts. This investigation probed the effect of temperature on the diastereoselectivity of cyclization with emphasis on the role of intersystem crossing on product ratios.

α -Arylacetophenones show variable product ratios at various temperatures. The Arrhenius plots are linear indicative of conformational equilibrium. The results show nonenthalpic factors to be as important as enthalpic differences at determining diastereoselectivity. The low diastereoselectivities observed for α -(2-benzylphenyl)-acetophenones is attributed to benzylic conjugation which imparts rotational freedom to both ends of the biradical intermediate. α -Aryl propiophenones show a large preference for the α -methyl group and the phenyl to be trans in the 2-phenyl-2-indanol product. This phenomenon seems to stem from the lowest energy "reactive ground state conformer" of the ketones which always mirrors one of the biradical minima.

Irradiation of α -arylacetones results in formation of indanols and α -cleavage products. Indanol formation involves a singlet state δ -hydrogen abstraction followed by Yang cyclization while α -cleavage occurs from the triplet state. The fact that α -cleavage is the predominant photoreaction at low temperatures has been attributed to a competition between hydrogen abstraction which has a barrier and a barrierless intersystem crossing process. α -Arylacetones show lower indanol diastereoselectivities than their acetophenone analogs. This has been attributed to conformational control, rather than ground state control, of diastereoselectivity. The low product quantum yields of α -arylacetones have been attributed to a well known radiationless decay process which competes with singlet state hydrogen abstraction.

o-tert-Butyl- α,α,α -trifluoroacetophenone, like *o-tert*-butylacetophenone, forms an indanol and an unsaturated alcohol upon irradiation in benzene and methanol. The unsaturated alcohol is the major product under all conditions. Capto-dative resonance thus does not provide sufficient stabilization to allow the hydroxy end of the biradical to twist out of benzylic conjugation to give higher indanol yields.

2-(2'-(2',3'-Dimethyl)butyl)benzophenone forms three isomeric indanols and an unsaturated alcohol upon irradiation in solution and in the solid state. Two different reaction sites, isopropyl and methyl, seem to have comparable reactivity which shows the insensitivity of hydrogen abstraction rates to orientational factors. Formation of the unsaturated alcohol mimics the *o-tert*-butylacetophenone derivatives and could explain the less than unity quantum yields previously observed for *tert*-amylbenzophenones.

This Thesis is Dedicated To My Grandmothers Who Passed away Before I Graduated

Acknowledgments

The Author wishes to thank Dr. Peter J. Wagner for his help, guidance, sense of humor and innumerable entertaining discussions during the course of this work.

The author is grateful to the National Science Foundation and Michigan State University for financial support in the form of teaching, research assistantships and the Hart fellowship. The author would also like to thank the Chemistry Department for the use of its excellent facilities.

The author also owes special thanks to friends in the Wagner research group. Their help and support made my graduate career much more enjoyable. Last, but by no means least, I would like to thank my family for their help, support and patience throughout my graduate career.

Table of Contents

TABLE OF CONTENTS	vi
LIST OF FIGURES	viii
LIST OF TABLES	x
LIST OF SCHEMES	xii
LIST OF ABBREVIATIONS	xiv
INTRODUCTION	1
I. MEASUREMENTS OF QUANTUM YIELDS AND EXCITED STATE LIFETIMES	3
II. A-CLEAVAGE REACTIONS	5
III. HYDROGEN ABSTRACTION	8
<i>A. Conformational Control of Photoreactivity</i>	<i>11</i>
<i>B. Orientational Requirements of Hydrogen Abstraction</i>	<i>14</i>
<i>C. δ-Hydrogen Abstraction</i>	<i>21</i>
<i>D. Nature of the Excited State- Singlet vs. Triplet</i>	<i>25</i>
<i>E. Effect of Environment</i>	<i>28</i>
<i>F. Biradical Lifetime</i>	<i>30</i>
<i>G. Diastereoselectivity</i>	<i>34</i>
<i>H. Photoenolization of α-(2,4,6-triisopropylphenyl)acetophenone</i>	<i>36</i>
IV. GOALS OF RESEARCH	38
RESULTS	40
I. A-ARYLACETOPHENONES AND DERIVATIVES	40
<i>A. General Preparation of the Ketones</i>	<i>40</i>
<i>B. Irradiation of Ketones</i>	<i>41</i>
<i>C. Steady-State Photokinetics</i>	<i>60</i>
II. A-ARYLACETONES	62
<i>A. General Preparation of the Ketones</i>	<i>62</i>
<i>B. Irradiation of Ketones</i>	<i>62</i>
<i>C. Identification of Photoproducts</i>	<i>63</i>
<i>D. Steady-State Photokinetics</i>	<i>70</i>
III. 2-TERT-BUTYL TRIFLOROACETOPHENONE	72
<i>A. Preparation</i>	<i>72</i>
<i>B. Irradiation Conditions</i>	<i>72</i>
<i>C. Identification of Photoproducts</i>	<i>72</i>
IV. 2'-(2,3-DIMETHYL-2-BUTYL)BENZOPHENONE	74
<i>A. General Preparation</i>	<i>74</i>
<i>B. Irradiation Conditions</i>	<i>74</i>
<i>C. Identification of photoproducts</i>	<i>75</i>
<i>D. Steady-State Photokinetics</i>	<i>78</i>
V. SEMIEMPIRICAL CALCULATIONS	79
DISCUSSION	90
I. CONFORMATIONAL CONTROL OF PRODUCT RATIOS FROM TRIPLET 1,5-BIRADICALS	90
II. PHOTOBEHAVIOR OF A-ARYLACETONES - A COMPARISON OF SINGLET AND TRIPLET BIRADICAL BEHAVIOR	110
III. PHOTOENOLIZATIONS OF A-(2,4,6-TRIIISOPROPYLPHENYL)ACETOPHENONE AND ACETONE	115

IV. PHOTOBHAVIOR OF O-TERT-BUTYLTRIFLUOROACETOPHENONE	118
V. PHOTOBHAVIOR OF 2-(2'-(2',3'-DIMETHYLBUTYL))BENZOPHENONE - EFFECT OF DIHEDRAL ANGLE ON HYDROGEN ABSTRACTION RATES	120
EXPERIMENTAL.....	131
I. GENERAL PROCEDURES	131
II. PREPARATION OF STARTING KETONES	132
<i>α</i> -(2-Ethylphenyl)- <i>β,β,β</i> -trideuteropropiophenone (4d ₃)	132
<i>α</i> -(2-Ethylphenyl)propiophenone (4).....	137
<i>α</i> -(2-Ethylphenyl)acetone (10)	138
<i>α</i> -Mesitylacetone (11).....	140
<i>α</i> -(2-Benzylphenyl)propiophenone (7)	142
<i>α</i> -(2,4,6-Triethylphenyl)- <i>β,β,β</i> -trideuteropropiophenone (5d ₃)	145
<i>α</i> -(2,4,6-Triethylphenyl)propiophenone (5)	150
<i>α</i> -(2,4,6-Triethylphenyl)acetone (12)	150
<i>α</i> -(2,4,6-Triisopropylphenyl)acetone (13).....	152
<i>α</i> -(2,4,6-Triisopropylphenyl)acetophenone (9)	155
<i>o</i> -tert-Butyl- <i>α,α,α</i> -trifluoroacetophenone (14)	157
<i>o</i> -(2,3-Dimethyl-2-butyl)benzophenone (15).....	160
III. PHOTOCHEMICAL EXPERIMENTS AND PROCEDURES	166
A. Purification of Chemicals.....	166
B. Equipment and Procedures.....	167
C. Identification of Photoproducts	169
D. Quantitative Measurements	219
REFERENCES:	251

List of Figures

FIGURE 1. SIMPLIFIED JABLONSKI DIAGRAM	1
FIGURE 2.....	15
FIGURE 3. ORIENTATIONAL REQUIREMENTS FOR H-ABSTRACTION	15
FIGURE 4. EFFECT OF DIHEDRAL ANGLE ON REACTIVITY	17
FIGURE 5. EFFECT OF DIHEDRAL ANGLE ON REACTIVITY	18
FIGURE 6. CORRELATION DIAGRAM.....	27
FIGURE 7. MINIMUM ENERGY GEOMETRIES OF A-(2-ETHYLPHENYL)ACETOPHENONE	80
FIGURE 8. MINIMUM ENERGY GEOMETRIES OF A-(2,4,6-TRIETHYLPHENYL)ACETOPHENONE	80
FIGURE 9. LOWEST ENERGY CONFORMERS OF A-(2-ETHYLPHENYL)PROIOPHENONE.....	81
FIGURE 10. LOWEST ENERGY GEOMETRIES OF A-(2,4,6-TRIETHYLPHENYL)PROIOPHENONE	82
FIGURE 11. MINIMUM GEOMETRIES OF A-(2-BENZYLPHENYL)ACETOPHENONE	83
FIGURE 12. LOWEST ENERGY CONFORMERS OF A-(2-BENZYLPHENYL)PROIOPHENONE.....	83
FIGURE 13. LOWEST ENERGY GEOMETRIES OF A-MESITYLPROIOPHENONE	84
FIGURE 14. LOWEST ENERGY GEOMETRY OF A-(2,4,6-TRISOPROPYLPHENYL)ACETOPHENONE	85
FIGURE 15. LOWEST ENERGY GEOMETRIES OF A-(2-ETHYLPHENYL)ACETONE	85
FIGURE 16. LOWEST ENERGY CONFORMERS OF A-MESITYLACETONE	86
FIGURE 17. LOWEST ENERGY GEOMETRIES OF A-(2,4,6-TRIETHYLPHENYL)ACETONE	87
FIGURE 18. LOWEST ENERGY GEOMETRY OF A-(2,4,6-TRISOPROPYLPHENYL)ACETONE.....	87
FIGURE 19. LOWEST ENERGY GEOMETRY OF 2- <i>tert</i> -BUTYLTRIFLUOROACETOPHENONE	88
FIGURE 20	89
FIGURE 21. LOWEST ENERGY BIRADICAL CONFORMATIONS OF 2.....	96
FIGURE 22. LOWEST ENERGY GROUND STATE CONFORMATIONS OF 2	97
FIGURE 23. LOWEST ENERGY BIRADICAL CONFORMATIONS OF 3.....	99
FIGURE 24. LOWEST ENERGY GROUND STATE CONFORMATIONS OF 8	100
FIGURE 25. LOWEST ENERGY BIRADICAL CONFORMATIONS OF 8.....	101
FIGURE 26. LOWEST ENERGY BIRADICAL CONFORMATIONS OF 5.....	105
FIGURE 27. LOWEST ENERGY GROUND STATE CONFORMATIONS OF 5	107
FIGURE 28. LOWEST ENERGY BIRADICAL CONFORMATIONS OF 4.....	108
FIGURE 29. LOWEST ENERGY GROUND STATE CONFORMATIONS OF 4	109
FIGURE 30. LOWEST ENERGY BIRADICAL CONFORMATIONS OF 10.....	114
FIGURE 31. LOWEST ENERGY GROUND STATE AND BIRADICAL CONFORMERS OF 9 AND 13.....	116
FIGURE 32.....	121
FIGURE 33. VARIABLE TEMPERATURE NMR OF A-(2,4,6-TRIETHYLPHENYL)-B,B,B-TRIDEUTERIO- PROIOPHENONE IN ACETONE- D_6	149
FIGURE 34. 1H NMR OF A-(2-ETHYLPHENYL)ACETOPHENONE BEFORE AND AFTER IRRADIATION IN TOLUENE ($\lambda > 290$ NM)	171
FIGURE 35. 1H NMR SPECTRA OF A-(2,4,6-TRIETHYLPHENYL)ACETOPHENONE BEFORE AND AFTER IRRADIATION IN TOLUENE ($\lambda > 290$ NM)	175
FIGURE 36. 1H NMR SPECTRA OF A-(2-ETHYLPHENYL)PROIOPHENONE BEFORE AND AFTER IRRADIATION IN TOLUENE ($\lambda > 290$ NM).....	182
FIGURE 37. 1H NMR SPECTRA OF A-(2,4,6-TRIETHYLPHENYL)PROIOPHENONE BEFORE AND AFTER IRRADIATION IN TOLUENE ($\lambda > 290$ NM)	186
FIGURE 38. 1H NMR SPECTRA OF A-(2-BENZYLPHENYL)ACETOPHENONE BEFORE AND AFTER IRRADIATION IN TOLUENE ($\lambda > 290$ NM).....	191
FIGURE 39. 1H NMR SPECTRA OF A-MESITYLPROIOPHENONE BEFORE AND AFTER IRRADIATION IN TOLUENE ($\lambda > 290$ NM).....	195
FIGURE 40. 1H NMR OF A-(2,4,6-TRISOPROPYLPHENYL)ACETOPHENONE AFTER IRRADIATION IN TOLUENE ($\lambda > 290$ NM).....	197
FIGURE 41. 1H NMR OF THE INDANOL MIXTURE FROM A-(2-ETHYLPHENYL)ACETONE IN BENZENE.....	203

FIGURE 42. ¹ H NMR OF THE METHYL REGION OF THE INDANOL MIXTURE FROM A-(2-ETHYLPHENYL)- ACETONE IN BENZENE	207
FIGURE 43. ¹ H NMR OF THE METHYLENE REGION OF THE INDANOL MIXTURE FROM A-(2- ETHYLPHENYL)ACETONE IN BENZENE.....	208
FIGURE 44. ¹ H NMR OF A-(2,4,6-TRIIISOPROPYLPHENYL)ACETONE AFTER IRRADIATION IN TOLUENE (λ > 290 NM, T= 297 K)	213

List of Tables

TABLE 1. A-SUBSTITUENT EFFECT ON <i>o</i> -TOLYLACETOPHENONE DERIVATIVES	24
TABLE 2. DIASTEREOSELECTIVITY IN PHOTOCYCLOADDITION OF BENZALDEHYDE TO CYCLOALKENES	35
TABLE 3. CHEMICAL YIELDS OF PHOTOPRODUCTS OF A-(2-ETHYLPHENYL)ACETOPHENONE IN TOLUENE AT VARIOUS TEMPERATURES ($\lambda > 290$).....	43
TABLE 4. CHEMICAL YIELDS OF PHOTOPRODUCTS OF A-(2,4,6-TRIETHYLPHENYL)ACETOPHENONE IN TOLUENE AT VARIOUS TEMPERATURES ($\lambda > 290$).....	45
TABLE 5. CHEMICAL YIELDS OF PHOTOPRODUCTS OF A-(<i>o</i> -TOLYL)PROPIOPHENONE IN TOLUENE AT VARIOUS TEMPERATURES ($\lambda > 290$)	46
TABLE 6. CHEMICAL YIELDS OF PHOTOPRODUCTS OF A-(2-ETHYLPHENYL)PROPIOPHENONE IN TOLUENE AT VARIOUS TEMPERATURES ($\lambda > 290$ NM)	49
TABLE 7. CHEMICAL YIELDS OF PHOTOPRODUCTS OF A-(2,4,6-TRIETHYLPHENYL) PROPIOPHENONE IN TOLUENE AT VARIOUS TEMPERATURES ($\lambda > 290$ NM)	50
TABLE 8. CHEMICAL YIELDS OF PHOTOPRODUCTS OF A-(2-BENZYLPHENYL)ACETOPHENONE IN TOLUENE AT VARIOUS TEMPERATURES ($\lambda > 290$ NM)	53
TABLE 9. CHEMICAL YIELDS OF PHOTOPRODUCTS OF A-MESITYLPROPIOPHENONE IN TOLUENE AT VARIOUS TEMPERATURES ($\lambda > 290$ NM).....	55
TABLE 10. MOLAR ABSORPTIVITY COEFFICIENTS ($M^{-1}CM^{-1}$) OF 9 AND ITS ENOL AT VARIOUS WAVELENGTHS.....	57
TABLE 11. PRODUCT QUANTUM YIELDS OF 9 AS A FUNCTION OF CONVERSION AND WAVELENGTH.....	58
TABLE 12. PRODUCT RATIOS OF IRRADIATION OF 9 UNDER VARIOUS CONDITIONS	59
TABLE 13. LIFETIMES OF TRIPLET ACETO- AND PROPIOPHENONES IN BENZENE	60
TABLE 14. QUANTUM YIELDS OF PHOTOPRODUCTS FROM ACETO- AND PROPIOPHENONES IN BENZENE	61
TABLE 15. CHEMICAL YIELDS OF PHOTOPRODUCTS FROM A-(2-ETHYLPHENYL)ACETONE IN TOLUENE AT VARIOUS TEMPERATURES ($\lambda > 290$ NM)	65
TABLE 16. CHEMICAL YIELDS OF PHOTOPRODUCTS FROM A-MESITYLACETONE IN TOLUENE AT VARIOUS TEMPERATURES ($\lambda > 290$ NM).....	67
TABLE 17. PRODUCT CHEMICAL YIELDS OF A-(2,4,6-TRIETHYLPHENYL)ACETONE IN TOLUENE AT VARIOUS TEMPERATURES ($\lambda > 290$ NM).....	68
TABLE 18. PRODUCT CHEMICAL YIELDS OF A-(2,4,6-TRISOPROPYLPHENYL)ACETONE AS A FUNCTION OF CONVERSION AND TEMPERATURE	70
TABLE 19. TRIPLET LIFETIMES OF A-ARYLACETONES IN BENZENE AT ROOM TEMPERATURE ($\lambda = 313$ NM).....	71
TABLE 20. QUANTUM YIELDS OF PHOTOPRODUCTS OF A-ARYLACETONES IN BENZENE AT ROOM TEMPERATURE ($\lambda = 313$ NM).....	71
TABLE 21. EFFECT OF TEMPERATURE AND MEDIUM ON PRODUCT RATIOS OF 15.....	77
TABLE 22. TRIPLET LIFETIMES AND PRODUCT QUANTUM YIELDS OF 2-(2'-(2',3'-DIMETHYL)BUTYL)-BENZOPHENONE AT ROOM TEMPERATURE ($\lambda = 313$ NM)	78
TABLE 23. EFFECT OF TEMPERATURE ON THE INDANOL RATIOS OF A-ARYLACETOPHENONES	91
TABLE 24. ARRHENIUS DATA FROM GRAPH 2	92
TABLE 25. ARRHENIUS DATA FROM GRAPH 3	103
TABLE 26. EFFECT OF TEMPERATURE ON PRODUCT RATIOS FROM A-ARYLACETONES	111
TABLE 27. EFFECT OF TEMPERATURE AND MEDIUM ON PRODUCT RATIOS OF 15	124
TABLE 28. DETAILS OF GLOBAL MINIMIZATIONS FOR COMPOUNDS 1-9.....	221
TABLE 29. DETAILS OF GLOBAL MINIMIZATIONS FOR COMPOUNDS 10-15	222
TABLE 30. GRID OF ENERGIES FOR THE GROUND STATE OPTIMIZATION OF A-(2-ETHYLPHENYL)ACETOPHENONE.....	223
TABLE 31. GRID OF ENERGIES FOR GLOBAL MINIMIZATION OF THE TRIPLET BIRADICAL OF A-(2,4,6-TRIETHYLPHENYL)ACETOPHENONE.....	224
TABLE 32. GRID OF ENERGIES FOR GLOBAL MINIMIZATION OF THE TRIPLET BIRADICAL OF A-(2-TOLYL)PROPIOPHENONE	225

TABLE 33. GRID OF ENERGIES FOR GLOBAL MINIMIZATION OF THE TRIPLET BIRADICAL OF A-(2-ETHYLPHENYL)PROPIOPHENONE	226
TABLE 34. GRID OF ENERGIES FOR GLOBAL MINIMIZATION OF THE TRIPLET BIRADICAL OF A-(2,4,6-TRIETHYLPHENYL)PROPIOPHENONE	227
TABLE 35. GRID OF ENERGIES FOR GLOBAL MINIMIZATION OF THE TRIPLET BIRADICAL OF A-MESITYLPROPIOPHENONE.....	228
TABLE 36. GRID OF ENERGIES FOR GLOBAL MINIMIZATION OF THE TRIPLET BIRADICAL OF A-(2-ETHYLPHENYL)ACETONE.....	229
TABLE 37. GRID OF ENERGIES FOR GLOBAL MINIMIZATION OF THE SINGLET BIRADICAL OF A-(2-ETHYLPHENYL)ACETONE.....	230
TABLE 38. GRID OF ENERGIES FOR GLOBAL MINIMIZATION OF THE TRIPLET BIRADICAL OF A-(2,4,6-TRISOPROPYLPHENYL)ACETONE.....	231
TABLE 39. PRODUCT QUANTUM YIELDS OF A-(2-ETHYLPHENYL)ACETOPHENONE IN BENZENE.....	234
TABLE 40. PRODUCT QUANTUM YIELDS OF A-(2,4,6-TRIETHYLPHENYL)ACETOPHENONE IN BENZENE	235
TABLE 41. PRODUCT QUANTUM YIELDS OF A-(2-BENZYLPHENYL)ACETOPHENONE IN BENZENE	236
TABLE 42. PRODUCT QUANTUM YIELDS OF A-(2-ETHYLPHENYL)PROPIOPHENONE IN BENZENE	237
TABLE 43. PRODUCT QUANTUM YIELDS OF A-(2,4,6-TRIETHYLPHENYL)PROPIOPHENONE IN BENZENE.....	238
TABLE 44. PRODUCT QUANTUM YIELDS OF A-(2-ETHYLPHENYL)ACETONE IN BENZENE	239
TABLE 45. PRODUCT QUANTUM YIELDS OF A-MESITYLACETONE IN BENZENE	240
TABLE 46. PRODUCT QUANTUM YIELDS OF A-(2,4,6-TRIETHYLPHENYL)ACETONE IN BENZENE	241
TABLE 47. PRODUCT QUANTUM YIELDS OF A-(2,4,6-TRISOPROPYLPHENYL)ACETOPHENONE IN BENZENE.....	242
TABLE 48. PRODUCT QUANTUM YIELDS OF A-(2-BENZYLPHENYL)PROPIOPHENONE IN BENZENE.....	243
TABLE 49. PRODUCT QUANTUM YIELDS OF A-(2,4,6-TRISOPROPYLPHENYL)ACETONE IN BENZENE	244
TABLE 50. PRODUCT QUANTUM YIELDS OF 2-(2'-(2',3'-DIMETHYL)BUTYL)BENZOPHENONE	245
TABLE 51. QUENCHING OF THE INDANOL FORMATION IN A-(2-ETHYLPHENYL)ACETOPHENONE WITH 2,5-DIMETHYL-2,4-HEXADIENE AT 313 NM IN BENZENE	246
TABLE 52. QUENCHING OF THE INDANOL FORMATION IN A-(2,4,6-TRIETHYLPHENYL) ACETOPHENONE WITH 2,5-DIMETHYL-2,4-HEXADIENE AT 313 NM IN BENZENE.....	246
TABLE 53. QUENCHING OF THE INDANOL FORMATION IN A-(2-BENZYLPHENYL)ACETOPHENONE WITH 2,5-DIMETHYL-2,4-HEXADIENE AT 313 NM IN BENZENE	247
TABLE 54. QUENCHING OF THE INDANOL FORMATION IN A-(2-ETHYLPHENYL)PROPIOPHENONE WITH 2,5-DIMETHYL-2,4-HEXADIENE AT 313 NM IN BENZENE	247
TABLE 55. QUENCHING OF THE INDANOL FORMATION IN A-(2,4,6-TRIETHYLPHENYL) PROPIOPHENONE WITH 2,5-DIMETHYL-2,4-HEXADIENE AT 313 NM IN BENZENE.....	248
TABLE 56. QUENCHING OF THE INDANOL FORMATION IN 2'-(2,3-DIMETHYL-2-BUTYL)BENZOPHENONE WITH 2,5-DIMETHYL-2,4-HEXADIENE AT 313 NM IN BENZENE.....	248
TABLE 57. QUENCHING OF THE DIARYLETHANE FORMATION IN A-(2-ETHYLPHENYL)ACETONE WITH 2,5-DIMETHYL-2,4-HEXADIENE AT 313 NM IN BENZENE	249
TABLE 58. QUENCHING OF THE DIARYLETHANE FORMATION IN A-MESITYLACETONE WITH 2,5-DIMETHYL-2,4-HEXADIENE AT 313 NM IN BENZENE.....	249
TABLE 59. QUENCHING OF THE DIARYLETHANE FORMATION IN A-(2,4,6-TRISOPROPYLPHENYL) ACETONE WITH 2,5-DIMETHYL-2,4-HEXADIENE AT 313 NM IN BENZENE.....	250

List of Schemes

SCHEME 1. A-CLEAVAGE REACTION	5
SCHEME 2. A-CLEAVAGE OF PIVALOPHENONE	5
SCHEME 3. CAGE AND NON-CAGE REACTIONS	6
SCHEME 4. A-CLEAVAGE IN CYCLIC KETONES	7
SCHEME 5. ORBITAL REQUIREMENTS OF TYPE II CLEAVAGE.....	10
SCHEME 6. ROLE OF BACK TRANSFER IN DETERMINATION OF QUANTUM EFFICIENCIES	11
SCHEME 7. CONFORMATIONAL, ROTATIONAL AND GROUND STATE CONTROL OF REACTIVITY	12
SCHEME 8. CONFORMATIONAL CONTROL OF REACTIVITY.....	12
SCHEME 9. GROUND STATE CONTROL OF REACTIVITY	13
SCHEME 10. ROTATIONAL CONTROL OF REACTIVITY	14
SCHEME 11. PHOTOCYCLIZATION OF 2,4,6-TRISOPROPYLBENZOPHENONES	17
SCHEME 12. BOAT-LIKE TRANSITION STATE FOR HYDROGEN ABSTRACTION	19
SCHEME 13. COMPETITION BETWEEN H-ABSTRACTION AND CYCLIZATION EFFICIENCIES.....	21
SCHEME 14. Δ -HYDROGEN ABSTRACTION IN OTBBP.....	22
SCHEME 15. PHOTOBHAVIOR OF OTAMBP	23
SCHEME 16. PHOTOCHEMISTRY OF BENZOIN ETHERS	29
SCHEME 17. PHOTOCHEMISTRY OF HEXAETHYLBENZIL	29
SCHEME 18. CRYSTALLINE STATE VS. SOLUTION PHOTOCHEMISTRY	30
SCHEME 19. PHOTOCYCLOADDITION OF BENZALDEHYDE TO CYCLOALKENES	35
SCHEME 20. ISC CONTROL OF DIASTEREOSELECTIVITY.....	36
SCHEME 21. PHOTOTAUTOMERIZATION OF ENOL TO KETONE	37
SCHEME 22. PHOTOBHAVIOR OF A-(2,4,6-TRISOPROPYLPHENYL)ACETOPHENONE.....	37
SCHEME 23. CHEMICAL SHIFTS OF METHYLS TRANS AND CIS TO PHENYL IN FIVE-MEMBERED RINGS	42
SCHEME 24. PHOTOCHEMISTRY OF 1.....	43
SCHEME 25. PHOTOCHEMISTRY OF 2.....	44
SCHEME 26. PHOTOCHEMISTRY OF 3.....	46
SCHEME 27. PHOTOCHEMISTRY OF 4.....	48
SCHEME 28. PHOTOBHAVIOR OF 5.....	50
SCHEME 29.....	51
SCHEME 30. PHOTOBHAVIOR OF 6.....	52
SCHEME 31. PHOTOBHAVIOR OF 7.....	54
SCHEME 32. PHOTOCHEMISTRY OF 8.....	55
SCHEME 33. PHOTOBHAVIOR OF 9.....	57
SCHEME 34. PHOTOPRODUCTS OF 10	65
SCHEME 35. PHOTOCHEMISTRY OF 11.....	66
SCHEME 36. PHOTOBHAVIOR OF 12.....	68
SCHEME 37. PHOTOCHEMISTRY OF 13.....	69
SCHEME 38. PHOTOBHAVIOR OF 14.....	73
SCHEME 39. PHOTOCHEMISTRY OF 15.....	76
SCHEME 40.....	90
SCHEME 41.....	95
SCHEME 42. LOWEST ENERGY BIRADICAL CONFORMATIONS OF 6	104
SCHEME 43. REACTIVE GROUND STATE CONFORMATIONS OF 10.....	115
SCHEME 44.....	119
SCHEME 45.....	119
SCHEME 46.....	120
SCHEME 47.....	123
SCHEME 48.....	125
SCHEME 49.....	126

SCHEME 50.....	127
SCHEME 51. SYNTHESIS OF A-(2-ETHYLPHENYL)PROPIOPHENONE	132
SCHEME 52. SYNTHESIS OF A-(2-ETHYLPHENYL)ACETONE.....	138
SCHEME 53. SYNTHESIS OF A-MESITYLACETONE	140
SCHEME 54. SYNTHESIS OF A-(2-BENZYLPHENYL)PROPIOPHENONE	142
SCHEME 55. SYNTHESIS OF A-(2,4,6-TRIETHYLPHENYL)-B,B,B-TRIDEUTEROPROPIOPHENONE	145
SCHEME 56. SYNTHESIS OF A-(2,4,6-TRIETHYLPHENYL)ACETONE	150
SCHEME 57. SYNTHESIS OF A-(2,4,6-TRIISOPROPYLPHENYL)ACETONE.....	152
SCHEME 58. SYNTHESIS OF A-(2,4,6-TRIISOPROPYLPHENYL)ACETOPHENONE	155
SCHEME 59. SYNTHESIS OF <i>O</i> - <i>TERT</i> -BUTYLTRIFLUOROACETOPHENONE	157
SCHEME 60. SYNTHESIS OF 2-(2'-(2',3'-DIMETHYL)BUTYL)BENZOPHENONE.....	161
SCHEME 61. PHOTOPRODUCTS OF A-(2-ETHYLPHENYL)ACETOPHENONE	169
SCHEME 62. PHOTOPRODUCTS OF A-(2,4,6-TRIETHYLPHENYL)ACETOPHENONE.....	172
SCHEME 63. PHOTOPRODUCTS OF A-TOLYLPROPIOPHENONE.....	176
SCHEME 64. PHOTOPRODUCTS OF A-(2-ETHYLPHENYL)-B,B,B-TRIDEUTEROPROPIOPHENONE	178
SCHEME 65. PHOTOPRODUCTS OF A-(2,4,6-TRIETHYLPHENYL)B,B,B-TRIDEUTERO PROPIOPHENONE	183
SCHEME 66. PHOTOPRODUCTS OF A-(2-BENZYLPHENYL)ACETOPHENONE.....	188
SCHEME 67. PHOTOPRODUCTS OF A-(2-BENZYLPHENYL)PROPIOPHENONE	190
SCHEME 68. PHOTOPRODUCTS FROM A-MESITYLPROPIOPHENONE	193
SCHEME 69. PHOTOPRODUCTS OF A-(2,4,6-TRIISOPROPYLPHENYL)ACETOPHENONE.....	196
SCHEME 70. PHOTOCHEMISTRY OF TRIMETHYLSILYLENOL ETHER OF 9	200
SCHEME 71. PHOTOPRODUCTS OF A-(2-ETHYLPHENYL)ACETONE	202
SCHEME 72. PHOTOPRODUCTS OF A-MESITYLACETONE	206
SCHEME 73. PHOTOPRODUCTS OF A-(2,4,6-TRIETHYLPHENYL)ACETONE	210
SCHEME 74. PHOTOPRODUCTS OF A-(2,4,6-TRIISOPROPYLPHENYL)ACETONE	212
SCHEME 75. PHOTOPRODUCTS OF <i>O</i> - <i>TERT</i> -BUTYLTRIFLUOROACETOPHENONE	214
SCHEME 76. PHOTOPRODUCTS OF <i>O</i> - <i>TERT</i> -AMYL BENZOPHENONE.....	216
SCHEME 77. PHOTOPRODUCTS OF 2-(2'-(2',3'-DIMETHYL)BUTYL)BENZOPHENONE.....	218

List of Abbreviations

OTBBP	<i>o-tert</i> -ButylBenzophenone
OTAMPB	<i>o-tert</i> -AmylBenzophenone
ISC	Intersystem Crossing
SOC	Spin-Orbit Coupling
nOe	Nuclear Overhauser Enhancement
CMC	Critical Micellar Concentration
PTLC	Preparative Scale Thin Layer Chromatography

Introduction

Many chemical reactions require the input of considerable energy to proceed. This energy is usually introduced as heat. Photochemical methods, however, provide an alternative way to add energy to reactants. The light absorbed by the photoactive portion of the molecule, the chromophore, provides energy to the system. Absorption of electromagnetic radiation by a molecule depends on a correspondence between the radiation energy and the energy of certain molecular transitions. The energy associated with ultraviolet and visible light is required to excite electrons in molecules. The first step in a photochemical reaction is excitation of a molecule through absorption of a photon. Whether this excited molecule leads to a chemical reaction or returns to the original ground state depends upon competition between various intramolecular and intermolecular interactions within the system.

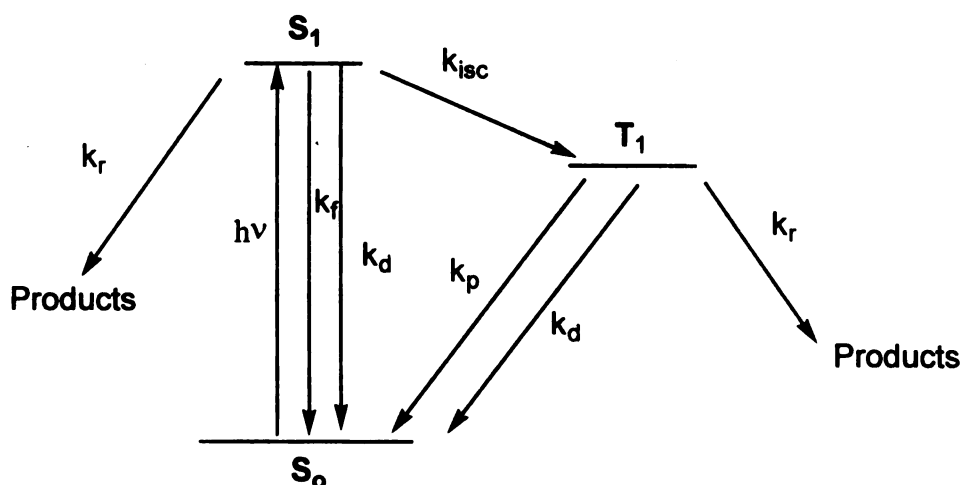
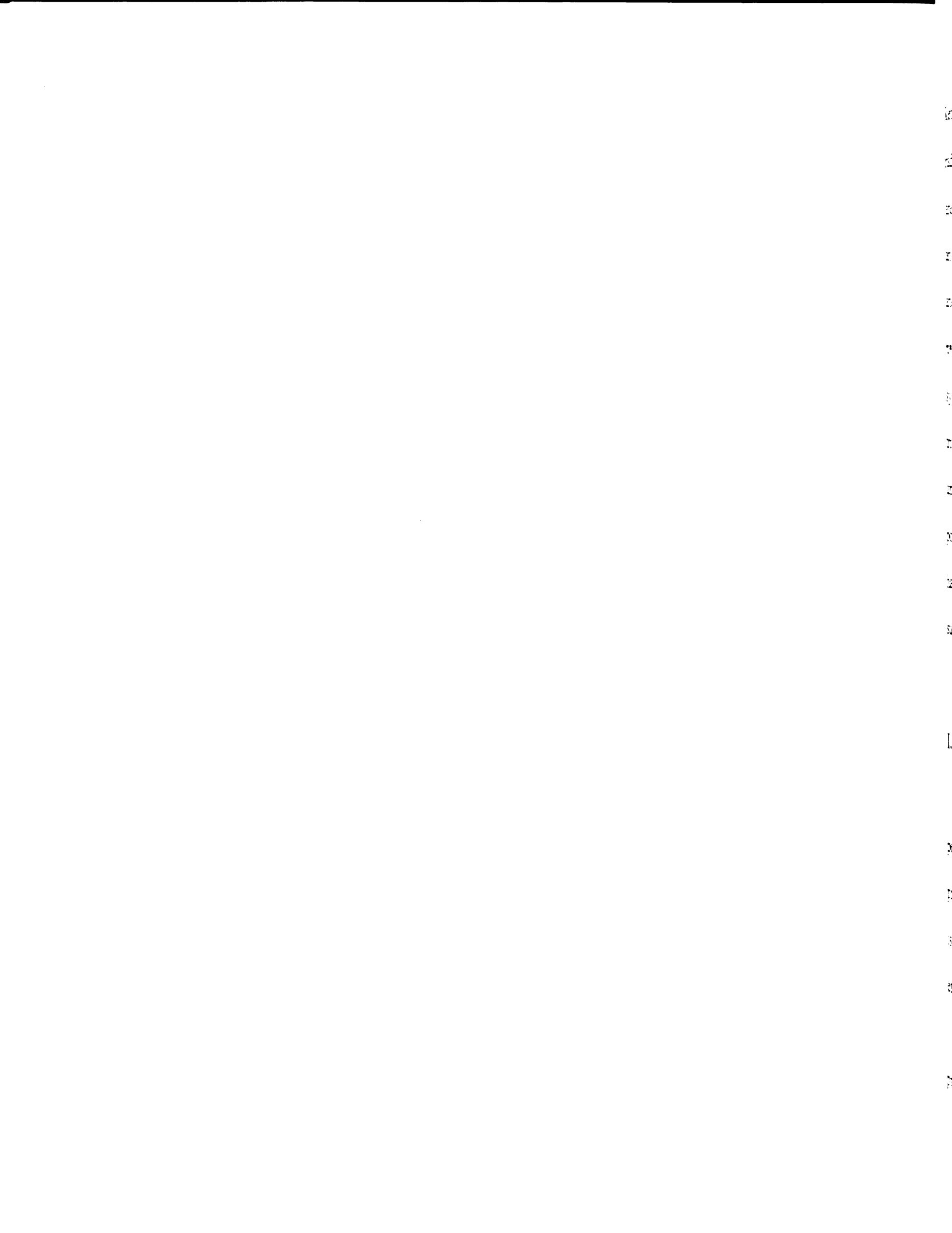


Figure 1. Simplified Jablonski Diagram

The photophysical and photochemical processes of molecules can best be described with the Jablonski diagram (Figure 1).¹ Absorption of a photon promotes a molecule from the ground state to the singlet excited state. The excited state molecule can decay to the ground state via emission of light (fluorescence) or radiationless decay. Rate constants for fluorescence and radiationless decay are on the order of 10^6 - 10^9 s⁻¹, and 10^5 - 10^8 s⁻¹ respectively.^{2,3} Photochemical reactions are also possible from the excited singlet. The excited singlet can undergo intersystem crossing to an excited triplet state. Typical rate constants for intersystem crossing (k_{isc}) are on the order of 10^7 - 10^{11} s⁻¹.^{2,3,4,5,6,7} The excited triplet can decay via radiative deactivation (phosphorescence) with a rate constant, k_p , of 10^1 - 10^6 s⁻¹.² It can also undergo radiationless decay and chemical reaction. Quenching of the excited triplet by energy transfer and/or charge transfer can occur with a rate constant as high as the rate of diffusion in a given solvent ($<10^{10}$ M⁻¹ s⁻¹).⁸

Photochemistry of the carbonyl group has been a major target of research for many decades. Aliphatic and aromatic ketones undergo similar photochemical reactions. However, the excited states leading to these reactions are somewhat different for the two. The reactive excited state of aliphatic ketones is the n,π^* state. On excitation, an electron from the oxygen nonbonding orbital is transferred to the π^* -antibonding orbital of the carbonyl group, creating an electron deficient oxygen. The singlet is initially formed, but intersystem crossing to the triplet occurs with rate constants of 10^8 - 10^{11} s⁻¹.^{2,3,4,5,6,7} Both S_1 (lowest excited singlet) and T_1 (lowest excited triplet) exhibit reactivity for aliphatic



ketones. The chemical behavior of the n,π^* triplet state is similar to that of an alkoxy radical. α -Cleavage, hydrogen abstraction, and charge transfer from an electron donor are the reactions frequently observed.^{9,10,11} Phenyl ketones have two low lying triplets, an n,π^* triplet and a π,π^* triplet, whose energy levels are affected by ring substituents and solvents. The π,π^* triplet arises from promotion of an electron from a π -bonding to a π^* -antibonding orbital. This results in a shift of electron density from the aromatic π -system to the carbonyl oxygen, generating an electron rich oxygen, and makes the π,π^* triplet much less reactive than the n,π^* triplet. Ketones with a π,π^* lowest triplet state do undergo typical n,π^* triplet reactions, but at a much slower rate, which reflects the population of the reacting n,π^* state at equilibrium.^{12,13,14} A wide variety of reactions have been reported in ketone photochemistry. Those relevant to this work are summarized below.

I. Measurements of Quantum Yields and Excited State Lifetimes

Quantum yields of photoreactions are defined as the molecules of product formed per photon of light absorbed. Thus, quantum yields can be obtained by measuring the product concentration and the light absorbed during the course of the reaction. The latter is usually measured using actinometers, which are compounds with known quantum efficiencies.

The quantum yield for any photochemical reaction can be expressed as the product of probabilities. Thus, for a triplet hydrogen abstraction,

$$\Phi = \Phi_{isc} k_H \tau P_{Br}$$

$$1/\tau = k_H + k_d$$

$$P_{Br} = k_r / (k_r + k_{Br})$$

Equation 1

where Φ_{isc} is the intersystem crossing quantum yield, k_H is the rate constant for hydrogen abstraction, k_d is the rate constant for triplet decay other than hydrogen abstraction, τ is the triplet lifetime, and P_{Br} is the probability that the intermediate will go to products. In the presence of an external quencher τ decreases and mathematically becomes:

$$1/\tau = k_H + k_d + k_q[Q]$$

Equation 2

where k_q is the bimolecular quenching rate constant. The Stern-Volmer equation is a mathematical relationship between quantum efficiencies in the absence (Φ^0) and presence (Φ) of quencher and is written as:

$$\Phi^0 / \Phi = 1 + k_q \tau [Q]$$

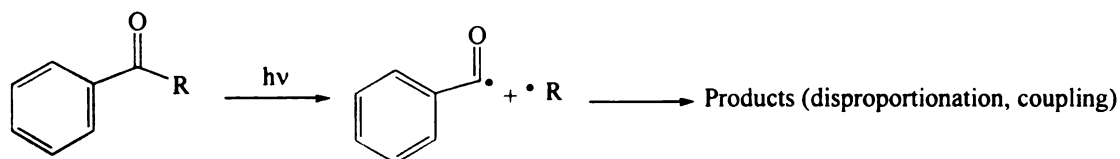
Equation 3

Thus a plot of Φ^0 / Φ versus $[Q]$ should give a straight line with an intercept of 1 and a slope of $k_q\tau$. In most cases, the rate of energy transfer quenching by dienes is diffusion controlled. For example, k_q is known to equal $5-6 \times 10^9 \text{ M}^{-1}\text{s}^{-1}$ in benzene at room temperature.^{8,15} Thus, the triplet lifetime can be calculated from the slope of the Stern-Volmer plot.

II. α -Cleavage reactions

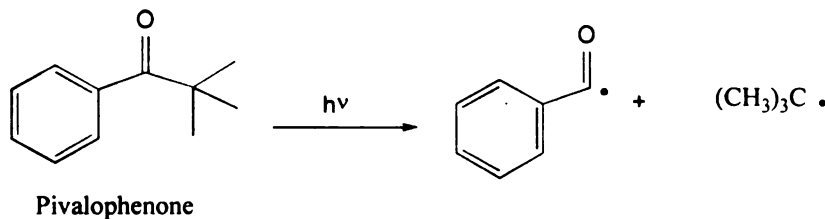
Photoexcited carbonyl compounds can undergo α -cleavage reactions (Scheme 1).

These reactions are commonly referred to as *Norrish type-I* reactions of the carbonyl compounds.¹⁶



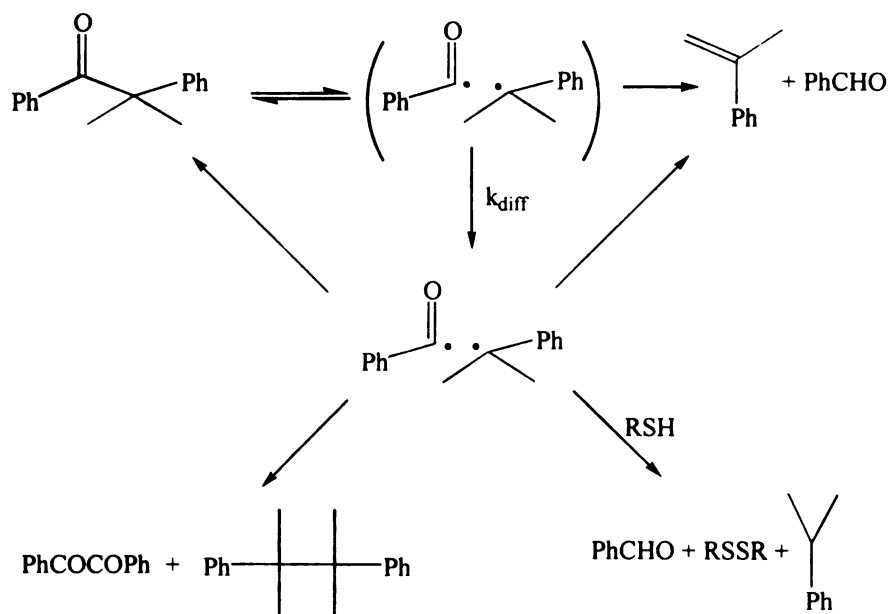
Scheme 1. α -Cleavage Reaction

The reaction's rate constant is dependent on the nature of the excited state, the relative stability of the alkyl radicals formed, and the degree of steric crowding in the reactant ketone. The reaction has been generally recognized to occur from an n,π^* excited state. The cleavage occurs due to the weakening of the α -carbon bond by overlap with the vacant n orbital which also happens in alkoxy radicals.^{17,18,19} When the excited state configuration is π,π^* , no such overlap is possible and the reaction does not occur. Pivalophenone, which has a lowest n,π^* triplet, cleaves with a rate constant of 10^7 s^{-1} , whereas *p*-methoxypivalophenone, with a π,π^* lowest triplet, cleaves much slower with a rate constant on order of 10^5 s^{-1} .²⁰



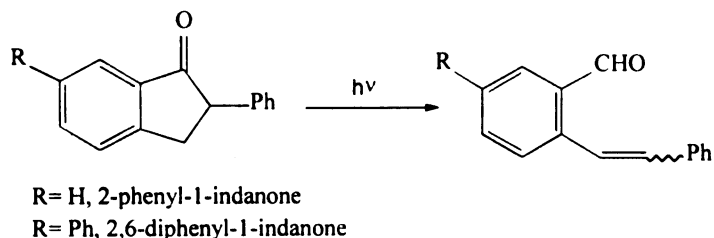
Scheme 2. α -Cleavage of Pivalophenone

The α -bond that produces the more stable carbon radical cleaves preferentially in unsymmetrically substituted ketones. Lewis has shown that the products obtained from the α -cleavage of ketones can be accounted for according to a mechanism shown in Scheme 3.²¹ The resulting radicals can recouple or disproportionate in the cage or diffuse apart and be trapped by other radicals, solvent or additives.



Scheme 3. Cage and Non-cage Reactions

Baum²² reported a similar study with 2-phenyl-1-indanone and 2,6-diphenyl-1-indanone. Although 2-phenyl-1-indanone cleaves efficiently to isomeric products, 2,6-diphenyl-1-indanone affords little product. This observation is consistent with the fact that 2-phenyl-1-indanone has an n,π^* lowest energy triplet and 2,6-diphenyl-1-indanone has a π,π^* lowest energy triplet.

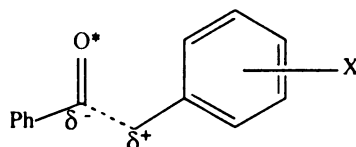


Scheme 4. α -Cleavage in Cyclic Ketones

The photochemical ring opening reactions of 2-hydroxyindan-1-ones have been reported to involve an initial Norrish type I cleavage followed by a 1,4-hydrogen transfer from a benzylic carbon.^{23,24} The possibility of 1,6-hydrogen transfer from the OH was ruled out when photolysis in methanol- d_4 resulted in no deuterium incorporation in the aldehyde.

In aliphatic ketones, where both singlet and triplet states can be populated, the triplet cleaves about 100 times faster than the singlet.^{25,26} Turro and co-workers have estimated the n,π^* singlet and triplet reactivities towards α -cleavage in several cyclic ketones. Their experimental results indicate that the triplet rate constant was larger than $5 \times 10^{10} \text{ s}^{-1}$, while the singlet rate constant was smaller than $2.5 \times 10^8 \text{ s}^{-1}$.²⁵ Yang has reported that the triplet state of di-*tert*-butyl ketone cleaves with a rate constant of $7.9 \times 10^9 \text{ s}^{-1}$, while the cleavage rate constant for the singlet is only $6 \times 10^7 \text{ s}^{-1}$.²⁶ Phenyl ketones undergo α -cleavage at much slower rates than aliphatic ketones. For example, triplet aliphatic *t*-butyl ketones α -cleave about 4000 times faster than triplet pivalophenone.²⁷

Electron donating groups on the α -phenyl ring enhance the reaction, indicating an early transition state with some ionic character.²¹ Other α -substituents also speed up the reaction, however, the rate constant for the reaction is dependent on the steric congestion in the ground state and was found to be independent of the stability of the resulting radicals.²¹



III. Hydrogen Abstraction

Photoexcited carbonyl compounds may undergo a characteristic hydrogen shift to the carbonyl oxygen from hydrogen donors.^{28,29} This process, known as hydrogen abstraction, can occur between an excited carbonyl and an external donor molecule (intermolecular hydrogen abstraction) or internally within the same molecule (intramolecular hydrogen abstraction). As for the α -cleavage reaction, hydrogen abstraction may occur from both singlet and triplet states in aliphatic ketones whereas the abstraction process occurs solely from the triplet excited state in the aromatic ketones. For aromatic ketones, the intersystem crossing of the initially formed singlet excited state is so fast ($\sim 10^{11} \text{ s}^{-1}$) that reactions of the S_1 state are usually not observed.³⁰

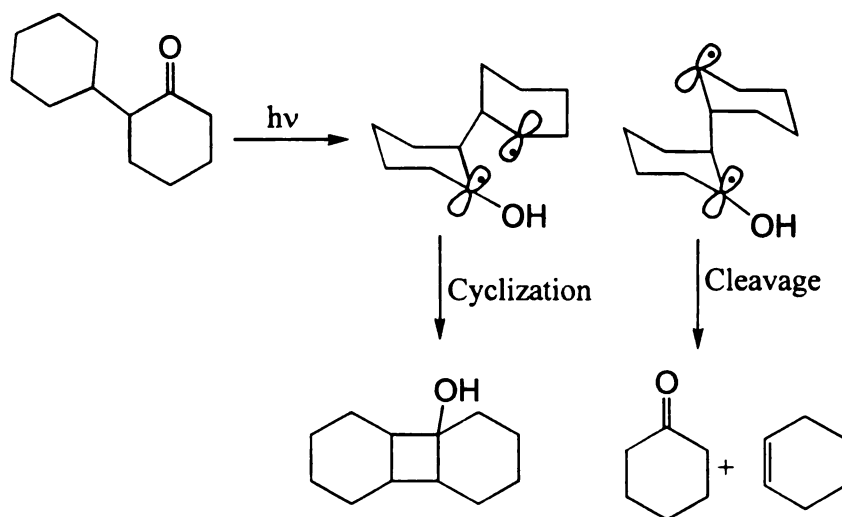
The reactive excited state for hydrogen abstraction is the n,π^* state. Carbonyl compounds with a π,π^* lowest excited state abstract hydrogen at much slower rates (from a thermally populated n,π^* state, or from the π,π^* state).^{13,14} This inefficiency is

attributed to a relatively high electron density on the oxygen atom in the π,π^* state. By comparison, the oxygen atom in the n,π^* state is more reactive toward hydrogen donors because of its radical like character. Hydrogen abstractions by triplet carbonyls are similar to those by alkoxy radicals.³¹ The n,π^* triplets, like alkoxy radicals have such a high electron demand that the transition states for hydrogen transfer are stabilized by charge transfer. Therefore, electron withdrawing groups near reactive hydrogens slow down the reaction.^{28,48}

Intramolecular hydrogen abstraction is the subject of this research and the material that follows will focus on this subject. Intramolecular hydrogen abstraction from the γ -carbon atom is favored but will occur from other positions when there are no hydrogens at the γ position and the molecular conformations allow other sites to come into close proximity to the excited carbonyl group. In acyclic systems the rate of abstraction from these sites is intrinsically lower since the transition state involves more strain and there is a lower probability that the molecule will attain the required conformation.^{32,48}

The γ -hydrogen abstraction yields a 1,4-biradical. Depending on the conformation of the initially formed 1,4-biradical, two different pathways are possible: (1) If the p orbitals of the radical centers can overlap, a cyclobutanol is the product. (2) If the p orbitals of the radical centers are parallel to the β -bond, this bond will cleave to yield an enol and an alkene (Scheme 5). These cyclization and cleavage reactions are termed the Norrish Type II reaction. The requirement that the orbitals be parallel to the β -bond is equivalent to the need for a planar transition state. This is illustrated in the reaction of α -

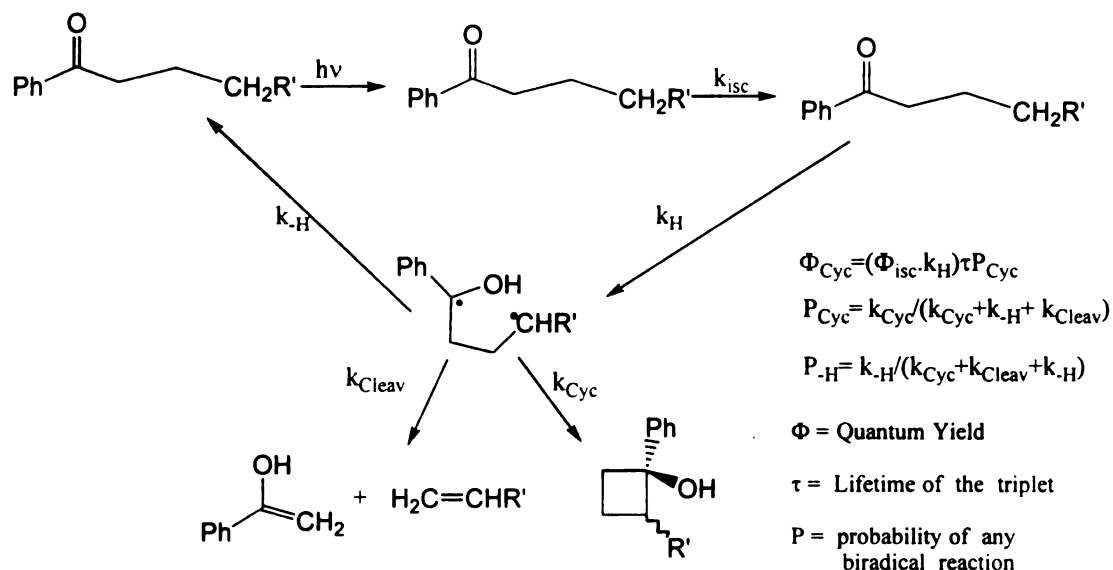
cyclohexyl-cyclohexanone in which the α,β -carbon-carbon bond must be axial in both rings for a cleavage conformation and, because of the limitations on this conformation, the cyclization process is preferred from both singlet and triplet states.³⁰ (Scheme 5)



Scheme 5. Orbital Requirements of Type II cleavage

One of the most important reactions of the intermediate biradicals is disproportionation to give back the starting ketone or back transfer. Quantum efficiencies for cyclization and cleavage are determined by the extent of the back transfer (Scheme 6).

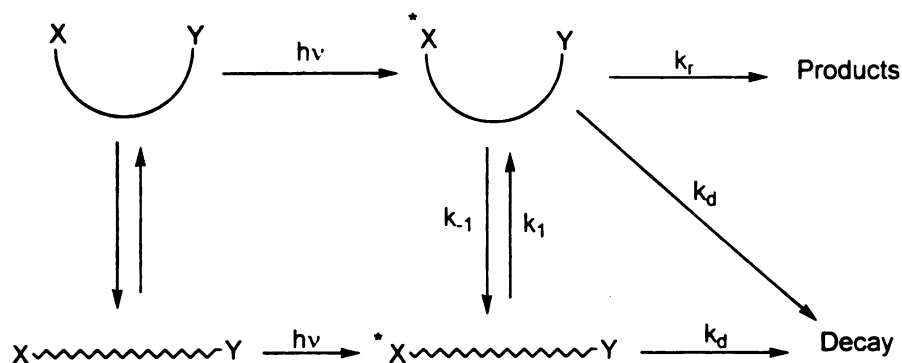
Quantum yields in Lewis base solvents are generally higher than in hydrocarbons since the former can hydrogen bond to the resulting hydroxybiradical and prevent the back transfer.³³



Scheme 6. Role of Back Transfer in Determination of Quantum Efficiencies

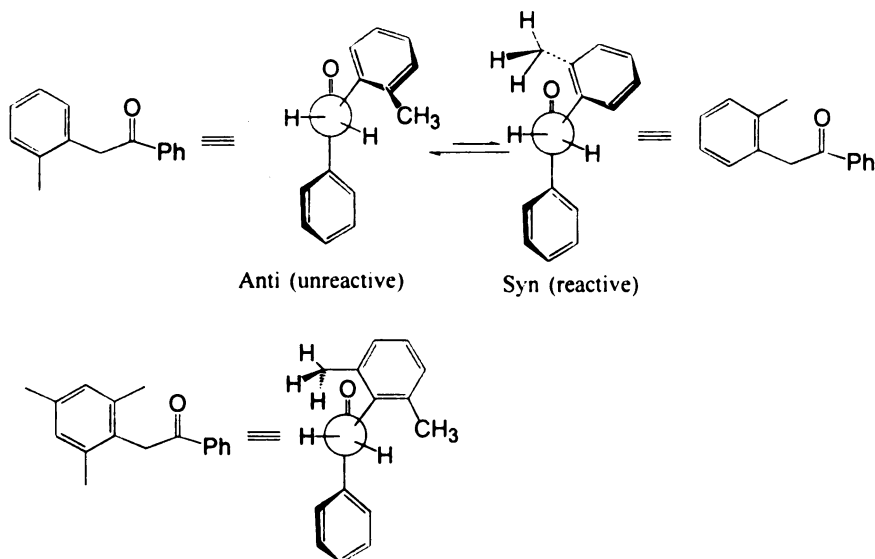
A. Conformational Control of Photoreactivity

The efficiency of hydrogen abstraction is dependent on the preferred ground state geometry, particularly since excited states can be very short-lived. Intramolecular hydrogen abstraction requires the carbonyl oxygen and the abstractable hydrogen to approach each other in such a way that proper orbital overlap and reaction can occur. This requirement makes photochemical intramolecular hydrogen abstractions sensitive to conformational equilibria, since competitive photochemical reactions can occur at rates faster than conformational motions.³⁴ The competition between conformational change, reaction, and decay (Scheme 7) provides three boundary conditions:³⁵ (1) Conformational equilibrium ($k_1, k_{-1} \gg k_r, k_d$) (2) Ground state control ($k_1, k_{-1} \ll k_r, k_d$) (3) Rotational control ($k_1 \sim k_d, k_{-1} < k_r$).³⁴



Scheme 7. Conformational, Rotational and Ground State Control of Reactivity

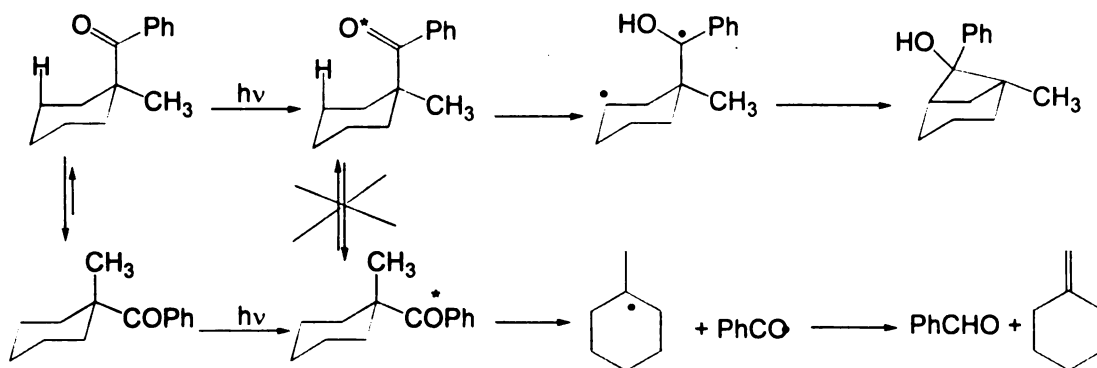
Wagner and Meador have reported that α -(*o*-alkylphenyl)acetophenones undergo efficient δ -hydrogen abstraction followed by cyclization to yield 2-indanols.³⁶ In their investigation, the rate of hydrogen abstraction by triplet α -mesitylacetophenone was found to be 7 times faster than that of triplet α -(*o*-tolyl)acetophenone. The slower hydrogen abstraction rate of α -(*o*-tolyl)acetophenone was attributed to a conformational equilibrium between the reactive *syn* and the unreactive *anti* conformers (Scheme 8).



Scheme 8. Conformational Control of Reactivity

In molecules where conformational changes are comparable or slower than photoreactions, either ground state control or rotational control may occur.

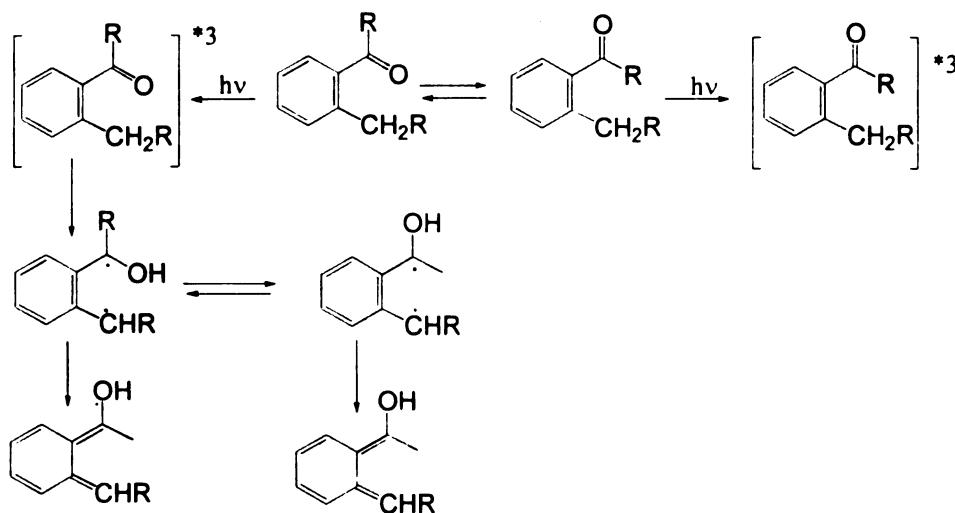
Several benzoylcyclohexane derivatives have provided the most clear-cut examples of ground state control in photoreactions. Lewis³⁷ investigated conformational effects in the photochemistry of 1-methylcyclohexyl phenyl ketone and a number of substituted analogs. Lewis found that for 1-methylcyclohexyl phenyl ketone, there exist two different ketone triplets, each leading to different photoproducts (Scheme 9). The ketone conformer with the benzoyl group in an axial position undergoes γ -hydrogen abstraction followed by cyclization to the corresponding 6-hydroxy-1-methyl-6-phenylbicyclo-[3.1.1]-heptane. The ketone conformer having the benzoyl group in an equatorial position cannot undergo hydrogen abstraction since the carbonyl group is oriented away from those hydrogens. Instead, it undergoes acyl cleavage giving rise to benzaldehyde as well as other products expected from the benzoyl and 1-methylcyclohexyl radicals.



Scheme 9. Ground State Control of Reactivity

Lewis found that the ratio of the products from the two different pathways is entirely dependent upon the ground state population of each ketone conformer.

An example of rotational control of photoreactivity is provided in the photoenolization of *o*-alkylphenylketones (Scheme 10).^{35,38} The anti rotamer is much less reactive than the syn rotamer. The lack of an H/D isotope effect on the rate of decay of the anti triplet led to the conclusion that the rate determining step was bond rotation and not hydrogen abstraction.³⁵



Scheme 10. Rotational Control of Reactivity

B. Orientational Requirements of Hydrogen Abstraction

One unresolved point that has been subject of much debate during the past twenty years has been the preferred transition state geometry for hydrogen abstraction process. In 1968, Turro reported that irradiation of cyclohexane solutions of *cis*- and *trans*-2-*n*-propyl-4-*t*-butylcyclohexanones results in strikingly different photochemistry (Figure 2).³⁹ Photolysis of the *cis* precursor resulted in the formation of 4-*t*-butylcyclohexanone,

while photolysis of the *trans* isomer gave the *cis* compound as the major product, presumably as the result of α -cleavage followed by reclosure with epimerization. Based on these results, Turro suggested that the striking contrast in the photochemistry of *cis* and *trans* isomers results from a stereoelectronic requirement for the Type II reaction, namely that the hydrogen on the γ -carbon to be extracted must be directed toward the half-vacant n orbital of the carbonyl oxygen atom.³⁹

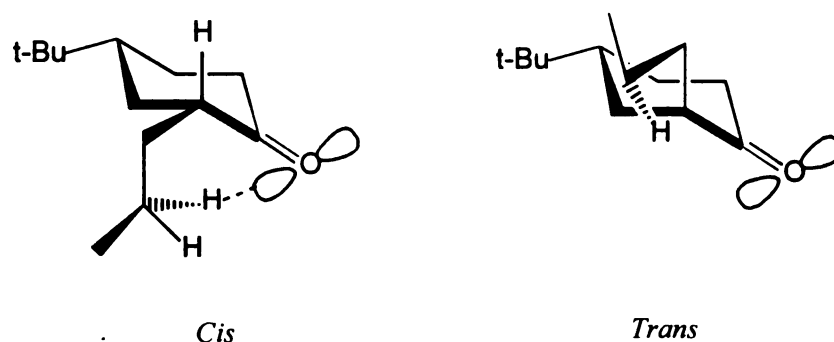


Figure 2

Scheffer has studied the Type II reaction in the crystalline state where the reactant geometry is fixed and measurable by x-ray diffraction methods.¹⁰⁵

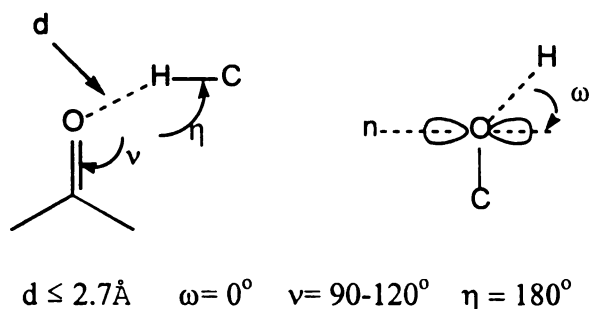


Figure 3. Orientational Requirements for H-Abstraction

In analyzing their reactivity, he considered the following ground state parameters, as depicted in Figure 3, to be the most important in determining the reactivity: d , the

distance between O and H; η , the O-H-C angle, ν , the C=O-H angle; and ω , the dihedral angle that the O-H vector makes with respect to the nodal plane of the carbonyl pi system. In several ketones, for which x-ray crystal structures were obtained, the value of d ranged from 2.3-3.1 Å, η from 85-120°, ν from 74-103°, and ω from 0-62°. ^{49,105,40,41} Scheffer suggests the theoretically “ideal” values for these parameters to be those shown in Figure 3. The distance of 2.7 Å is the sum of the H and O van der Waals radii. Scheffer points that when hydrogen is this close in the ground state, minimal molecular motion is required for hydrogen abstraction in the crystal. Molecular flexibility can, however, allow hydrogen abstraction to occur at longer distances. The deviations from ideality in case of η and ω have long been known from the reactivity of many steroidal ketones. ^{11,48}

Morrison and coworkers reported *ab initio* studies (3-21G basis set) for hydrogen abstraction from methane by triplet formaldehyde. ⁴² The calculated saddle point for the reaction had the following parameters: $d=1.18$ Å, $\nu=109^\circ$, $\omega=9^\circ$, $\eta=176^\circ$.

Sugiyama has reported that in some bridged polycyclic ketones (Figure 4), photolysis results in no hydrogen abstraction, although the hydrogens are extremely close to the carbonyl oxygen. ⁴³ He attributed this to the unfavorable dihedral angle between the hydrogens and the C-C=O plane. An alternative explanation could be that the abstraction is indeed occurring, but the biradical does not cyclize and instead disproportionates to the starting material. This seems reasonable since cyclization will put additional strain on an already strained ring system.

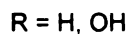
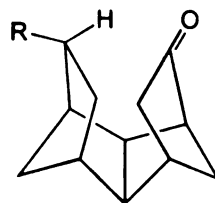
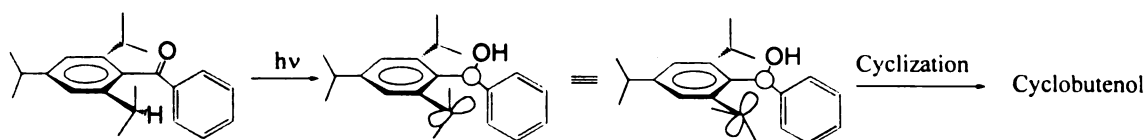


Figure 4. Effect of Dihedral Angle on Reactivity

Photochemical studies of solid complexes of desoxycholic acid and acetophenone derivatives provide examples of intermolecular hydrogen abstraction from the perpendicular direction of the carbonyl plane, but it was concluded that molecular motions within the crystal lattice permitted approach of the reactive hydrogen to the locus of the n orbital of the excited ketone.⁴⁴

Matsuura suggested that photocyclization of 2,4,6-triisopropylbenzophenones (Scheme 11), where abstractable hydrogens lie between 55 - 60° out of the plane of the carbonyl group, occurs from the π, π^* state.⁴⁵ This was because the reaction from the n, π^* state requires rotation about several bonds and therefore, is topochemically unfavorable in the solid state.



Scheme 11. Photocyclization of 2,4,6-Triisopropylbenzophenones

Sauers and *co-workers* designed polycyclic ketones that contain hydrogen atoms fixed in the plane of the π system (Figure 5) with the aim of setting limits on reactivity

based on out of plane angles.⁴⁶ They reported that even when theoretical models did not reveal any barriers attributable to unusual steric strain, no reaction occurred. The short triplet lifetimes of these ketones were attributed to a reversible Norrish type I cleavage that generates very short lived biradicals.⁴⁷

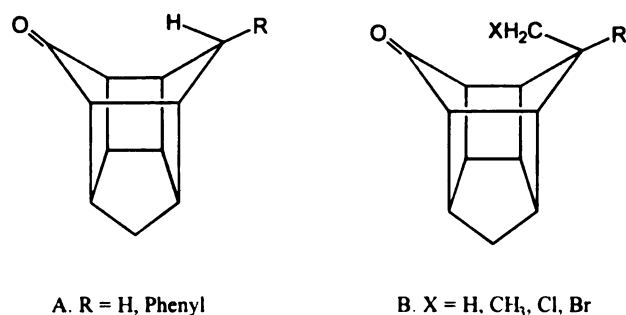
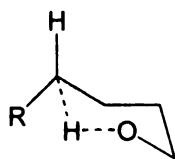
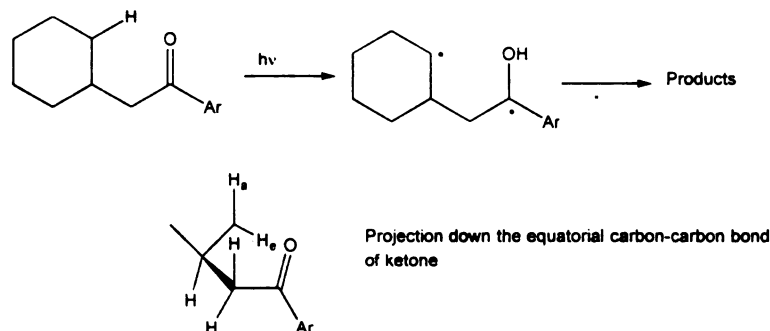


Figure 5. Effect of Dihedral Angle on Reactivity

Wagner suggested that the ease of 1,5-hydrogen transfers in acyclic systems reflects primarily a torsion free, chair-like, six-membered cyclic transition state such that the C-H-O angle is tetrahedral.⁴⁸ This angle is much less than the linear arrangement calculated by theoretical models. It was also proposed that the torsional strain present in the cycloheptane-like transition state for 1,6-hydrogen transfers is responsible for the slower rate of δ -hydrogen abstraction in straight chain systems. Wagner also suggested that coplanar hydrogen abstraction is not a strict requirement for the Type II process and proposed a $\cos^2\omega$ dependence for abstraction.¹¹

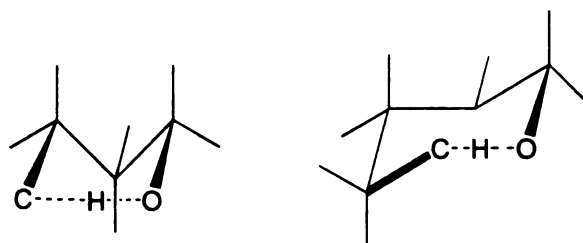


Scheffer has reported a boat rather than a chair transition state for hydrogen abstraction in a few cases (Scheme 12).⁴⁹ His studies further reinforced the notion that hydrogen and the carbonyl need not be coplanar for the abstraction process to take place.

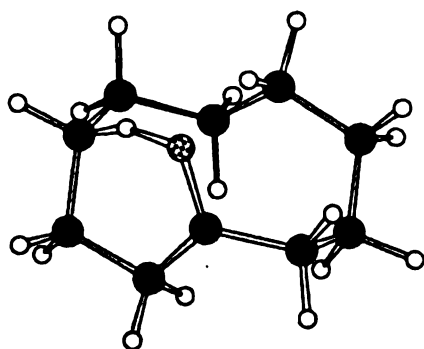


Scheme 12. Boat-Like Transition State for Hydrogen Abstraction

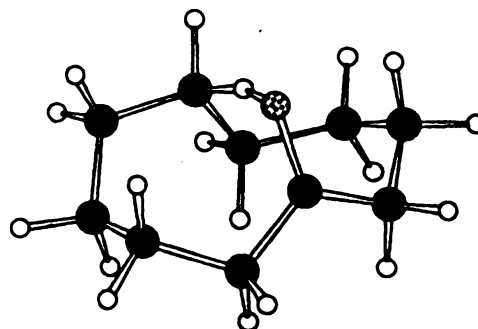
Houk noted that a chair-like cyclohexane transition state requires a severely nonlinear geometry for hydrogen transfer.⁵⁰ He carried out both *ab initio* molecular orbital calculations and force field modeling which predict the six-membered transition structure for γ -hydrogen abstraction (butoxy radical) resembles a five membered ring of heavy atoms, having an envelope shape like that of a cyclopentane, but with one long bond (2.5 Å) between C_a and O.⁵⁰ The seven-membered cyclic transition structure for δ -hydrogen abstraction (pentoxy radical) also had a chair form much like that of cyclohexane, but with one long bond. In both transition structures the CHO angle was nearly linear. Based on their calculations, Houk and co-workers have suggested that the preference for a six-membered over a seven-membered transition state is the result of a more favorable entropy of activation for the six-membered transition state.⁵⁰ Similar transition state geometries were calculated for the γ - and δ -hydrogen abstractions of triplet butanal and pentanal, respectively.⁵¹



Sauers and *co*-workers found a correlation between the overall reaction and the transition state steric energy. Using computational methods, they calculated the transition structure energies for intramolecular hydrogen abstraction at γ vs. ϵ positions for triplet cyclodecanone.^{52,53} In the lowest energy conformation of cyclodecanone, a γ -hydrogen lies close (2.54 Å) to the carbonyl group. The ϵ -hydrogen, on the other hand, is not only remote (4.12 Å), but is on the wrong side of the molecule. However, another low energy conformation was found in which the ϵ -hydrogen lies close (2.48 Å) to the carbonyl moiety.⁵³ The out of plane angles are 56° and 90.2° for the γ and ϵ hydrogens in the two structures, respectively. Irradiations in cyclohexane are reported to yield only 10-decalols, products of ϵ -hydrogen abstraction. Computed transition structure energies show a clear preference for reaction via a 6-membered ring, over an 8-membered ring.



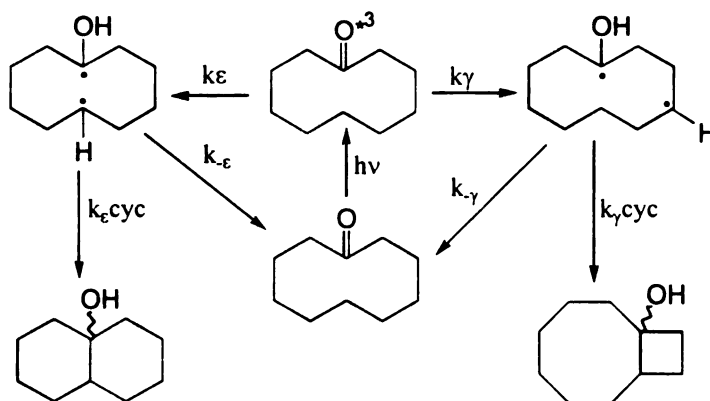
Steric Energy=21.4 kcal/mol



Steric Energy=23.8 kcal/mol

The reason for this apparent paradox lies in the ratio of cyclization vs. disproportionation rates, since there would be a large difference in ease of formation of the two ring systems:

decalin vs. bicyclo[6.2.0]decane (Scheme 13).⁵³ This hypothesis was confirmed with the observation that irradiation in *tert*-butanol produced 1-hydroxybicyclo[6.2.0]decane as the major product. This is due to stabilization of biradical by H-bonding to the solvent which will increase the biradical lifetime and the amount of cyclization.



Scheme 13. Competition Between H-Abstraction and Cyclization Efficiencies

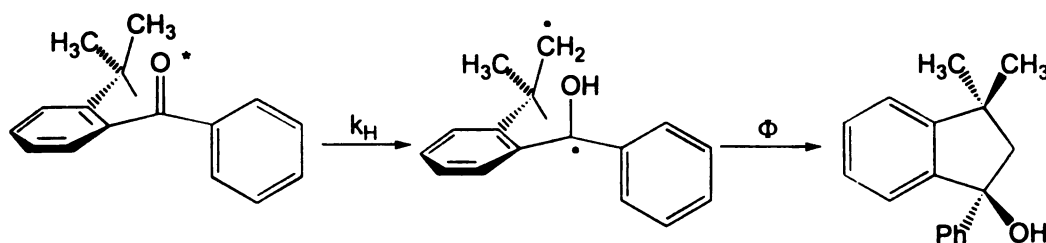
The above mentioned studies show that in most cases the transition state for hydrogen abstraction deviates from ideality. Furthermore, the dependence of reactivity on the value of ω is not clearly understood. This point will be addressed later in this thesis.

C. δ -Hydrogen Abstraction

Intramolecular hydrogen abstraction by the carbonyl function occurs from sites other than the γ -position when this position has no hydrogens or when the chemical or geometrical features of the molecule allow for effective competition from other positions. In δ -methoxy-valerophenone, for example, δ -hydrogen abstraction has the same rate as the γ -abstraction due to activation of the δ -position and deactivation of the γ -position by the methoxy group.³⁰ The biradicals produced from these δ -abstractions,

however, cannot undergo simple cleavage to give electron paired products and in some cases cyclize very efficiently.

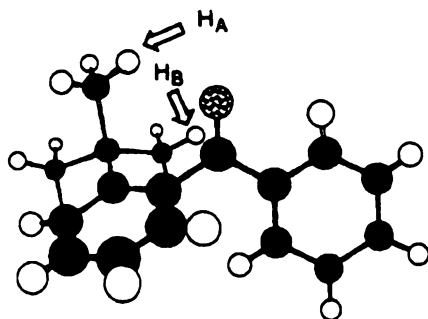
Wagner reports that irradiation of *o*-*tert*-butylbenzophenone (OTBBP) as a solid or in solution results in its quantitative cyclization to 1-phenyl-3,3-dimethyl-1-indanol.^{54,55,56} A large solvent effect was also reported on the quantum efficiency and the lifetime of the 1,5-biradical (Scheme 14).



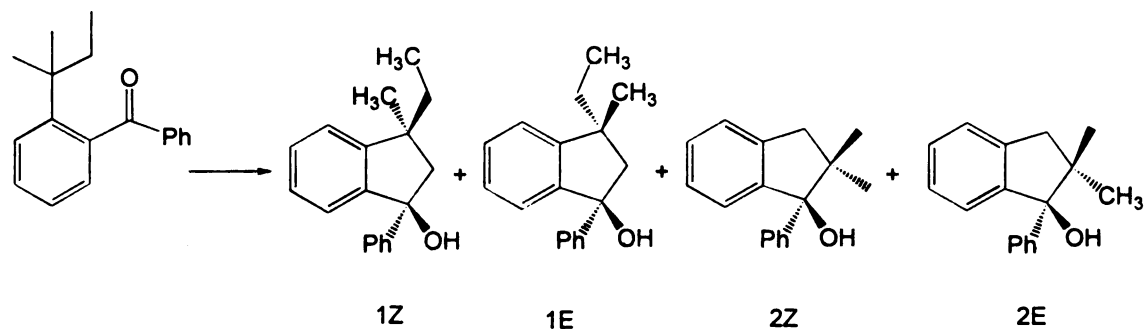
$k_H > 10^9 \text{ M}^{-1} \text{ S}^{-1}$ at 25° ; $E_a = 2.5 \text{ kcal/mole}$; $\log A = 10.6$
 biradical lifetime = 43 ns in methanol, 4ns in toluene
 $\Phi_{\text{benzene}} = 0.04$ $\Phi_{\text{methanol}} = 1.00$

Scheme 14. δ -Hydrogen Abstraction in OTBBP

The large value of k_H for OTBBP is attributed to an ideal conformation for hydrogen abstraction. The x-ray structure shows that one of the *tert*-butyl hydrogens is 2.46 Å from the carbonyl oxygen (H_A , $\omega = 40^\circ$), while another is 2.67 Å away (H_B , $\omega = 90^\circ$).

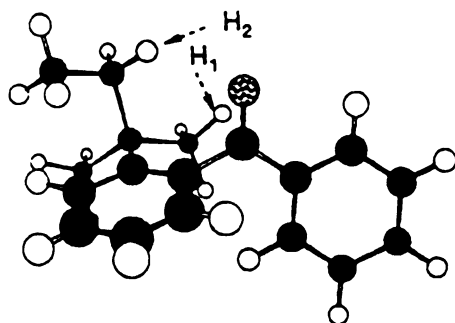


In order to determine which hydrogen is attacked, an unsymmetrical analog, *o*-*tert*-amylbenzophenone was investigated. *o*-*tert*-Amylbenzophenone (OTABMP) was reported to yield a 60:40 ratio for hydrogen abstraction from methyl (1E and 1Z) and ethyl (2E and 2Z) groups of the *tert*-amyl unit when irradiated in benzene at ambient temperatures (Scheme 15).⁵⁷ Furthermore, solid state irradiation of OTABP resulted in abstraction from ethyl and methyl positions at a ratio of 70:30.



Scheme 15. Photobehavior of OTABMP

This was an interesting result since the primary and secondary hydrogens in OTABP adopt different positions in the crystal. The x-ray structure shows the closest ethyl hydrogen is 2.63Å from the oxygen ($\omega = 45^\circ$), while the methyl hydrogen is 2.53Å away but with a different dihedral angle ($\omega = 95^\circ$).



The abstraction of methyl hydrogens in the crystal is engaging since theoretically these hydrogens should not be abstracted.

It was mentioned earlier that α -(*o*-alkylphenyl)acetophenones undergo efficient cyclization to 2-indanols. Introduction of an α -substituent not only decreases the efficiency of indanol formation but also introduces α -cleavage as an alternative pathway for triplet relaxation (Table 1).⁵⁸

This phenomenon was explained in terms of the starting geometry of ketones. In the unsubstituted acetophenones, the most stable conformer is the one with the α -aryl group eclipsing the carbonyl. This geometry is very close to the reactive geometry. For the α -substituted acetophenones, however, the α -alkyl substituent eclipses the carbonyl and the α -aryl group is twisted away, thus creating a poor geometry for hydrogen abstraction. As shown in Table 1, as the rate of hydrogen abstraction drops, due to a poor starting geometry, reactions such as α -cleavage begin to compete.

Table 1. α -Substituent Effect on *o*-Tolylacetophenone Derivatives

Ketone	Φ_{cyc}	Φ_{cleav}	$1/\tau, 10^8 \text{ S}^{-1}$
α -(<i>o</i> -Tolyl)acetophenone	1.0	0	1.2
α -(<i>o</i> -Tolyl)propiofenone	0.05	0.28	0.6
α -(<i>o</i> -Tolyl)isobutyrophenone	0	0.38	0.5
α -(<i>o</i> -Tolyl)valerophenone	0.014	0.03 ^a 0.34 ^b	2.2

a) Type I cleavage b) Type II cleavage

D. Nature of the Excited State- Singlet vs. Triplet

One of the most intriguing questions in organic photochemistry is whether the differences in spin multiplicity between singlet and triplet states will be reflected in their reactivity in primary photochemical processes. Yang has shown that in aliphatic ketones the rate of cleavage from the triplet is about 100 times faster than the singlet.²⁶ Dialkylketones are known to undergo hydrogen abstraction in both the T_1 and S_1 states.^{59,60,28} Photolysis of the optically active ketone (S)-(+)-5-methyl-2-heptanone showed that photoracemization occurs from the triplet state, suggesting the existence of a triplet biradical sufficiently long lived to allow racemization at the γ -carbon.⁶¹ The results obtained with the optically active ketone showed that the total quantum yield of observed events from T_1 is only 0.14.⁶¹ Since Φ_{isc} was determined to be 0.11 and the quantum yield for reaction from S_1 is 0.07, the remaining quantum yield of 0.79 must represent non radiative decay from S_1 .⁶¹ This decay appears to lead to no racemization and is not affected by changes in the solvent, which implies that if it does involve formation of a singlet biradical and subsequent back hydrogen transfer, then the biradical must be extremely short-lived. Stephenson, *et al.*, have also presented evidence which is consistent with the intermediacy of a singlet biradical in the type II reaction.⁶²

It has also been suggested that the type II reaction from S_1 state may occur via a concerted pathway.²⁸ Heller has proposed that the electronic energy might be transferred into vibrational stretching energy of a C-H bond, with further partitioning into a pair of

radicals (or biradical) or to a relaxed ground state.⁶³ Hammond has also postulated that chemical reactions of the excited states are special forms of radiationless decay.⁶⁴

Salem has calculated the activation energies and surface crossings for singlet and triplet state hydrogen abstractions.⁶⁵ He showed that simple symmetry considerations indicate that the n,π^* singlet of the carbonyl correlates with the singlet diradical product, whereas the ground state correlates with a zwitterionic species.⁶⁵ Since the plane of symmetry is not maintained in most hydrogen abstractions, an avoided crossing between the excited and ground state surfaces occur (Figure 6). Hydrogen abstraction therefore requires a radiationless decay which can occur easiest at the point of the smallest energy difference between the two surfaces.^{11,65} Conversion of the electronic energy into vibrational energy populates the ground state at a maximum, from which relaxation to diradical product or to ground state reactant can occur.^{11,65} In other words, singlet hydrogen abstraction is inherently inefficient.

Scaiano *et al.* have studied fluorescence quenching of acetone by several hydrogen donors.⁶⁶ They report the excited singlet of acetone to be 2-10 times more reactive than the triplet toward hydrogen donors. They have ascribed this to a more exothermic reaction from the singlet (singlet being higher in energy than triplet) which results in a lower activation energy for hydrogen abstraction. Furthermore, the lower quantum yield for product formation from the singlet relative to triplet was attributed to a lower efficiency of photoreduction from the singlet, i.e., the actual rate of transfer for the hydrogen atom to the excited singlet is lower than in the triplet.^{60,63} The authors attribute

this inefficiency to deactivation of the excited state to yield the reactants from an avoided crossing (Figure 6) before a radical pair is reached.

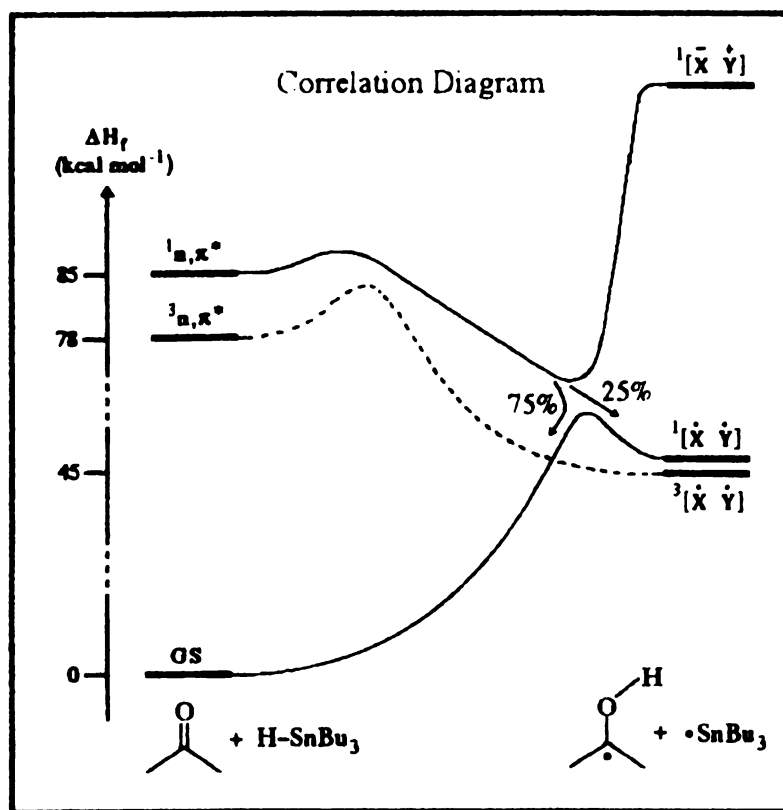
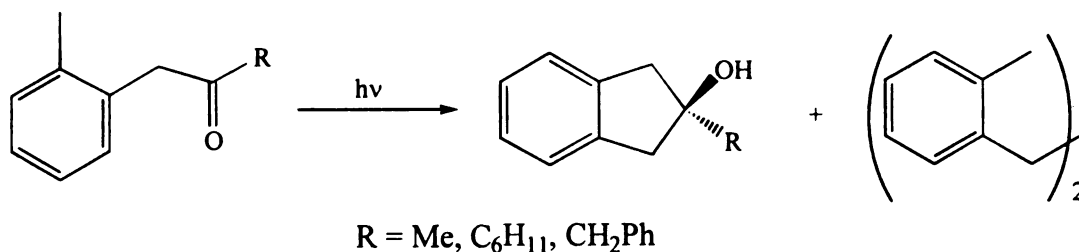


Figure 6. Correlation Diagram

It was concluded that the interaction of the singlets with hydrogen donors is not a chemical reaction but a physical quenching mechanism, where the hydrogen donor causes deactivation by accepting part of the electronic excitation energy as vibrational energy and promoting internal conversion from S₁ to S₀.^{60,65}

Turro recently reported that α -(*o*-tolyl)acetones undergo δ -hydrogen abstraction followed by cyclization to yield 2-indanols.⁶⁷ Quenching studies indicate that δ -hydrogen abstraction occurs from the singlet while α -cleavage occurs from the triplet. The rate constants of hydrogen abstraction and intersystem crossing from the singlet in tolylbenzyl

ketone were reported to be 2×10^9 and $5 \times 10^8 \text{ s}^{-1}$, respectively.⁶⁷ α -(*o*-Tolyl)acetophenone, in contrast, does not cleave but undergoes an efficient ($\Phi=1.0$) δ -hydrogen abstraction followed by cyclization from the triplet.⁸⁷ The rate constant for intramolecular hydrogen abstraction of α -(*o*-tolyl)acetophenone was reported to be $1.6 \times 10^8 \text{ s}^{-1}$,⁸⁷ ten-times lower than the singlet abstraction rate reported by Turro⁶⁷.

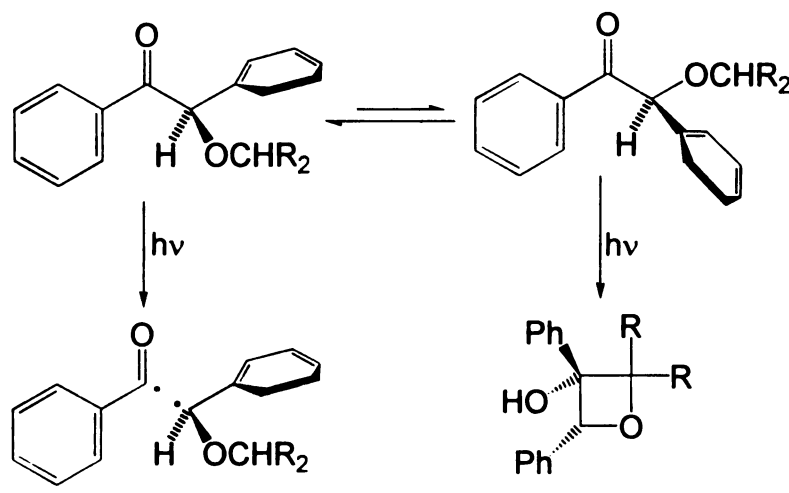


E. Effect of Environment

Turro has studied the photochemistry of α,α -dimethylvalerophenone in several zeolites.⁶⁸ Product distribution varied depending on the zeolite cavity size. Type I cleavage is the main photoreaction when the cavities are too small to allow conformational changes necessary for the Type II reaction. (The cage effect precludes observation of Type I products unless the resulting radicals rearrange or disproportionate while coupling.)

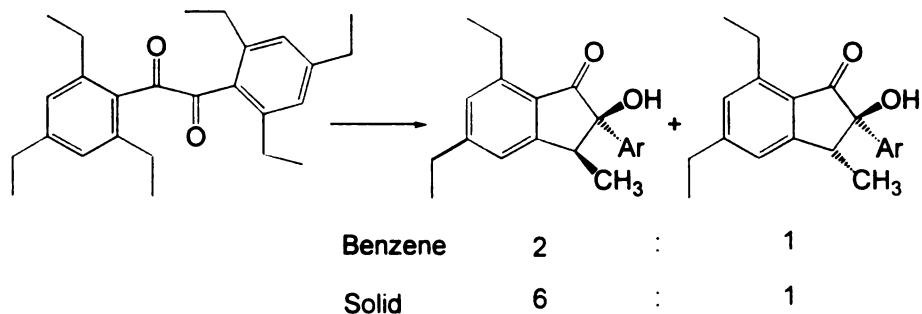
Turro has also studied the photochemistry of α -(*o*-tolyl)acetones in aqueous surfactant solution.⁶⁷ He has shown an increase in cyclization product (indanol) yields in micelles compared to solution. This is due to the well-known cage effect.⁸¹

DeMayo studied the photochemistry of benzoin ethers, which only α -cleave in solution, on silica.⁶⁹ He reported an 85:15 ratio of Type I/ Type II products and attributed this to a more reactive ketone geometry and reversibility of cleavage due to poor translational mobility on the silica surface. (Scheme 16)



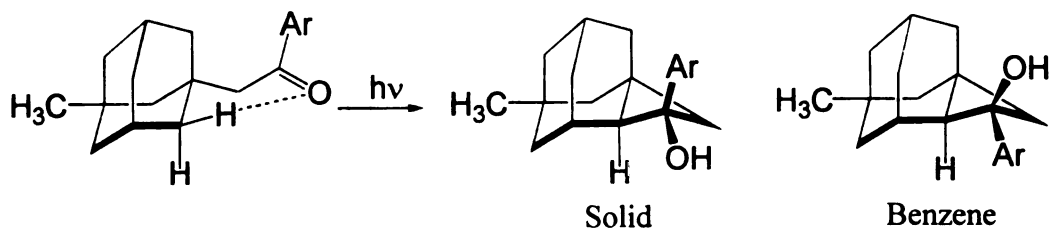
Scheme 16. Photochemistry of Benzoin Ethers

The crystalline and amorphous solid states can provide unique behavior and product stereoselectivity. Wagner and coworkers have reported that irradiation of solid 2,4,6,2',4',6'-hexaethylbenzil (Scheme 17) has resulted in a three-fold Z:E increase over solution chemistry.⁷⁰



Scheme 17. Photochemistry of Hexaethylbenzil

Perhaps, the most striking results in crystalline state photochemistry can be found in Scheffer's work. He has shown that when a compound crystallizes in a chiral space group the crystalline state irradiation, in most cases, will result in high enantio- and/or diastereoselective photoproducts. For example, the achiral ketone α -(3-methyladamant-1-yl)acetophenone crystallizes in a chiral space group.⁷¹ Irradiation in crystal results in a 70% yield of a single cyclobutanol in 82% enantiomeric excess with the configuration depending on the configuration of crystal. The solution photochemistry, however, results in a racemic mixture of products (Scheme 18).^{72,73}



Scheme 18. Crystalline State vs. Solution Photochemistry

F. Biradical Lifetime

Triplet biradicals must undergo intersystem crossing (ISC) to form singlet products. The rate of triplet biradical decay is thus determined by the rate of ISC, since the chemical reactions of the singlet biradicals presumably are so fast that ISC is effectively irreversible. Scaiano has postulated that singlet biradicals maintain conformational memory of their triplet precursor and undergo no conformational change because they react so rapidly.⁷⁴ The long lifetimes of triplet biradicals, coupled with generally fast bond rotations, assure that the biradicals usually attain conformational equilibrium before ISC. Different biradical conformations may or may not have the same

NC

an

NC

DA

in

to

in

nt

es

oc

to

es

no

in

to

to

es

to

to

ISC rate. Several interesting questions can thus be raised. What causes ISC? What conformational factors enhance the rate of ISC? When does ISC occur?

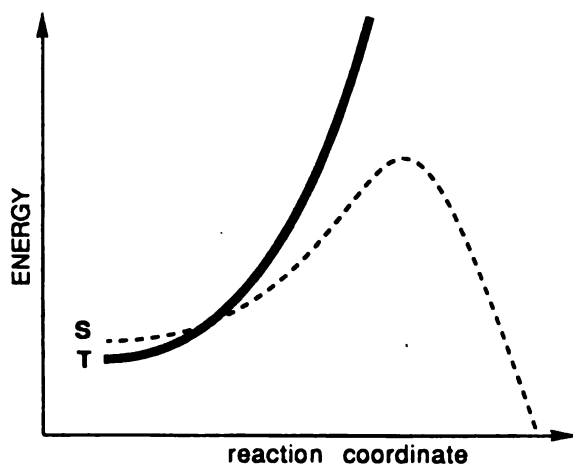
Salem and Rowland proposed that three factors are important in determining the ISC rates. These include: orthogonality of the axes of the two p orbitals, distance between two biradical centers and ionic (zwitterionic) character of the singlet state.⁷⁵ These factors influence spin-orbit coupling which is the predominant cause of ISC in short biradicals.

Recently Michl has performed calculations similar to those of Salem and Rowland to determine the factors that result in spin-orbit coupling (SOC).⁷⁶ His results show that in order for SOC between singlet and triplet to be large, (a) the most localized orthogonal orbitals A and B singly occupied in triplet must interact covalently through a non-zero resonance integral and/or be sufficiently different in energy for one to have electron occupancy near two in the singlet (b) the biradical contains one or more atoms (heavier than hydrogen) at which one p orbital contributes to A and another to B (through bond contributions) and (c) the contributions from these p orbitals must add rather than cancel.

Scaiano has studied solvent effects on biradical lifetimes. Lewis bases tend to increase the quantum yields of product formation in hydroxy biradicals.⁷⁷ It was interesting to see whether a lifetime increase would parallel an increase in quantum yield due to suppression of a major chemical path, namely disproportionation back to starting ketone. Scaiano, however, showed that lifetime and quantum yield increases are not correlated.⁷⁸ For example, the lifetimes of γ -methylvalerophenone in wet acetonitrile⁷⁹ (76 ns) and pyridine (121 ns) differ by almost a factor of two, while the quantum yield for product formation remains essentially unity. Similarly, 2% water in acetonitrile is

sufficient to achieve or closely approach the maximum quantum yield of unity, while lifetimes keep increasing until the concentration of water reaches ~20%.⁷⁹

Wagner has proposed that the concept of “conformational memory” in singlet biradicals is only relevant in 1,4-biradicals since they can form products from most conformations. He has suggested that for 1,5- and longer biradicals, ISC and the chemical reaction (cyclization) are coupled.⁸⁰ Both singlet and triplet surfaces rise in energy as movement along the reaction coordinate develops electronic and steric strain. The singlet surface, however, is soon stabilized by the developing bond while the triplet keeps rising in energy. This will lead to surface crossing at points that represent low activation energies (Graph 1). Since the biradical ends approach each other as the reaction proceeds, the ISC at this point benefits from large spin-orbit interactions as well as state degeneracy.



Graph 1. Triplet-Singlet Interconversion

Turro suggests that spin multiplicity cannot change during the elementary chemical step of bond formation or bond cleavage because the rate of spin motion is too

slow relative to the time scale for an elementary step.⁸¹ He indicates that hyperfine and exchange interactions are important factors leading to ISC in α -cleavage reactions and that when the two radical centers are close, strong exchange interactions inhibit spin inversions.

Closs argued that a triplet biradical goes through a large number of conformations in which triplet and singlet are nearly degenerate and its wave function is a rapidly oscillating mixture of singlet and triplet character, with triplet dominant at all times.⁸² He proposed that ISC will take place only when the biradical reaches a geometry in which two surfaces separate in energy, with a probability given by the average weight of singlet character in the wave function.

Michl's calculations suggest that SOC will be strong in those geometries in which there is a significant covalent interaction between the two radical centers.⁷⁶ This interaction stabilizes S_0 and destabilizes T_1 . He suggests that a small but a non-zero activation energy is needed for the triplet to reach the best geometries for ISC and that after ISC the molecule should find itself part way down a steep path in the S_0 surface leading to products. He thus concludes that ISC in triplet biradicals should be concerted with the formation of a new bond.⁷⁶

Wagner has also suggested that if ISC occurs discretely, the solvent and structural effects at early stages of reaction can be treated as entropic factors.⁸⁰ For example, lifetime increase in hydroxybiradicals in the presence of Lewis bases can be explained in terms of a biradical having a lower probability of finding an ISC path since a major path

for reaction and ISC has been eliminated. Thus, ISC is disfavored entropically and lifetime increases.

G. Diastereoselectivity

Unlike singlet reactions, pure steric arguments alone can not explain or predict product stereoselectivities in triplet reactions. Triplets must first intersystem cross to the singlet surface before they can form products. An interesting question can be raised. Do bond rotations occur after ISC and before product formation or does the singlet react so fast that it does not undergo any conformational change from its triplet precursor? Since rate constants for singlet biradical reactions have not been measured, one cannot answer this question with any degree of certainty. However, most investigators have ignored bond rotations in the singlet biradical and have assumed that product stereoselectivities are determined on the triplet surface. Even with such an approximation, prediction of product stereoselectivities from the triplet surface is not trivial since one must also consider ISC. It was mentioned earlier that different biradical conformations may have different ISC rates. Thus one must consider both the population of various conformers and their relative intersystem crossing rates to address product stereoselectivities. Griesbeck has recently attempted to attribute the observed diastereoselectivities in 2+2 photocycloaddition of benzaldehyde to cyclic olefins in terms of relative rates of ISC from various reactive conformations (Scheme 19).^{83,84} By excluding non-reactive conformers (although the author doesn't mention this point), he assumes ISC to be coupled to the reaction, in agreement with Wagner, Closs and Michl. Griesbeck has

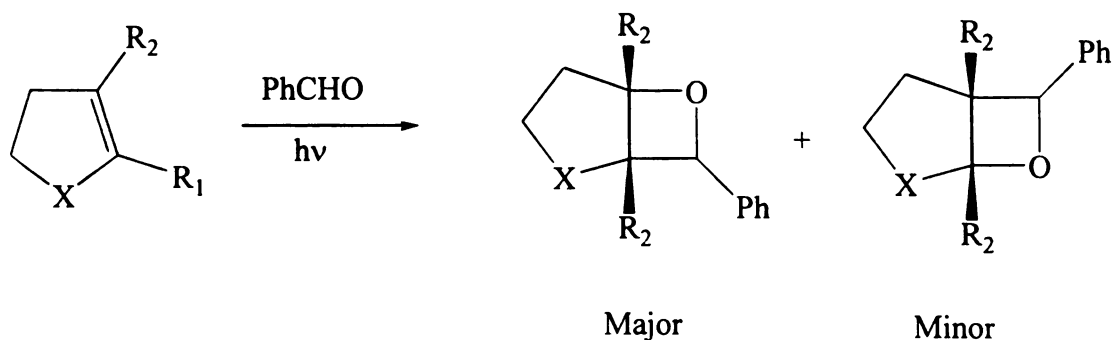
observed good endo selectivity between aromatic aldehydes and unsubstituted cycloalkenes while methyl groups at position 1 or 2 on the cycloalkene lower the amount of endo oxetane.

The biradical conformers A and B (Scheme 20) were considered in the reaction between benzaldehyde and cycloalkenes, with conformer A, which forms the endo product, being more populated due to fewer steric interactions.

Table 2. Diastereoselectivity in Photocycloaddition of Benzaldehyde to Cycloalkenes

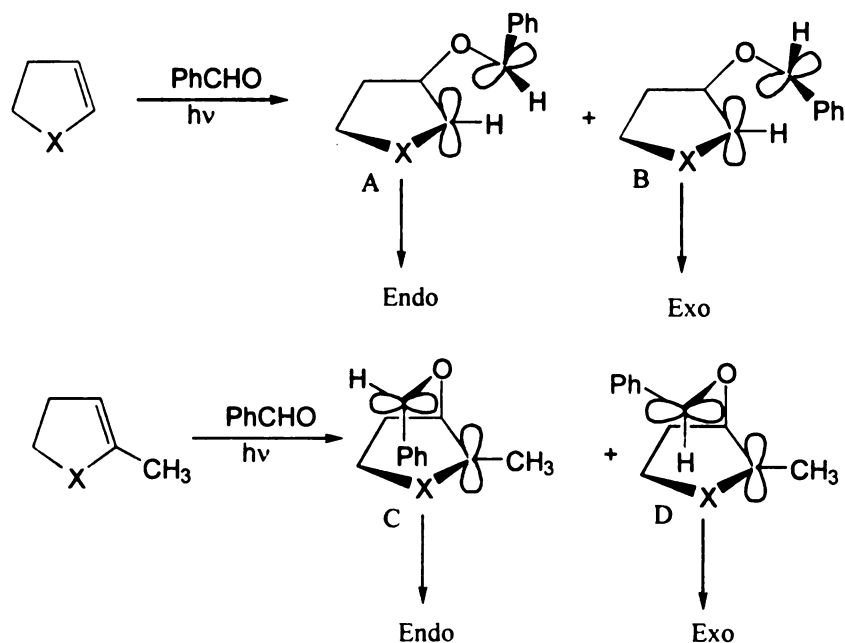
X	R ₁	R ₂	Endo/Exo ^a
CH ₂	H	H	61:39
CH ₂	CH ₃	H	16:94
O	H	H	88:12
O	CH ₃	H	65:35

a) For the major product only



Scheme 19. Photocycloaddition of Benzaldehyde to cycloalkenes

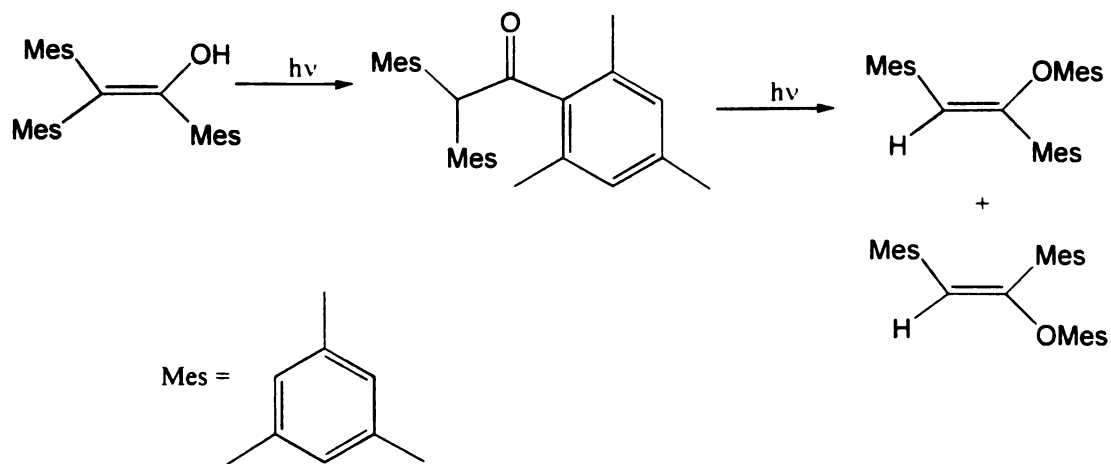
Methyl substitution at position 1, however, forces the oxygen bridge to twist toward the middle of the cycloalkene ring due to steric interactions between the methyl and phenyl or hydrogen of the aldehyde. Thus, conformer D, being more populated due to fewer steric interactions, leads to an increase in the amount of exo product. The author emphasizes that these conformers are not real minima on the triplet surface and that they merely represent geometries for rapid ISC, due to orthogonality of the p-orbitals at radical centers.



Scheme 20. ISC Control of Diastereoselectivity

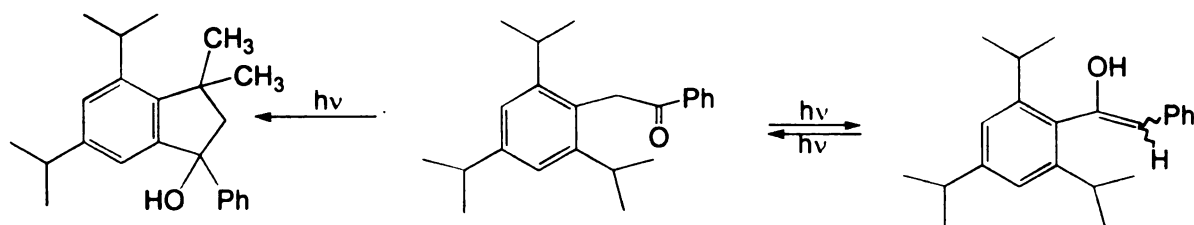
H. Photoenolization of α -(2,4,6-triisopropylphenyl)acetophenone

Hart has reported that irradiation of 1,2,2-trimesitylethenol gives 1,2,2-trimesitylethanone, as an intermediate, en route to formation of enol ethers (Scheme 21).^{85,86} Thus a precedence for phototautomerization of enol to ketone was established.



Scheme 21. Phototautomerization of Enol to Ketone

Wagner and Meador reported that irradiation of α -(2,4,6-triisopropylphenyl)acetophenone results in formation of its enol and an indanol in a 10:1 and 1:1 ratios in dioxane and benzene, respectively (Scheme 21).^{36a,b}



Scheme 22. Photobehavior of α -(2,4,6-triisopropylphenyl)acetophenone

An interesting question can be raised. Is the indanol formed by δ -hydrogen abstraction followed by cyclization from the ketone or as a result of a rearrangement from the enol? The authors suggested that the enol photoreverts to ketone and acts merely as an internal filter, lowering the quantum yield for cyclization.⁸⁷ We have performed experiments to test this hypothesis. The results of our investigation are given in this thesis.

IV. Goals of Research

1) Triplet biradicals must intersystem cross to the singlet surface in order to form products. When two biradical conformers lead to formation of different products, ISC must play a key role in determining the product ratios. Furthermore, certain biradical geometries have been postulated to cause more efficient ISC.^{75,76} The effect of temperature on product ratios from α -(*o*-alkylphenyl) and α -(2,4,6-trialkylphenyl)acetophenones, and propiophenones has been investigated. The results of these studies have been rationalized in terms of population and reaction rates, which encompass ISC rates of various biradical conformers.

2) The singlet state reactions have been postulated to occur via either a concerted path or very short-lived biradical intermediates that do not allow equilibration (bond rotation).^{11,60,61,62,63} We have studied the photobehavior of several α -(*o*-alkylphenyl) and α -(2,4,6-trialkylphenyl)acetones at various temperatures to gain a better understanding of the factors that control singlet state and/or singlet biradical reactivity. These results in conjunction with the results of acetophenones have been used to compare and contrast singlet vs. triplet reactivity.

3) As mentioned earlier, four ground state parameters: d , the distance between O and H; η , the O-H-C angle, ν , the C=O-H angle; and ω , the dihedral angle that the O-H vector makes with respect to the nodal plane of the carbonyl have been considered to be the most important in determining the rate and efficiency of hydrogen abstraction. To examine the influence of these factors, in particular the dihedral angle, we have investigated the photochemistry of *o*-(2'-(2',3'-dimethyl)butyl)benzophenone. The results

of this investigation along with semiempirical calculations have been used to explain the importance of dihedral angle on reactivity.

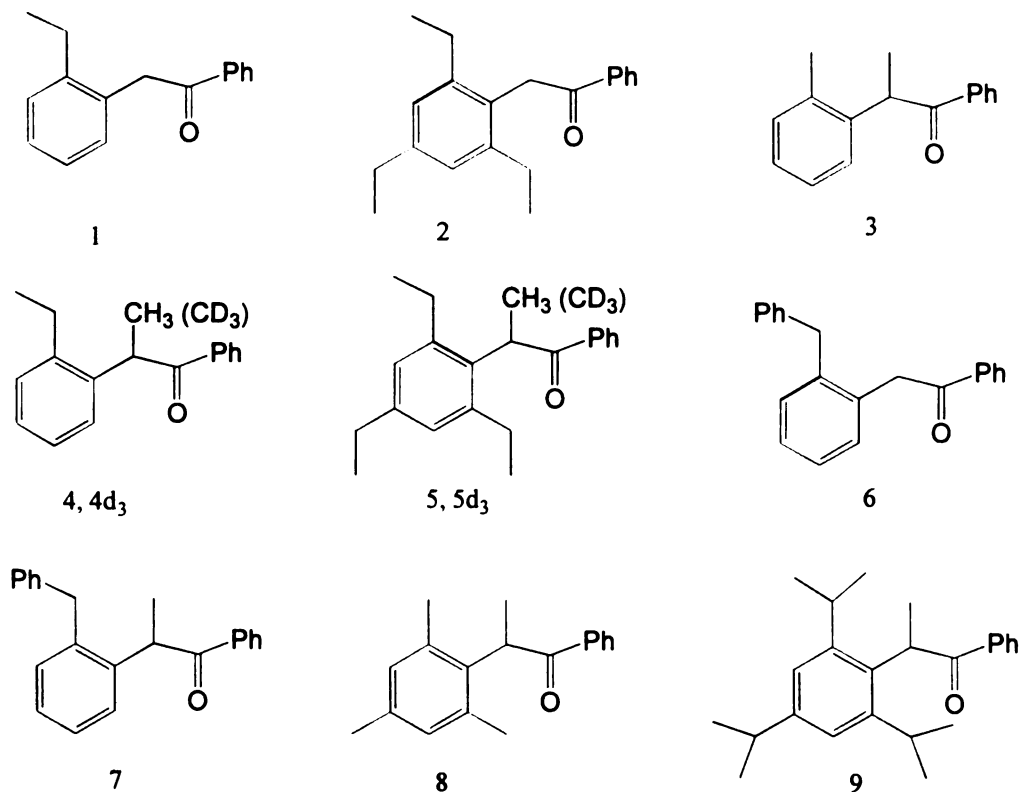
Results

I. α -Arylacetophenones and derivatives

A. General Preparation of the Ketones

α -(*o*-Alkylphenyl)acetophenones and α -(2,4,6-trialkylphenyl)acetophenones had been prepared by Park⁸⁸ and were used without any further purification.

α -(*o*-Alkylphenyl)propiophenones and α -(2,4,6-trialkylphenyl)propiophenones were similarly prepared from *o*-arylacetonitriles by α -methylation with LDA and methyl iodide followed by coupling with phenyl Grignard or phenyl lithium reagents. As a result, the following compounds were prepared and/or used in this study.

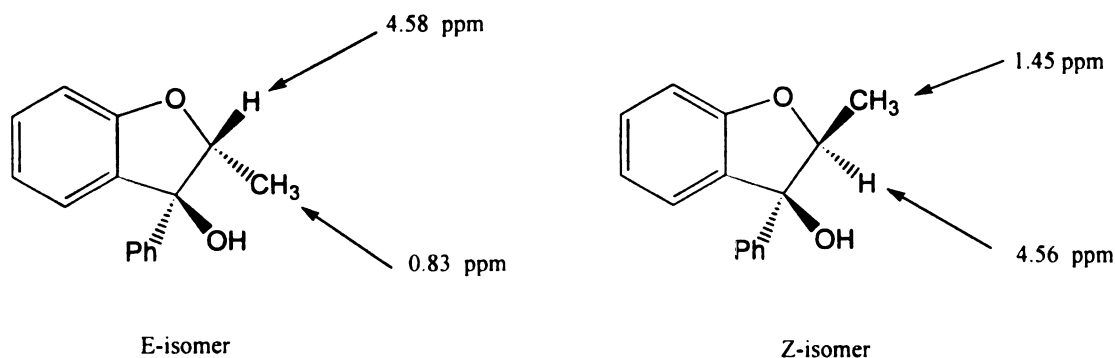


B. Irradiation of Ketones

NMR scale irradiations were carried out on 0.01 M solutions of ketones in deuterated solvents. In order to achieve n,π^* excitation, the ketones were irradiated through Pyrex (>290 nm) or Uranium glass (>334 nm) filters. For solid state irradiations, crystals were packed in capillary tubes and irradiated. The resulting solid (crystal) was then dissolved in CDCl_3 and analyzed by NMR. The irradiation sources included a medium pressure mercury arc lamp and a Rayonet reactor. The ketones were irradiated at -72° , 0° , room temperature (24°) and 110°C to determine the effect of temperature on product ratios. The desired temperatures were attained by dry ice-ethanol, ice-water, water (at RT) and heated silicon oil baths, respectively. Irradiation solvents included deuterated benzene, toluene and methanol. In most cases the starting ketones disappeared after 30-40 minutes of irradiation with the corresponding appearance of diastereomeric mixtures of 2-phenyl-2-indanols. In all cases material balances were > 95%. In the cases of compounds 3, 4 and 7, type I cleavage products were also formed. Irradiation of compound 4 at -72°C , however, did not result in type I cleavage. For compound 9, longer wavelength irradiation (366 nm) was necessary to determine the quantum efficiency, since the enol product absorbs strongly between 300 and 340 nm. Chemical yields were measured by irradiating 0.01 M solutions of ketones in benzene- d_6 or toluene- d_8 at room temperature (24°C), with methyl benzoate as an internal standard. The resulting mixtures were then analyzed by NMR or GC or both. Chemical yields at other temperatures were calculated based on product ratios and overall chemical yield at room temperature. The values at high temperature were checked by heating samples that had been irradiated at

room temperature to 110°C for three hours. Subsequent analysis gave the same product yields as before, indicating that dehydration was not effecting the product ratios.

The structural assignments of indanols were straightforward in most cases. Methyl doublets at 0.6-1.5 ppm were most informative because it is generally accepted that a methyl cis to the phenyl is significantly shielded relative to one trans, as previously observed in a number of such products.^{89,90} For example, in photoproducts from *o*-ethoxybenzophenone, the chemical shift of methyl group of E isomer was shifted much more upfield than that of Z isomer, as shown in Scheme 23.⁹¹

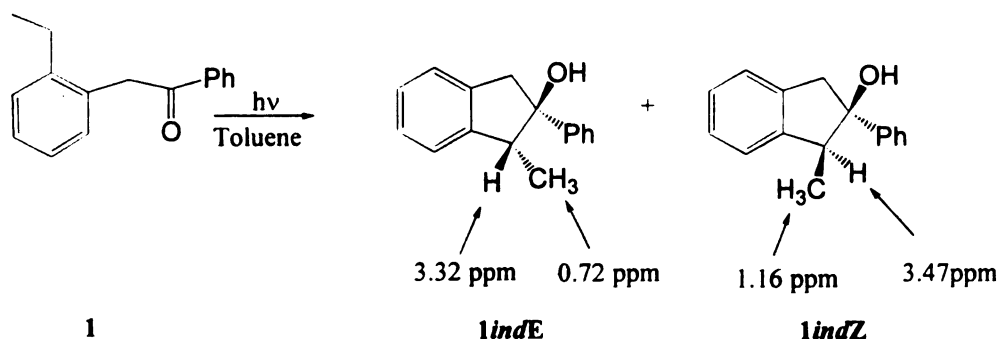


Scheme 23. Chemical Shifts of Methyls Trans and Cis to Phenyl in Five-Membered Rings

a. α -(*o*-Ethylphenyl)acetophenone (1**)**

Irradiation of **1** in benzene or methanol resulted in formation of isomeric 2-phenyl-2-indanols, previously identified by Park.^{87,88} Preparative scale irradiation of **1** in benzene followed by preparative scale TLC (PTLC) using 3% ethyl acetate in hexane as eluent resulted in separation of the two products which were identified as two isomeric 2-phenyl-2-indanols (**1indZ** and **1indE**) by their NMR spectra in CDCl₃ (Scheme 24). The signal of the trans methyl appears at 1.16 ppm, while that of the cis methyl appears at

0.72 ppm. It is also noteworthy that the methine hydrogen cis to the OH is more shielded than one cis to phenyl.



Scheme 24. Photochemistry of 1

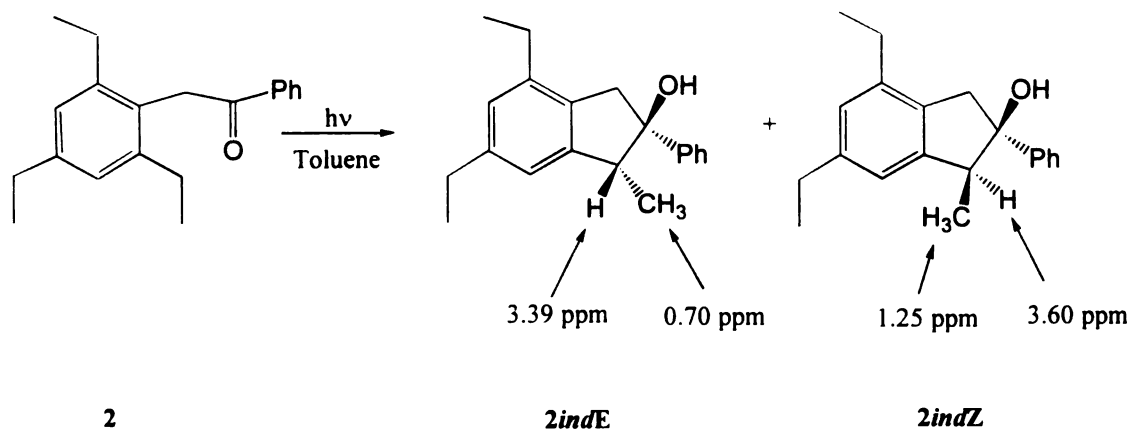
Quantitative analysis of product ratios at several temperatures was achieved by irradiating 0.01 M solutions of **1** in toluene- d_8 through a Pyrex filter followed by NMR analysis. GC analysis of the mixtures showed similar product ratios as NMR. Quantitative results of temperature studies for compounds **1-8** are listed in Table 23. Irradiation of crystalline **1** at 0°C resulted in formation of **1indZ** and **1indE** in a ratio >30:1. The chemical yields are listed in Table 3.

Table 3. Chemical Yields of Photoproducts of α -(2-Ethylphenyl)acetophenone in Toluene at Various Temperatures ($\lambda > 290$)

Temperature (°C)	1indZ	1indE
-72	92.5%	3.5%
0	91%	5%
24	90%	6%
110	88%	8%

. b. α -(2,4,6-Triethylphenyl)acetophenone (2)

Irradiation of a 0.01 M solution of **2** in benzene- d_6 resulted in formation of two isomeric 2-phenyl-2-indanols (**2indZ** and **2indE**, Scheme 25) previously identified by Park.^{87,88} Preparative scale irradiation of **2** in benzene followed by PTLC, using 5% ethyl acetate in hexane as eluent, resulted in isolation of the photoproducts, which were identified from their corresponding NMR spectra in $CDCl_3$. Each isomer showing a methyl doublet, a methine quartet and an AB quartet signal with coupling constants similar to previously identified indanols.^{87,88} The NMR signal of the trans methyl appears at 1.25 ppm while that of the cis methyl appears at 0.70 ppm.



Scheme 25. Photochemistry of 2

The product ratios were determined by integration of the methyl doublet signals of each isomer and by GC analysis. Photolysis of crystalline **2** resulted in **2indZ** as the only detectable photoproduct. Chemical yields are listed in Table 4.

Table 4. Chemical Yields of Photoproducts of α -(2,4,6-Triethylphenyl)acetophenone in Toluene at Various Temperatures ($\lambda > 290$)

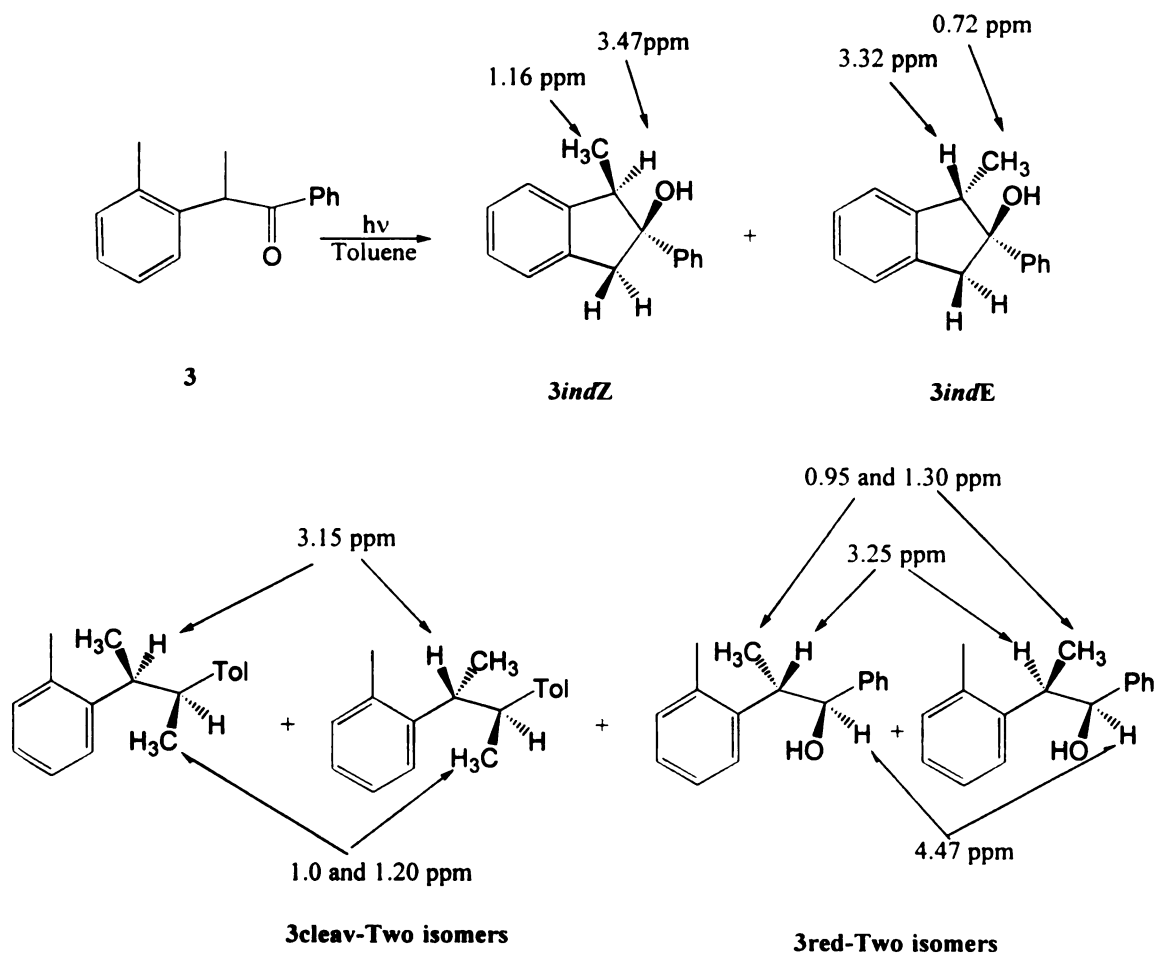
Temperature (°C)	<i>2indZ</i>	<i>2indE</i>
-72	97%	3%
0	96%	4%
24	95%	5%
110	94%	6%

*c. α -(*o*-Tolyl)propiophenone (3)*

Photochemistry of **3** was previously studied by Wagner and Zhou.⁵⁸ However, in our effort to study the effect of temperature on product ratios we reinvestigated its photochemistry. Preparative scale irradiation of **3** in methanol followed by PTLC resulted in isolation of eight products, identified by their NMR spectra in CDCl₃ as two isomeric 2-phenyl-2-indanols (*3indZ* and *3indE*), two isomeric 1-phenyl-2-tolyl-1-propanols (photoreduction products- *3red*), two isomeric diarylethanes (α -cleavage products- *3cleav*), β -tolylpropiophenone and benzaldehyde. Isolation of two indanol isomers was surprising since the previous investigators had reported the formation of only the Z-isomer.⁵⁸ The two indanols isolated had the same spectroscopic data as those isolated from **1**. The signal of the trans methyl appears at 1.16 ppm while that of the cis methyl appears at 0.72 ppm. Table 23 contains the product ratios of irradiation of **3** at various temperatures. Chemical yields are listed in Table 5.

Table 5. Chemical yields of Photoproducts of α -(*o*-Tolyl)propiophenone in Toluene at Various Temperatures ($\lambda > 290$)

Temperature ($^{\circ}\text{C}$)	<i>3indZ</i>	<i>3indE</i>	β -Phenylpropiophenone	α -Cleavage
-72	48%	1%	-	17%
0	36%	2%	8%	31%
24	30%	2%	8%	35%
110	20%	2%	12%	44%



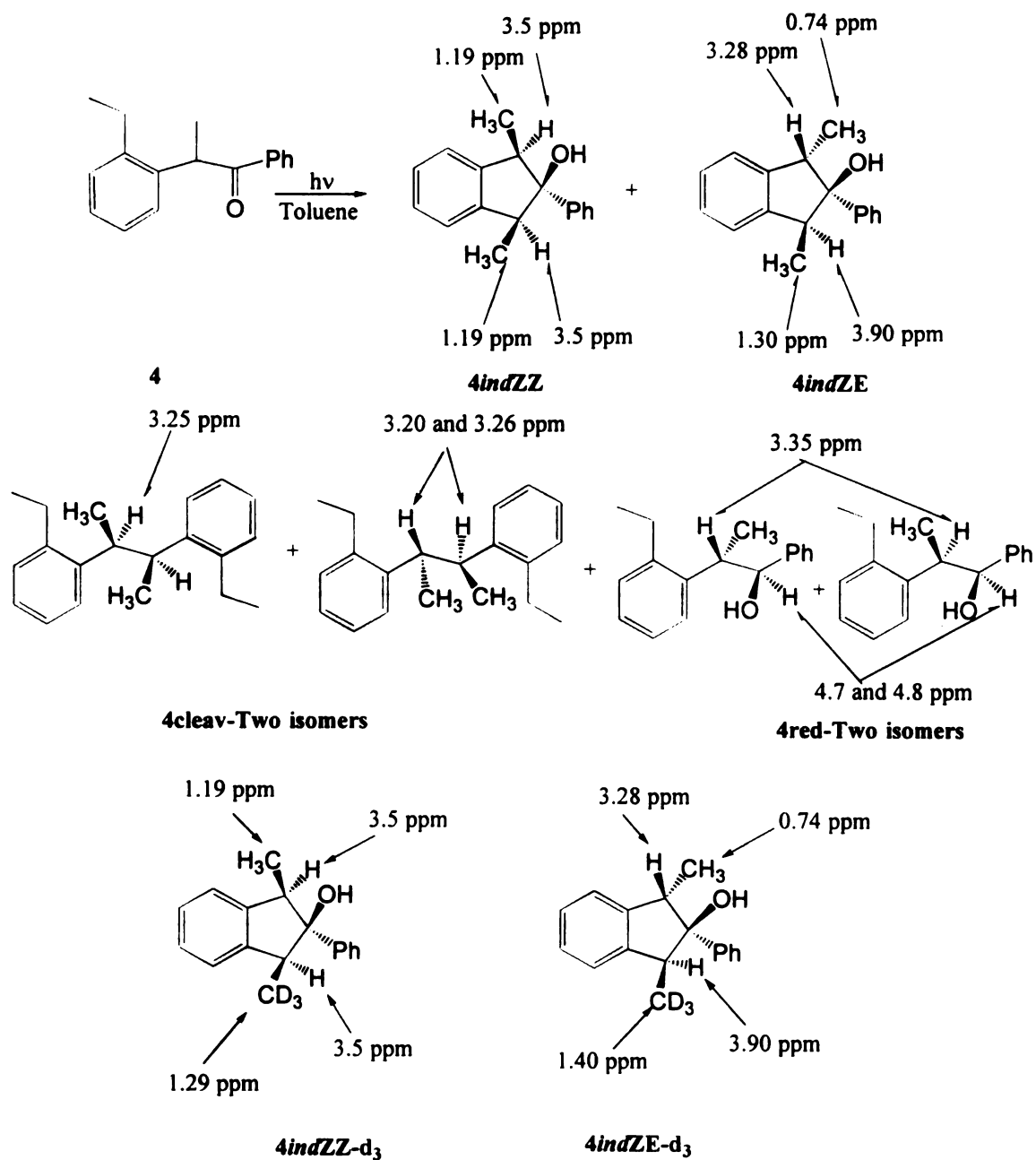
Scheme 26. Photochemistry of 3

d. α -(*o*-Ethylphenyl)propiophenone (4, 4d₃)

Irradiation of **4** at room temperature in benzene or methanol results in formation of a mixture of products, most of which were previously identified by Park.⁸⁸ Preparative scale irradiation of **4** in methanol followed by PTLC, using 3% ethyl acetate in hexane, resulted in isolation of these photoproducts. The products were identified (by their NMR spectra in CDCl₃) as two isomeric 2-phenyl-2-indanols (**4indZZ** and **4indZE**), two isomeric diethylphenylbutanes (α -cleavage products- **4cleav**), two isomeric 1-phenyl-2-(*o*-ethylphenyl)-1-propanols (photoreduction products- **4red**) and benzaldehyde. The symmetric ZZ-indanol had a doublet signal at 1.19 ppm corresponding to both methyls while the ZE isomer had two distinct methyl doublet signals, the methyl trans to phenyl appearing at 1.3 ppm, and the methyl cis to phenyl at 0.74 ppm. Furthermore, the spectrum of the ZZ isomer shows only one methine signal due to the symmetry of the structure while that of the ZE isomer shows two distinct methine signals. Product ratios were determined by NMR integration and GC analysis. The ratio of the two isomeric indanols (**4indZZ** and **4indZE**) from **4** were 5:1 and 1:1 in benzene and methanol respectively.

It was important to know which methyl group ends up cis to phenyl in the ZE isomer. Irradiation of the α -trideuteriomethyl **4** showed that only the ethyl methyl ends up cis to phenyl in the ZE isomer, since the ZE-indanol had a methyl doublet signal at 0.74 ppm but not one at 1.3 ppm (Scheme 26). The ²H NMR spectra of the ZZ and the ZE-indanols show broad singlets at 1.29 and 1.4 ppm, respectively. These chemical shifts

are 0.1 ppm higher than those from the fully protonated **4**. The difference could be due to using the DMSO- d_6 sample rather than $CDCl_3$ as the reference.



Scheme 27. Photochemistry of **4**

An interesting solvent effect was observed in the photolysis of compound **4**. Irradiation in toluene- d_8 results in a 1:9 ZZ/ZE ratio at -72°C (Table 23). However, irradiation at -72°C in methanol results in formation of **4indZE** as the exclusive photoproduct. Type I cleavage products were not observed in the low temperature irradiation mixtures. Irradiation of crystalline **4** was unsuccessful since the crystals melted during photolysis. Indanols were the only products observed in the oil obtained from crystal irradiations, in a 1:2 ZZ/ZE ratio. Low temperature irradiation of crystals at 0 and -72°C resulted in no reaction. Chemical yields are listed in Table 6.

Table 6. Chemical Yields of Photoproducts of α -(2-Ethylphenyl)propiophenone in Toluene at Various Temperatures ($\lambda > 290$ nm)

Temperature ($^\circ\text{C}$)	4indZZ	4indZE	α -Cleavage
-72	9%	91%	-
0	27%	18%	47%
24	41%	7%	46%
110	37%	4%	56%

e. α -(2,4,6-Triethylphenyl)propiophenone (5)

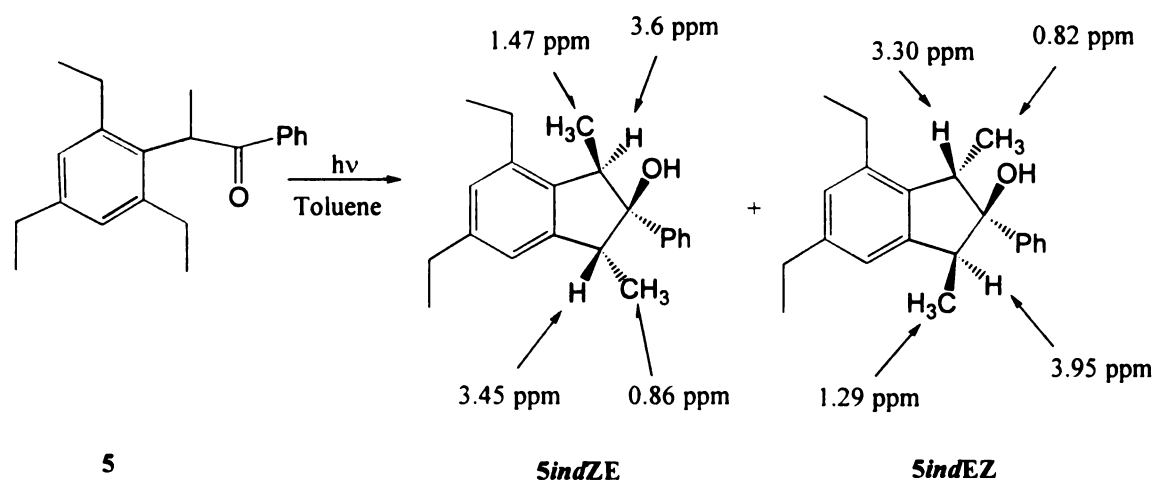
Irradiation of 0.01 M solutions of **5** in benzene- d_6 and methanol- d_4 at room temperature results in formation of two isomeric 2-phenyl-2-indanols (**5indZE** and **5indEZ**, Scheme 28) previously identified by Park.⁸⁸ Preparative scale irradiation of **5** in toluene followed by PTLC, using 7% ethyl acetate in hexane, results in isolation of

photoproducts which were identified by their corresponding NMR spectra in CDCl₃.

Chemical yields are listed in Table 7.

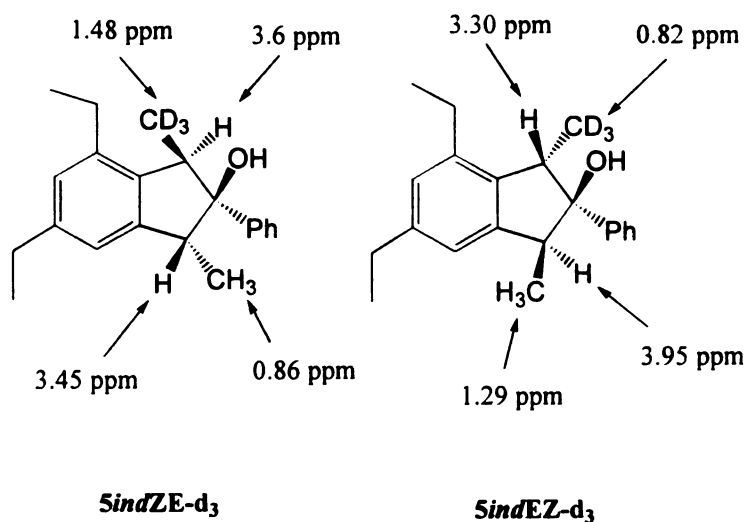
Table 7. Chemical Yields of Photoproducts of α -(2,4,6-Triethylphenyl) propiophenone in Toluene at Various Temperatures ($\lambda > 290$ nm)

Temperature (°C)	<i>SindZE</i>	<i>SindEZ</i>
-72	86%	14%
0	60%	40%
24	54%	46%
110	40%	60%



Scheme 28. Photobehavior of 5

The structural assignment for the isomeric indanols *SindZE* and *SindEZ* was a difficult task in the fully protonated species since both isomers had NMR signals corresponding to methyl doublets cis and trans to the phenyl ring. (Scheme 29)

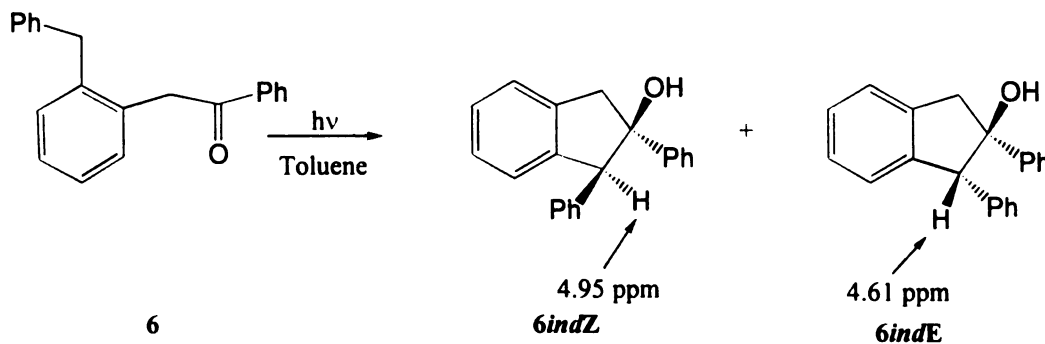


Scheme 29

In the ZE isomer, the trans methyl signal appears at 1.47 ppm while that of the cis methyl appears at 0.86 ppm. In the EZ isomer, the trans methyl signal appears at 1.29 ppm while that of the cis methyl appears at 0.82 ppm. Introduction of an α -CD₃ group in place of α -CH₃ made the assignments much easier, since the ZE isomer displayed only the methyl doublet signal cis to phenyl, while the EZ isomer had one trans to phenyl. The ²H NMR spectra of the ZE and the EZ-indanols show singlets at 1.48 and 0.82 ppm (CDCl₃ reference), respectively. Low temperature irradiation at -72°C in toluene and methanol resulted in 6:1 and 12:1 ZE/EZ ratios, respectively. Irradiation of crystalline **5** results in formation of *SindZE* as the only observable product (5% conversion). Irradiation of crystal for 22 hours resulted in an oil, the NMR of which indicated the presence of both indanols *SindZE* and *SindEZ* in a 17 to 1 ratio. Irradiation of **5** on silica resulted in a 10:1 ZE/EZ ratio of indanols. Table 23 contains the product ratios of irradiation of **5** at various temperatures.

*f. α -(*o*-Benzylphenyl)acetophenone(6)*

Irradiation of **6** in benzene resulted in formation of two isomeric 2-phenyl-2-indanols (**6indZ** and **6indE**, Scheme 30) previously identified by Park.⁸⁸ Preparative scale irradiation in toluene followed by PTLC, using 5% ethyl acetate in hexane, resulted in isolation of the photoproducts which were identified by their corresponding NMR spectra. Stereochemical assignment of the two isomers was made using nuclear Overhauser enhancement (nOe) experiments. Irradiation of the doubly benzylic methine signal at 4.61 ppm in the E-isomer in benzene- d_6 resulted in enhancement of the OH signal at 2.45 ppm (5%), while similar irradiation in the Z-isomer resulted in no such enhancement. The signal at 2.45 ppm disappeared upon addition of two drops of D_2O to the solution. The product ratios were determined by NMR and GC analysis. For the NMR analysis, the ratio of the AB quartet signals of the Z-isomer, which appears at 3.4 and 3.65 ppm, to that of the E-isomer, which appears at 3.3 and 3.85 ppm, was used. Table 8 contains the product ratios of irradiation of **6** at various temperatures. Irradiation of **6** in methanol resulted in a 1:1 ratio of indanols. Irradiation of crystalline **6** also results in a 1:1 Z/E indanol ratio. Chemical yields are listed in Table 8.



Scheme 30. Photobehavior of 6

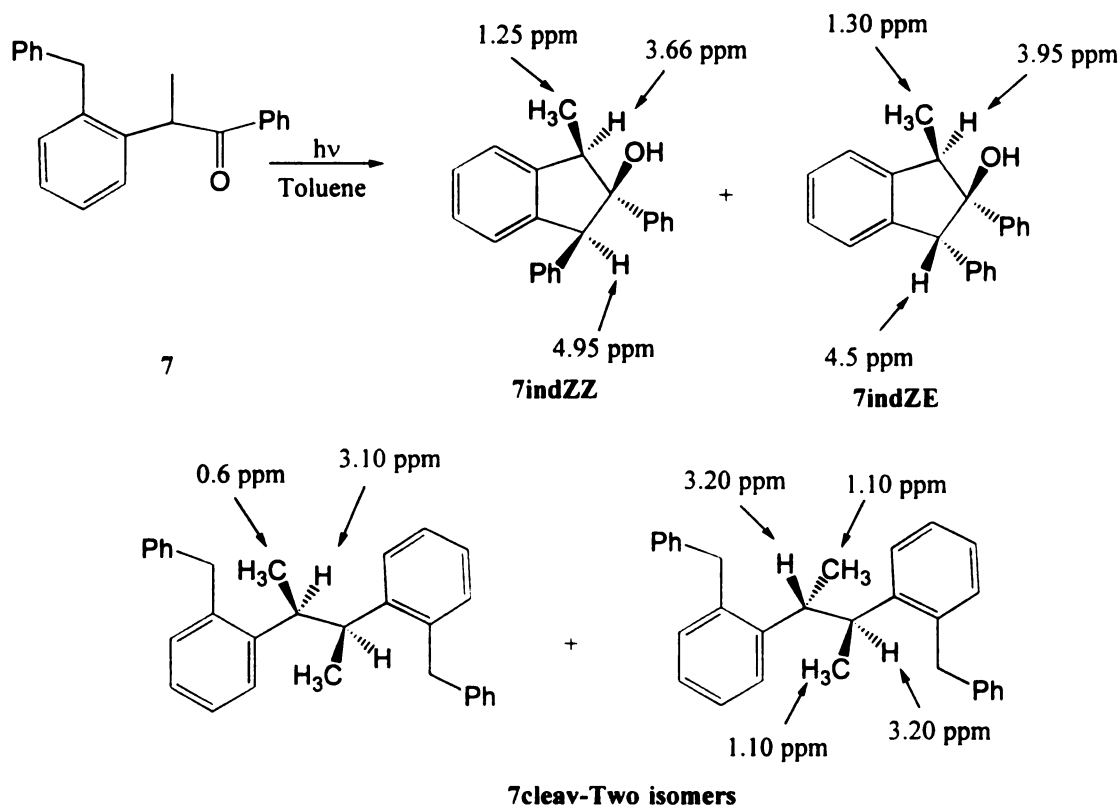
Table 8. Chemical Yields of Photoproducts of α -(2-Benzylphenyl)acetophenone in Toluene at Various Temperatures ($\lambda > 290$ nm)

Temperature ($^{\circ}\text{C}$)	<i>6indZ</i>	<i>6indE</i>
-72	41%	59%
0	50%	50%
24	55%	45%
110	60%	40%

g. α -(*o*-Benzylphenyl)propiofenone (7)

Irradiation of a 0.01 M solution of **7** at room temperature in benzene- d_6 resulted in formation of a mixture of products. Preparative scale irradiation in toluene followed by PTLC, using 3% ethyl acetate in hexane, resulted in isolation of photoproducts which were identified by their NMR spectra (in CDCl_3) as two isomeric 2-phenyl-2-indanols (*7indZZ* and *7indZE*), two isomeric di(benzylphenyl)butanes (α -cleavage products-*7cleav*) and benzaldehyde (Scheme 31). Although the chemical shift of the methyl doublet signals from both indanols indicated a trans configuration relative to the 2-phenyl, the stereochemical orientation of the 3-phenyl groups in the two isomers was ambiguous. NOe experiments were performed. Irradiation of the benzylic methine signal of one isomer at 4.50 ppm resulted in a small enhancement (0.47%) of the methyl doublet at 1.30 ppm. However, irradiation of the benzylic methine signal of the other isomer at 4.95 ppm did not result in signal enhancement of the methyl doublet at 1.25 ppm. Thus,

the former was assigned as the ZE while the latter was assigned as the ZZ isomer. Irradiation of **7** at -72°C resulted in formation of both type I and type II products. Two indanols were formed in a 1:1 ratio at all temperatures studied. The chemical yields were measured by NMR analysis and were 55% and 35% for indanols and α -cleavage products at room temperature, respectively.



Scheme 31. Photobehavior of **7**

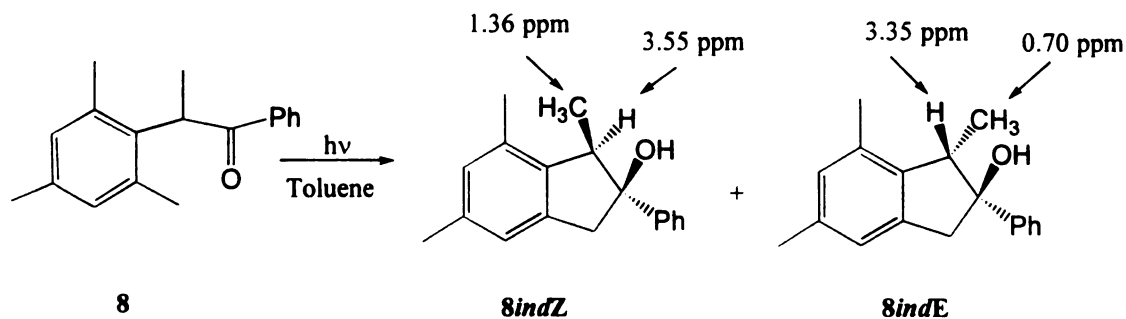
h. α -Mesitylpropiophenone (**8**)

The photochemistry of compound **8** was previously studied by Wagner and Zhou,⁵⁸ but temperature effects on the diastereoselectivity of the biradical closure were not studied. Irradiation of **8** in benzene results in formation of two isomeric 2-phenyl-2-

indanols (**8indZ** and **8indE**, Scheme 32). Preparative scale irradiation followed by PTLC, using 3% ethyl acetate in hexane, resulted in isolation of photoproducts which were identified by their NMR spectra in CDCl_3 . Analysis of product ratios by NMR was simple since the methyl doublet signal from the Z-isomer appeared at 1.36 ppm while that for the E-isomer appeared at 0.7 ppm. The product ratios were determined by both NMR and GC analysis. Table 23 contains the product ratios at various temperatures. Chemical yields are listed in Table 9.

Table 9. Chemical Yields of Photoproducts of α -Mesitylpropiophenone in Toluene at Various Temperatures ($\lambda > 290 \text{ nm}$)

Temperature ($^{\circ}\text{C}$)	8indZ	8indE
-72	96%	4%
0	94%	6%
24	91%	9%
110	82%	18%



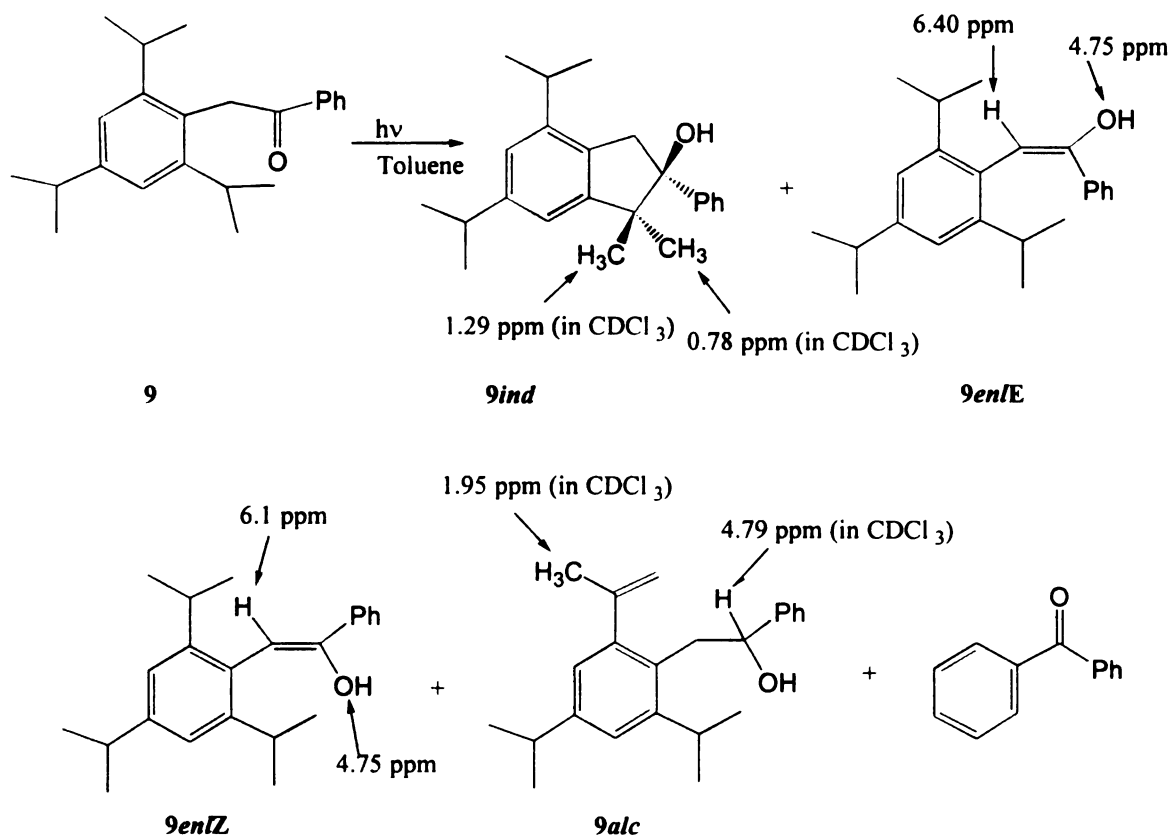
Scheme 32. Photochemistry of 8

i. α -(2,4,6-Triisopropylphenyl)acetophenone (9)

The photochemistry of **9** (Scheme 33) was previously studied by Wagner, Meador and Zhou.⁸⁷ Here, a systematic study of product ratios as a function of temperature and conversion is presented. Irradiation of **9** at -72 °C in both methanol and toluene forms only enols (**9enlZ** and **9enlE**), together with 5-10% benzaldehyde. Only Z-enol was observed in toluene at low temperature, while a 4:1 Z/E enol ratio was observed in methanol. The Z-enol was identified by the following NMR signals in toluene: a vinylic CH signal at 6.1 ppm, an OH signal at 4.8 ppm and methyl doublet signals at 1.2-1.30 ppm. The E-enol has a vinylic CH signal at 6.4 ppm, an OH signal at 4.75 ppm and methyl doublet signals at 1.1-1.2 ppm (in toluene-d₈). The vinylic CH signal of the Z-isomer is further upfield than that of the E-isomer presumably due to partial shielding by the phenyl group. The enols are stable for days at room temperature in the dark, but tautomerize completely to ketone within 5 hours at 90 °C. Upon irradiation at 313 nm at room temperature they revert to **9**, whereas the Z-trimethylsilyl enol ether of **9**, synthesized by treating **9** with KH and trimethylsilylchloride, affords only the E-isomer. The Z:E enol ratio in toluene decreases as irradiation time increases, ranging from 10:1 to 2:1. A study of product yields as a function of conversion, temperature, and excitation wavelength (Table 12) indicated that indanol (**9ind**) builds up very slowly following several interconversions between ketone and enol at 313 nm excitation but is obtained in a constant quantum yield at 366 nm (Table 11), where the enol does not absorb (Table 10). Irradiation of **9** at 366 nm thus results in a constant 8:1 enol/indanol ratio. Irradiation of crystals of **8** produces only Z-enol up to 20% conversion.

Table 10. Molar Absorptivity Coefficients ($M^{-1}cm^{-1}$) of **9 and its Enol at Various Wavelengths**

Compound	ϵ_{313}	ϵ_{336}	ϵ_{366}
9	79	70	6.2
Enol of 9	1230	22	0
Z-Trimethylsilylenol ether of 9	1912	98	0



Scheme 33. Photobehavior of **9**

Table 11. Product Quantum Yields of 9 as a Function of Conversion and Wavelength

λ (nm)	%Conversion	[Enol]	$\Phi_{\text{enol}}^{\text{a}}$	[Indanol]	$\Phi_{\text{indanol}}^{\text{a,b}}$
313	6	0.0065	0.35	-	-
313	15	0.013	0.234	0.003	0.062
313	19	0.014	0.15	0.006	0.059
313	24	0.014	0.09	0.009	0.052
366	10	0.13	0.64	-	-
366	18	0.18	0.64	0.024	0.085
366	25	0.24	0.64	0.034	0.085

a) Quantum yields were measured by NMR (b) Quantum yields were measured by GC

[Ketone]= 0.0143 M (GC studies), [Ketone]= 0.0983 M (NMR studies)

[Valerophenone]= 0.024 M (GC studies), [Valerophenone]= 0.1165 M (NMR studies)

[C20 standard]= 0.0033 M (GC studies), [Methyl benzoate-standard]= 0.03 M (NMR studies)

Table 12. Product Ratios of Irradiation of 9 Under Various Conditions

T (°C)	λ (nm)	Solvent	% Conv.	9ind	9en/Z	9en/E	Cleavage
-72	>290	Toluene	>95	0	90	0	10
-72	>290	Methanol	>95	0	72	18	10
24	>290	Benzene	40	20	73	7	0
24	>290	Benzene	50	28	62	7	3
24	>290	Benzene	64	30	53	7	10
24	>290	Benzene	70	50	16	8	26
24	>334	Benzene	17	29	71	-	-
24	>334	Benzene	23	24	63	13	-
24	>334	Benzene	46	26	59	15	-
24	>334	Benzene	66	20	53	24	23
24	>334	Benzene	>95	55	0	0	45
90	>290	Toluene	24	17	66	17	0
90	>290	Toluene	38	35	52	13	0
90	>290	Toluene	70	69	25	6	0
90	>290	Toluene	>95	100	0	0	0

C. Steady-State Photokinetics.

The quantum yields were measured by irradiation of degassed solutions of ketones (0.025-0.04 M) in tubes containing a fixed amount of internal standard parallel to valerophenone actinometer. For quenching studies, these tubes also contained varying amounts of 2,5-dimethyl-2,4-hexadiene quencher. Product yields at 5-18% were measured using GC or NMR and were converted to quantum yields. Stern-Volmer plots were linear with slopes equal to $k_q\tau$. The kinetic data are listed in Table 13 and Table 14. Triplet lifetimes, based on a k_q value of $6 \times 10^9 \text{ M}^{-1}\text{s}^{-1}$, are also listed.³⁰ The errors represent deviation of 2-4 measured values from the average.

Table 13. Lifetimes of Triplet Aceto- and Propiophenones in Benzene

Ketones	$k_q\tau, \text{M}^{-1}$	$1/\tau, 10^9 \text{s}^{-1}$
1	8.04 ± 0.4	0.75
2	6.95 ± 0.3	0.86
4	17.40 ± 0.8	0.34
5	7.98 ± 0.4	0.75
6	3.99 ± 0.2	1.5

Table 14. Quantum Yields of Photoproducts from Aceto- and Propiophenones in Benzene

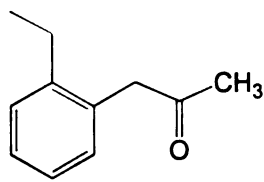
Ketones	Φ_{Cyc}	Φ_{Cleavage}
1	0.48 ± 0.02	-
2	0.48 ± 0.02	-
4	0.064 ± 0.004	0.43 ± 0.02
5	0.27 ± 0.015	-
6	0.40 ± 0.011	-
7	0.10 ± 0.005	0.06 ± 0.005
9	$0.055, 0.085^{\text{a}} \pm 0.003$	-

a) Quantum Yield measured at 366 nm.

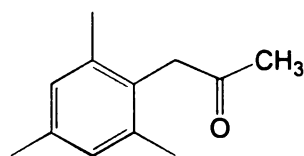
II. α -Arylacetones

A. General Preparation of the Ketones.

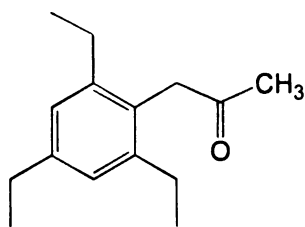
α -Arylacetones were prepared by chloromethylation of the appropriate arylbenzene, cyanation with sodium cyanide, hydrolysis with concentrated hydrochloric acid, and coupling with methyl lithium. As a result, the following compounds were prepared and/or used in this study.



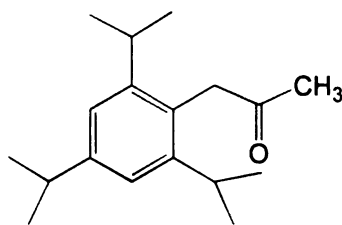
10



11



12



13

B. Irradiation of Ketones

NMR scale irradiations were carried out using 0.01 M solutions of ketones in deuterated benzene and toluene. The solutions were irradiated through a Pyrex filter (>290 nm). The ketones were irradiated at -72° , 24° and 110°C to determine the effect of temperature on product ratios. In most cases, the starting ketones disappeared after 24 hours of irradiation with corresponding appearance of mixtures of 2-methyl-2-indanols

and α -cleavage products. In the case of compounds 10 and 12, two isomeric indanols were detected after irradiation. The isomeric ratios of these indanols were determined by GC and/or NMR. Chemical yields were measured by irradiating 0.01 M solutions of ketones in benzene- d_6 at room temperature (24°C) using methyl benzoate as an internal standard. The resulting mixtures were then analyzed by NMR or GC or both. Chemical yields at other temperatures were calculated based on product ratios and overall chemical yield at room temperature. The values at high temperature were checked by heating the solution, which had been irradiated at room temperature, to 110°C for three hours followed by analysis to ensure that dehydration of indanols was not affecting the product ratios. In most cases material balances were > 95%. Stern-Volmer quenching experiments using 2,5-dimethyl-2,4-hexadiene as quencher, show a quenchable α -cleavage reaction while no quenching of indanol formation was observed. Our experiments thus indicate that δ -hydrogen abstraction occurs from the singlet while α -cleavage occurs from the triplet in α -alkylphenylacetones, in agreement with Turro's⁶⁷ results.

C. Identification of Photoproducts

a. α -(2-Ethylphenyl)acetone (10)

The behavior of 10 is temperature and environment dependent. Irradiation of 10 in benzene resulted in formation of a mixture of compounds. Preparative scale irradiation followed by PTLC, using 3% ethyl acetate in hexane, resulted in separation of photoproducts which were identified as two isomeric 2-methyl-2-indanols (**10indZ** and **10indE**, Scheme 34) and 1,2-di-(*o*-ethylphenyl) ethane (α -cleavage product- **10cleav**).

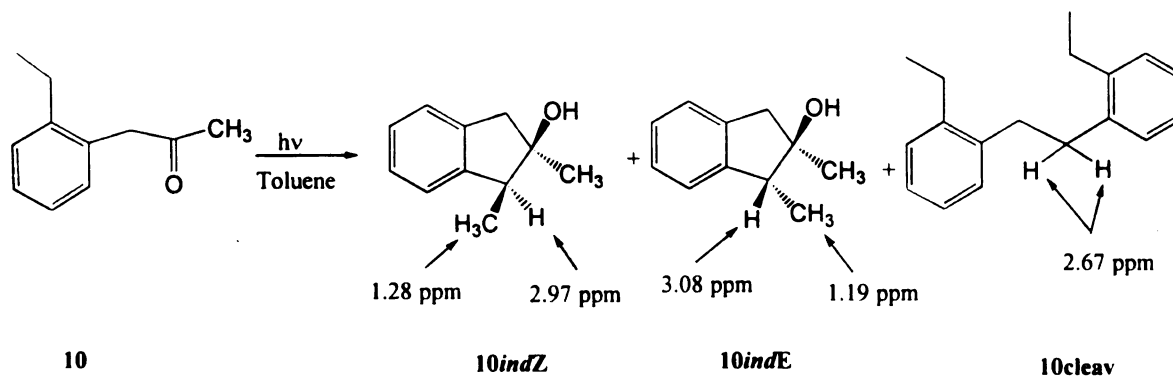
Analysis of product ratios in benzene by NMR was not easy due to overlapping peaks, thus irradiations were performed in toluene which gave much better peak separations. The structural assignment for the isomeric indanols **10indZ** and **10indE** proved to be a difficult task since all methyl signals appeared in close proximity to each other in the NMR spectrum. The NMR spectra of the cis and trans 1-methyl-2-indanols were previously reported in literature⁹², however, the presence of the methyl group at the 2-position should change the chemical shifts, so comparisons are not reliable. The structural assignments of the indanols were based on the use of shift reagents and nOe experiments. Addition of Rondeau's reagent, tris(6,6,7,7,8,8,8-heptafluoro-2,2-dimethyl-3,5-octanedionato) praseodymium, to 0.01 M solutions of each indanol in CDCl₃ caused an upfield shift of all proton signals. The methine signal at 3.08 ppm of the minor isomer moved upfield (to 2.97 ppm) twice as much as its methyl signal at (1.19 ppm to 1.16 ppm), while the upfield shift of both methyl (1.28 to 1.0 ppm) and methine (2.97 to 2.68 ppm) signals of the major isomer were comparable. Addition of europium shift reagent caused a similar downfield shift of the signals but caused peak broadening which made assignments difficult. Furthermore, irradiation of the methine signal in the minor isomer caused an nOe enhancement of the OH signal. These data strongly suggest that the minor isomer has E-stereochemistry. The product ratios and indanol diastereoselectivities were measured by NMR analysis. The Z:E indanol ratio was determined by the ratio of the methyl doublet signal of the Z-isomer at 1.12 ppm to that of the E-isomer at 1.0 ppm in toluene-d₈. Irradiation of **10** resulted in 20:80, 50:50 and 60:40 indanol/diarylethane ratios at -72°C, 24°C and 90°C, respectively. Furthermore, the ratio of the two isomeric

indanols (**10indZ**: **10indE**) were 3.2:1, 2.5:1 and 1.4:1 at 0°C, 24 °C and 90 °C , respectively. Irradiation of **10** inside sodium dodecylsulfate micelles (0.4 g in 100 ml of water, 14 mM, critical micellar concentration (CMC) = 10 mM)⁹³ at 24°C resulted in a 75:25 indanol/ α -cleavage ratio, while the **10indE**: **10indZ** ratio remained 2.5:1. Chemical yields are listed in Table 15.

Table 15. Chemical Yields of Photoproducts from α -(2-Ethylphenyl)acetone in Toluene at Various Temperatures ($\lambda > 290$ nm)

Temperature (°C)	10indZ	10indE	10cleav
-72	20% ^a	- ^a	80%
0	34%	11%	47%
24	33%	13%	48%
110	28%	28%	39%

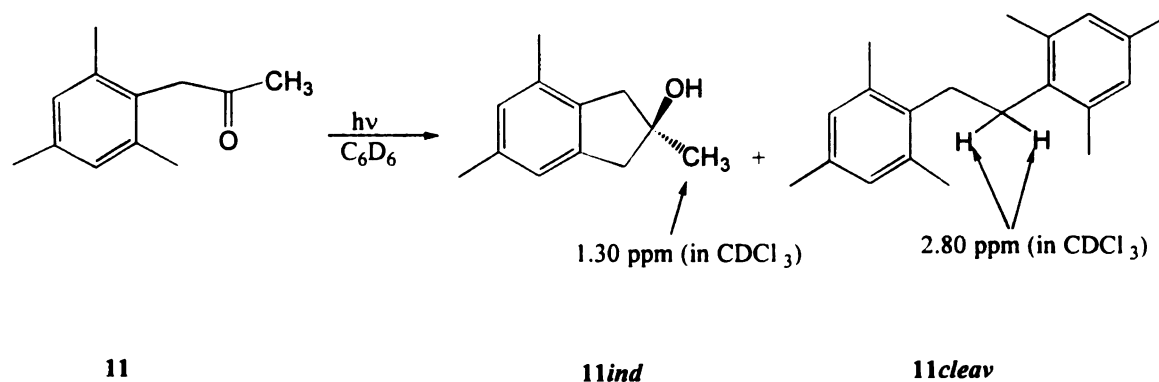
a. Only the Z-indanol was observed in the product mixture irradiated at -72°C, the E-isomer might have been present in trace amounts but could not be detected by NMR.



Scheme 34. Photoproducts of 10

b. α -Mesitylacetone (11)

Irradiation of compound **11** (Scheme 35) in toluene- d_8 resulted in formation of two products which were identified as an indanol (**11ind**) and a diarylethane (**11cleav**) by their NMR spectra. Preparative scale irradiation in toluene followed by PTLC, using 3% ethylacetate in hexane, resulted in separation of photoproducts. The product ratios were determined by comparing the NMR integration of the AB quartet signal of the indanol at 3.0 ppm to that of the methylene signal of the diarylethane at 2.8 ppm. Irradiation of **11** at -72°C , 24°C and 110°C resulted in a 0:100, 60:40, and 70:30 indanol/diarylethane ratio, respectively. No reaction takes place upon irradiation of crystals. Chemical yields are listed in Table 16.



Scheme 35. Photochemistry of 11

Table 16. Chemical Yields of Photoproducts from α -Mesitylacetone in Toluene at Various Temperatures ($\lambda > 290$ nm)

Temperature ($^{\circ}\text{C}$)	11ind	11cleav
-72	0	98%
24	56%	42%
110	69%	29%

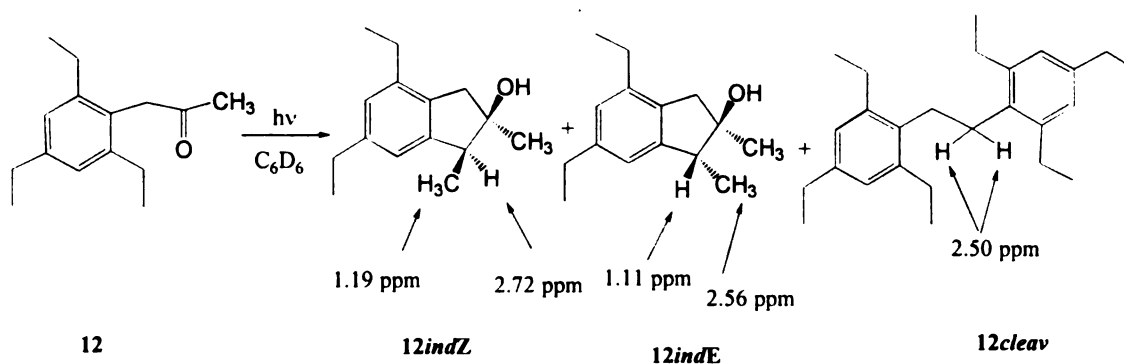
c. α -(2,4,6-Triethylphenyl)acetone (12)

Irradiation of compound **12** in benzene- d_6 or toluene- d_8 resulted in formation of a mixture of two isomeric indanols (**12indZ** and **12indE**) and α -cleavage products, **12cleav** and acetaldehyde (Scheme 36). Preparative scale irradiation in benzene followed by PTLC, using 5% ethyl acetate in hexane, resulted in separation of the indanols as a mixture from the diarylethane. The indanol/diarylethane ratios were measured by NMR analysis to be 20:80, 70:30, and 85:15 at -72°C , 24°C , and 110°C , respectively. They were determined from the ratio of the methyl signal of the *Z*-indanol at 1.26 ppm to that of the methylene of the diarylethane at 2.5 ppm. The ratio of the two isomeric indanols, measured by NMR and GC, was 10:1 in favor of the *Z*-isomer for irradiations at 24°C in benzene. The indanol ratios were determined by NMR integration of the methyl doublet signal of the *Z*-indanol at 1.19 ppm to that of the *E*-indanol at 1.11 ppm in C_6D_6 . The peaks for the two isomeric indanols overlap and separation is difficult. The *Z*-stereochemistry for the major indanol was based on the comparison of the peaks to that of the *Z*-indanol of *o*-(ethylphenyl)acetone. Chemical yields are listed in Table 17.

Table 17. Product Chemical Yields of α -(2,4,6-Triethylphenyl)acetone in Toluene at Various Temperatures ($\lambda > 290$ nm)

Temperature ($^{\circ}\text{C}$)	12indZ	12indE	12cleav
-72	17%	$\sim 2\%^a$	71%
24	58%	6%	27%
110	71%	$\sim 6\%^a$	12%

a) The yield of the **12indE** was estimated based on the **12indZ** yield and a constant 10:1 indanol ratio, since ratios at other temperatures were hard to determine due to overlapping peaks.

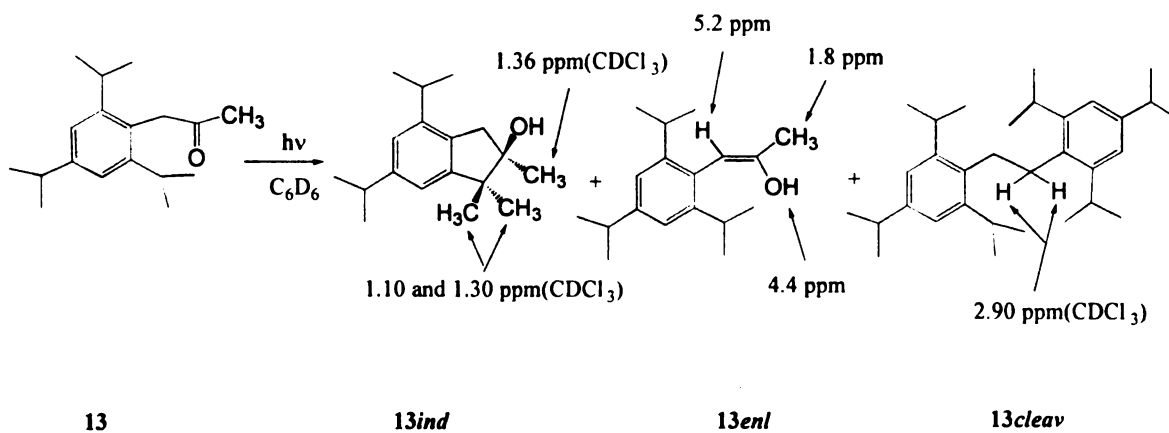


Scheme 36. Photobehavior of 12

d. α -(2,4,6-Triisopropylphenyl)acetone (13)

The photobehavior of **13** (Scheme 37) at room temperature is conversion dependent. At low conversions the *Z*-enol (**13enI**) is the major photoproduct. It was identified by the following NMR signals in benzene: an allylic methyl at 1.8 ppm, a vinylic CH at 5.4 ppm and a OH at 4.4 ppm. The *Z*-stereochemistry was assigned based on its stability relative to the *E*-isomer and by comparison of its NMR data to the

literature values (*Z*-enol of phenylacetone is reported to have a vinylic CH signal at 5.0 ppm in benzene).⁹⁴ At high conversions an indanol (**13ind**) and a diarylethane (**13cleav**) are the only observable photoproducts. The indanol is identified by the following NMR signals in benzene-*d*₆: three methyl singlet signals at 1.10 at 1.30 and 1.36 ppm, an OH signal at 1.8 and an AB quartet signal at 2.95 at 2.99 ppm (in CDCl₃). Formation of the enol is interesting since it mimics the behavior of the acetophenone analog. The enol of **13**, however, is not as stable as acetophenone enols and tautomerizes back to ketone in a few hours in the dark at 24°C, and in a few minutes at 110°C. The behavior of **13**, like its analogs, is also temperature dependent. At -72°C, only cleavage products are formed while at 110°C indanol is the only photoproduct. At room temperature *Z*-enol, indanol and cleavage products are formed but no reaction takes place upon irradiation of crystals. Table 18 lists product chemical yields as a function of conversion and temperature. The product ratios are determined by NMR integration of the vinylic CH signal of the enol, the methyl singlet signal of the indanol and the methylene singlet signal of the diarylethane.



Scheme 37. Photochemistry of 13

Table 18. Product Chemical Yields of α -(2,4,6-Triisopropylphenyl)acetone as a Function of Conversion and Temperature

Temperature(°C)	Solvent	%Conversion	13en/Z	13ind	13cleav
-72	Toluene	>95	0	0	100
24	Benzene	36	46	40	14
24	Benzene	55	33	45	22
24	Benzene	74	23	47	30
24	Benzene	80	17	48	35
110	Toluene	>95	0	100	0

D. Steady-State Photokinetics.

The quantum yields were measured by irradiation of degassed solutions of ketones (0.02-0.03 M) in tubes containing a fixed amount of internal standard parallel to a valerophenone actinometer. For quenching studies, these tubes also contained varying amounts of 2,5-dimethyl-2,4-hexadiene quencher. Product yields at 5-18% were measured using GC or NMR and were converted to quantum yields. Stern-Volmer plots were linear with slopes equal to $k_q\tau$. The kinetic data are listed in Table 19 and Table 20. Triplet lifetimes, based on a k_q value of $6 \times 10^9 \text{ M}^{-1} \text{ s}^{-1}$, are also listed.³⁰ The errors represent deviation of 2-4 measured values from the average.

Table 19. Triplet Lifetimes of α -Arylacetonnes in Benzene at Room Temperature ($\lambda = 313$ nm)

Ketones	$k_q\tau, M^{-1}$	$1/\tau \times 10^9 s^{-1}$
10	6.7 ± 0.3	0.89
11	31.4 ± 1.5	0.31
13	107.1 ± 5	0.009

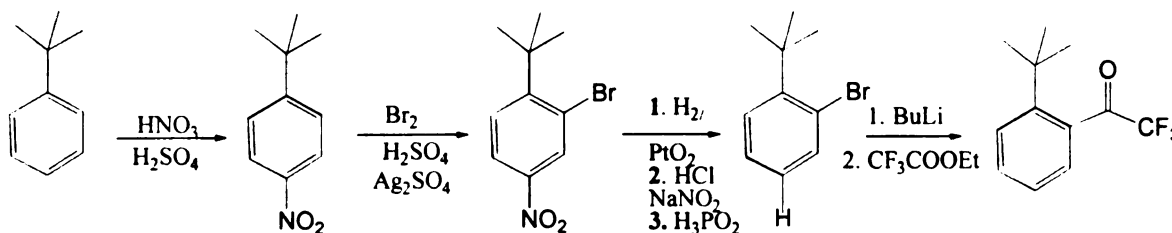
Table 20. Quantum Yields of Photoproducts of α -Arylacetonnes in Benzene at Room Temperature ($\lambda = 313$ nm)

Ketones	Φ_{Cyc}	$\Phi_{Diarylethane}$
10	0.0128 ± 0.0005	0.0156 ± 0.0005
11	0.085 ± 0.003	0.054 ± 0.002
12	0.036 ± 0.003	0.018 ± 0.002
13	$0.012 (\Phi_{Enol} = 0.028)$	0.005 ± 0.0002

III. 2-*tert*-Butyl trifluoroacetophenone

A. Preparation

2-*tert*-Butyl trifluoroacetophenone (**14**) was prepared by nitration of the *tert*-butylbenzene followed by bromination, reduction of nitro group, formation and reduction of diazonium salt, formation of Grignard and reaction with ethyl trifluoroacetate.



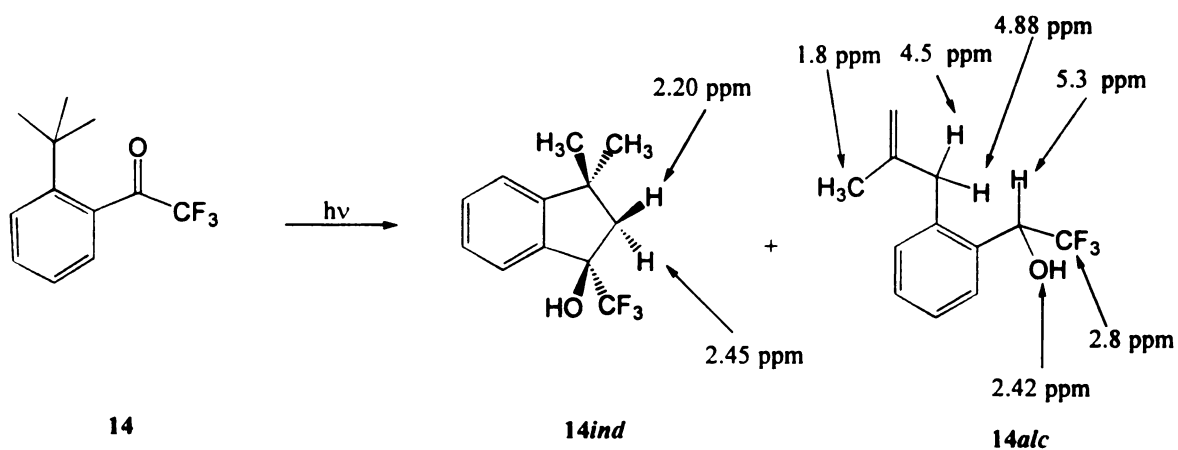
B. Irradiation Conditions

NMR scale irradiations were carried out using 0.01 M solutions of **14** in deuterated benzene, methanol or toluene. The solutions were irradiated through a Pyrex filter. The starting ketone disappeared after 2 hours of irradiation with corresponding appearance of mixtures of 3,3-dimethyl-1-trifluoromethyl-1-indanol (**14ind**) and 1-{2'-(3-(2''-methyl)propargyl)-phenyl}trifluoromethylethanol (**14alc**). Material balance was > 95%.

C. Identification of Photoproducts

Large scale irradiation was performed in benzene. The products were isolated by PTLC using 30% ethyl acetate in hexane solution as eluent. The products are an

unsaturated alcohol and an indanol and are formed in a 10:1 ratio (Scheme 38). The unsaturated alcohol was the predominant photoproduct in both methanol and hydrocarbon solvents (benzene). The unsaturated alcohol is identified by the following NMR signals: an allylic methyl signal at 1.8 ppm, an OH signal at 2.4 ppm (d, $J=4.8$ Hz), an AB quartet signal at 3.4 ppm, two vinylic CH signals at 4.5 and 4.8 ppm and a methine (dq, $J=4.8, 6.8$ Hz) signal at 5.3 ppm (in CDCl_3). Furthermore, ^{19}F NMR of the alcohol showed a doublet ($J=6.8$ Hz) signal at -2.0 ppm relative to ethyl trifluoroacetate standard. The indanol had two methyl singlet signals at 1.37 and 1.42 ppm and an AB quartet at 2.2 and 2.45 ppm (in CDCl_3). A weak w-type coupling was observed in the indanol between the CF_3 group and the trans hydrogen on the five-membered ring (2.2 ppm). Chemical yields were measured by irradiating 0.01 M solutions of **14** in benzene- d_6 at room temperature in the presence of a methyl benzoate standard. NMR analysis of the resulting mixture showed it to consist of 88% **14alc**, and 9% **14ind**.

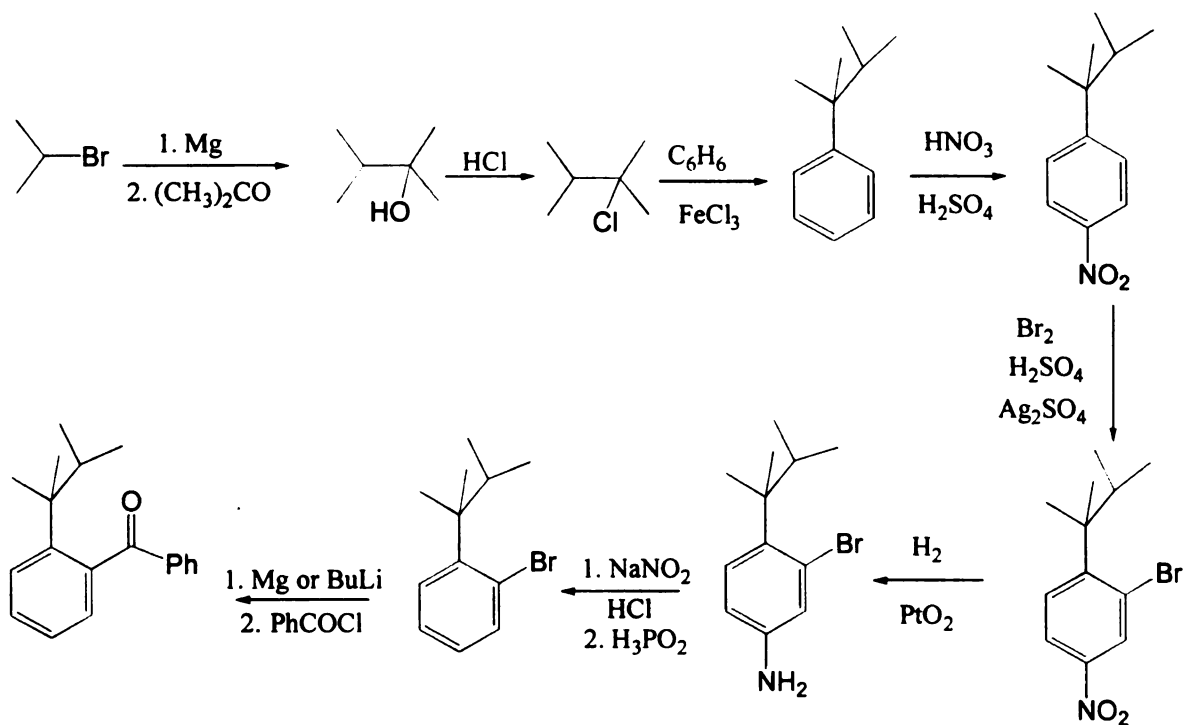


Scheme 38. Photobehavior of 14

IV. 2'-(2,3-Dimethyl-2-butyl)benzophenone

A. General Preparation

o-(2,3-Dimethyl-2-butyl)benzophenone was prepared by addition of isopropyl Grignard to acetone, treatment of the resulting alcohol with concentrated HCl, Friedel-Crafts alkylation of benzene with the resulting alkyl chloride, nitration, bromination, reduction of nitro group, formation and reduction of diazonium salt, formation of Grignard and coupling to benzoyl chloride.



B. Irradiation Conditions

NMR scale irradiations were carried out using 0.01 M solutions of 2'-(2,3-dimethyl-2-butyl)benzophenone in deuterated benzene, methanol and toluene. The

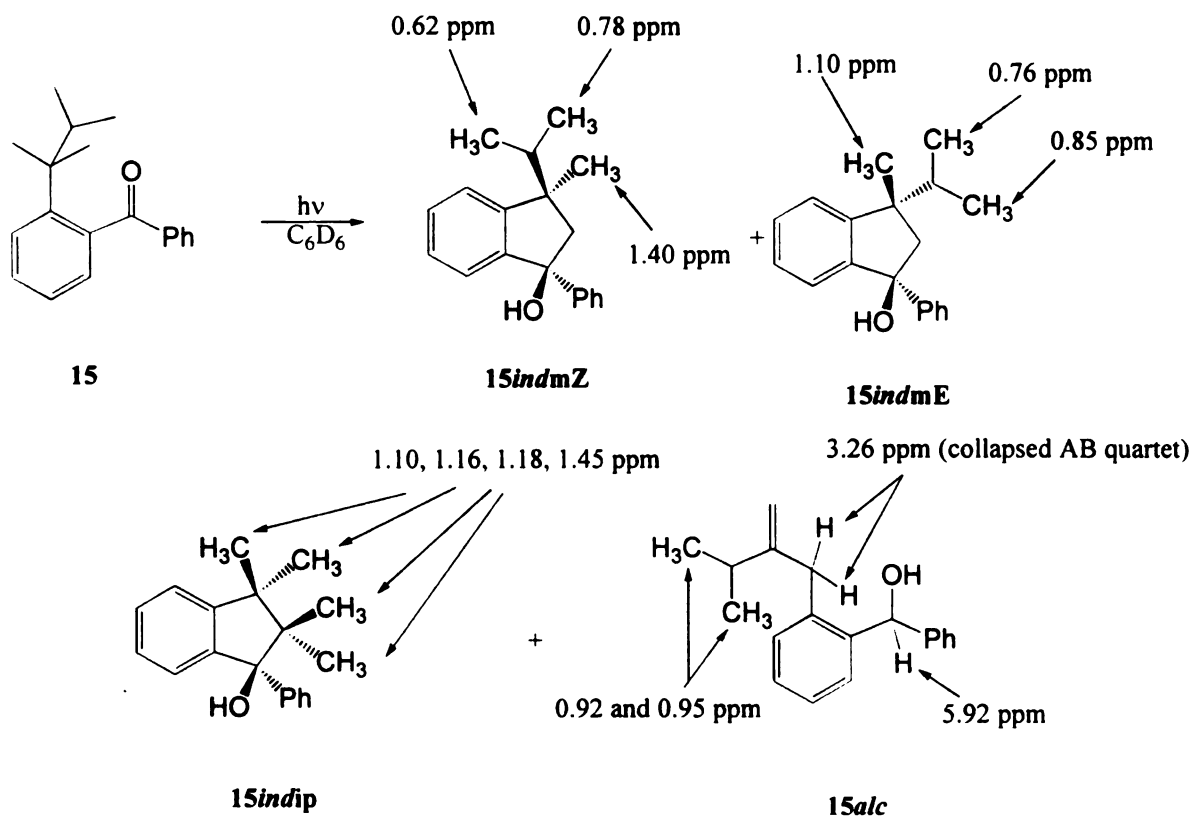
solutions were irradiated through a Pyrex filter. In most cases the starting ketone disappeared after 30 minutes of irradiation with corresponding appearance of mixtures of isomeric indanols (**15indmZ**, **15indmE**, **15indip**, **15alc**). The quantum efficiencies were higher in methanol than in benzene. Chemical yields were measured by irradiating 0.03 M solutions of **15** in benzene and methanol with methyl benzoate as a standard. The resulting solutions were then analyzed by NMR. In all cases, material balances were >95%.

C. Identification of photoproducts.

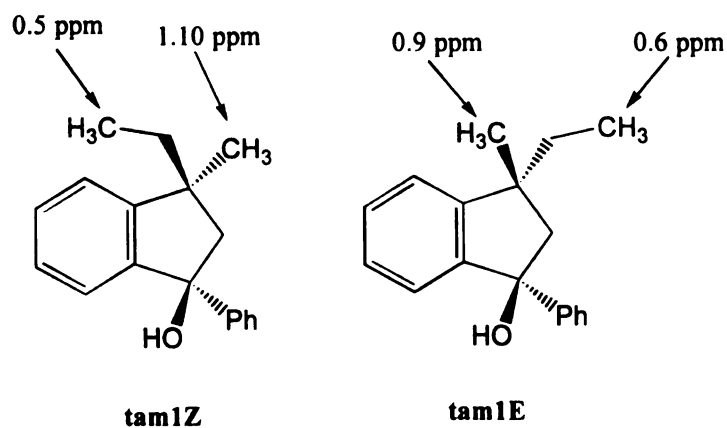
The indanol products were difficult to isolate because of rapid dehydration on silica gel. An unsaturated alcohol similar to those obtained from irradiation of *o*-*tert*-butylaceto- and trifluoroacetophenones was also observed as a photoproduct.

o-(2,3-Dimethyl-2-butyl)benzophenone (0.01 M) in deuterated benzene was irradiated with Pyrex-filtered light from a medium pressure mercury arc lamp. The reaction was complete within 1.5 hours of irradiation and four products formed (Scheme 39). The reaction mixture had to be analyzed immediately after irradiation because photoproducts dehydrated rapidly. **15indmE**, **15indmZ** and **15alc** (Scheme 39) measure abstraction of a primary methyl hydrogen while **15indip** measures abstraction of a tertiary hydrogen. This reaction was repeated in several solvents and product ratios were determined by NMR. The stereochemical assignments of **15indmE** and **15indmZ** were made by comparison of the NMR data to those of E- and Z-3-ethyl-3-methyl-1-phenyl-1-indanol (**tam1E** and **tam1Z**), photoproducts of OTAMPB.⁵⁷ The NMR data of **tam1E**

and **tam1Z** in benzene indicate that the methyl group of the ethyl substituent appears at 0.6 ppm in the E-isomer with a methyl singlet signal at 0.90 ppm which are, respectively, upfield and downfield relative to the signals in the Z-isomer (0.5 and 1.10 ppm respectively).



Scheme 39. Photochemistry of 15



Thus, the isomer with the isopropyl doublet signals at higher field and the methyl singlet signal at lower field was assigned the E-stereochemistry. **15indmZ** has two isopropyl doublet signals at 0.62 at 0.78 ppm and a methyl singlet signal at 1.40ppm while the isopropyl and methyl signals of **15indmE** appear at 0.76, 0.85 and 1.10 ppm, respectively. Identification of **15alc** by NMR was also simple, since **15alc** shows similar NMR signals to the unsaturated alcohol of **14** with two vinylic CH signals appearing at 4.47 and 4.84 ppm, a bibenzylic OH signal at 5.92 ppm, an AB quartet signal at 3.26 ppm and two isopropyl doublet signals at 0.92 and 0.95 ppm. The reaction proceeds in solid as well as solution similar to *tert*-amylbenzophenone Table 21 shows the chemical yield in benzene and methanol at room temperature along with product ratios under various conditions.

Table 21. Effect of Temperature and Medium on Product Ratios of 15

Reaction medium	T (°C)	15indmZ	15indmE	15alc	15indip
Benzene	24	27	52	7	14
Methanol	24	32	32	13	23
Toluene	110	22	29	8	41
Toluene	-72	33	48	5	14
solid	24	23	27	-	50

D. Steady-State Photokinetics

The quantum yields were measured by irradiation of degassed solutions of ketones (0.15 M) in tubes containing a fixed amount of internal standard parallel to valerophenone actinometer. For quenching studies, these tubes also contained varying amounts of 2,5-dimethyl-2,4-hexadiene as a quencher. Product yields at 5-18% were measured using GC or NMR and were converted to quantum yields. Stern-Volmer plots were linear with slopes equal to $k_q\tau$. The kinetic data are listed in Table 22. Triplet lifetimes, based on a k_q value of $6 \times 10^9 \text{ M}^{-1}\text{s}^{-1}$, are also listed.³⁰ The errors represent deviations from the average.

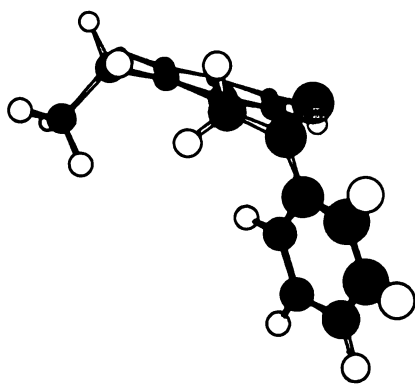
Table 22. Triplet Lifetimes and Product Quantum Yields of 2-(2'-(2',3'-Dimethyl)butyl)-benzophenone at Room Temperature ($\lambda = 313 \text{ nm}$)

Solvent	$k_q\tau, \text{M}^{-1}$	$1/\tau \times 10^9 \text{S}^{-1}$	$\Phi_{15\text{indmE}}$	$\Phi_{15\text{indmZ}}$	$\Phi_{14\text{alc}}$	$\Phi_{14\text{indip}}$
Benzene	20.8 ± 0.9	0.29	0.052 ± 0.003	0.026 ± 0.001	0.0060 ± 0.0003	0.010 ± 0.005
Methanol	-	-	0.130 ± 0.007	0.120 ± 0.006	0.061 ± 0.003	0.110 ± 0.005

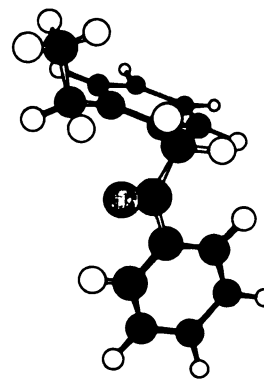
V. Semiempirical Calculations

In order to gain a better understanding of our experimental results, we performed calculations on the ground state as well as triplet biradical geometries of all of our compounds. The results of our triplet biradical calculations are presented and discussed in the discussion part of this thesis. The results of our ground state calculations are presented below:

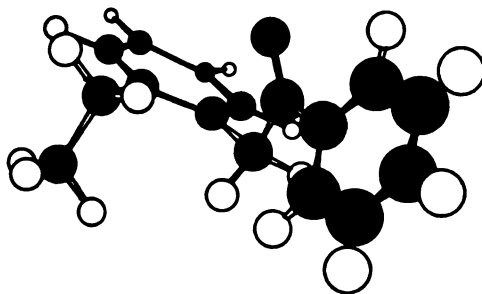
Global minimizations (semiempirical- AM1 level) with dihedral drivers around phenyl- α -carbon and α -carbon-carbonyl bonds have shown that the lowest energy geometry of **1** does not have the phenyl group eclipsing the carbonyl (Figure 7). However, geometry (**1B**) exists as a local minimum 0.8 kcal/mole higher than global minimum. In geometries **1B** ($d=2.32 \text{ \AA}$, $\omega=48^\circ$) and **1C** ($d=2.77 \text{ \AA}$, $\omega=62^\circ$) but not in **1A**, hydrogens are close enough for abstraction. MMX minimizations had shown **1C** to be the lowest energy geometry.⁸⁷ The reason for the discrepancy between molecular mechanics and semiempirical results is attributed to the inability of molecular mechanics to account for electronic interactions such as torsional interactions and resonance.



1A. Lowest Energy Geometry of **1**



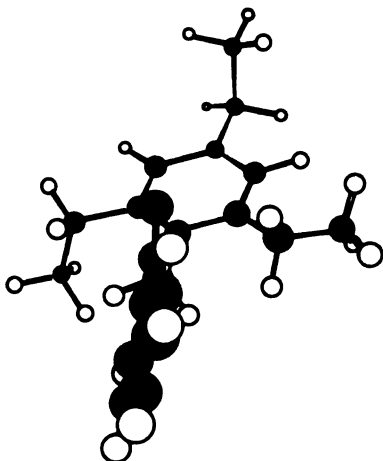
1B. 0.5 kcal/mole less stable than **1A**



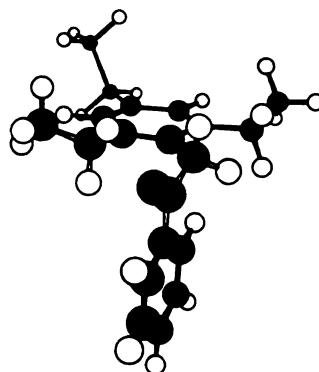
1C. 0.8 kcal/mole less stable than 1A

Figure 7. Minimum Energy Geometries of α -(2-Ethylphenyl)acetophenone

Similar minimizations (AM1) reveal that **2** has two energy minima within 0.7 kcal/mole of each other (Figure 8). In both **2A** ($d=2.72$ Å, $\omega=110^\circ$) and **2B** (two hydrogens are available for abstraction, one pointing up one down, $d_{\text{up}}=2.42$ Å, $\omega_{\text{up}}=67^\circ$, $d_{\text{down}}=2.71$ Å, $\omega_{\text{down}}=96^\circ$) hydrogens are close enough for abstraction.



2A. Lowest Energy Geometry of **2**

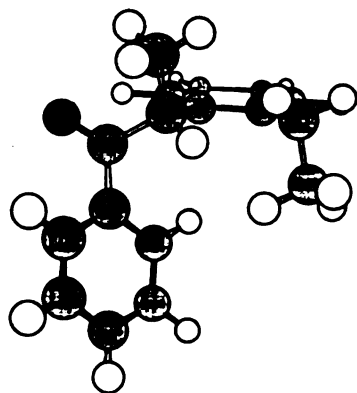


2B. 0.7 kcal/mole less stable than 2A

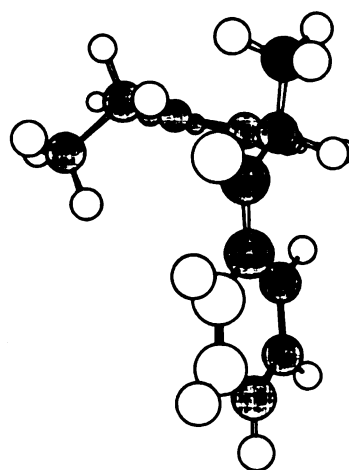
Figure 8. Minimum Energy Geometries of α -(2,4,6-Triethylphenyl)acetophenone

The lowest energy geometry of **4** is calculated to be the one in which the methyl eclipses the carbonyl (Figure 9). In this geometry, however, the methylene hydrogens are too far to be abstracted since the carbonyl is twisted away from them. Global

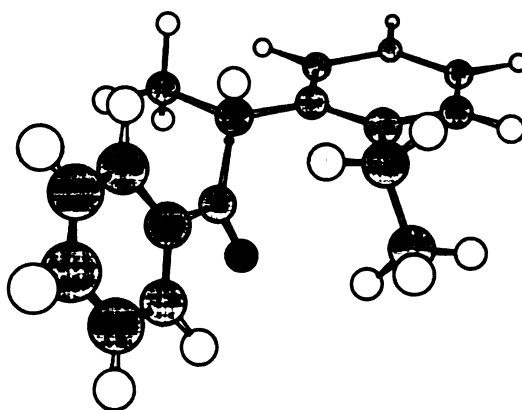
minimizations with dihedral drivers (10° increments) around the benzene- α -carbon bond reveal two other minima; in both, methylene hydrogens are close enough to be abstracted. These conformers are 1.4 and 2.4 kcal/mole higher in energy than the global minimum. In the lower energy conformer ($d=3.0 \text{ \AA}$, $\omega=86.8^\circ$), ethyl derived methyl is pointing down and the α -phenyl is eclipsing the carbonyl, while in the higher energy conformer ($d_1=2.5 \text{ \AA}$, $\omega_1=61.5^\circ$, $d_2=2.7 \text{ \AA}$, $\omega_2=99.45^\circ$), ethyl derived methyl is relatively coplanar with the α -phenyl and α -methyl eclipsing the carbonyl.(Figure 9)



4A. Lowest Energy Geometry of 4



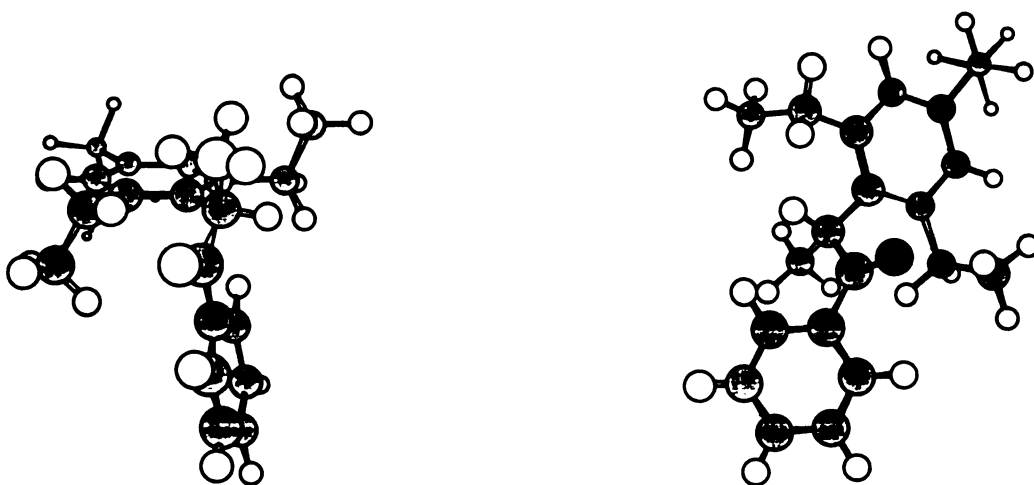
4B. 1.4 kcal/mole less stable than 4A



4C. 2.4 kcal/mole less stable than 4A

Figure 9. Lowest Energy Conformers of α -(2-Ethylphenyl)propiophenone

The lowest energy geometry of **5** is has the α -methyl eclipsing the carbonyl (AM1). In this geometry, the closest methylene hydrogen is 2.2 Å away and makes a dihedral angle of 50° with the carbonyl σ plane. Another geometry, **5B**, which lies 1.8 kcal/mole above the global minimum with the phenyl and methyl gauche to each other. In this geometry the closest hydrogen is 2.8 Å from the carbonyl oxygen and makes a dihedral angle of 103° with the carbonyl nodal plane.(Figure 10)

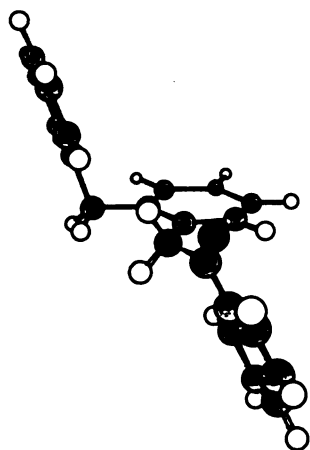


5A

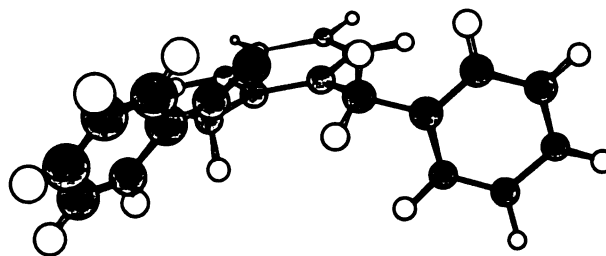
5B. 1.8 kcal/mole less stable than 5A

Figure 10. Lowest Energy Geometries of α -(2,4,6-Triethylphenyl)propiofenone

Semiempirical calculations show that in the lowest energy geometry of **6** the α -hydrogen eclipses the carbonyl (**6A**, Figure 11). In this geometry, the benzylic hydrogens are too far away for abstraction. In another geometry (**6B**) both benzylic hydrogens are close enough for abstraction ($d_{up}=2.46$ Å, $\omega_{up}=161.8^\circ$, $d_{down}=2.68$ Å, $\omega_{down}=142.2^\circ$).



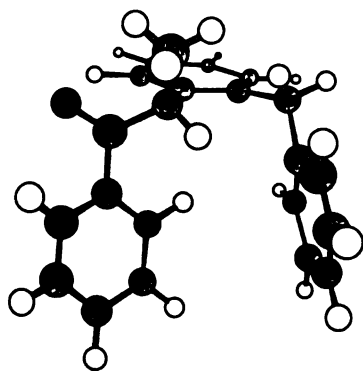
6A. Lowest Energy Geometry of 6



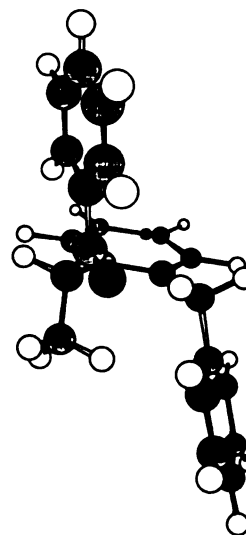
6B. 0.4 kcal/mole less stable than 6A

Figure 11. Minimum Geometries of α -(2-Benzylphenyl)acetophenone

Global minimizations reveal that in the lowest energy geometry of 7 (7A, Figure 12) benzylic hydrogens are too distant for abstraction ($d = 4.8 \text{ \AA}$). Another minimum (7B, $d = 2.32 \text{ \AA}$, $\omega = 48^\circ$) higher in energy than 7A by 2.0 kcal/mole, has hydrogens close enough for abstraction.



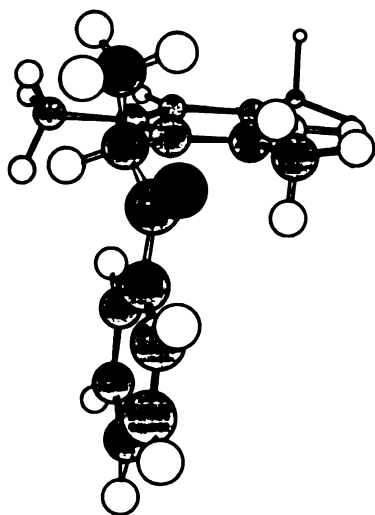
7A. Lowest Energy Geometry of 7



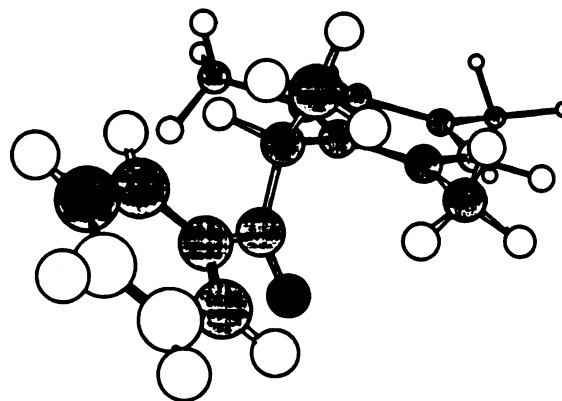
7B. 2.0 kcal/mole less stable than 7A

Figure 12. Lowest Energy Conformers of α -(2-Benzylphenyl)propiophenone

The minimum energy geometry of **8** has an α -methyl group eclipsing the carbonyl (AM1, **8A**, Figure 13). In this geometry, two hydrogens on the same methyl group are close enough for abstraction ($d_{\text{up}}=2.45 \text{ \AA}$, $\omega_{\text{up}}=122.7^\circ$, $d_{\text{down}}=2.67 \text{ \AA}$, $\omega_{\text{down}}=84.4^\circ$). There is another geometry (**8B**) 2.1 kcal/mole higher in energy than **8a** in which methyl and phenyl are gauche to each other. In this geometry closest hydrogen is 2.7 \AA from carbonyl oxygen and makes a dihedral angle of 105° with the nodal plane of carbonyl.



8A. Lowest Energy Geometry of **8**



8B. 2.1 kcal/mole less stable than **8A**

Figure 13. Lowest Energy Geometries of α -Mesitylpropiophenone

The lowest energy geometry of **9** has the α -phenyl eclipsing the carbonyl. In this geometry, the benzylic hydrogen closest to the carbonyl is 2.85 \AA from oxygen. (Figure 14)

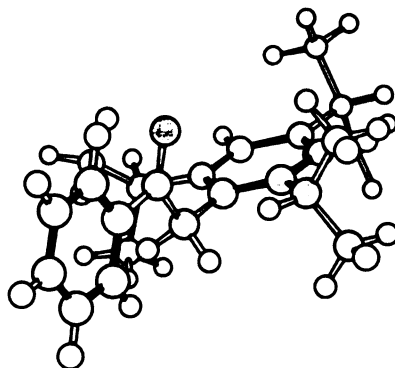
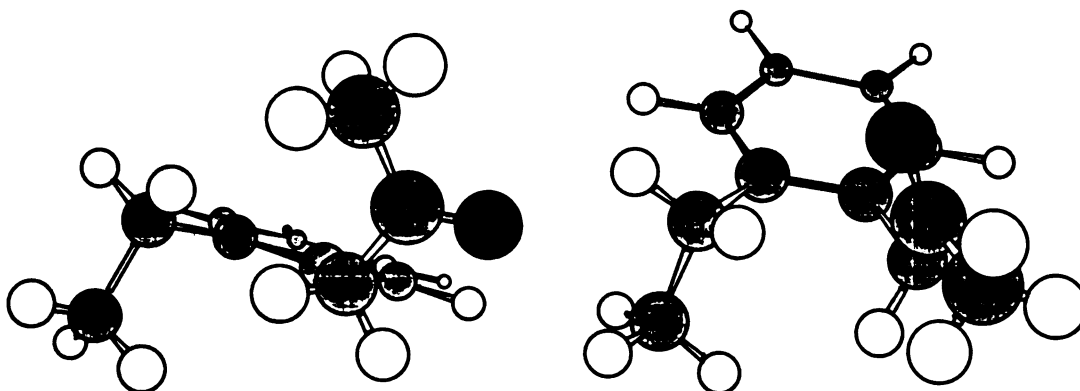


Figure 14. Lowest Energy Geometry of α -(2,4,6-Triisopropylphenyl)acetophenone

Molecular mechanics and semiempirical calculations were performed on **10**. In its lowest energy geometry (**10A**), no hydrogens are close enough for abstraction. Global minimizations with dihedral drivers (10° increments) around benzene- α -carbon and α -carbon-carbonyl bonds reveal another minimum (**10B**, 0.6 kcal/mole higher than global minimum) in which methylene hydrogens are close enough to be abstracted ($d=2.64 \text{ \AA}$, $\omega=63^\circ$, Figure 15)

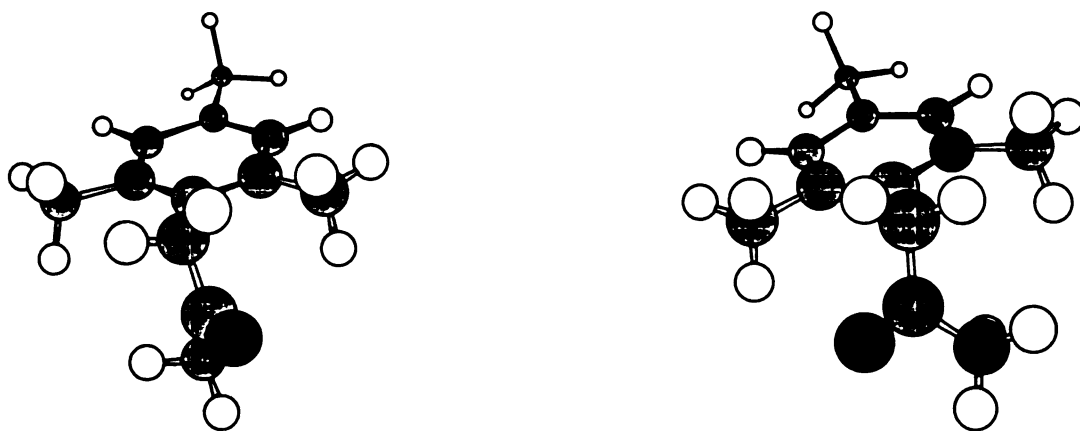


10A. Lowest Energy Geometry of 10

10B. 0.6 kcal/mole less stable than 10A

Figure 15. Lowest Energy Geometries of α -(2-Ethylphenyl)acetone

Global minimizations show that hydrogen abstraction in **11** must occur from a geometry (**11B**, $d=2.9 \text{ \AA}$, $\omega=58^\circ$) other than its global minimum (**11A**, $d=3.26 \text{ \AA}$), since no hydrogens are close enough for abstraction in the latter (Figure 16).

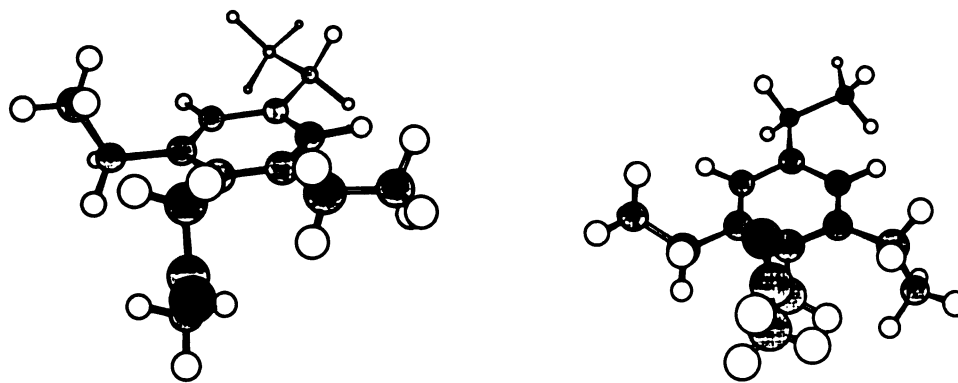


11A. Lowest Energy Geometry of **11**

11B. 0.4 kcal/mole less stable than **11A**

Figure 16. Lowest Energy Conformers of α -Mesitylacetone

The lowest energy geometry of **12** is one with an α -hydrogen eclipsing the carbonyl (Figure 17). In this geometry, however, the methylene hydrogens are too far to be abstracted. Global minimizations with dihedral drivers (10° increments) around benzene- α -carbon and α -carbon-carbonyl bonds reveal another minimum in which methylene hydrogens are close enough to be abstracted ($d=2.7 \text{ \AA}$, $w=60^\circ$). This conformer is 2.0 kcal/mole higher in energy than the global minimum (Figure 17).



12A. Lowest Energy Geometry of 12

12B. 2.0 kcal/mole less stable than 12A

Figure 17. Lowest Energy Geometries of α -(2,4,6-Triethylphenyl)acetone

Semiempirical calculations were performed on 13 to show the lowest energy geometry is one with the α -phenyl eclipsing the carbonyl. In this geometry, the benzylic hydrogens closest to the carbonyl is 3.14 Å from the oxygen. (Figure 18)

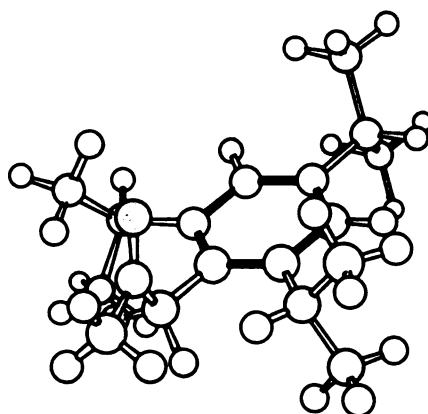


Figure 18. Lowest Energy Geometry of α -(2,4,6-Triisopropylphenyl)acetone

Molecular mechanics calculation reveal that in its minimum energy geometry, 14 like OTBBP, has hydrogens on two methyl groups close enough for abstraction. (Figure 19)

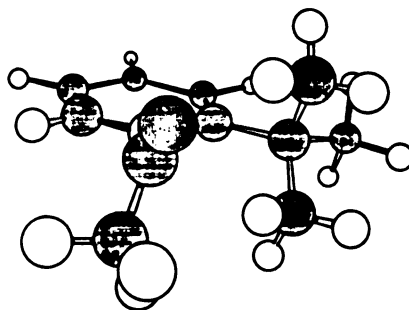
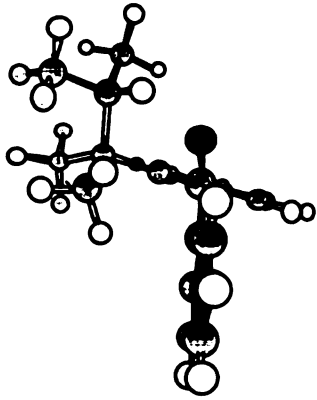
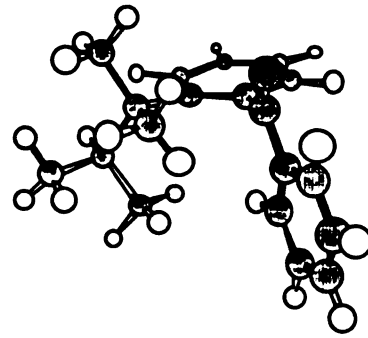


Figure 19. Lowest Energy Geometry of 2-*tert*-Butyltrifluoroacetophenone

Semiempirical calculations at AM1 level were performed on 2'-(2,3-Dimethyl-2-butyl)benzophenone. The lowest energy geometry was calculated to be the one with the isopropyl group pointing up with its hydrogen pointing over the benzene ring. There are two hydrogens at an abstractable distance from the carbonyl oxygen, but with different dihedral angles. The isopropyl hydrogen is closer and better aligned ($d=2.28 \text{ \AA}$, $\omega=42.8^\circ$) than the methyl hydrogen ($d=2.46 \text{ \AA}$, $\omega = 96.4^\circ$). Minimizations (semiempirical-AM1 level) were also performed with a dihedral driver (10° increments) for rotation around the benzene-*t*-hexyl bond to detect conformations with methyl hydrogens better aligned for abstraction. The calculations revealed another minimum 1.0 kcal/mole higher in energy than the global minimum. In this conformation, only methyl hydrogens are close enough for abstraction ($d=2.31 \text{ \AA}$, $\omega=78.9^\circ$, Figure 20).



15A. Lowest Energy Geometry of 15



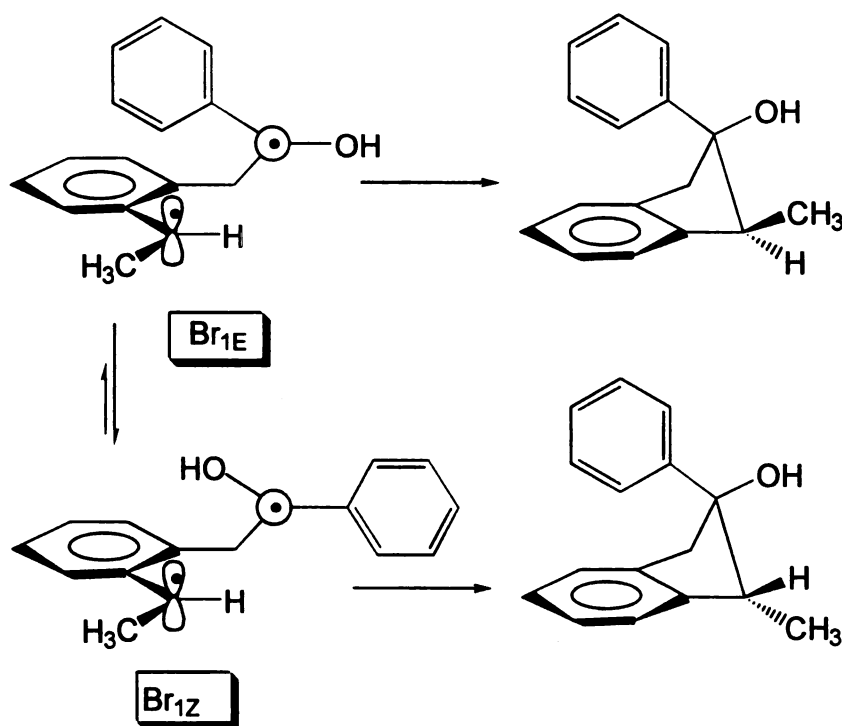
15B. 1.0 kcal/mole less stable than 15A

Figure 20

Discussion

I. Conformational Control of Product Ratios from Triplet 1,5-Biradicals

The high diastereoselectivity observed in the photocyclization of α -(*o*-alkylphenyl) and α -(2,4,6-trialkylphenyl)acetophenones was attributed to differences in energy of two hydroxy-biradical rotamers by Park and Wagner.^{87,88} For example, the observed 20:1 indanol ratio in the photocyclization of α -(*o*-ethylphenyl)acetophenone was attributed to a 20:1 population of biradical conformers Br_{1Z} and Br_{1E} (Scheme 40).

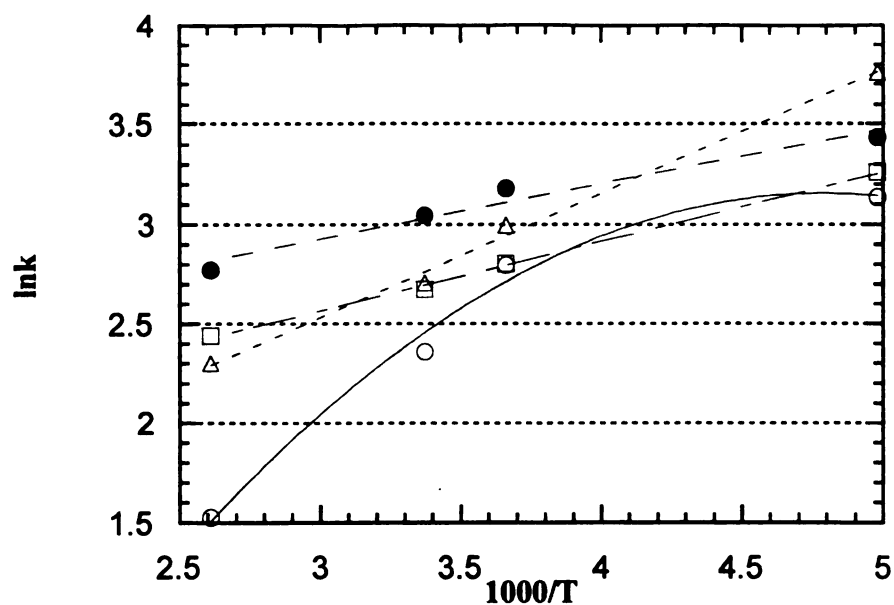


Scheme 40

Our temperature studies along with semiempirical calculations, however, indicate that not only activation enthalpies, but also the entropies (the A factors in the Arrhenius equation, $k = Ae^{-E_a/RT}$), which may reflect the intersystem crossing rates of the biradical rotamers, are responsible for the observed diastereoselectivities.

Table 23. Effect of Temperature on the Indanol Ratios of α -Arylacetophenones

T (°C)	Solvent	1Z:1E	2Z:2E	3Z:3E	4ZZ:4ZE	5ZE:5ZE	6Z:6E	8Z:8E
-72	Toluene	26:1	31:1	44:1	1:9	6:1	0.68:1	23:1
-72	Methanol	-	-	-	0:100	15:1	-	-
0	Toluene	16.5:1	24:1	20:1	1.6:1	1.5:1	1.04:1	16:1
24	SiO ₂	-	>30:1	>30:1	1:2.5	10:1	1:1	16:1
24	Methanol	2:1	-	5:1	1:1	12:1	-	-
24	Crystal	>30:1	100:0	-	-	100:0	1:1	-
24	Toluene	14.5:1	21:1	15:1	5:1	1.2:1	1.3:1	10:1
110	Toluene	11.5:1	16:1	10:1	10:1	1:1.5	1.5:1	4.5:1



1(\circ), 2(\bullet), 3(Δ), 8(\square)

Graph 2. Arrhenius Plot 1

Table 24. Arrhenius Data from Graph 2

Ketone	A_Z/A_E	ΔE_{\bullet} , Kcal/mole
1	$A_Z/A_E = 4.6$	$E_E - E_Z = 0.69$
2	$A_Z/A_E = 8.2$	$E_E - E_Z = 0.55$
3	$A_Z/A_E = 2.0$	$E_E - E_Z = 1.2$
8 ^a	$A_E/A_Z = 7.0$	$E_E - E_Z = 2.4$

a) from the three lowest points

Product ratios are influenced by the energies and hydrogen abstraction rates of reactive excited state conformers as well as interconversion and cyclization rates of

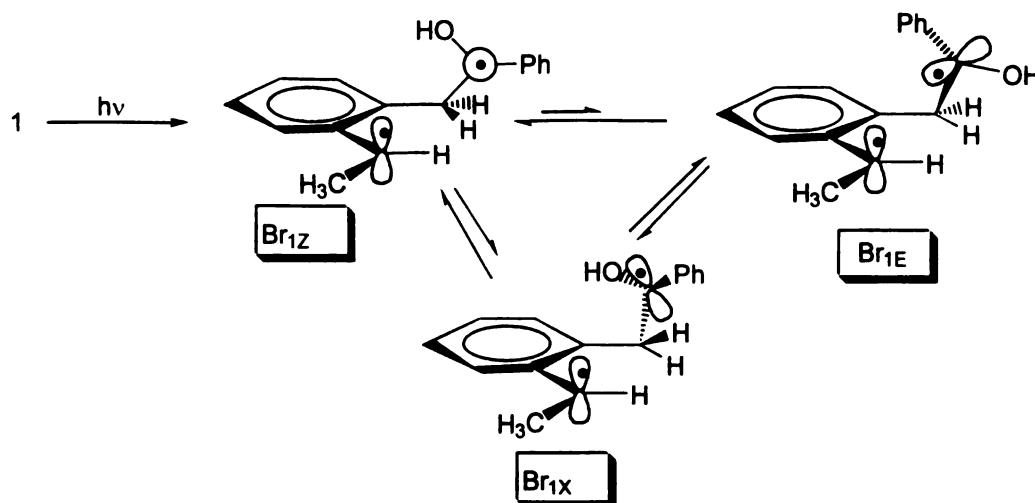
biradical rotamers. Energies of reactive triplet conformers mirror those of reactive ground state minima since the only significant change in geometry due to n,π^* excitation is a slight lengthening of the C-O bond.¹⁰⁷ The hydrogen abstraction rates are dependent on the orientation of the abstractable hydrogen relative to the nodal plane of the carbonyl group⁹⁵ and are assumed to be similar for various conformers. These factors control the product ratios only when cyclization is faster than interconversion of biradical rotamers (ground state control). When biradicals interconvert faster than they cyclize, which is the case for most triplet biradicals due to their long lifetime, only energies and cyclization rates of various conformers influence product ratios (conformational control). Thus, in cases where the photocyclization is conformationally controlled, the product ratios can be calculated using Equation 4,

$$Z/E = (X_Z/X_E) \cdot (k_{Cyc}^Z/k_{Cyc}^E)$$

Equation 4

where X_Z and X_E are the populations of the biradicals leading to Z and E indanols and k_{Cyc}^Z and k_{Cyc}^E are the rates of the cyclizations for different conformers. The populations of different rotamers are determined by the difference in their free energies which are presumed to be dominated by enthalpies. There are several known mechanisms for ISC of biradicals.⁹⁶ In short biradicals, ISC is mainly driven by spin-orbit coupling, which is known to be very much dependent upon the distance and orientation of radical centers.^{76,97,98,99} The observed diastereoselectivities can, thus, be explained by the calculated energies, which reflect the conformational population, and cyclization rates which contain the intersystem crossing term. Semiempirical calculations have been

performed on the conformational distribution of the hydroxybiradical from **1**. In these calculations, only the biradicals with the methyl at the δ -radical site trans to the hemipinacol radical moiety were considered, since the syn isomer was found to lie 4 kcal/mole above the trans. There are only two minima within 5 kcal/mole of the global minimum (Br_{1Z}). Only one of these conformers (Br_{1E}), which lies 0.5 kcal/mole above the global minimum, can cyclize directly. The other conformer (Br_{1X}) requires a rotation around the ethylphenyl ring to achieve a cyclizable geometry. Br_{1X} can form Br_{1Z} and Br_{1E} by small rotations around bonds a and b, respectively. Analysis of the minimization map reveal that these interconversions have similar barriers such that Br_{1Z} (2.3 kcal/mole) and Br_{1E} (3.1 kcal/mole) are formed in a 3:1 ratio from Br_{1X} . This results in almost the same population ratio expected from a 0.5 kcal/mole energy difference. Thus, even though Br_{1X} can not cyclize directly, it acts as a transitional geometry from which either one of the two reactive (cyclizable) geometries can be formed. It was also observed that the rotamer with the hydroxyl group pointing toward the central benzene ring is more stable (about 1.0-2.0 kcal/mole) than the one with the hydroxy group pointing away. This phenomenon represents hydrogen bonding of the OH to the benzene ring^{100,101} and is prevented by Lewis base solvents. The large solvent effects on the photobehavior of **1** strongly support such a stabilizing effect in the biradical. In Br_{1E} , the two singly occupied p orbitals are almost orthogonal but not pointed at each other as they are in Br_{1Z} . These different orbital orientations seemingly lead to less triplet-singlet mixing in Br_{1E} and to less efficient intersystem crossing, which appears as a lower pre-exponential factor for cyclization (Scheme 41).



Scheme 41

If we assume that intersystem crossing is independent of cyclization and that at each minimum the system intersystem crosses to the singlet surface, then we must determine what happens to Br_{1X} after it becomes a singlet. Since Br_{1X} cannot cyclize directly, it must convert into either Br_{1Z} or Br_{1E} . The calculated rotational barriers noted above suggest that Br_{1X} can form Br_{1Z} 3-times more efficiently than it can Br_{1E} . Boltzman population ratios of Br_{1Z} , Br_{1X} and Br_{1E} are 0.42, 0.42 and 0.16, respectively. If we assume that Br_{1Z} intersystem crosses faster than Br_{1X} and Br_{1E} , due to a better orbital orientation, the ratio of intersystem crossing rates at room temperature can be measured, as follows, from the product ratios.

$$15 = (0.42 (k_{isc1}/k_{isc2}) + 0.28)/(0.16+0.14) \text{ thus } k_{isc1}/k_{isc2} = 10$$

Where k_{isc1} and k_{isc2} are the intersystem crossing rates of Br_{1Z} and Br_{1X} or Br_{1E} , respectively. This ratio seems too high to arise simply from different orbital orientations. Thus, it is believed that Br_{1X} converts into Br_{1Z} and Br_{1E} prior to intersystem crossing.

The fact that **1** yields only Z-indanol in the crystal confirms that Br_{1Z} is the predominant initial biradical geometry and rotations around the hydroxyradical site are necessary for formation of E-indanol.

Similar explanation can be offered for the photobehavior of **2** at various temperatures. The Arrhenius plot is linear which indicates that the biradical conformers are equilibrated at all temperatures. Semiempirical minimizations reveal the presence of two minima (**2A** and **2B**) within 1.2 kcal/mole of each other. The global minimum **2A** is in the pro-Z geometry while **2B** is in the pro-E geometry. The calculated enthalpic difference between the two biradical rotamers is twice the measured value (Table 24).

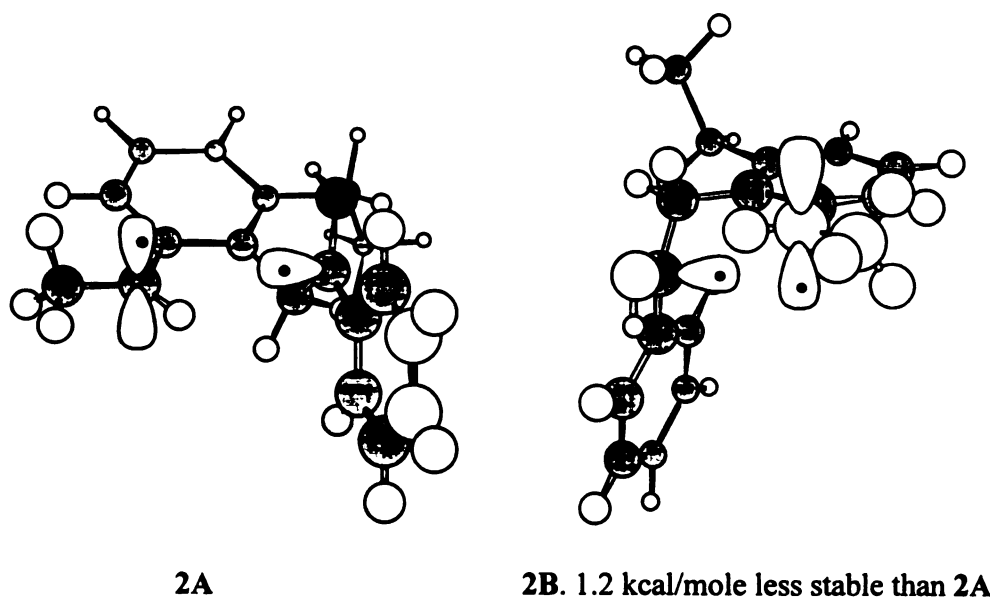
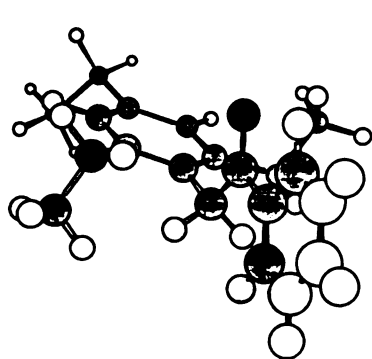


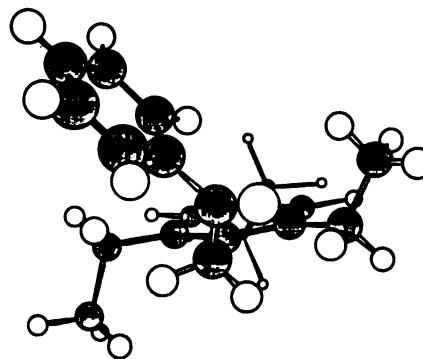
Figure 21. Lowest Energy Biradical Conformations of 2

It was thought that ground state control might be operative. Global minimizations of the ground state ketone show the presence of two minima (**2C** and **2D**) within 0.6 kcal/mole of each other, with the global minimum **2C** in the pro-Z geometry. However,

analysis of the lowest energy rotational path for the interconversion of the two biradical conformers did not reveal significant barriers (4-5 kcal/mole). Thus, biradical minima can interconvert and ground state control can not be operative. It is believed that reactivity is rotationally controlled, with the discrepancy between the calculated and measured values attributable to over estimation of calculated pro-E energy. The large difference in the A factors may be attributed to: 1) the pro-Z biradical cyclizing faster than the pro-E biradical and 2) a larger entropic loss for the pro-E relative to pro-Z biradical due to phenyl and methyl ending up cis to each other in the E-isomer.



2C

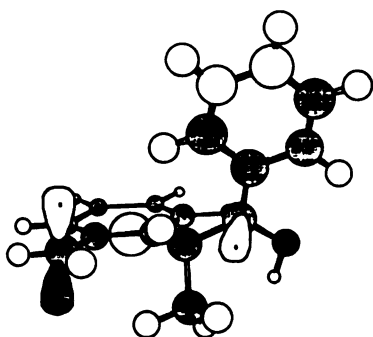
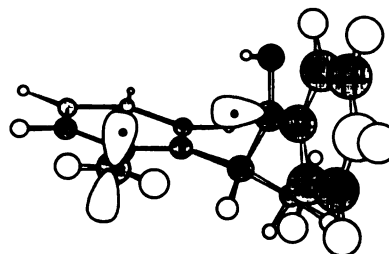
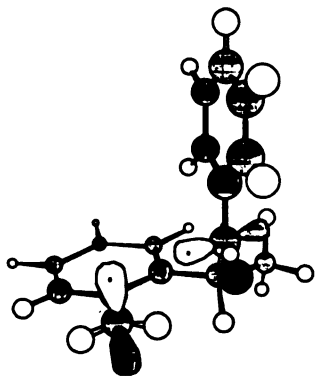
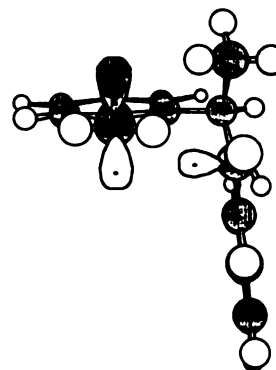


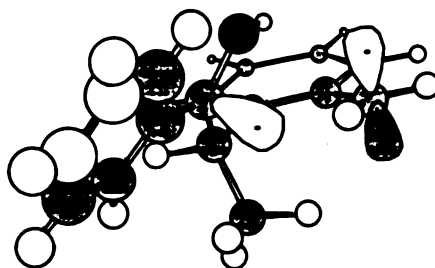
2D. 0.6 kcal/mole less stable than 2C

Figure 22. Lowest Energy Ground State Conformations of 2

Arrhenius data for **3** indicate that the conformation leading to **3Z** should be 1.2 kcal/mole more stable than that one leading to **3E**. Our minimizations, however, reveal the presence of 5 minima within 2 kcal/mole of each other. Three of these (**3A**, **3B** and **3D**) are in a pro-Z and the other two (**3C** and **3E**) are in a pro-E geometry. The global minimum (**3A**) has the hydroxyradical end twisted away from the benzylic radical such that cyclization requires a rotation around tolyl- α -carbon bond. Conformations **3B**, **3C**

and **3D** are respectively 0.1, 1.0 and 1.3 kcal/mole higher in energy than **3A**. The highest energy conformer (**3D**) is 2.0 kcal/mole higher than **3A** and will not contribute much to the overall yield of **3indE**. Thus, the observed product ratios in case of **3** are the result of products stemming from three conformations. In all reactive conformers (**3B**, **3C**, and **3D**), the two singly occupied p orbitals are orthogonal and are pointing toward each other. Thus, the A factor ratio simply represents the ratio of number of conformers leading to Z and E (Table 24). It is worth noting that the measured 1.2 kcal/mole enthalpy difference reflects an 88:12 ratio of pro-Z: pro-E conformers at RT. This ratio is also achieved by the Boltzman population of the three calculated conformers [**3B**(76%), **3C**(15%), **3D**(9%)].

**3A****3B**. 0.1 kcal/mole less stable than **3A****3C**. 1.0 kcal/mole less stable than **3A****3D**. 1.3 kcal/mole less stable than **3A**



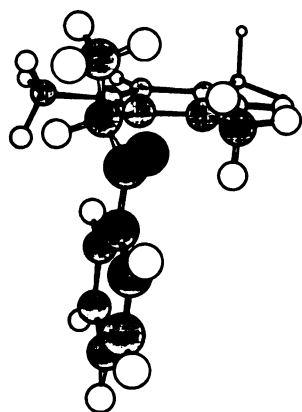
3E. 2.0 kcal/mole less stable than 3A

Figure 23. Lowest Energy Biradical Conformations of 3

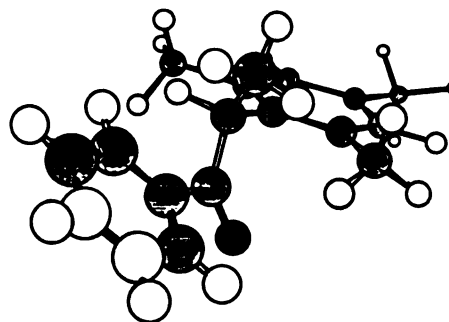
The Arrhenius plot of **8** is curved. It was thought that the curvature could be associated with the dehydration of indanols at high temperatures, thus leading to erroneous product ratios. However, control experiments revealed that dehydrations do not occur during the timeline of irradiations. This curvature can, however, be explained by one of the following:

1) A curved Arrhenius plot means a change in the mechanism of the reaction. Thus the curvature can be attributed to a change in the factors that control the reactivity. The measured isomeric ratio at -72°C is much less than the expected value predicted by the line through the other three points. Therefore, it is reasonable to assume that a mechanism other than conformational control is operative. The stereoselectivity of **8** depends on geometric variations at the α -hydroxy radical site. Rotation of the mesityl ring is too slow to compete with biradical decay at low temperatures.^{36g,102} If rotations around the α -carbon-hydroxy radical site are also slow (semiempirical calculations show a 6.0 kcal/mole barrier), then the biradical must react from the geometry in which it is formed and ground state control becomes operative. Semiempirical minimizations have revealed the presence of two reactive ground state minima; with the low energy minimum in a pro-

Z and the high energy one in the pro-E geometry. The difference in energy of 2.1 kcal/mole, however, warrants a Z:E ratio of 250:1, much greater than the 25:1 observed ratio. The 10-fold contrast between calculated and measured ratios can, however, be attributed to the difference in partitioning of the resulting biradicals, with the pro-E biradical cyclizing 10-times more efficiently than the pro-Z. Indeed, the ratio of A factors shows that the pro-E biradical cyclizes 7-times more efficiently than the pro-Z biradical.



8A. Lowest Energy Geometry of **8**

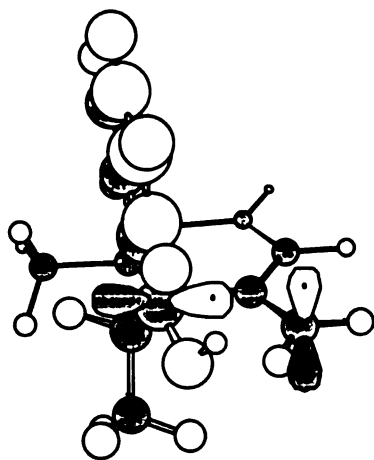
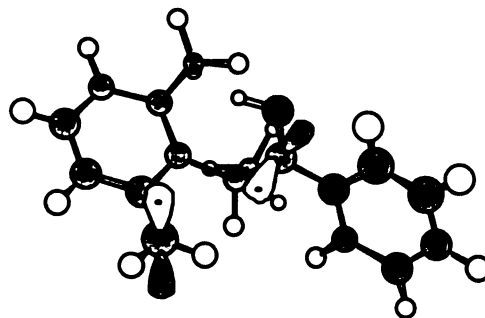
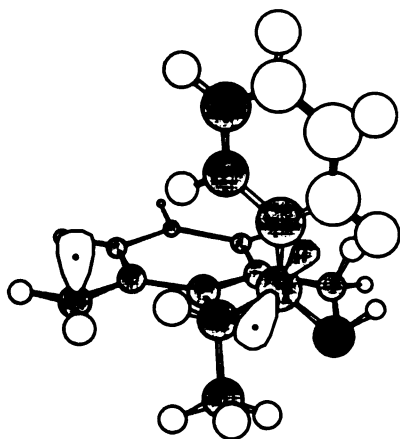
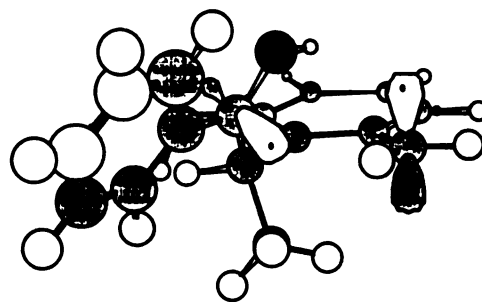


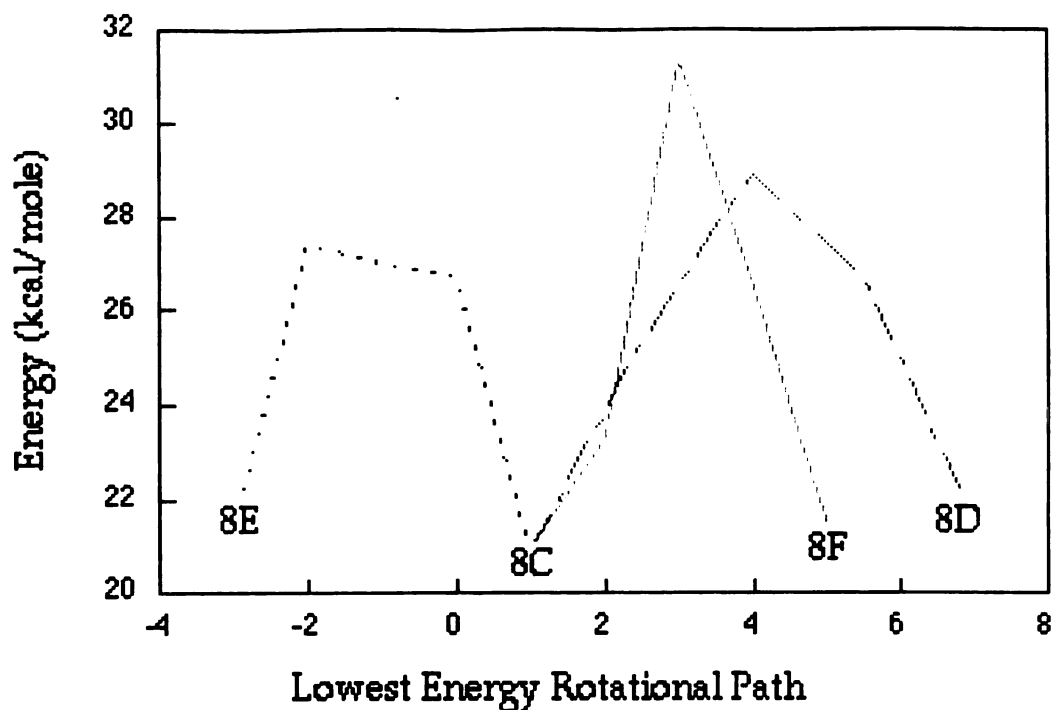
8B. 2.1 kcal/mole less stable than **8A**

Figure 24. Lowest Energy Ground State Conformations of 8

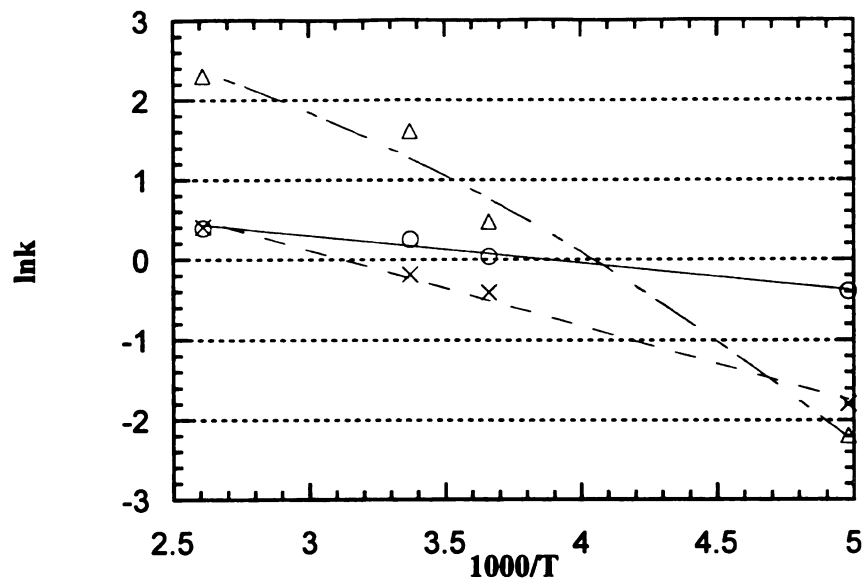
2) Global minimizations on the hydroxybiradical from **8** reveal the presence of 4 minima within 1.0 kcal/mole of each other. Three of these conformations (**8C**, **8D**, **8E**) are in a pro-Z geometry. Of these conformations, **8E** has the hydroxyradical end twisted away from the benzylic radical such that cyclization requires 180° rotation around the mesityl- α -carbon bond. It was mentioned earlier that this rotation is too slow to compete with biradical decay at low temperatures, as seen from variable temperature NMR which shows coalescence of the ortho-methyl groups of **8** near 0°C. Thus, even though cyclization is possible from **8E** and **8G** above 0°C, it can not happen at -72°C which

should lead to a lower than expected Z:E ratio at this temperature. This explanation, however, can be disregarded if one considers the rotational map that shows the interconversion of these conformers. Conversion of **8C**, which is essentially the initial biradical geometry, to the other conformers suffers from relatively high barriers (6-9 kcal/mole). This means that at low temperatures biradical interconversion can not compete with cyclization which in turn means that ground state control is operative.

**8C****8D**. 0.5 kcal/mole less stable than **8C****8E**. 0.7 kcal/mole less stable than **8C****8F**. 0.8 kcal/mole less stable than **8C****Figure 25. Lowest Energy Biradical Conformations of 8**



Photobehavior of **8** at higher temperatures is assumed to be conformationally controlled. The Arrhenius data indicate the pro-Z biradical to be 2.4 kcal/mole more stable than the pro-E. This gives a Z: E population ratio of 98:2. Our calculations, however, indicate a lower population ratio of 85:15 based on the energies of cyclizable minima **8C**, **8D** and **8F**. This discrepancy may be attributed to competition between ground state and biradical controls at 0°C (since it is not clear at what point the plot starts to curve, one can not be sure of such competition). The difference in the A factors is attributed to a more efficient cyclization of the pro-E conformer.

4 (O), 5(Δ), 6(x)

Graph 3. Arrhenius Plot 2

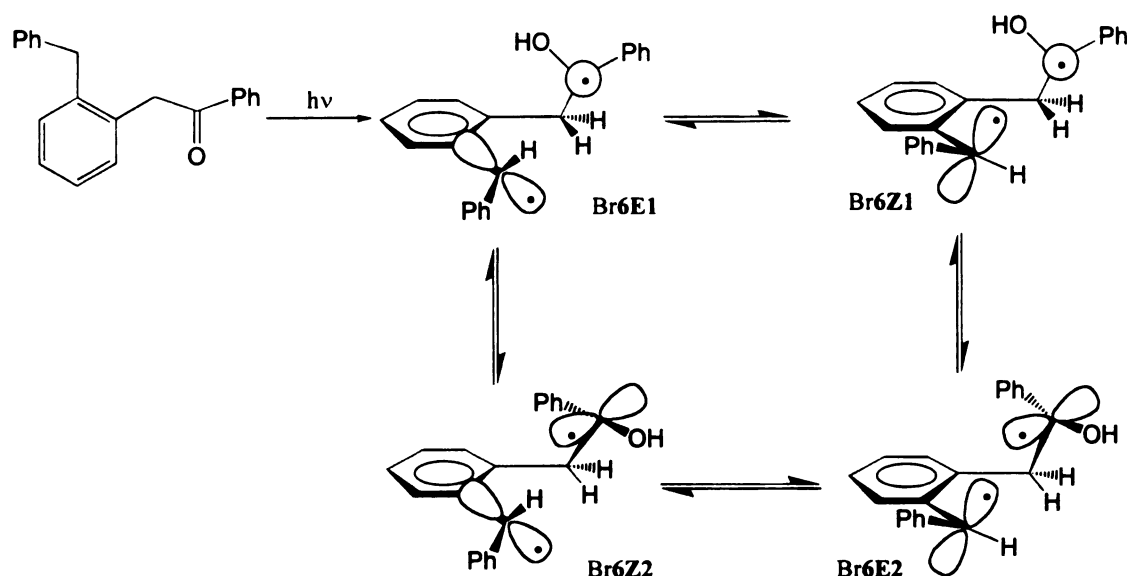
Table 25. Arrhenius Data from Graph 3

Ketone	A_Z/A_E	ΔE_p , Kcal/mole
4 ^a	$A_{ZZ}/A_{ZE} = 2325$	$E_{ZE} - E_{ZZ} = 4.0$
5	$A_{EZ}/A_{ZE} = 18.8$	$E_{EZ} - E_{ZE} = 1.88$
6	$A_Z/A_E = 3.7$	$E_Z - E_E = 0.67$

a) from the best-fit line

The lack of stereoselectivity in photocyclization of **6** is similar to earlier results from the Wagner group.^{54.103} The two biradical geometries with phenyl tilted up or down

are very similar in energy but have different orbital orientations which leads to different cyclization rates (Scheme 42).



Scheme 42. Lowest Energy Biradical Conformations of 6

Arrhenius data for **5** indicate the pro-ZE precursor to be enthalpically more stable than the pro-EZ one by 1.88 kcal/mole. Global minimizations on the biradical from **5** reveal the presence of 3 minima within 0.5 kcal/mole of each other. The global minimum (**5A**) is in a pro-EZ while the other two (**5B** and **5C**) are in a pro-ZE geometries. The fact that the global minimum has a pro-EZ geometry contrasts with the Arrhenius data. Another interesting observation is that the Arrhenius plot of **5**, unlike **8**, is not curved. The curvature in the plot of **8** was rationalized in terms of either 1) ground state control or 2) lack of cyclization of several biradical conformations. Option 2 is not valid for **5** since the next closest minimum is 2.4 kcal/mole higher in energy than **5A** and will not contribute much to the product ratios. This suggests that photobehavior of **5** is ground state controlled. The rotational energy map for interconversion of **5A** to **5B** indicates an

11 kcal/mole barrier. This barrier is much too large for the interconversion of these biradical conformers to compete with cyclization. Thus, ground state control of reactivity must be operative.

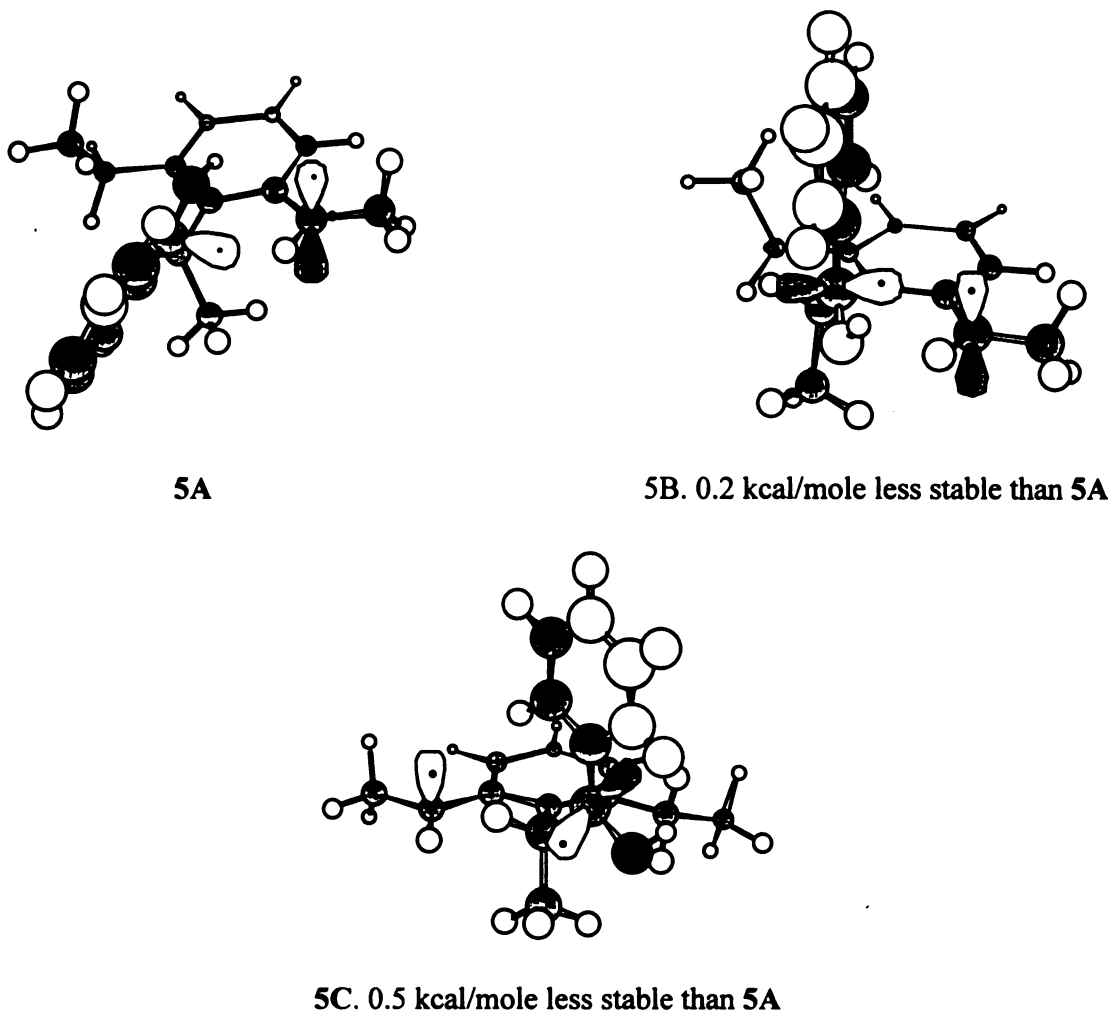
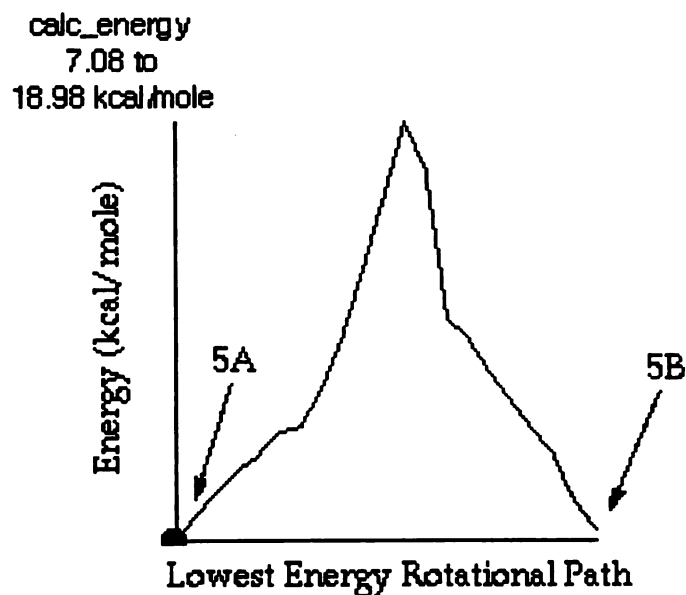


Figure 26. Lowest Energy Biradical Conformations of 5

Semiempirical minimizations on the ground state of 5 revealed two minima (5E and 5F) within 1.8 kcal/mole of each other. If bond rotations are slow as expected and ground state control is operative, then these geometries should give the products in the correct ratios. Arrhenius data predict the two reactive geometries to be different in energy



by 1.88 kcal/mole (good agreement with calculated results) with the lower energy geometry resulting in the ZE-isomer. Indeed, the global ground state minimum is in the pro ZE-geometry.



The difference in the A factors is attributed to the difference in rotational entropies of the two conformers. The pro-ZE conformer has a higher rotational freedom than the pro-EZ conformer since in the latter phenyl and methyl are cis (gauche) to each other. Thus, for the ground state control of reactivity, interconversion of the pro-EZ conformer to the pro-ZE one is entropically favored while the reverse is entropically disfavored. The fact that quantum efficiencies of formation for the ZE (0.14) and EZ

indanols (0.12) are similar indicates that the pro-EZ biradical is cyclizing more efficiently.

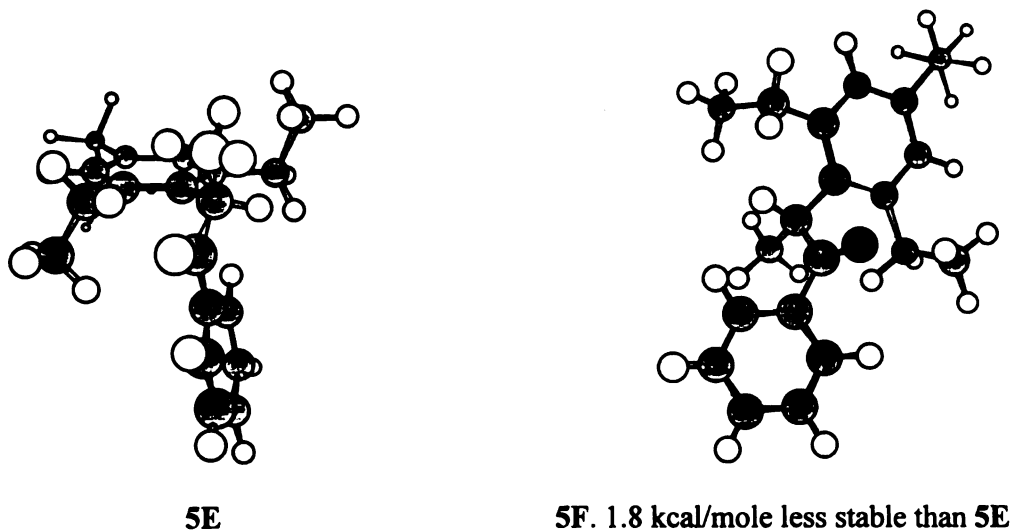
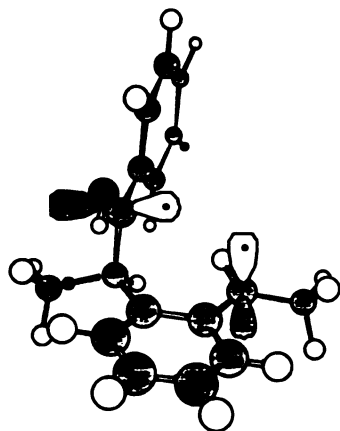
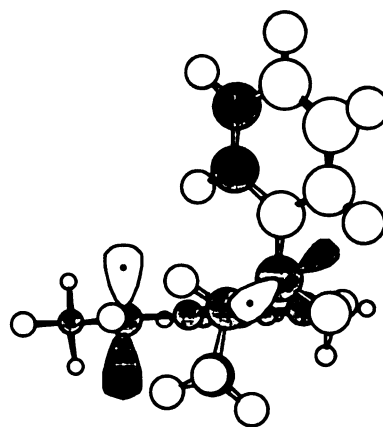


Figure 27. Lowest Energy Ground State Conformations of 5

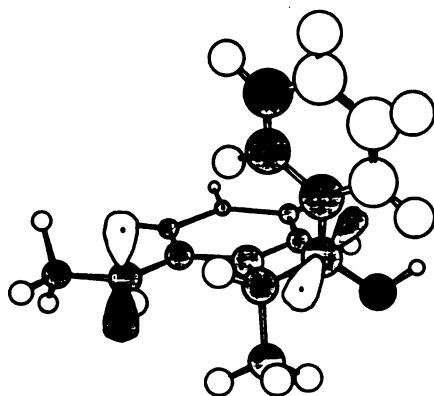
The photobehavior of **4** is striking in that the ZE isomer, the minor indanol formed at room temperature, is the predominant product at low temperatures in hydrocarbon solvents and is the only product at low temperature in methanol. The Arrhenius plot of **4**, similar to that of **8**, is curved. Furthermore, the Arrhenius data obtained from the best fit line have unrealistic values of ΔE_a and A for an equilibrated system. The data would indicate the pro-ZE biradical to be more stable than the pro-ZZ by 4.0 kcal/mole. Global minimizations on the biradical of **4**, however, show the global minimum to have a pro-ZZ geometry, with the closest cyclizable pro-ZE biradical (**4D**) 1.5 kcal/mole higher in energy.



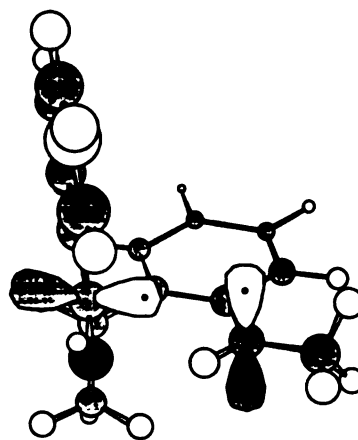
4A



4B. 0.2 kcal/mole less stable than 4A



4C. 0.5 kcal/mole less stable than 4A

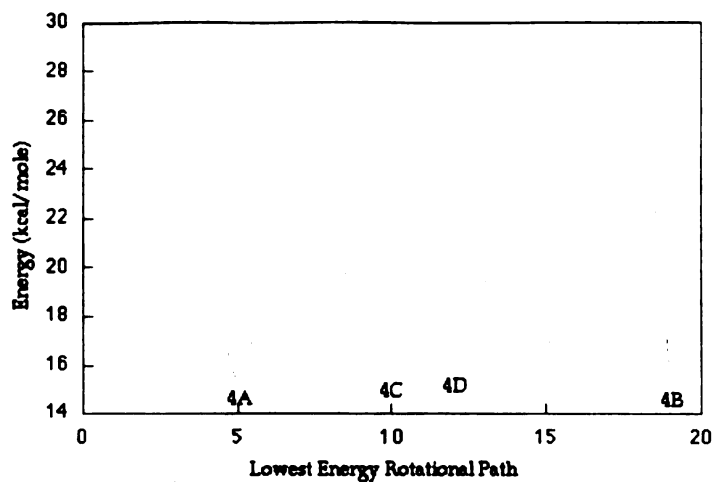


4D. 1.5 kcal/mole less stable than 4A

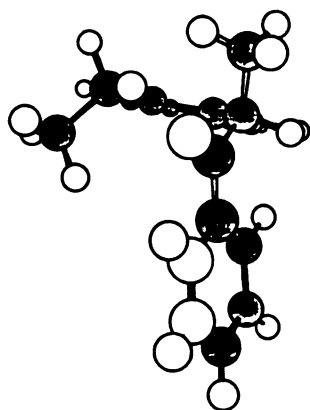
Figure 28. Lowest Energy Biradical Conformations of 4

The curvature in the plot is believed to involve competition between bond rotation and cyclization in the hydroxybiradical at low temperatures. The lowest energy rotational map for interconversion of these biradical conformers shows 4-10 kcal/mole barriers. At low temperatures slow bond rotation in the biradical can not compete with cyclization, as in **5** and **8**, and ground state control is operative. As temperature increases, the rotation

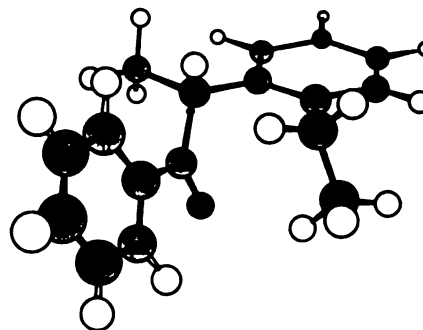
becomes faster and competes with cyclization. At or near room temperature, rotation becomes faster than cyclization and conformational control takes over.



The ZE:ZZ ratio of 9:1 at -72°C thus must be the result of the ground state control. Global minimizations on ground state of **4** reveal the presence of two minima within 1.0 kcal/mole of each other, with the lower energy one being in the pro-ZE geometry. It is thus believed that these two conformers are responsible for the observed 9:1 ZE:ZZ ratio at -72°C .



4E

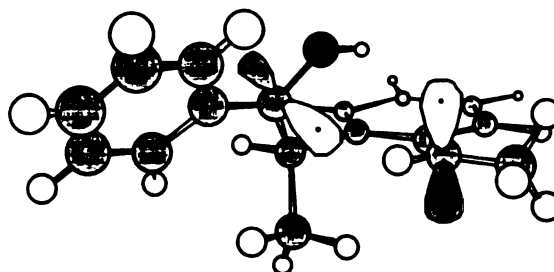


4F. 1.0 kcal/mole less stable than 4E

Figure 29. Lowest Energy Ground State Conformations of 4

The low quantum efficiency for cyclization (0.06) in **4** is attributed to a competing α -cleavage reaction and an efficient back transfer which occurs at geometries along the rotational path of interconversion of calculated minima.

Finally, the absence of the EZ-isomer from photoproducts of **4** can be explained by considering that the lowest energy biradical conformer leading to EZ lies 2.2 kcal/mole above the global minimum and thus is scarcely populated.



4G. Pro-EZ biradical

II. Photobehavior of α -Arylacetones - A Comparison of Singlet and Triplet Biradical Behavior

The main goal of this project was to determine the similarities and differences in reactivity and selectivity of 1,5-singlet and triplet biradicals. From a mechanistic point of view, the difference in the reactivity of the singlet and triplet 1,5-biradicals and the role of environmental and conformational factors in determining the overall efficiency and chemical yield of indanol formation must be addressed.

As mentioned earlier, the reactive excited states for aliphatic ketones are both singlet and triplet states. Thus, the excited states responsible for the two observed photoreactions in α -arylacetones, namely δ -hydrogen abstraction and α -cleavage, have to

be determined. Turro has shown that in α -(*o*-tolyl)acetones δ -hydrogen abstraction occurs only from the singlet while α -cleavage occurs only from the triplet.⁶⁷ Our quenching studies corroborate Turro's results.

Table 26. Effect of Temperature on Product Ratios from α -Arylacetones

Compound	Indanol/Diarylethane	Indanol/Diarylethane	Indanol/Diarylethane
	-72 °C	24 °C	110 °C
10	20:80	50:50 (3:1-Z:E)	60:40 (1.4:1 Z:E)
11	0:100	60:40	70:30
12	15:85	70:30 (10:1-Z:E)	85:15
13	0:100	70:30	100:0

Temperature effects on quantum yields are quite interesting. Diphenylethanes (DPEs) are the major and sometimes the only products at low temperature while indanol yields increase with increasing temperature. The high yield of DPEs, which result from α -cleavage followed by coupling of the resulting free radicals, demonstrates that there is an enthalpic barrier to hydrogen abstraction at low temperature whereas intersystem crossing has none. Thus, as temperature decreases, intersystem crossing to the triplet which only α -cleaves becomes predominant. Indanol yield increases with increasing temperature. This may be due to two reasons: First, a higher population of excited singlets undergoing hydrogen abstraction because they have higher kinetic energy; and

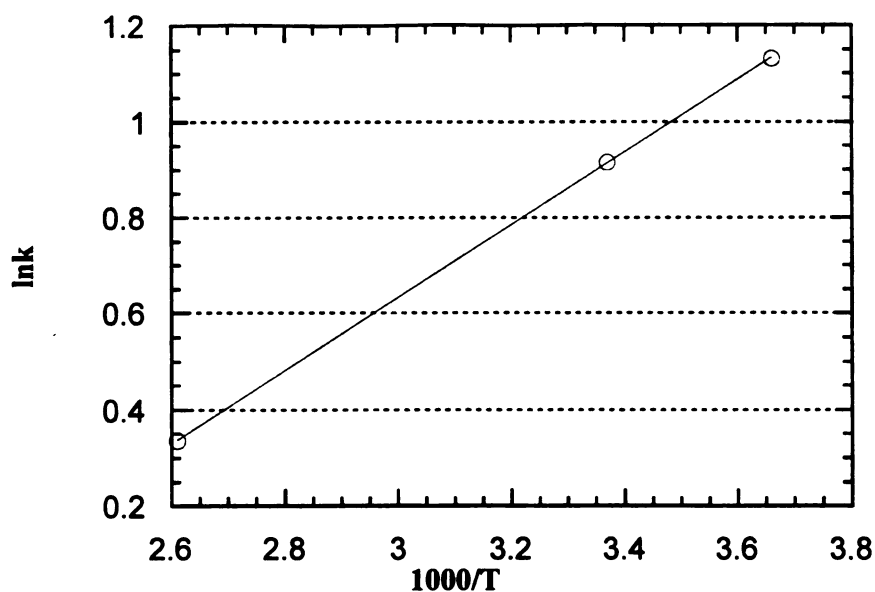
second, a higher percent of the resulting singlet biradicals cyclizing rather than disproportionating. The latter would support Wagner's suggestion that cyclization reactions have large barriers (due to loss of rotational freedom, ring strain and steric crowding around the forming bond) even on the singlet surface.⁸⁷

The decrease in the quantum efficiencies of indanol formation in the trialkyl series from mesityl to the triisopropyl can be attributed to an increasingly more efficient disproportionation of the singlet biradical as the size of the alkyl group increases (which impedes cyclization due to increased strain during cyclization).

Wagner *et al.* reported that α -mesitylacetophenone has a more rapid hydrogen abstraction but a lower indanol quantum yield than α -(*o*-tolyl)acetophenone, which they attributed to a charge-transfer quenching process competing with hydrogen abstraction in the former.⁸⁷ An increase in indanol quantum yield in the acetone series from α -tolyl to α -(*o*-ethylphenyl) to α -mesitylacetone indicates the absence of any significant charge transfer quenching process from the singlet state.

The effect of environment on the reactivity of acetones has also been addressed by Turro⁶⁷ who reports a significant increase in indanol chemical yield in micellar solutions relative to homogeneous solutions. Our results show a 25% increase in indanol yield in micellar solutions.

The conformational factors involved in hydrogen abstraction of α -arylacetoness might be expected to be similar to those for α -arylacetonophenones. However, a 2-6 fold decrease in diastereoselectivity was observed in acetones.



$$A_E/A_Z=5 \quad E_Z-E_E=1.6 \text{ kcal/mole}$$

Graph 4. Arrhenius Plot of α -(*o*-Ethylphenyl)acetone

The singlet biradicals have very short lifetimes and the ground state control might be assumed to control their reactivity. However, our results with α -(*o*-ethylphenyl) acetone seem to indicate conformational control of reactivity in photocyclization of singlet biradicals. Experimental results show the *Z*-indanol to be the major cyclization product under all conditions. Ground state global minimizations indicate the presence of two reactive geometries, a low energy in a pro-*E* and a pro-*Z* geometry 0.55 kcal/mole higher in energy (Scheme 43). Furthermore, semiempirical minimizations on the biradical of **10** show the presence of three minima within 1.8 kcal/mole of each other. The global minimum (**10A**) is not in a good geometry to cyclize, but the two higher energy

conformations can and are in a pro-Z (**10B**) and pro-E (**10C**) geometries, and can cyclize. **10C** is higher in energy than **10B** by 1.6 kcal/mole, in good agreement with the experimental values. The difference in A factors can be attributed to a faster cyclization rate of the pro-E precursor, due to its higher energy which in turn means a lower activation energy for cyclization. Therefore, the photocyclization of α -(2-ethylphenyl)acetone is believed to be conformationally controlled which means that the singlet biradical lives long enough to allow equilibration. Furthermore, the difference in the A factors indicates that there needs to be an activation energy for cyclization.

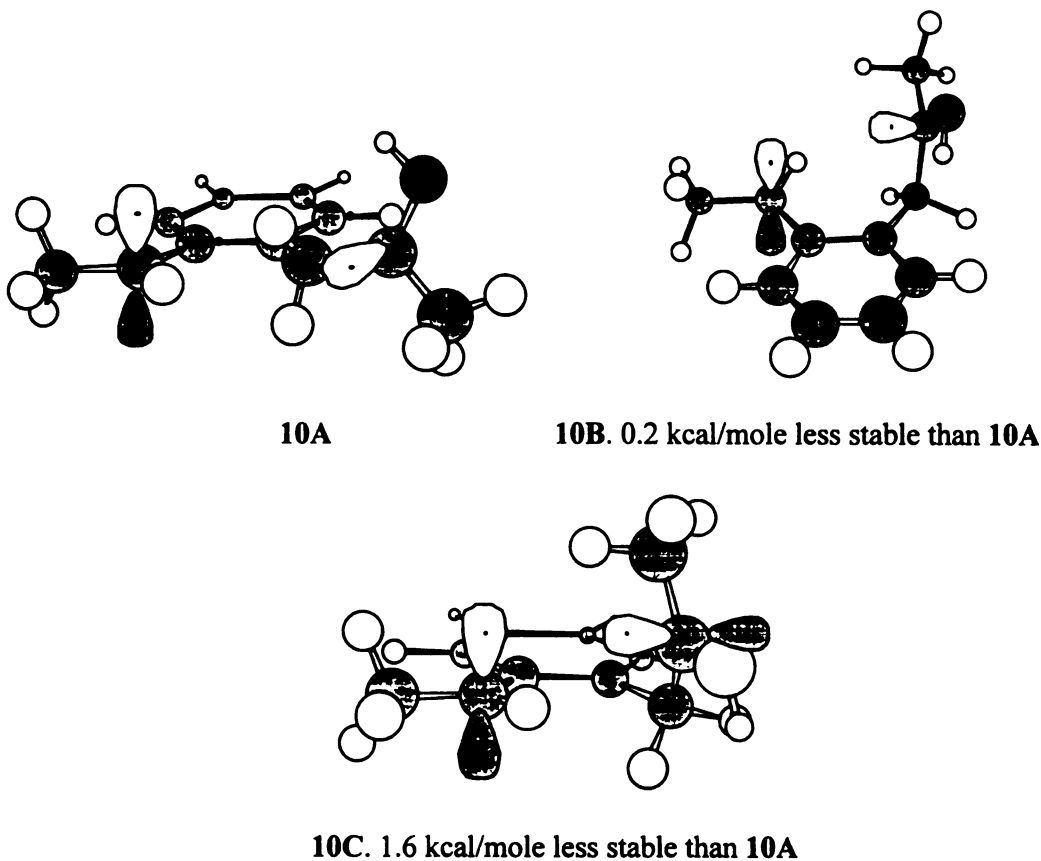
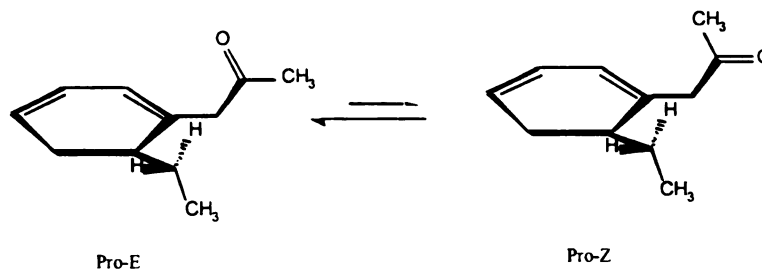


Figure 30. Lowest Energy Biradical Conformations of 10

Another explanation for the observed diastereoselectivity is that ground state control is operative but the pro-E biradical disproportionates 9 times more efficiently than the pro-Z biradical. This could be the case since the cyclization of the pro-E biradical suffers from larger steric/non-bonded interactions during the closure than the pro-Z.



Scheme 43. Reactive Ground State Conformations of 10

III. Photoenolizations of α -(2,4,6-Triisopropylphenyl)acetophenone and Acetone

Formation of enol from compound **9** had already been documented.^{36a,80,87} Our reinvestigation of this reaction along with temperature and phase effects indicate that the enol is the only initial product formed under all conditions. Furthermore, our investigation into the photobehavior of α -(2,4,6-triisopropylphenyl)acetone (**13**) reveals that enol formation also occurs from the singlet states. We have demonstrated that in both cases enol photochemically and thermally reverts back to ketone. Thus the formation of enol and its reversion to ketone with hydrogen exchange between the benzylic and α -carbons demonstrates that disproportionation involving a 1,4-hydrogen transfer can compete with cyclization. The large preference for formation of enols from **9** and **13** might be blamed on the normal steric hindrance to cyclization of two tertiary radical sites.

However, since α -(2,5-diisopropylphenyl)acetophenone cyclizes quite efficiently, the effect of the second *o*-isopropyl group warrants scrutiny.^{36a,87} The semiempirical calculations strongly suggest that the other isopropyl group forces the biradical into a geometry in which one α -hydrogen is pointed directly at the other radical site, thus inviting disproportionation. Cyclization, on the other hand, requires bond rotation which may be impeded by the second isopropyl. The fact that enol is the only product at low temperature and from crystalline **9** demands that the indanol-forming biradical conformation be different from that initially formed. The minimized geometries of ketones **9** and **13** lead to the minimum energy biradical geometries, which favor disproportionation, as just noted. For this reason, the singlet and triplet biradicals behave very similarly.

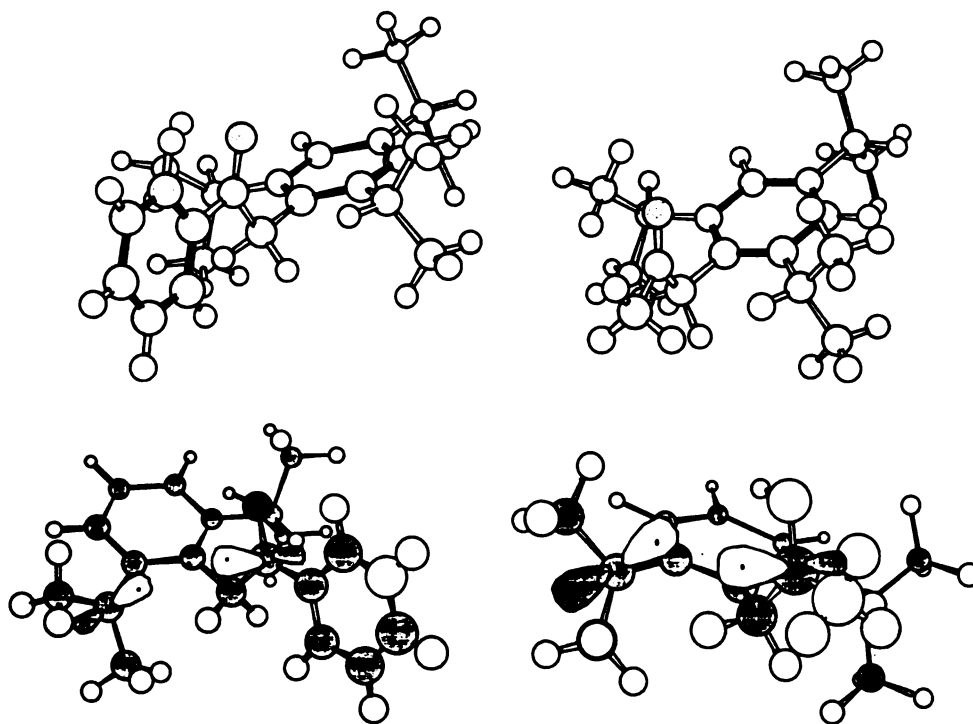


Figure 31. Lowest Energy Ground State and Biradical Conformers of 9 and 13

An explanation is required for the fact that the enol is a stable product at long wavelength irradiation but not at shorter wavelengths. A solution containing only enols, obtained by low temperature irradiation, showed strong UV absorption below 330 nm, with λ_{max} near 270 nm. Initially, the indanol is formed in low yield but the yield increases with conversion. This means that enol is converted photochemically to indanol, and is in agreement with the observed decrease in enol quantum yield with time for irradiations at wavelengths where the enol absorbs strongly. Our time dependent studies for irradiation of both ketone and enol show that indanol is not formed directly from enol but only from ketone, which must be regenerated continually from the enol. The mechanism of this disproportionation is unclear. Hart has proposed a simple 1,3-hydrogen shift, which seems reasonable even though the trimethylsilyl enol ether of **9** does not undergo the same 1,3-shift.

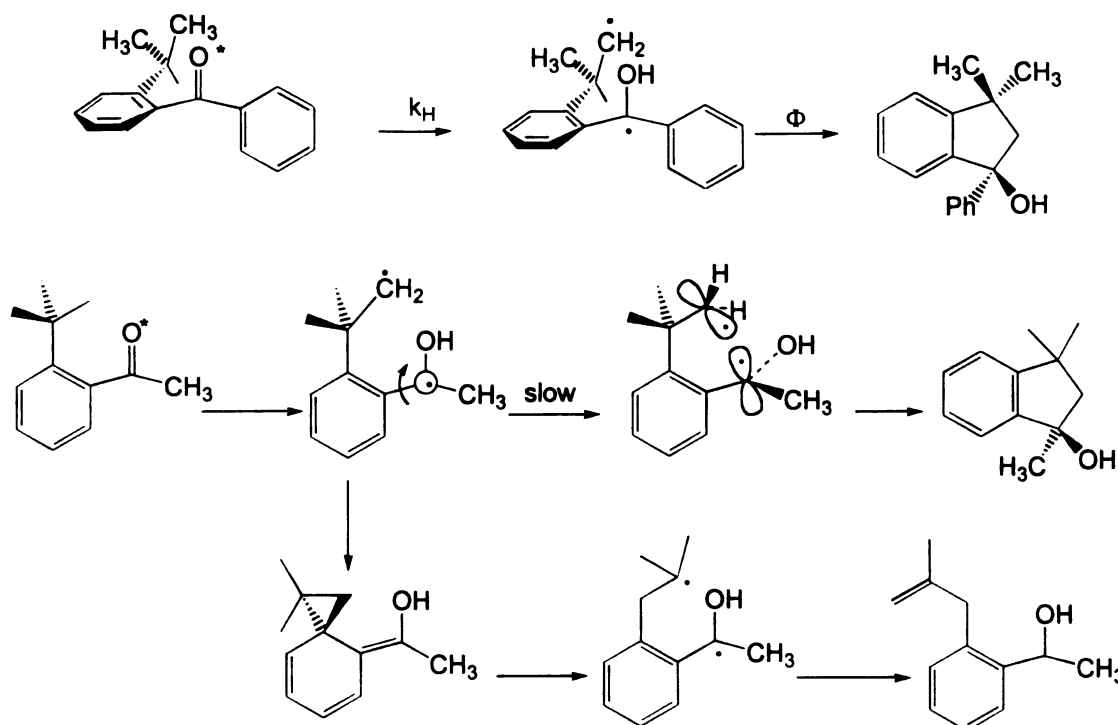
For ketone **13**, α -cleavage is the only photoreaction at low temperature. This demonstrates that there is an enthalpic barrier to hydrogen abstraction, whereas intersystem crossing has none. Thus, as temperature decreases, the intersystem crossing to a triplet that undergoes only radical cleavage becomes predominant. The overall quantum efficiency is low for **13** because of the well known highly efficient radiationless decay that accompanies singlet state hydrogen transfers.¹¹ The stability of solid **13** is attributed to the large ground state C=O---H distance (3.2 Å).

We have considered the possibility of similar enol formation for the other α -aryl acetones and acetophenones studied. In our investigations, however, we were unable to detect any, except maybe for α -(2,4,6-triethylphenyl)acetone where a vinyl peak was

observed in the NMR spectrum of the photolysis mixture but disappeared too quickly to allow careful analysis. The less hindered enols are expected to be much less stable with respect to ketone and if formed apparently are too short-lived to detect.

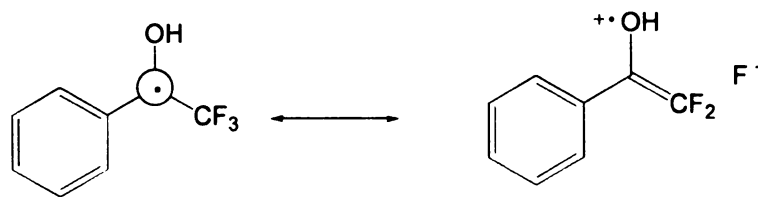
IV. Photobehavior of *o*-*tert*-Butyltrifluoroacetophenone

Wagner *et al.* reported a sharp contrast in the photobehavior of *o*-*tert*-butylacetophenones and benzophenones.^{54,56} Irradiation of benzophenones results in efficient formation of indanols while that of acetophenones results mainly in an unsaturated alcohol. Rotation of the 1,5-biradical produced by δ -hydrogen abstraction in *o*-*tert*-butylphenyl ketones is necessary for cyclization but destroys the benzylic conjugation. π -Conjugation is more important in excited states than in ground state.¹⁰⁴ In the benzophenone derivatives, the benzylic radical center of the biradical can remain unconjugated with the unsubstituted phenyl ring while the butylphenyl ring rotates. The absence of the second phenyl ring in the acetophenone derivatives causes a retarded rotation. Thus, the difference in behavior was attributed to the retarded rotation of the benzylic center of the biradical which slows down the indanol formation and allows the biradical to undergo a less favorable reaction, namely rearrangement to an unsaturated alcohol. The authors cited two possibilities for the formation of the unsaturated alcohol, disproportionation of a rearranged 1,5-biradical or a 1,5-sigmatropic hydrogen shift in a spiroenol.⁵⁴



Scheme 44

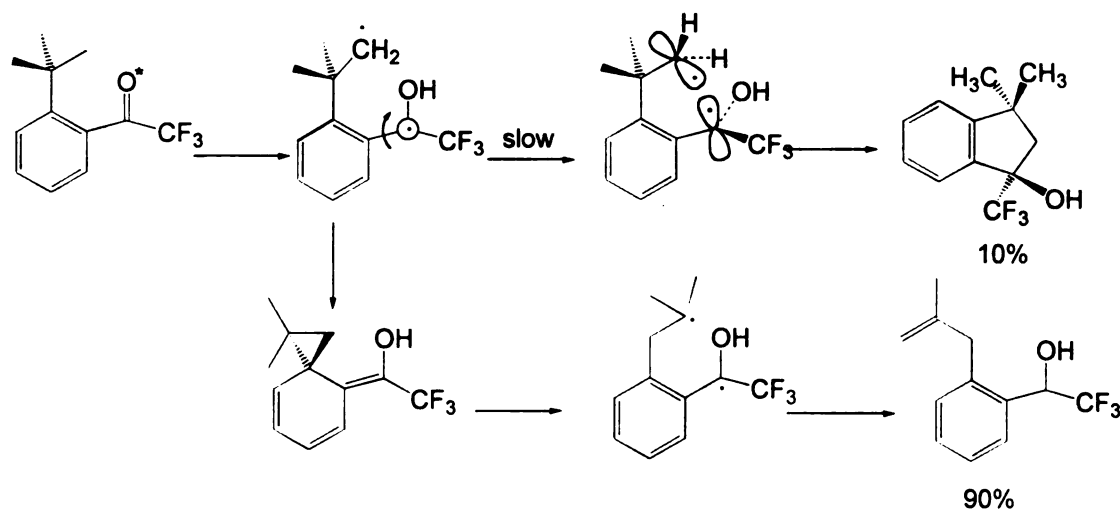
The photobehavior of *o*-*tert*-butyltrifluoroacetophenone was investigated to determine whether the capto-dative resonance of the benzylic radical center to the trifluoromethyl group is sufficient to allow a free rotation of the benzylic center, leading to an indanol as a major product.



Scheme 45

Our results clearly indicate that capto-dative resonance is not sufficient to allow a free rotation of the benzylic radical center since the unsaturated alcohol comprised ~90%

of the products in all solvents. Our calculated barrier to rotation of the benzylic radical center of acetophenone and trifluoroacetophenone totally out of conjugation is 8 kcal/mole. If the benzylic center has to rotate only 45° to get into a geometry suitable for cyclization the barrier drops to 4 kcal/mole. Clearly, capto-dative resonance does not provide 4 kcal/mole stabilization to speed up cyclization process, thus the less favorable rearrangement to unsaturated alcohol remains the predominant relaxation pathway.



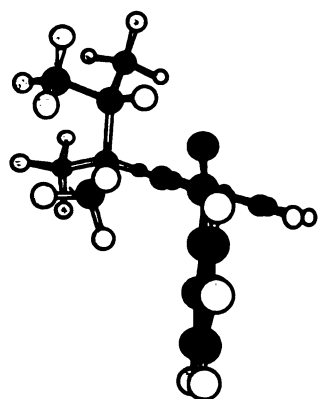
Scheme 46

V. Photobehavior of 2-(2'-(2',3'-Dimethylbutyl))benzophenone - Effect of Dihedral Angle on Hydrogen Abstraction Rates

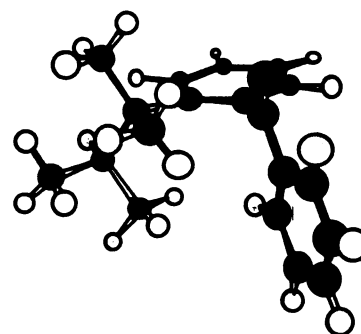
The primary purpose of this study was to gain insight into the orbital orientational requirements for hydrogen abstraction by triplet carbonyls.

Global minimizations (AM1) with dihedral drivers around phenyl-*tert*-carbon bond have revealed the presence of two distinct minima on the energy surface of **15** (Figure 32). The lowest energy minimum (**15A**) has the isopropyl group perpendicular to

the plane of the phenyl and occupying the same side of the plane as the carbonyl oxygen. In this geometry both isopropyl (H_A , $d= 2.3 \text{ \AA}$) and methyl hydrogens (H_B , $d= 2.5 \text{ \AA}$) are close enough for abstraction. In the other minimum (**15B**), which lies 1.0 kcal/mole above **15A**, only methyl hydrogens ($d=2.3 \text{ \AA}$) are close enough for abstraction. The global minimum **15A** has a geometry similar to the X-ray structure of OTAMPB.⁵⁷



15A. Lowest Energy Geometry of 15



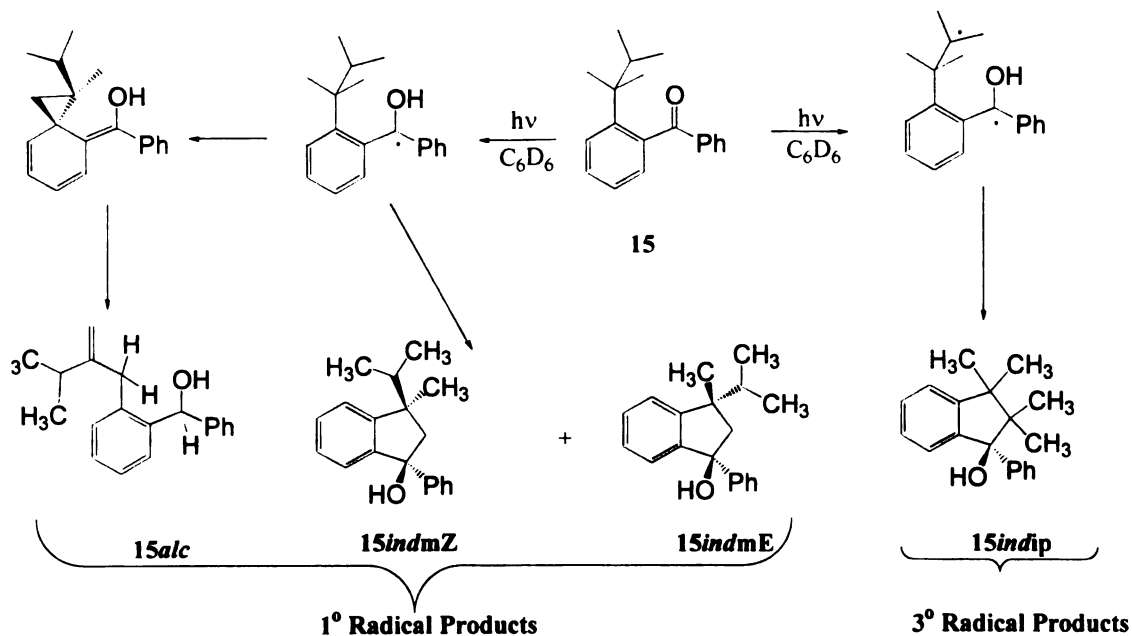
15B. 1.0 kcal/mole less stable than 15A

Figure 32

Our calculations have revealed that a methyl hydrogen is within abstraction distance of the carbonyl oxygen over a wide range of geometries. Scheffer¹⁰⁵ has established that distance is the principal determinant of reactivity,¹⁰⁶ so the reaction can occur from a geometry other than the two minima. However, the very low activation energy for triplet decay in OTBBP⁵⁶ rules out more than slight departures from conformational minima in reaching the transition state. Despite favorable distances, the methyl hydrogens have different dihedral angles with respect to the nodal plane of the carbonyl in the two minima. In **15A**, the angle ω is 96° while in **15B** ω is 79° . If we

consider a $\cos^2\omega$ dependence on reactivity, as has been proposed by Wagner,⁴⁸ methyl hydrogens in both conformations should be unreactive toward abstraction. Despite this, **15** forms indanol photoproducts that represent 50-90% hydrogen abstraction from a poorly positioned methyl group. Even in the crystalline state 50% of the products originate from methyl abstraction. It is conceivable that the flexibility of the *tert*-hexyl group might cause significant improvements in ω at the transition state relative to the reactant. It is also noteworthy that the reactant is the triplet, not the ground state on which the calculations have been performed. This, however, shouldn't alter our treatment since the only significant change in geometry due to n,π^* excitation is slight lengthening of the C-O bond.¹⁰⁷

Biradical Partitioning. The quantitative treatment of our results involves converting product ratios into relative rate constants for hydrogen abstraction. Scheme 47 depicts the competition that produces the observed product ratios. The product ratios are determined by the ratios of hydrogen abstraction rates times the partitioning of biradical between coupling and reversion back to ketone. An extra feature of the photobehavior of **15** is the formation of **15alc**. To our knowledge, such intermediates (spiro-intermediate) and photoproducts have been observed for *o*-alkoxy and *o-tert*-butylacetophenones but not benzophenones.⁵⁴ Formation of the unsaturated alcohol from a spiro intermediate in 2,4-di-*tert*-butylacetophenone has quantum efficiencies of 0.02-0.05 in benzene and methanol.⁵⁴ Thus, the biradical and the spiro intermediate revert back to starting ketone with a combined 95-98% efficiency.



Scheme 47

If one considers that the biradical from OTBBP forms the indanol product with a quantum efficiency of 1 and that both biradicals from OTBBP and 2,4-di-tert-butylacetophenone are solvated to the same extent, we can conclude that all of the 95% disproportionation back to ketone in methanol arises from the spiro intermediate. However, such values are not available for benzophenone derivatives and the mechanism of reversion of the spiro-intermediate back to ketone (radical or ionic) is unknown. Thus, for simplicity, two boundary conditions have been considered:

a) The spiro-intermediate which leads to formation of **15alc** has a quantum efficiency of 1 for product formation, so that all partitioning is presumed to occur in the biradical. Thus product ratios can be determined using Equation 5.

$$1/3 = (15indmZ + 15indmE + 15alc) / 15indip = (k_{meH} / k_{ipH}) (P_{Br1} / P_{br3})$$

Equation 5

One must understand how the P_{Br1}/P_{Br3} ratio can vary in order to correctly deduce k_{mcH}/k_{ipH} ratios from product ratios. There is a large solvent effect on product ratios and quantum efficiencies.

Table 27. Effect of temperature and Medium on Product Ratios of 15

Reaction media	T (°C)	15indmZ	15indmE	15alc	15indip
Benzene	24	27	52	7	15
Methanol	24	32	32	13	23
Toluene	110	22	29	8	41
Toluene	-72	33	48	5	15
solid	24	23	27	-	50

This solvent effect shows that the two biradicals cyclize with different efficiencies. In benzene, all biradicals from OTBBP, OTAMBP and **15** disproportionate to starting ketone with high efficiency. In methanol, all of the biradicals from OTBBP cyclize but not quite half of those from OTAMBP and **15** cyclize. The P_{Br} value for the biradical from OTBBP is 0.04 in benzene but rises to unity in methanol, where hydrogen bonding to solvent suppresses biradical disproportionation back to the ground state ketone. Similarly, the P_{Br} value for a solvated biradical is unity in OTAMBP, while those for unsolvated biradicals are 0.05 and 0.028 for a primary (methyl) and secondary (ethyl) radicals, respectively. The low quantum yields for **15** and the methanol induced increase

in the yield of **15indip** suggest that P_{Br_3} cyclizes less efficiently than does P_{Br_1} . The fact that P_{Br_3} is more sterically crowded than P_{Br_1} will lead to a lower rate of cyclization in unsolvated biradicals. This point will be emphasized when the temperature effects on product ratios are considered.

Since methanol increases the total quantum yield of **15** only to 42%, its biradicals, similar to those of OTAMPB, hydrogen bond to solvent less efficiently than the less sterically crowded biradical of OTBBP. Because methanol traps only 42% of biradicals, we rely on an estimate of Br_3/Br_1 for the 58% that still revert to starting ketone. We have assumed two boundary conditions, described below, in order to calculate the ratios of hydrogen abstraction rates.

One option is to assume that all primary biradicals cyclize with 100% efficiency in methanol as is the case for the biradical from OTBBP. In this case, Br_3/Br_1 is 2.2 and P_{Br_3}/P_{Br_1} becomes 6 and 19 in methanol and benzene, respectively. Therefore, k_{Hip}/k_{Hmc} is calculated to be 2.24 in methanol and benzene. However, this treatment would demand an unlikely P_{Br_1} value of 0.27 in benzene, seven times higher than that of OTBBP ($P_{Br} = 0.04$ in benzene).

$$\Phi_{1(\text{benzene})} = 0.0835 \quad \Phi_{1(\text{methanol})} = 0.309 \quad \Phi_{2(\text{benzene})} = 0.01 \quad \Phi_{2(\text{methanol})} = 0.107$$

$$Br_3/Br_1 = 69/31 = 2.2$$

In Methanol:

$$P_{Br_1}/P_{Br_3} = 1/0.155 = 6.45$$

$$k_{Hip}/k_{Hmc} = 2.24$$

In Benzene:

$$P_{Br_1}/P_{Br_3} = 0.27/0.015 = 18.75$$

$$k_{Hip}/k_{Hmc} = 2.24$$

Scheme 48

Another option is to assume that the $k_{\text{Hip}}/k_{\text{Hmc}}$ is the same as the product ratios. Partial suppression of disproportionation is common in bulky hydroxybiradicals and is thought to reflect an equilibrium between hydrogen-bonded and free biradicals, with none of the former disproportionating. Since Br_1 and Br_3 share a common conformational preference, the equilibrium constant for solvation should be similar for both biradicals and the Br_3/Br_1 ratio should approximate $k_{\text{Hip}}/k_{\text{Hmc}}$. In this situation, P_{Br_1} and P_{Br_3} become 0.108 and 0.05 respectively for the unsolvated biradicals. It is important to note that ~95% of the reaction in methanol arises from the solvated biradicals.

$$\Phi_{1(\text{benzene})} = 0.0835 \quad \Phi_{1(\text{methanol})} = 0.309 \quad \Phi_{2(\text{benzene})} = 0.01 \quad \Phi_{2(\text{methanol})} = 0.107$$

$$k_{\text{Hmc}}/k_{\text{Hip}} = 77/23$$

In Methanol: $\Phi_1/\Phi_3 = (77/23)\{0.34 + 0.67(0.108)/0.34 + 0.66(0.05)\} = 0.309/0.107$

In Benzene: $\Phi_1/\Phi_3 = (77/23)(0.108/0.05) = 0.0835/0.01$

Scheme 49

b) It has been assumed that ~90% of the spiro intermediate formed in methanol reverts to the starting ketone, similar to the acetophenone derivatives. The percent of biradicals which form indanol becomes 39% and the efficiency of indanol formation from this fraction is 0.91 if one considers that all solvated primary biradicals form product with 100% efficiency. The $k_{\text{Hmc}}/k_{\text{Hip}}$ value is 1.78 in benzene and methanol.

$$\Phi_{1\text{ind}(\text{benzene})} = 0.0775 \quad \Phi_{1\text{ind}(\text{methanol})} = 0.248 \quad \Phi_{2(\text{benzene})} = 0.01 \quad \Phi_{2(\text{methanol})} = 0.107$$

$$\Phi_{1\text{Salc}(\text{benzene})} = 0.006 \quad \Phi_{1\text{Salc}(\text{methanol})} = 0.061 \quad P_{\text{Br-spiro}(\text{methanol})} = 0.61$$

$P_{\text{Br-ind(methanol)}} = 0.39$	$\Phi_{\text{ind(methanol)}} = 0.355$	Efficiency = $0.355/0.39 = 0.91$
	$\text{Br}_3/\text{Br}_1 = 25/15 = 1.78$	
In Methanol:	$P_{\text{Br1}}/P_{\text{Br3}} = 1/0.75 = 1.34$	$k_{\text{Hip}}/k_{\text{Hmc}} = 1.78$
In Benzene:	$P_{\text{Br1}}/P_{\text{Br3}} = 0.31/0.07 = 18.75$	$k_{\text{Hip}}/k_{\text{Hmc}} = 1.78$

Scheme 50

The high efficiency of indanol formation in methanol for **15** is similar to that of OTBBP.⁵⁶ The low quantum yields for product formation in OTAMBP relative to OTBBP was surprising and no products arising from the spiro intermediate was observed. However, based on our results from **15**, an explanation for the low observed quantum efficiencies in OTAMBP can be offered. It is believed that spiro intermediate is indeed formed in OTAMBP, but that it disproportionates back to ketone with a higher efficiency than **15**, and thus no products stemming from the spiro compound could be observed. Formation of the spiro intermediate from the biradical only allows a fraction of biradicals to be available for cyclization. It is also believed that this fraction is very close to the observed quantum yield of 0.42 and that the indanol formation from solvated biradicals is highly efficient.

Temperature Effects. The lack of change in product ratios as temperature decreases indicates that hydrogen abstraction is derived by relief of steric strain, as proposed by Wagner, rather than by intrinsic CH reactivity.⁵⁷ The fact that the amount of **15indip** increases 3-fold at high temperature but is unchanged at low temperature, reflects a higher efficiency of tertiary biradical closure at higher temperatures. It is, however, conceivable that changes in conformational equilibria can affect the observed relative

rates for hydrogen abstraction.^{11,108} For example if **15B**, in which only a methyl can react, is slightly lower in energy in certain solvents (due to solvation) than **15A**, then the 1/3 ratio would increase with change in solvent provided that no change in P values also occur. This effect along with changes in P values due to solvation can account for different 1/3 ratios in methanol and toluene.

Phase Effects. Lower selectivity is observed in the crystal than in solution. The solid state product ratios can not easily be converted into $k_{\text{Hme}}/k_{\text{Hip}}$ ratios, since quantum efficiencies and biradical lifetimes are not available in the solid. If all biradicals have similar P_{Br} values, then $k_{\text{Hip}}/k_{\text{Hme}} = 1.0$. If the *tert*-hexyl rotation is slow in the solid, then the competition between rotation of Br_2 into a geometry necessary for cyclization and disproportionation back to ketone may be even less favorable than in solution, where bond rotations are rapid but cyclization is only 2-5% efficient. Since Br_1 does not need to rotate, its partitioning should be independent of the environment. The solvent effects on product ratios suggest different biradical partitioning efficiencies, thus $k_{\text{Hip}}/k_{\text{Hme}}$ should be much higher than unity and closer to the solution values.

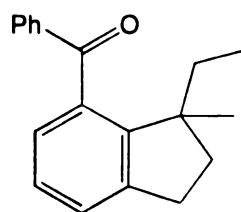
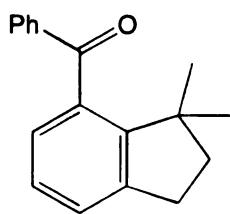
Diastereoselectivity. The lower diastereoselectivity of Br_1 in methanol is attributed to the solvation of hydroxy biradicals to Lewis bases which is known to greatly influence the diastereoselectivity of their cyclization. A variety of 1,4- and 1,5-biradicals that show significant preferences for cyclizing with alkyl group trans to phenyl in hydrocarbon solvents show reduced selectivity in alcohols.^{33,80,109,110} Br_1 shows a large 2.0 E/Z selectivity in benzene and toluene but almost no selectivity in methanol. In solid, the observed selectivity always reflects a least-motion picture of biradical cyclization and in

most cases shows enhanced diastereoselectivity relative to solution.¹¹¹ The general conclusion is that low molecular flexibility in crystals may reduce but not totally prevent inversion of radical sites by rotation. Br₁, however, does not show an appreciable selectivity in solid. This can be explained in two ways: either photochemistry occurs at defect sites or the *tert*-hexyl bond rotations in solid are faster than biradical cyclization.

The lower 1/3 ratio in solid compared to solution reinforces our assumption that bond rotations in solid are faster than cyclization. In the solid, one would expect P_{Br3} to be lower than solution due to rotations necessary for cyclization, thus the significant amount of **3** obtained in the solid either reflects a higher hydrogen abstraction rate, similar bond rotation rates as solution, or a combination of both. The higher hydrogen abstraction rates in solid may reflect predominant population of **15A** in which isopropyl hydrogen is in good geometry for abstraction. One would expect **15A** to be the predominant conformation at low temperature in solution as well, however, the ratios of 1/3 did not change much from those at room temperature. Since we don't know the effect of solvation on various conformations, we tentatively suggest that a combination of predominant population of **15A** and fast bond rotations is responsible for the low 1/3 ratios in solid. The apparent absence of **15alc** may represent a topochemically unfavorable reaction for formation of spiro intermediate.

Our results indicate that significant amount of reaction takes place at methyl hydrogen oriented at $\omega = 90^\circ$ at ground state. It is possible, however, that conformational flexibility causes $\omega < 90^\circ$ in solution and to a lesser extent in solid. In order to better address the effect of dihedral angle on hydrogen abstraction rates, molecules with low molecular

flexibility with hydrogens at $\omega=90^\circ$ angles with respect to nodal plane of carbonyl need be synthesized. A few examples of such molecules are given below:



Experimental

I. General Procedures

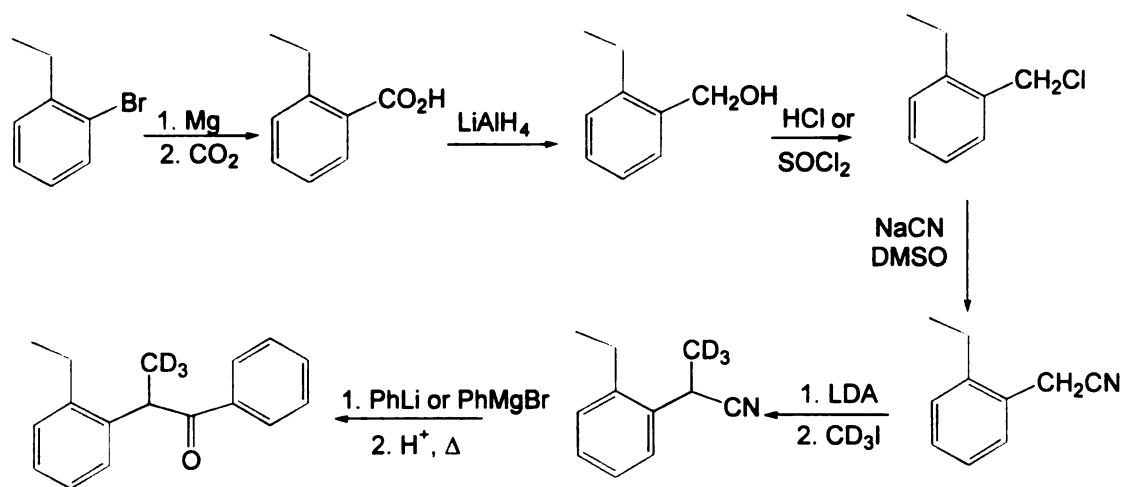
^1H and ^{13}C NMR spectra were obtained using either a 300 MHz Varian Gemini, a 300 MHz Varian VXR-300 or a 500 MHz Varian VXR-500 instrument. IR spectra were recorded using solutions in CCl_4 or CHCl_3 on a Nicolet IR-42 Fourier Transform IR spectrometer. UV spectra were recorded on a Shimadzu UV-160 spectrometer. Low resolution mass spectra were recorded on a Hewlett-Packard 5890 GC/MS Trio-1 and high resolution mass spectra were obtained using a Joel JMS-HX110 Mass spectrometer in the MSU Mass Spectroscopic facility. The electron impact (EI) and direct probe methods were used.

Gas chromatographic analyses were performed on a Varian 1400 or 3400 machine with flame ionization detectors. The GC was connected to a Hewlett-Packard 3393A or 3392A Integrating recorder. Two types of columns were used for GC analysis; Megabore DB1 and Megabore DB225. HPLC analyses were performed on a Rainin apparatus equipped with a Dynamax UV-D absorbance detector using a silica column. For the preparative TLC, Analtech Uniplate silica gel plates (20 x 20 cm, 1000 micron) were used.

II. Preparation of Starting Ketones

α -(2-Ethylphenyl)- β,β,β -trideuteropropiophenone (**4d₃**)

α -(2-Ethylphenyl)- β,β,β -trideuteropropiophenone was prepared by the reaction of the phenyl Grignard reagent with *o*-ethylphenyl- β,β,β -propionitrile following the route given below. Attempts to make this compound from α -(2-ethylphenyl)acetophenone, LDA and methyl iodide resulted in O-methylation.



Scheme 51. Synthesis of α -(2-Ethylphenyl)propiophenone

2-Ethyl benzoic acid

In a 250 mL three necked round bottom flask equipped with a condenser and purged with argon was placed 2.0 grams (0.085 moles) of oven dried magnesium and 10 mL of freshly distilled ether. A solution of 2-ethylbromobenzene (13 g, 0.07 moles, Aldrich) in ether was added dropwise over a period of an hour to the magnesium. The reaction was initiated with a heat gun or by adding small amounts of 1,2-dibromoethane.

After the addition was complete, the mixture was allowed to stir at room temperature for an hour and was refluxed for two hours to ensure the Grignard formation. A large excess of dry ice was completely ground with a pestle. After the Grignard had cooled to room temperature, it was poured into a flask containing the freshly ground dry ice. The resulting slush was stirred vigorously and was allowed to warm to room temperature. The work-up consisted of adding 50 mL of 10% HCl to the mixture and separating the layers. The organic layer was then washed with water and dilute alkali solution. The alkaline layer was acidified with 10% HCl solution until a white precipitate could be observed. The precipitate was extracted into ether, and the ether layer was washed twice with water and dried over anhydrous magnesium sulfate. Solvent was removed to afford 6.1 g (58% yield) of product as an oily solid. This solid was used without further purification in the next step.

$^1\text{H NMR}(\text{CDCl}_3)$: $\delta(\text{ppm})$ 1.15 (t, 3H), 2.96 (q, 2H), 7.1-7.4 (m, 3H), 7.91 (d, 1H)

IR(CCl_4): 3400 (broad), 2976, 2876, 1695, 1576, 1530

2-Ethylbenzyl alcohol

A solution of 2-ethylbenzoic acid (6.1 g, 0.041 moles) in 20 mL of anhydrous ether was added dropwise over a period of 30 minutes to a stirred suspension of lithium aluminum hydride (3.34 g, 0.088 moles) in 100 mL of anhydrous ether under an argon atmosphere. The resulting mixture was stirred at room temperature for an hour and was refluxed for 7 hours before being cooled to room temperature. The excess lithium aluminum hydride was decomposed with careful addition of ice. Acidic workup afforded

5.1 grams (92% yield) of product as a yellow oil which was used without purification in the next step.

$^1\text{H NMR}(\text{CDCl}_3)$: δ 1.25 (t, 3H), 2.72 (q, 2H), 2.12 (broad s, 1H), 4.73 (s, 2H), 7.2-7.4 (4H, m)

$\text{IR}(\text{CCl}_4)$: 3618, 3067.2, 2970.7, 2876.2, 1550.9, 1253.8, 1217.2, 1062.9, 1003.1

2-Ethylbenzyl chloride

In a 250 mL round bottom flask was placed 5.1 grams (0.038 moles) of 2-ethylbenzyl alcohol and 200 mL of concentrated hydrochloric acid. The mixture was stirred at room temperature overnight. The mixture was then slowly added to 500 mL of cold water and was extracted with two 50 mL portions of ether. The combined organic layer was washed with water, saturated sodium bicarbonate and saturated sodium chloride solutions and was dried over anhydrous magnesium sulfate. Solvent was evaporated to yield 5.8 grams (100% yield) of product as a dark yellow oil which was used without purification in the next step.

$^1\text{H NMR}(\text{CDCl}_3)$: δ 1.12 (t, 3H), 2.63 (q, 2H), 4.48 (s, 2H), 7.0-7.3 (m, 4H)

α -(2-Ethylphenyl) acetonitrile

2.0 Grams (0.04 moles) of sodium cyanide was added to a flask containing 150 mL of dimethylsulfoxide. The mixture was heated to 80-90°C until all of the sodium cyanide dissolved at which time a solution of 2-ethylbenzyl chloride (5.8 grams, 0.038 moles) in DMSO was added dropwise over a period of an hour. The mixture was heated at 80-90°C for an additional 5 hours and then allowed to cool to room temperature. The

mixture was poured into a flask containing 500 mL of cold water. The aqueous layer was washed with two 50 mL portions of ether. The combined ethereal layer was washed 10 times with water and dried over anhydrous magnesium sulfate. Solvent was evaporated to afford 5.5 grams (100% yield) of a yellow oil which was used without purification in the next step.

$^1\text{H NMR}(\text{CDCl}_3)$: δ 1.23 (t, 3H), 2.68 (q, 2H), 3.71 (s, 2H), 7.2-7.4 (m, 4H)

$\text{IR}(\text{CCl}_4)$: 2961.1, 2856.9, 2253, 1261.6, 1010.8

α -(2-Ethylphenyl)- β,β,β -trideuteriopropionitrile

In a 100 mL round bottom flask equipped with a condenser and purged with argon was placed 20 mL of dry THF along with 4.1 grams (0.041 moles) of diisopropyl amine. The solution was cooled in an ice water bath. Butyl lithium (29 mL of 1.4 M solution) was added dropwise to the mixture and it was allowed to stir at 0°C for an additional 30 minutes to ensure the complete formation of LDA. The mixture was then cooled to -78°C in an acetone/dry ice bath while a solution of α -(2-ethylphenyl)acetonitrile (5.5 g, 0.038 moles) in THF was added dropwise. The solution turned dark-red in color. The solution was allowed to warm to room temperature and stir for 2 hrs. before 2.5 mL of CD_3I (5.8 g, 0.04 moles) was added. The mixture was stirred at room temperature for an hour and was refluxed overnight. The solvent was removed to leave an oily residue which was washed with ether/water mixture. The layers were separated and the water layer was washed twice with ether. The combined organic layer was washed with water and dried over anhydrous magnesium sulfate. Solvent was removed to yield 4.3 grams (70%) of a

brown oil. Kugelrohr distillation of the brown oil resulted in recovery of 4.1 g of product as a colorless liquid.

$^1\text{H NMR}(\text{CDCl}_3)$: δ 1.28 (t, 3H), 2.69 (q, 2H), 4.11 (broad s, 1H), 7.2-7.5 (m, 4H)

$\text{IR}(\text{CCl}_4)$: 3155.9, 2985.2, 2902.3, 2254.1, 1470.9, 1383.2, 1096.7

α -(2-Ethylphenyl)- β,β,β -trideuteriopropiophenone

A solution of α -(2-ethylphenyl)- β,β,β -trideuteriopropionitrile (4.1 g, 0.025 moles) in 30 mL of anhydrous ether was added dropwise over a period of 30 minutes to a stirred solution of phenyl magnesium bromide (prepared from 5.18 g (0.033 moles) of bromobenzene and 0.8 g (0.033 moles) of magnesium in 50 mL of anhydrous ether). After the addition was complete, the mixture was refluxed for 10 hours and allowed to cool to room temperature. The mixture was then added to 100 mL of 10% HCl and layers were separated. The aqueous layer was placed in a round bottom flask and was heated at 90°C overnight. The mixture was allowed to cool to room temperature, ether was added and layers were separated. The aqueous layer was washed twice with ether and the combined organic layer was washed with water, saturated sodium bicarbonate, and saturated sodium chloride solutions. The organic layer was then dried over anhydrous magnesium sulfate. Solvent removal resulted in a yellow oil which after chromatography (by flash chromatography using 97:3 hexane/ethylacetate solution as eluent) afforded 2.9 grams (48% yield, 0.012 moles) of pale-yellow oil which crystallized upon cooling in the refrigerator.

$^1\text{H NMR}(\text{CDCl}_3)$: δ 1.32 (t, $J= 7.5\text{Hz}$, 3H, CH_3), 2.84 (AB quartet of q, $J= 7.6, 4.5\text{Hz}$, 2H, CH_2), 4.78 (broad s, 1H, CHCD_3), 7.04 (dt, $J= 7.8\text{ Hz}$, $J= 1.71\text{ Hz}$, 2H, Ar), 7.15 (dd, $J= 6.7, 1.71\text{ Hz}$, 1H, Ar), 7.20 (broad d, 1H, Ar), 7.32 (dd, $J= 7.14\text{ Hz}$, $J= 7.62\text{ Hz}$, 2H, Ar), 7.41 (t, $J= 7.6\text{ Hz}$, 1H, Ar), 7.82 (d, $J= 7.11\text{ Hz}$, 2H, Ar)

$^2\text{H NMR}(\text{CDCl}_3)$: δ 1.18 (s, 3D)

$^{13}\text{C NMR}(\text{CDCl}_3)$: δ 15.11, 18.15 (septet, CD_3), 25.46, 43.76, 126.49, 126.99, 127.17, 128.38, 128.46, 128.96, 132.53, 136.72, 139.30, 140.37, 201.15

$\text{IR}(\text{CCl}_4)$: 3067, 3026, 2967, 2928, 2876, 2233, 1686, 1217, 1006

m.p.: 36-38°C

HRMS: 241.15429 calculated for $\text{C}_{17}\text{H}_{15}\text{D}_3\text{O}$; found: 241.1547

α -(2-Ethylphenyl)propiophenone (4)

α -(2-Ethylphenyl)propiophenone was synthesized using the same procedure as α -(2-ethylphenyl)- β,β,β -trideuteropropiophenone with the exception of using methyl iodide instead of CD_3I .

$^1\text{H NMR}(\text{CDCl}_3)$: δ 1.32 (t, $J= 7.5\text{Hz}$, 3H, CH_3), 1.49 (d, $J=6.8\text{ Hz}$, 3H, CH_3CH), 2.84 (AB quartet of q, $J= 7.6, 4.5\text{Hz}$, 2H, CH_2), 4.78 (q, $J= 6.8\text{ Hz}$, 1H, CHCH_3), 7.04 (dt, $J= 7.8\text{ Hz}$, $J= 1.71\text{ Hz}$, 2H, Ar), 7.15 (dd, $J= 6.7, 1.71\text{ Hz}$, 1H, Ar), 7.20 (broad d, 1H, Ar), 7.32 (dd, $J= 7.14\text{ Hz}$, $J= 7.62\text{ Hz}$, 2H, Ar), 7.41 (t, $J= 7.6\text{ Hz}$, 1H, Ar), 7.82 (d, $J= 7.11\text{ Hz}$, 2H, Ar)

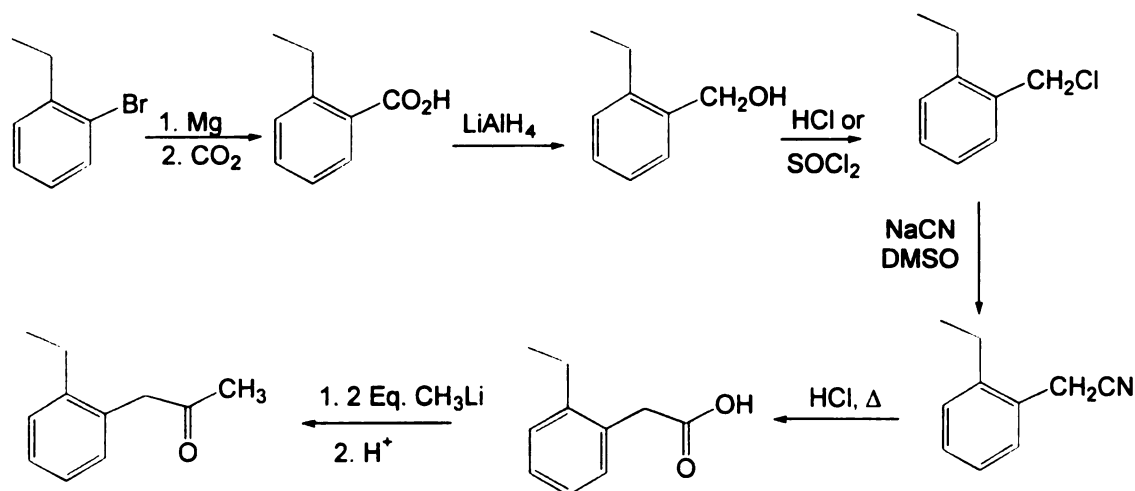
$^{13}\text{C NMR}(\text{CDCl}_3)$: δ 15.11, 18.15, 25.46, 43.76, 126.49, 126.99, 127.17, 128.38, 128.46, 128.96, 132.53, 136.72, 139.30, 140.37, 201.15

IR(CCl_4) : 3067, 3026, 2967, 2928, 2876, 1686, 1217, 1006

m.p.: 36-38°C

α -(2-Ethylphenyl)acetone (10)

α -(2-Ethylphenyl)acetone was prepared by the reaction of methyl lithium and α -(2-ethylphenyl)acetic acid following the route given below:



Scheme 52. Synthesis of α -(2-Ethylphenyl)acetone

α -(2-Ethylphenyl)acetic acid

In a 250 mL round bottom flask equipped with a condenser was placed 5.0 g (0.035 moles) of α -(2-ethylphenyl)acetonitrile along with 200 mL of concentrated hydrochloric acid. The mixture was refluxed for 48 hours, allowed to cool to room temperature and was poured slowly into a flask containing 500 mL of ice cold water. The aqueous layer was extracted with ether several times and the combined ether layer was washed twice with 5% NaOH solution. The alkaline layer was acidified with 10% HCl

solution until a white precipitate could be observed. The precipitate dissolved upon ether extraction and the organic layer was washed with water and saturated sodium chloride solutions and dried over anhydrous magnesium sulfate. Solvent was evaporated to leave 3.5 g (60% yield, 0.021 moles) of product as white powder which was used without purification in the next step.

$^1\text{H NMR}(\text{CDCl}_3)$: δ 1.2 (t, 3H), 2.65 (q, 2H), 3.68 (s, 2H), 7.1-7.2 (m, 4H)

$\text{IR}(\text{CCl}_4)$: 3350, 2960, 1686, 1456.4, 1201.8, 1057.2

α -(2-Ethylphenyl)acetone

To a solution of α -(2-ethylphenyl)acetic acid (3.5 g, 0.021 moles) in 50 mL anhydrous ether at 0°C under an argon atmosphere, was added 36 mL of 1.4 M methyl lithium. The mixture was allowed to warm to room temperature and was stirred overnight. The mixture was then poured into a flask containing 30 mL of 10% HCl and was stirred for 30 minutes before layers were separated. The aqueous layer was washed with ether twice and the combined organic layer was washed with water and saturated sodium chloride solution and dried over anhydrous magnesium sulfate. Solvent was removed to yield 2.7 g (80%) of product as a pale yellow oil.

$^1\text{H NMR}(\text{CDCl}_3)$: δ 1.17 (t, 7.56 Hz, 3H, CH_3), 2.13 (s, 3H), 2.56 (q, 7.53 Hz, 2H, CH_2), 3.71 (s, 2H), 7.1-7.3 (m, 4H)

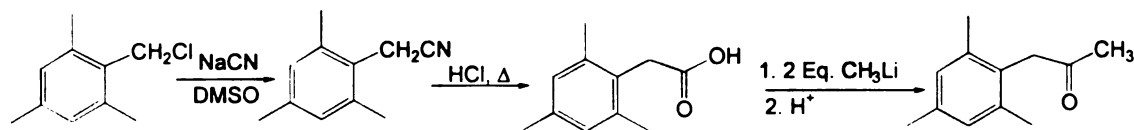
$^{13}\text{CNMR}(\text{CDCl}_3)$: δ 14.79, 25.78, 29.26, 48.59, 126.18, 127.60, 128.67, 130.63, 132.4, 142.62, 206.75

$\text{IR}(\text{CCl}_4)$: 3069, 3022, 2970, 2936, 2876, 1707, 1358, 1159, 1057

HRMS: 162.10446 calculated for C₁₁H₁₄O; found: 162.1080

α -Mesitylacetone (11)

α -Mesitylacetone was prepared by the reaction of methyllithium with α -mesitylacetic acid following the route described below:



Scheme 53. Synthesis of α -Mesitylacetone

α -Mesitylacetone nitrile

A mixture of sodium cyanide (8.7 g, 0.19 moles) in DMSO was heated at 90°C until all of the sodium cyanide dissolved. α -2,4,6-Trimethylbenzyl chloride (20 g, 0.12 moles) was added dropwise over a period of an hour and the mixture was heated for an additional 5 hours. The mixture was then allowed to cool to room temperature and was poured into 500 mL of ice-cold water. The resulting solution was extracted with ether three times and the combined ether layer was washed with water and dried. Solvent was evaporated to leave the desired product (18 g, 92%) as a yellow solid. The crude product was used without further purification.

¹H NMR(CDCl₃): δ 2.30 (s, 3H), 2.38 (s, 6H), 3.60 (s, 2H), 6.93 (s, 2H)

IR(CCl₄): 2921, 2240, 1404.4

α -Mesitylacetic acid

α -Mesitylacetonitrile (18 g, 0.11 moles) was poured into 300 mL of concentrated HCl and the mixture was refluxed for two days. The mixture was then allowed to cool to room temperature and was poured into 1 L of water. The resulting solution was extracted with ether several times. The ether layers were combined and washed with 10% NaOH solution. The alkaline layer was acidified and extracted with ether twice. The combined ether layer was washed with water and dried. Solvent was evaporated, giving the product as a white solid (15.3 g, 76%). This was used without further purification.

$^1\text{H NMR}(\text{CDCl}_3)$: δ 2.3 (s, 3H), 2.41 (s, 6H), 3.50 (s, 2H), 6.95 (s, 2H)

$\text{IR}(\text{CCl}_4)$: 3383, 2921.8, 1686, 1458.4, 1325.3, 1228.8, 1188.3, 852.6

 α -Mesitylacetone

To a solution of α -mesitylacetic acid (5 g, 0.027 moles) in 50 mL anhydrous ether at 0°C under an argon atmosphere, was added 40 mL of 1.4M methyl lithium. The mixture was allowed to warm to room temperature and was stirred overnight. The mixture was then poured into a flask containing 30 mL of 10% HCl and was stirred for 30 minutes before layers were separated. The aqueous layer was washed with ether twice and the combined organic layer was washed with water and saturated sodium chloride solution and dried over anhydrous magnesium sulfate. Solvent was removed to yield 3.4 g (72%) of product as an off-white solid. The product was recrystallized from methanol.

$^1\text{H NMR}(\text{CDCl}_3)$: δ 2.12 (s, 3H), 2.19 (s, 6H), 2.25 (s, 3H), 3.71 (s, 2H), 6.86 (s, 2H)

$^{13}\text{C NMR}(\text{CDCl}_3)$: δ 20.2, 20.9, 29.3, 44.8, 128.9, 129.1, 136.5, 136.6, 206.7

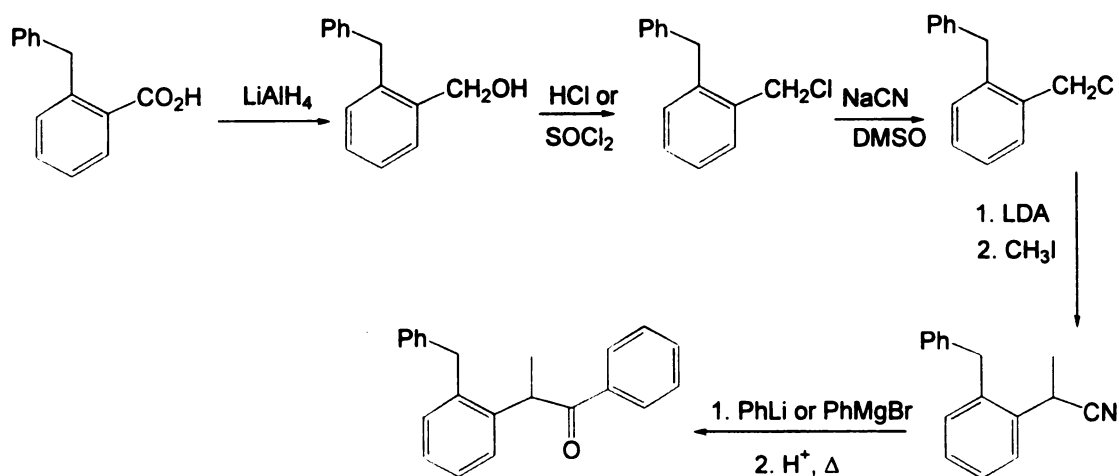
IR(CCl₄): 2920.6, 1711.1, 1417.8, 1167.1

m.p.: 60-62°C

HRMS: 176.12012 calculated for C₁₂H₁₆O; found: 176.1203

***α*-(2-Benzylphenyl)propiophenone (7)**

α-(2-Benzylphenyl)propiophenone was prepared by the reaction of phenyl magnesium bromide with *α*-(2-benzylphenyl)propionitrile following the route described below.



Scheme 54. Synthesis of *α*-(2-Benzylphenyl)propiophenone

***o*-Benzylbenzyl alcohol**

A solution of *o*-benzylbenzoic acid (0.033 moles, 7 g, Aldrich) in 15 mL of anhydrous ether was added dropwise to an argon purged stirred suspension of lithium aluminum hydride (2.7 g, 0.071 moles) in 50 mL of anhydrous ether. After addition was complete, the mixture was refluxed for 7 hours and allowed to cool to room temperature. Excess lithium aluminum hydride was quenched by careful addition of ice.

Acidic workup afforded 5.5 g (84% yield) of product as a yellow oil which was used in the next step without purification.

$^1\text{H NMR}(\text{CDCl}_3)$: δ 4.10 (s, 2H), 4.68 (s, 2H), 7.1-7.5 (m, 9H)

***o*-Benzylbenzyl chloride**

In a 250 mL round bottom flask was placed 5.5 g of *o*-benzylbenzyl alcohol along with 200 mL of concentrated hydrochloric acid. The mixture was stirred at room temperature overnight and was poured slowly into a flask containing 500 mL of ice cold water. Ether was added and layers were separated. The aqueous layer was washed twice with ether and the combined organic layer was washed with water, saturated sodium bicarbonate and saturated sodium chloride solutions and was dried over anhydrous magnesium sulfate. Removal of solvent resulted in recovery of 5.85 g (100% yield) of product as a yellow oil. This was used without purification in the next step.

$^1\text{H NMR}(\text{CDCl}_3)$: δ 4.19 (s, 2H), 4.58 (s, 2H), 7.1-7.4 (m, 9H)

***α* -(2-Benzylphenyl)acetonitrile**

A solution of (2-benzyl)benzyl chloride (5.85 g, 0.027 moles) in 10 mL of DMSO was added dropwise to a stirred solution of sodium cyanide (1.8 g, 0.036 moles) in 100 mL of DMSO. The mixture was refluxed overnight, allowed to cool to room temperature and was poured into a flask containing 500 mL of ice cold water. Ether was added and layers were separated. The aqueous layer was washed twice with ether and the combined organic layer was washed 10 times with water and dried over anhydrous magnesium

sulfate. Solvent removal afforded 5.1 g (91% yield) of product as a brownish oil which was used without purification in the next step.

$^1\text{H NMR}(\text{CDCl}_3)$: δ 3.35 (s, 2H), 4.01 (s, 2H), 7.0-7.4 (m, 9H)

α -(2-Benzylphenyl)propionophenone

A solution of α -(2-benzylphenyl)propionitrile (2.5 g, 0.011 moles) in anhydrous ether was added dropwise to a stirred solution of phenyl magnesium bromide (prepared from 2.0 g, 0.013 moles of bromobenzene and 0.32 g of magnesium) in 50 mL of ether. The mixture was refluxed overnight and cooled to room temperature before it was poured into a flask containing 100 mL of 10% HCl. Layers were separated and the aqueous layer was heated at 80-90°C for 7 hours. Ether was added and the layers were separated. The aqueous layer was washed twice with ether and the combined organic layer was washed with water and saturated sodium chloride and dried. Solvent removal yielded 1.8 g (54%) of crude product as a dark yellow oil. The oil was chromatographed (by flash chromatography using 95/5 hexane/ethyl acetate mixture as eluent) to yield 1.3 g of pure product as a pale yellow oil.

$^1\text{H NMR}(\text{CDCl}_3)$: δ 1.36 (d, 6.7 Hz, 3H, CH_3), 4.16 (s, 2H), 4.73 (q, 6.7 Hz, 1H, CHCH_3), 7.02 (dd, $J = 7.62, 1.59$ Hz, 1H, Ar), 7.1-7.4 (m, 11H, Ar), 7.46 (d, $J = 7.14$ Hz, 2H, Ar)

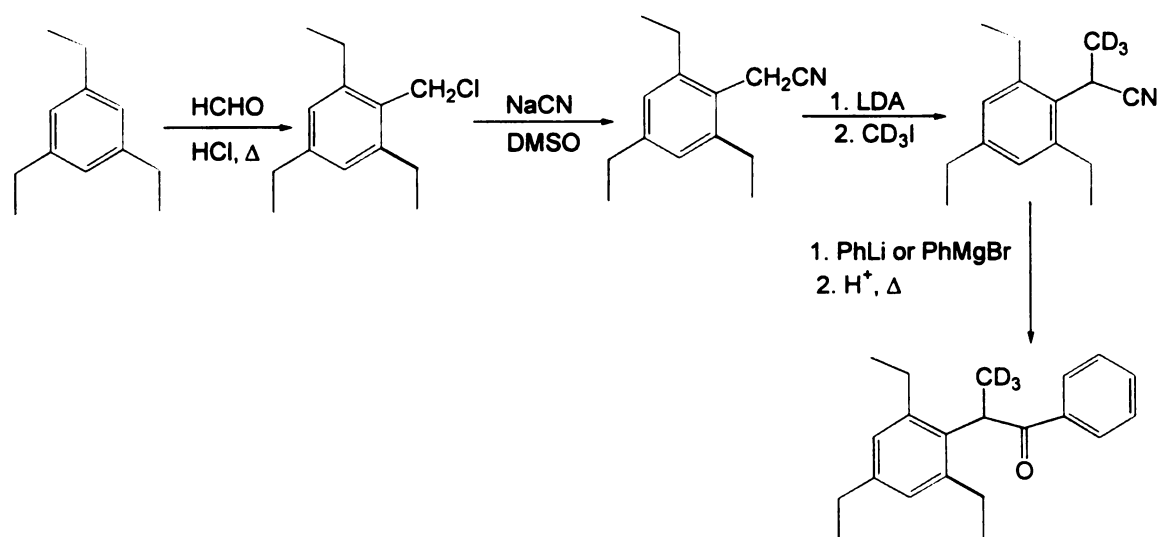
$^{13}\text{CNMR}(\text{CDCl}_3)$: δ 18.54, 39.50, 43.93, 126.37, 126.90, 127.39, 127.57, 128.24, 128.42, 128.63, 128.90, 131.59, 132.41, 136.34, 137.13, 140.01, 140.19, 200.93

$\text{IR}(\text{CCl}_4)$: 3067, 3028, 2964, 2932, 1688, 1452, 1261, 1022

HRMS: 300.15142 calculated for $C_{22}H_{20}O$; found: 300.1521

α -(2,4,6-Triethylphenyl)- β,β,β -trideuteropropiophenone (5d₃**)**

α -(2,4,6-Triethylphenyl)- β,β,β -trideuteropropiophenone was prepared by reaction of phenyl magnesium bromide with α -(2,4,6-triethylphenyl) β,β,β -trideuteropropionitrile according to the route outlined below.



Scheme 55. Synthesis of α -(2,4,6-Triethylphenyl)- β,β,β -trideuteropropiophenone

2,4,6-Triethylbenzyl chloride

In a 250 mL round bottom flask was placed 10.0 g (0.062 moles) of 1,3,5-triethylbenzene along with 2.0 g (0.066 moles, Aldrich) of paraformaldehyde and 200 mL of concentrated hydrochloric acid. The mixture was refluxed for 48 hours, allowed to cool to room temperature and was poured into a flask containing 500 mL of 20% NaOH solution. The mixture was stirred at room temperature for an hour. Ether was added and

layers were separated. The aqueous layer was washed twice with ether and the combined organic layer was washed with water, dilute alkali and saturated sodium chloride solutions and dried. Solvent was removed to yield a reddish-brown oil which upon analysis was shown to contain both starting material and the desired product. Kugelrohr distillation of this oil resulted in recovery of 11.6 g (89% yield) of a yellow oil as pure product.

$^1\text{H NMR}(\text{CDCl}_3)$: δ 1.22 (t, 3H), 1.26 (t, 6H), 2.60 (q, 2H), 2.75 (q, 4H), 4.70 (s, 2H), 6.90 (s, 2H)

α -(2,4,6-Triethylphenyl)acetonitrile

A solution of 2,4,6-triethylbenzylchloride (11.6 g, 0.055 moles) in 10 mL of DMSO was added dropwise to a stirred solution of sodium cyanide (0.06 moles in 100 mL DMSO) at 80°C. The mixture was heated at 80-100°C overnight, allowed to cool to room temperature and was poured into a flask containing 500 mL of ice cold water. Ether was added and the layers were separated. The aqueous layer was washed twice with ether and the combined organic layer was washed 10 times with water and dried (MgSO_4). Solvent was removed to afford 7.02 g (63.5% yield, 0.035 moles) of an off-white solid as product which was used in the next step without further purification.

$^1\text{H NMR}(\text{CDCl}_3)$: δ 1.2 (t, 3H), 1.25 (t, 6H), 2.6 (q, 2H), 2.68 (q, 4H), 3.62 (s, 2H), 6.9 (s, 2H)

$\text{IR}(\text{CCl}_4)$: 2961.1, 2235.8, 1608.8, 1456.4, 1251.9, 873.8

α -(2,4,6-Triethylphenyl)- β,β,β -trideuteropropionitrile

In a 250 mL round bottom flask equipped with a condenser and purged with argon was placed 4.00 g (0.04 moles) of diisopropylamine in 30 mL of dry THF. The solution was cooled to 0°C in an ice-water bath. Butyl lithium (28 mL of 1.4 M solution) was added and the mixture was allowed to warm to room temperature and stirred for half an hour. The mixture was then cooled to -78°C in an acetone/dry ice bath and 7.02 g (0.035 moles) of α -(2,4,6-triethylphenyl) acetonitrile in 20 mL of dry THF was added dropwise. After addition was complete, the mixture was allowed to warm to room temperature and was stirred for 4 hours before 2.6 mL (5.8 g, 0.04 moles) of CD₃I was added. The mixture was stirred at room temperature for an hour and refluxed overnight. After cooling to room temperature, solvent was evaporated to yield a pale yellow oil which was washed with an ether/water mixture. Layers were separated and the water layer was washed three times with ether. The combined organic layer was washed with water and saturated sodium chloride and dried. Removal of solvent resulted in recovery of 4.36 g (57% yield, 0.02 moles) of product as a crystalline solid. This was used in the next step without purification.

¹H NMR(CDCl₃): δ 1.20 (t, 3H), 1.25 (t, 6H), 2.60 (q, 2H), 2.75 (AB quartets of q, 4H), 4.23 (broad s, 1H), 6.92 (broad s, 2H)

 α -(2,4,6-Triethylphenyl)- β,β,β -trideuteropropiophenone

A solution of α -(2,4,6-triethylphenyl)- β,β,β -trideuteropropionitrile (4.36 g, 0.02 moles) in 20 mL of anhydrous ether was added dropwise to a stirred solution of phenyl

magnesium bromide (prepared from 3.6 g (0.022 moles) of bromobenzene and 0.95 g (0.022 moles) of dry magnesium) in 100 mL of anhydrous ether. The mixture was refluxed overnight, cooled to room temperature and poured into a flask containing 100 mL of 10% HCl solution. Layers were separated and the aqueous layer was heated at 80-90°C, for four hours. After cooling to room temperature, ether was added and the layers were separated. The aqueous layer was washed twice with ether and the combined organic layer was washed with water, saturated sodium bicarbonate and saturated sodium chloride and dried. Solvent removal resulted in recovery of 3.2 g (54% yield) of product as an off-white powder.

$^1\text{H NMR}(\text{CDCl}_3)$: δ 1.15 (broad, 6H, 2CH₃), 1.19 (t, J= 7.5 Hz, 3H, CH₃), 2.55 (q, J= 7.5 Hz, 2H, CH₂), 2.6 (broad, 4H, 2CH₂), 4.48 (broad s, 1H, CHCD₃), 6.86 (broad s, 2H, Ar), 7.23 (dd, J= 7.3, 7.6 Hz, 2H, Ar), 7.36 (t, J= 7.3Hz, 1H, Ar), 7.67 (d, J= 7.6Hz, 2H, Ar)

$^2\text{H NMR}(\text{CDCl}_3)$: δ 1.18 (s, 3D)

$^{13}\text{C NMR}(\text{CDCl}_3)$: δ 15.20, 17.2 (septet, CD₃), 28.4, 29.65, 29.69, 45.41, 126.74, 128.11, 128.57, 132.23, 135.76, 137.10, 141.4, 142.58, 202.89

IR(CCl₄): 2978, 2936, 2866, 1684, 1383, 1217, 1006 cm⁻¹

m.p.: 75-76°C

HRMS: 297.21689 calculated for C₂₁H₂₃D₃O; found: 297.2168

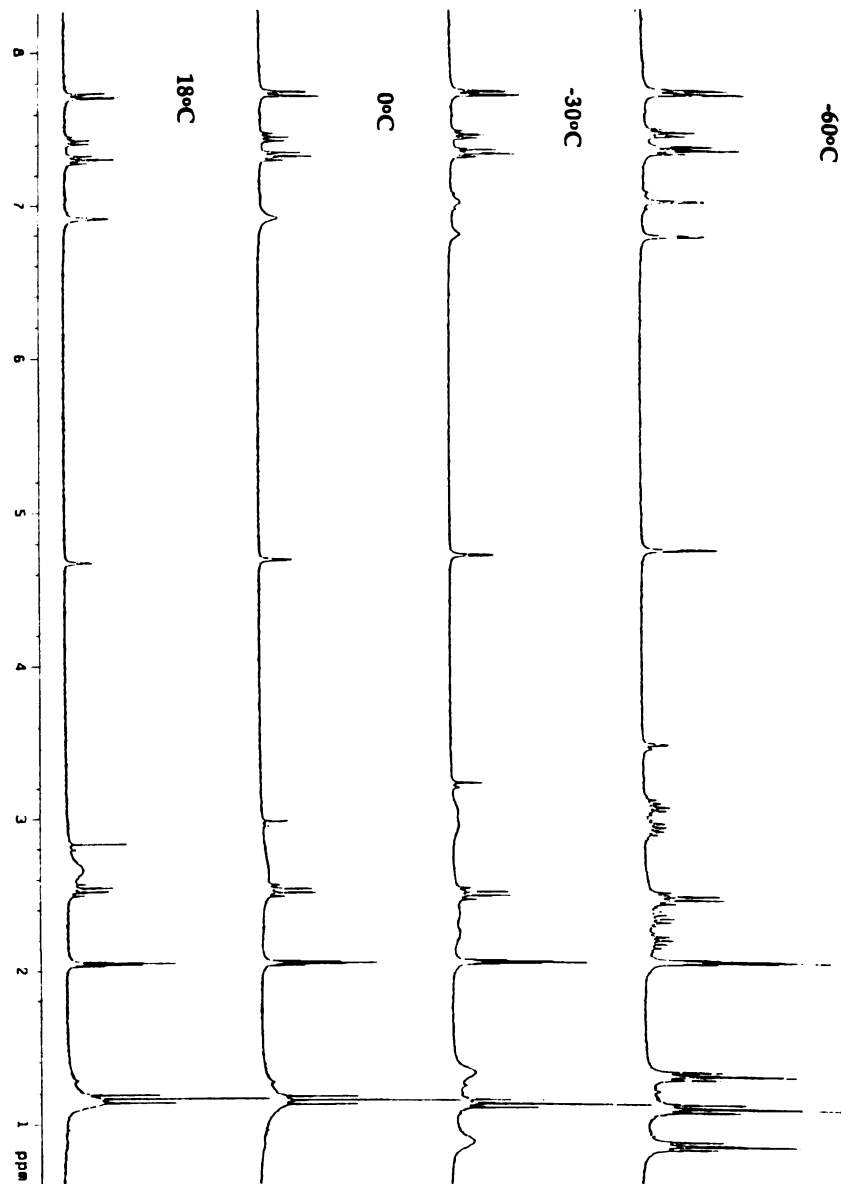


Figure 33. Variable Temperature NMR of α -(2,4,6-Triethylphenyl)- β,β,β -trideuterio-propionophenone in $\text{Acetone-}d_6$

α -(2,4,6-Triethylphenyl)propiophenone (5)

α -(2,4,6-Triethylphenyl)propiophenone was synthesized using the same procedure as α -(2,4,6-triethylphenyl)- β,β,β -trideuteriopropiophenone with the exception of using CH_3I instead of CD_3I .

$^1\text{H NMR}(\text{CDCl}_3)$: δ 1.15 (broad, 6H, 2CH_3), 1.19 (t, $J = 7.5$ Hz, 3H, CH_3), 1.55 (d, $J = 6.8$ Hz, 3H, CH_3CH), 2.55 (q, $J = 7.5$ Hz, 2H, CH_2), 2.6 (broad, 4H, 2CH_2), 4.48 (q, $J = 6.8$ Hz, 1H, CHCH_3), 6.86 (broad s, 2H, Ar), 7.23 (dd, $J = 7.3, 7.6$ Hz, 2H, Ar), 7.36 (t, $J = 7.3$ Hz, 1H, Ar), 7.67 (d, $J = 7.6$ Hz, 2H, Ar)

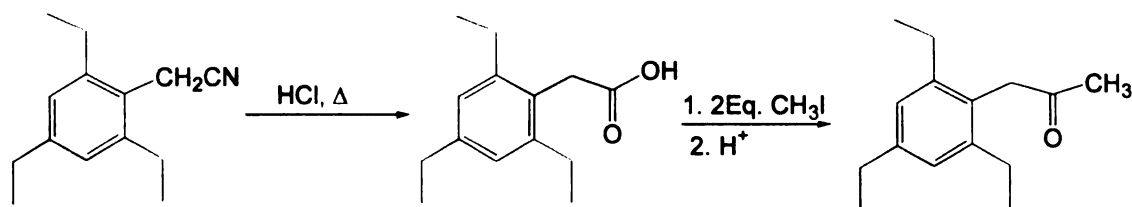
$^{13}\text{C NMR}(\text{CDCl}_3)$: δ 15.20, 17.2, 28.4, 29.65, 29.69, 45.41, 126.74, 128.11, 128.57, 132.23, 135.76, 137.10, 141.4, 142.58, 202.

$\text{IR}(\text{CCl}_4)$: 2978, 2936, 2866, 1684, 1383, 1217, 1006 cm^{-1}

m.p.: 75-76 $^\circ\text{C}$

 α -(2,4,6-Triethylphenyl)acetone (12)

α -(2,4,6-Triethylphenyl)acetone was synthesized by reaction of methyl lithium with α -(2,4,6-triethylphenyl)acetic acid according to the route described below:



Scheme 56. Synthesis of α -(2,4,6-Triethylphenyl)acetone

α -(2,4,6-Triethylphenyl)acetic acid

A solution of α -(2,4,6-triethylphenyl)acetonitrile (3.0 g, 0.015 moles) in concentrated hydrochloric acid was refluxed for two days. After cooling to room temperature, the solution was poured onto cold water and extracted with ether several times. The combined ether layer was washed twice with 1N NaOH solution. The alkaline layer was acidified with 10% hydrochloric acid until a white precipitate was formed. The precipitate was extracted into ether, washed twice with water and dried. Solvent removal afforded 3.2 g (100% yield) of product as a white solid. This was used in the next step without further purification.

$^1\text{H NMR}(\text{CDCl}_3)$: δ 1.18 (t, 6H), 1.21 (t, 3H), 2.58 (q, 2H), 2.61 (q, 4H), 3.72 (s, 2H), 6.9 (s, 2H)

IR(CCl_4): 3354.6, 2961, 1686, 1251.9, 1057.2, 1014.7

 α -(2,4,6-Triethylphenyl)acetone

Methyl lithium (14 mL of 1.4 M solution) was added dropwise to a stirred solution of α -(2,4,6-triethylphenyl)acetic acid (1.8 g, 0.008 moles) in 100 mL of anhydrous ether at 0°C. The mixture was warmed to room temperature, refluxed for 48 hours, and poured into a flask containing 100 mL of 10% HCl solution. Layers were separated and the aqueous layer was washed twice with ether. The combined organic layer was washed with water, dilute alkali and water and dried. Solvent removal afforded a yellow oil which was chromatographed (by flash chromatography using 99:1

hexane/ethyl acetate mixture as eluent) to give 1.6 g (73% yield) of product as a pale yellow oil.

$^1\text{H NMR}(\text{CDCl}_3)$: δ 1.18 (t, $J=7.5$ Hz, 6H, 2CH_3), 1.23 (t, $J=7.5$ Hz, 3H, CH_3CO), 2.16 (s, 3H, CH_3), 2.53 (q, $J=7.5$ Hz, 4H, 2CH_2 CH_3), 2.60 (q, $J=7.5$ Hz, 2H, CH_2CH_3), 3.78 (s, 2H, CH_2CO), 6.92 (s, 2H, Ar)

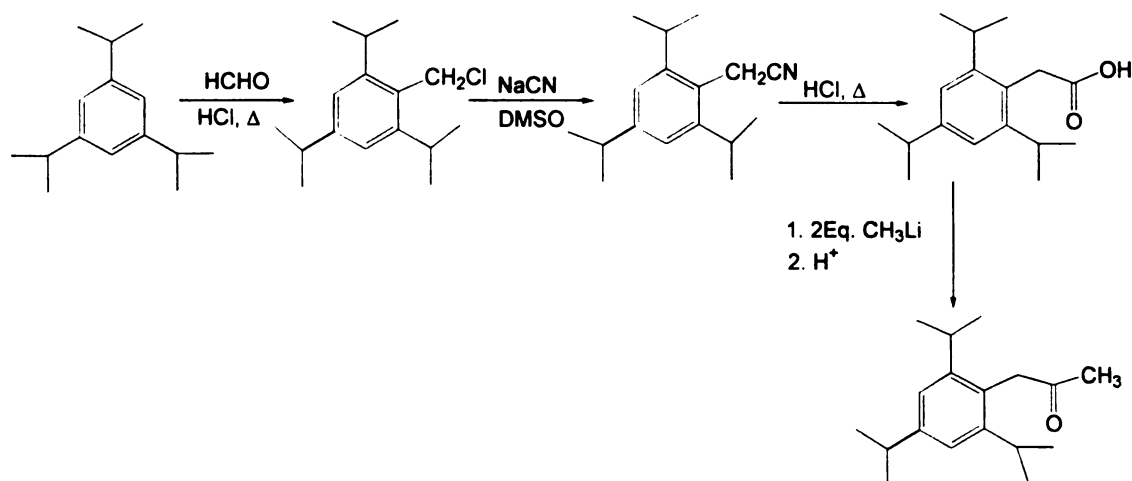
$^{13}\text{C NMR}(\text{CDCl}_3)$: δ 15.05, 15.40, 26.56, 28.58, 29.40, 43.74, 125.90, 127.76, 142.66, 143.12, 207.40

IR(neat): 2965, 2932, 2874, 1716.9, 1458.4, 1157.4

HRMS: 218.16706 calculated for $\text{C}_{15}\text{H}_{22}\text{O}$; found: 218.1664

α -(2,4,6-Triisopropylphenyl)acetone (13)

α -(2,4,6-Triisopropylphenyl) acetone was synthesized by reaction of methyl lithium with α -(2,4,6-triisopropylphenyl)acetic acid according to the route outlined below.



Scheme 57. Synthesis of α -(2,4,6-Triisopropylphenyl)acetone

2,4,6-Triisopropylbenzyl chloride

In a 250 mL round bottom flask was placed 10 g (0.049 moles, Aldrich) of triisopropylbenzene along with 1.56 g (0.052 moles) of paraformaldehyde and 200 mL of concentrated hydrochloric acid. The mixture was refluxed for three days, cooled to room temperature and was poured into a flask containing 500 mL of 20% NaOH solution. The mixture was stirred at room temperature for two hours before ether was added. Layers were separated and the aqueous layer was washed twice with ether. The combined organic layer was washed with water, dilute alkali and water and dried. Removal of solvent resulted in recovery of a yellow oil. Analysis of the oil showed it to contain both the starting material and the desired product. Kugelrohr distillation resulted in recovery of 3.8 g (30% yield) of the product as a yellow oil.

$^1\text{H NMR}(\text{CDCl}_3)$: δ 1.22 (d, 3H), 1.26 (d, 6H), 2.85 (septet, 1H), 3.28 (septet, 2H), 4.71 (s, 2H), 7.0 (s, 2H)

 α -(2,4,6-Triisopropylphenyl)acetonitrile

A solution of 2,4,6-triisopropylbenzyl chloride (3.8 g, 0.015 moles) in 10 mL of DMSO was added dropwise to a stirred solution of sodium cyanide (0.9 g, 0.018 moles) in 50 mL DMSO at 90°C. The mixture was stirred overnight, cooled to RT and was poured into a flask containing 500 mL of water. Ether was added and layers were separated. The aqueous layer was washed twice with ether and the combined organic layer was washed 10 times with water and dried. Solvent removal afforded 3.6 g (100% yield) of product as a yellow solid.

$^1\text{H NMR}(\text{CDCl}_3)$: δ 1.22 (d, 3H), 1.27 (d, 6H), 2.85 (septet, 1H), 3.13 (septet, 2H), 3.71 (s, 2H), 7.02 (s, 2H)

IR(CCl_4): 2966, 2238.2, 1456.5, 727.3

α -(2,4,6-Triisopropylphenyl)acetic acid

A stirred mixture of α -(2,4,6-triisopropylphenyl)acetonitrile (3.6 g, 0.015 moles) in 200 mL of concentrated hydrochloric acid was refluxed for 48 hours. The mixture was allowed to cool to room temperature and was poured slowly into a flask containing 500 mL of ice cold water. Ether was added, layers were separated and the organic layer was washed with dilute NaOH solution. The alkaline layer was acidified with 10% HCl solution until a white precipitate could be observed. Ether was added and layers were separated. The organic layer was washed twice with water and dried. Solvent removal afforded 1.2 g (30% yield) of product as a white solid.

$^1\text{H NMR}(\text{CDCl}_3)$: δ 1.21 (t, 6H), 1.23 (t, 3H), 2.87 (septet, 1H), 3.10 (septet, 2H), 3.80 (s, 2H), 7.0 (s, 2H)

IR(CCl_4): 3350.6, 2966, 1687, 1058.1

α -(2,4,6-Triisopropylphenyl)acetone

Methyl lithium (6.8 mL of 1.4 M solution) was added dropwise to a stirred solution of α -(2,4,6-triisopropylphenyl)acetic acid (1.2 g, 0.0045 moles) in 100 mL of anhydrous ether at 0°C. The mixture was warmed to room temperature, refluxed overnight, and poured into a flask containing 100 mL of 10% HCl solution. Layers were separated and the aqueous layer was washed twice with ether. The combined organic

layer was washed with water, dilute alkali and water and dried. Solvent removal afforded a yellow oil which was chromatographed (by flash chromatography using 99:1 hexane/ethyl acetate mixture as eluent) to give 0.35 g (30% yield) of product as a white solid.

$^1\text{H NMR}(\text{CDCl}_3)$: δ 1.19 (t, $J=6.8$ Hz, 12H, 4 CH_3), 1.23 (t, $J=6.9$ Hz, 6H, 2 CH_3), 2.18 (s, 3H, CH_3CO), 2.85 (septet, $J=6.8$ Hz, 1H, $\text{CH}(\text{CH}_3)_2$), 2.90 (septet, $J=6.8$ Hz, 2H, 2 $\text{CH}(\text{CH}_3)_2$), 3.84 (s, 2H, CH_2CO), 7.00 (s, 2H, Ar)

$^{13}\text{C NMR}(\text{CDCl}_3)$: δ 23.98, 29.48, 29.73, 30.05, 34.15, 43.17, 121.11, 121.16, 146.96, 147.58, 207.8

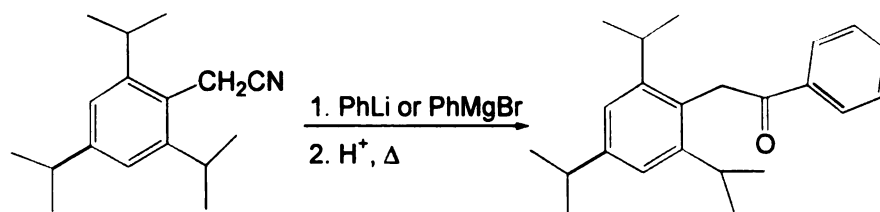
IR(neat): 2959.2, 2928.3, 2870.4, 1711.1, 1360, 1159.4

m.p.: 57-59°C

HRMS: 260.21402 calculated for $\text{C}_{18}\text{H}_{28}\text{O}$; found: 260.2141

α -(2,4,6-Triisopropylphenyl)acetophenone (9)

α -(2,4,6-Triisopropylphenyl)acetophenone was synthesized by reaction of phenyl magnesium bromide with α -(2,4,6-triisopropylphenyl)acetonitrile according to the route outlined below:



Scheme 58. Synthesis of α -(2,4,6-Triisopropylphenyl)acetophenone

α -(2,4,6-Triisopropylphenyl)acetophenone

A solution of α -(2,4,6-triisopropylphenyl)acetonitrile (0.012 moles, 3.0 g) in anhydrous ether was added dropwise to a stirred solution of phenyl magnesium bromide (prepared from 2.2 g of bromobenzene and 0.35 g of magnesium) in anhydrous ether. The mixture was stirred at room temperature for an hour and refluxed overnight. After cooling to room temperature, 50 mL of 10% hydrochloric acid solution was added and layers were separated. The aqueous layer was heated at 90°C for four hours and cooled to room temperature. Ether was added and layers were separated. The organic layer was washed with water, saturated sodium bicarbonate and saturated sodium chloride solutions and dried. Solvent was evaporated to leave a yellow oil which was chromatographed (by flash chromatography using 95:5 hexane/ethyl acetate mixture as eluent) to leave 2.3 g (60% yield) of product as a white solid.

$^1\text{H NMR}(\text{CDCl}_3)$: δ 1.18 (d, $J=6.8$ Hz, 12H, 4CH₃), 1.26 (d, $J=6.8$ Hz, 6H, 2CH₃), 2.85 (septet, $J=6.8$ Hz, 2H, 2CH(CH₃)₂), 2.89 (septet, $J=6.8$ Hz, 1H, CH(CH₃)₂), 4.45 (s, 2H, CH₂CO), 7.04 (s, 2H, Ar), 7.51 (dd, $J=7.35, 7.2$ Hz, 2H, Ar), 7.61 (tt, $J=7.2, 1.35$ Hz, 1H, Ar), 8.08 (dd, $J=7.35, 1.35$ Hz, 2H, Ar)

$^{13}\text{C NMR}(\text{CDCl}_3)$: δ 24.03, 24.08, 30.30, 34.24, 37.67, 121.0, 126.54, 128.09, 128.73, 133.13, 137.12, 147.12, 147.42, 197.75

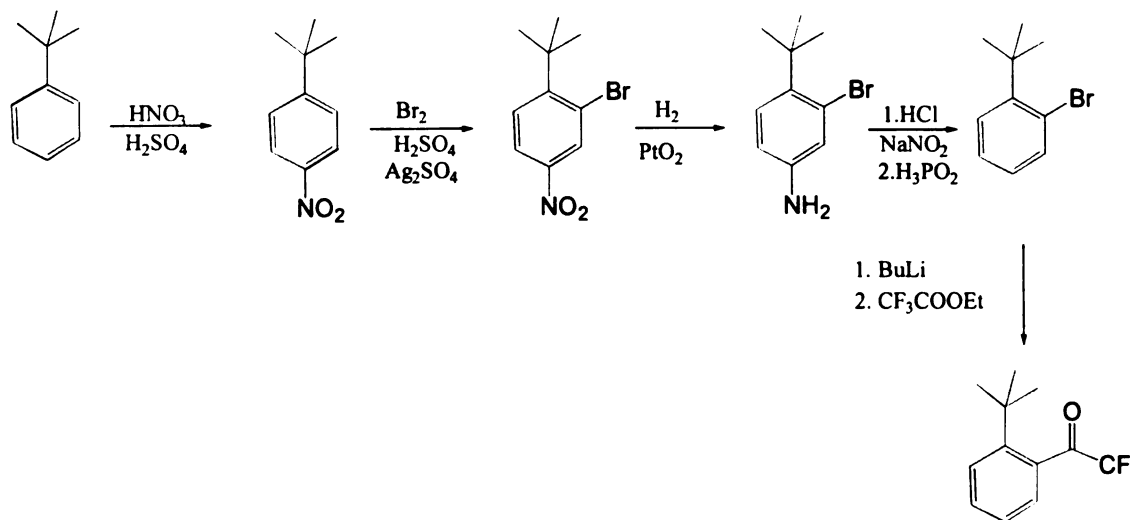
IR (CCl₄): 2965, 1691, 1448, 1216

HRMS: 322.22966 calculated for C₂₃H₃₀O; found: 322.2307

m.p.: 107-109°C

***o*-tert-Butyl- α,α,α -trifluoroacetophenone (14)**

o-tert-Butyl- α,α,α -trifluoroacetophenone was synthesized by reaction of *o*-tert-butyl phenyllithium with ethyl trifluoroacetate according to the route outlined below:



Scheme 59. Synthesis of *o*-tert-Butyltrifluoroacetophenone

***4*-tert-Butyl nitrobenzene**

A solution of nitric acid (2.5 mL of 15.5 M solution) in 15 mL of concentrated sulfuric acid was added dropwise to 5 g (0.037 moles, Aldrich) of *tert*-butylbenzene at 0°C. After the addition was complete, the mixture was stirred at 0°C for an hour, warmed to room temperature and poured into a separatory funnel. Layers were separated and the organic layer was washed with water twice and dried. The resulting yellow oil was distilled through a fractionating column to separate the para isomer. The desired product (5.7 g, 85% yield) was obtained as a pale yellow oil.

¹H NMR(CDCl₃): δ 1.32 (s, 9H), 7.5 (d, 2H), 8.14 (d, 2H)

3-Bromo-4-tert-butylnitrobenzene

In a 500 mL three necked round bottom flask was placed 5.7 g (0.032 moles) of 4-*tert*-butylnitrobenzene, silver sulfate (10 g, 0.032 moles), and 300 mL of concentrated hydrochloric acid. The mixture was stirred for 0.5 hours before 1.7 mL (0.032 moles) of bromine was added dropwise over a period of an hour. The mixture was allowed to stir at room temperature for an additional five hours and then poured into 1 liter of dilute sodium sulfite solution. The silver bromide was collected by suction filtration. The filtrate was extracted three times with ether and the combined ether layer was washed with water, 10% NaOH, water and dried over anhydrous magnesium sulfate. Solvent removal afforded 7.2 g (87%, 0.028 moles) of product as a yellow oil. This was used in the next step without further purification.

$^1\text{H NMR}(\text{CDCl}_3)$: δ 1.51 (s, 9H), 7.6 (d, 1H), 8.05 (dd, 1H), 8.4 (d, 1H)

3-Bromo-4-tert-butylanilinium chloride

3-Bromo-4-*tert*-butylnitrobenzene (7.2 g, 0.028 moles) was reduced in a Parr hydrogenator in the presence of 0.15 g platinum(IV) oxide (Aldrich, Adam's catalyst) in a mixture containing 100 mL of 95% ethanol and 15 mL of concentrated hydrochloric acid at a pressure of 47-50 psi of hydrogen at room temperature. The hydrogenation took approximately 18 hours. The reaction mixture was filtered through a celite pad to remove the catalyst. Solvent removal afforded 7.3 g (100% yield, 0.028 moles) of amine hydrochloride as a yellow solid.

$^1\text{H NMR}(\text{CDCl}_3)$: δ 1.5 (s, 9H), 7.48 (dd, 1H), 7.71 (d, 1H), 7.81 (d, 1H)

2-tert-Butylbromobenzene

In a 250 mL round bottom flask was placed 7.3 g (0.028 moles) of 3-bromo-4-*tert*-butylanilinium chloride and 30 mL of concentrated hydrochloric acid. The mixture was diluted with water to 100 mL and ice chips were added to cool the mixture to 0°C. A solution of sodium nitrite (2.0 g, 0.030 moles) in 10 mL of water was added to the mixture over a period of two minutes. The mixture was stirred at 0°C for an additional 15 minutes before it was vacuum filtered to give a clear yellow solution which was kept at 0°C. A 50% solution of hypophosphorous acid (70 mL) was added to the filtrate and the mixture was kept in the freezer for 48 hours. The mixture was then allowed to warm to room temperature and was extracted with ether three times. The combined ether layer was washed with water and dried over anhydrous magnesium sulfate. Solvent was evaporated to give a brownish oil which upon Kugelrohr distillation yielded 3.6 g (62% yield, 0.017 moles) of product as a colorless liquid.

¹H NMR(CDCI₃): δ 1.5 (s, 9H), 7.01 (ddd, 1H), 7.22 (ddd, 1H), 7.43 (dd, 1H), 7.57 (dd, 1H)

2-tert-Butyl- α,α,α -trifluoroacetophenone

To a stirred solution of 2-*tert*-butylbromobenzene (3.6 g, 0.017 moles) in 50 mL of anhydrous ether at -78°C, was added 11 mL of 2.0 M *n*-butyllithium (0.022 moles). The solution was allowed to warm to 0°C and was stirred at this temperature for 4 hours before 3.1 g (0.022 moles) of ethyl trifluoroacetate in 10 mL of anhydrous ether was added. The mixture was allowed to warm to room temperature and was refluxed

overnight. After cooling to room temperature, the mixture was poured onto 150 mL of saturated ammonium chloride solution and layers were separated. The organic layer was washed twice with saturated sodium chloride solution and dried. Solvent was evaporated to leave a brownish oil which was chromatographed (by flash chromatography using 90:10 hexane/ethyl acetate mixture as eluent) to afford 2.76 g (72% yield) of product as a colorless oil.

^1H NMR(CDCl_3): δ 1.37 (s, 9H, $\text{C}(\text{CH}_3)_3$), 7.28 (dd, $J = 6.81, 1.10$ Hz, 1H, Ar), 7.30 (broad, 1H, Ar), 7.46 (ddd, $J = 8.2, 6.81, 1.85$ Hz, 1H, Ar), 7.57 (dd, $J = 8.2, 1.1$ Hz, 1H, Ar)

^{13}C NMR(CDCl_3): δ 32.0, 36.0, 116 (q, $J = 291.4$ Hz), 125.3, 126.3, 127.9, 131.33, 132.6, 149.9, 189 (q, $J = 35.2$ Hz)

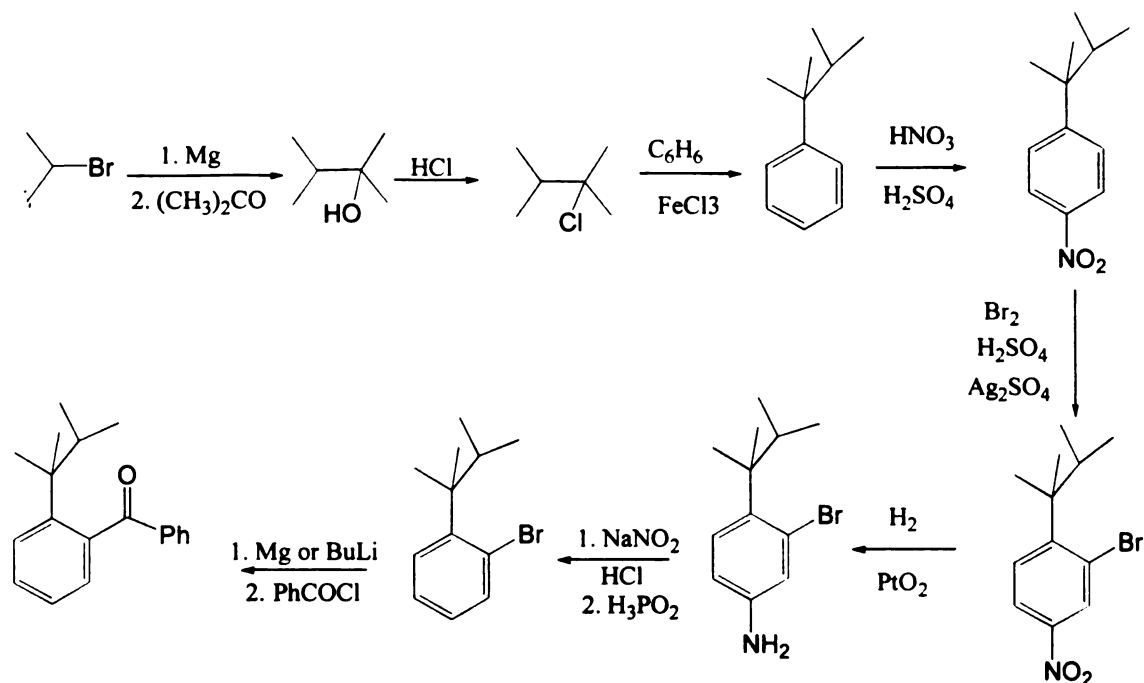
^{19}F NMR(CDCl_3): δ 1.83 (s, 3F, CF_3) reference: ethyl trifluoroacetate

IR(CCl_4): 2968.8, 1741.9, 1207.5, 1182.5, 1155.5

HRMS: 230.09185 calculated for $\text{C}_{12}\text{H}_{13}\text{OF}_3$; found: 230.0919

***o*-(2,3-Dimethyl-2-butyl)benzophenone (15)**

o-(2,3-Dimethyl-2-butyl)benzophenone was synthesized by reaction of *o*-(2,3-dimethyl-2-butyl)phenyl magnesium bromide with benzoyl chloride according to the route given below:



Scheme 60. Synthesis of 2-(2'-(2',3'-Dimethyl)butyl)benzophenone

2,3-Dimethyl-2-butanol

A solution of anhydrous acetone (44.5 g, 0.77 moles) in dry ether was added dropwise to a stirred mixture of isopropyl magnesium bromide (prepared from 48 g (0.4 moles) of isopropylbromide and 10 g (0.42 moles) magnesium) in ether at -78°C . The addition took approximately an hour. The mixture was then stirred at room temperature for an hour and was refluxed overnight. After cooling to room temperature, 50 mL of 10% HCl was added and layers were separated. The aqueous layer was washed four times with ether and the combined organic layer was washed with water, saturated sodium bicarbonate and saturated sodium chloride solutions and dried. Solvent removal afforded a pale yellow oil which was distilled to give 24.8 g (60% yield, 0.24 moles) of product as a colorless liquid.

^1H NMR(CDCl_3): δ 0.9 (d, 6H), 1.1 (s, 6H), 1.63 (septet, 1H), 2.15 (1H, s, OH)

2-Chloro-2,3-dimethylbutane

To 24.8 g (0.24 moles) of 2,3-dimethyl-2-butanol was added 100 mL of concentrated hydrochloric acid and the mixture was stirred at room temperature overnight. The mixture was then poured into a separatory funnel and layers were separated. The organic layer was washed with water and dried to afford 28.9 g (100% yield) of the product as a colorless liquid.

^1H NMR(CDCl_3): δ 0.99 (d, 6H), 1.52 (s, 6H), 1.85 (septet, 1H)

2,3-Dimethyl-2-butyl)benzene

A solution of 2-chloro-2,3-dimethylbutane (11 g, 0.11 moles) in 10 mL of benzene was added dropwise to a stirred suspension of ferric chloride (27 g, 0.17 moles) in benzene (30 mL, 0.44 moles) at 0°C. The mixture was allowed to warm to room temperature and was stirred for 2 hours. The mixture was then allowed to sit and the top fraction (liquid portion) was removed leaving the solid catalyst behind. Ether was added and the organic layer was washed with water and dilute alkali and dried. Solvent was removed to leave 10 g (56%, 0.06 moles) of product as a colorless oil.

^1H NMR(CDCl_3): δ 0.74 (d, 6H), 1.23 (s, 6H), 1.9 (septet, 1H), 7.1-7.4 (m, 5H)

4'-(2,3-Dimethyl-2-butyl)nitrobenzene

A solution of nitric acid (3.9 mL of 15.5 M solution) in 10 mL of concentrated sulfuric acid was added dropwise to 10 g (0.06 moles) of (2,3-dimethyl-2-butyl)benzene

at 0°C. After addition was complete, the mixture was allowed to stir in the ice bath for 0.5 hours before it was poured into a separatory funnel. Layers were separated and the organic layer was washed with saturated sodium chloride, water, 2N NaOH, and saturated sodium chloride and dried to leave a yellow oil which was analyzed to contain both ortho and para isomers. Fractional distillation resulted in recovery of 11.1 g (90% yield) of the desired product as a pale yellow oil.

$^1\text{H NMR}(\text{CDCl}_3)$: δ 0.74 (d, 6H), 1.25 (s, 6H), 2.91 (septet, 1H), 7.45 (d, 2H), 8.13 (d, 2H)

2'-Bromo-4'-(2,3-dimethyl-2-butyl)nitrobenzene

In a 500 mL three necked round bottom flask was placed 11.1 g (0.054 moles) of 4'(2,3-dimethyl-2-butyl)nitrobenzene, silver sulfate (17 g, 0.055 moles), and 300 mL of concentrated hydrochloric acid. The mixture was stirred for 0.5 hours before 2.9 mL (0.054 moles) of bromine was added dropwise over a period of an hour. The mixture was allowed to stir at room temperature for an additional five hours and then poured into 1 liter of dilute sodium sulfite solution. The silver bromide was collected by suction filtration. The filtrate was extracted three times with ether and the combined ether layer was washed with water, 10% NaOH, water and dried. Solvent removal afforded 9.6 g (62%, 0.034 moles) of product as a yellow oil. This was used in the next step without further purification.

$^1\text{H NMR}(\text{CDCl}_3)$: δ 0.75 (d, 6H), 1.4 (s, 6H), 3.0 (septet, 1H), 7.5 (d, 1H), 8.05 (dd, 1H), 8.4 (d, 1H)

3'-Bromo-4'-(2,3-dimethyl-2-butyl)anilinium chloride

3'-Bromo-4'-(2,3-dimethyl-2-butyl)nitrobenzene (9.6 g, 0.034 moles) was reduced in a Parr hydrogenator in the presence of 0.15 g platinum(IV) oxide (Aldrich, Adam's catalyst) in a mixture containing 150 mL of 95% ethanol and 15 mL of concentrated hydrochloric acid at a pressure of 47-50 psi of hydrogen at room temperature. The hydrogenation took approximately 24 hours. The reaction mixture was filtered through a celite pad to remove the catalyst. Solvent removal afforded 9.93 g (100% yield, 0.034 moles) of amine hydrochloride as an off-white solid.

$^1\text{H NMR}(\text{acetone-}d_6)$: δ 0.75 (d, 6H), 1.42 (s, 6H), 3.0 (septet, 1H), 7.46 (dd, 1H), 7.65 (d, 1H), 7.80 (d, 1H)

2'-(2,3-Dimethyl-2-butyl)bromobenzene

To 9.93 g (0.034 moles) of 3'-bromo-4'-(2,3-dimethyl-2-butyl)anilinium chloride was added 30 mL of concentrated hydrochloric acid. The mixture was diluted with water to 100 mL and ice chips were added to cool the mixture to 0°C. A solution of sodium nitrite (2.5 g, 0.036 moles) in 10 mL of water was added to the mixture over a period of two minutes. The mixture was stirred at 0°C for an additional 15 minutes before it was vacuum filtered to give a clear yellow solution which was kept at 0°C. A 50% solution of hypophosphorous acid (70 mL) was added to the filtrate and the mixture was kept in the freezer for 48 hours. The mixture was then allowed to warm to room temperature and was extracted with ether three times. The combined ether layer was washed with water and dried over anhydrous magnesium sulfate. Solvent was evaporated to give a yellow oil

which upon Kugelrohr distillation yielded 4.8 g (58% yield, 0.020 moles) of product as a colorless liquid.

$^1\text{H NMR}(\text{CDCl}_3)$: δ 0.75 (d, 6H), 1.40 (s, 6H), 3.0 (septet, 1H), 7.0 (dd, 1H), 7.20 (dd, 1H), 7.35 (d, 1H), 7.56 (d, 1H)

2'-(2,3-Dimethyl-2-butyl)benzophenone

A solution of benzoyl chloride (3.5 mL, 4.2 g, 0.03 moles) in 20 mL of anhydrous ether was added dropwise to a stirred solution of 2'-(2,3-dimethyl-2-butyl)phenyl magnesium bromide (prepared from 4.8 g (0.020 moles) 2'-(2,3-dimethyl-2-butyl)bromobenzene and 0.6 g magnesium) in anhydrous ether at 0°C. The mixture was stirred at room temperature for an hour and refluxed overnight. After cooling to room temperature, water was added and layers were separated. The organic layer was washed with water, sodium hydroxide, and water and dried. Solvent was evaporated to leave a yellow oil which was chromatographed (using hexane as eluent) to leave 2.0 g (38% yield) of product as an off-white solid which was recrystallized from hexane.

$^1\text{H NMR}(\text{CDCl}_3)$: δ 0.72 (d, $J=6.8$ Hz, 6H, $(\text{CH}_3)_2\text{CH}$), 1.17 (s, 6H, $(\text{CH}_3)_2\text{C}$), 2.20 (septet, $J=6.8$ Hz, 1H, $\text{CH}(\text{CH}_3)_2$), 7.01 (dd, $J=7.62, 1.56$ Hz, 1H, Ar), 7.18 (ddd, $J=7.53, 7.35, 1.23$ Hz, 1H, Ar), 7.36 (ddd, $J=8.22, 7.35, 1.59$ Hz, 1H, Ar), 7.41 (dd, $J=7.35, 7.0$ Hz, 2H, Ar), 7.48 (dd, $J=8.22, 1.12$ Hz, 1H, Ar), 7.54 (tt, $J=7.35, 1.44$ Hz, 1H, Ar), 7.80 (dd, $J=7.0, 1.44$ Hz, 2H, Ar)

$^{13}\text{C NMR}(\text{CDCl}_3)$: δ 18.0, 25.7, 37.0, 42.4, 124.5, 127.9, 128.3, 128.5, 128.6, 130.4, 133.1, 137.9, 138.9, 148.3, 200.1

IR(neat): 3063.4, 2961.1, 2932.1, 1670.5, 1450.6, 1269.3, 1176.7, 1109.2

HRMS: 266.16707 calculated for C₁₉H₂₂O; found: 266.1665

m.p.: 63-64°C

III. Photochemical Experiments and Procedures

A. Purification of Chemicals

1. Solvents

Benzene- 3.5 liter of reagent grade benzene was mixed with 0.5 liter conc. sulfuric acid and the mixture was stirred for 2-3 days. The benzene layer was separated and was washed with 100 mL portions of conc. sulfuric acid several times until the sulfuric acid layer did not turn yellow. The benzene was then washed with distilled water and saturated sodium bicarbonate solution. The benzene was separated, dried over magnesium sulfate and filtered into a 5 L round bottom flask. Phosphorus pentoxide (100 g) was added and the solution was refluxed for 48 hours. After refluxing, the benzene was distilled through a one meter column packed with stainless steel helices. The first and the last 10% were discarded. (b.p.: 78°C)

Methanol- Reagent grade absolute methanol was refluxed over magnesium turnings for 2 hrs. and distilled through a half meter column packed with glass helices. The first and last 10% were discarded.

2. Internal Standards

Pentadecane (C₁₅)- Pentadecane (Columbia Organics) was washed with sulfuric acid and distilled by Dr. Peter J. Wagner.

Hexadecane (C₁₆)- Hexadecane (Aldrich) was washed with sulfuric acid and distilled by Dr. Peter J. Wagner.

Heptadecane (C₁₇)- Heptadecane (Aldrich) was washed with sulfuric acid and distilled by Dr. Peter J. Wagner.

Nonadecane (C₁₉)- Nonadecane (Chemical Samples Company) was recrystallized from ethanol by Dr. Bong-Ser Park

Eicosane (C₂₀)- Eicosane (Aldrich) was purified by recrystallization from ethanol.

Methyl benzoate (MB)- Methyl benzoate was purified by fractional distillation by Dr. Kung-Lung Cheng.

B. Equipment and Procedures

1. Glassware

All photolysis glassware (pipettes, syringes, volumetric flasks, etc.) were rinsed with acetone and distilled water and boiled in a solution of Alconox laboratory detergent in distilled water for 24 hrs. They were rinsed with water and boiled in distilled water for 3-4 days with the water changed every 24 hrs. After a final rinse with distilled water, the glassware was oven dried at 140 °C overnight and cooled to room temperature before use.

Ampoules used for irradiation were made from 13 x 100 mm Pyrex culture tubes by flame heating them approximately 2 cm from the top with an oxygen-natural gas torch and drawing them to a uniform 15 cm length.

2. Sample Preparations

All solutions were prepared by directly weighing the desired material into volumetric flasks or by dilution of stock solutions. Equal volumes (3.0 mL) of sample were placed via syringes into each ampoule.

3. Degassing Procedure

Irradiation ampoules were attached to a vacuum line. The ampoules were degassed by three consecutive freeze-pump-thaw cycles. The ampoules were then sealed with an oxygen-natural gas torch while still under vacuum.

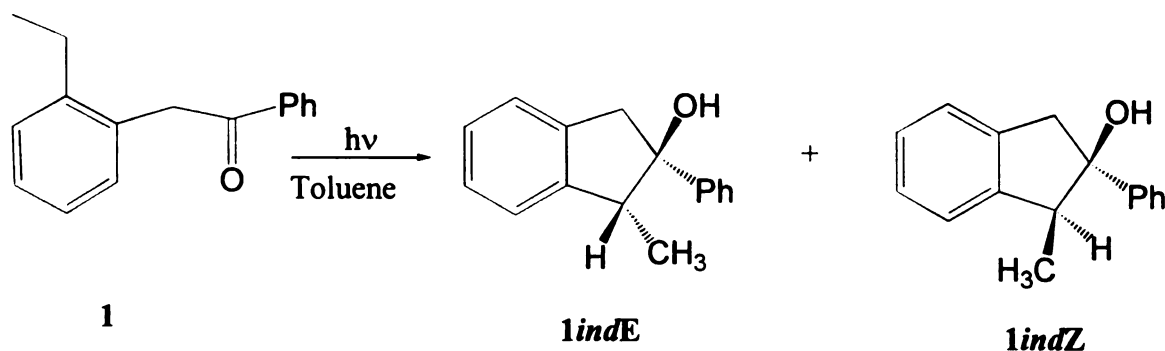
4. Irradiation Procedures

Small scale irradiations were made by irradiating 0.01 M degassed solutions of the sample in NMR tubes. The irradiation sources included a medium pressure mercury arc lamp and a Rayonet reactor. The light from the source was filtered through a Pyrex or Uranium glass or 313 and 366 nm filter solutions.

C. Identification of Photoproducts

Products From α -(2-Ethylphenyl)acetophenone (1)

α -(2-Ethylphenyl)acetophenone (0.0031 g) in 0.75 mL benzene- d_6 was irradiated through Pyrex filter for 15 minutes at room temperature. The signals of two photoproducts were detectable by NMR. The effect of temperature on product ratios was investigated by conducting the photochemistry in dry ice-acetone/ethanol, ice-water and silicon oil (110°C) baths. The diastereomeric ratio of the products were determined by NMR integration of the methyl doublet signals corresponding to each isomer. Large scale irradiation using 0.4 g of α -(2-ethylphenyl)acetophenone in 150 mL of toluene was performed until no trace of starting material could be observed by NMR. The product mixture was then separated by PTLC, using 3% ethyl acetate in hexane solution, to separate the two indanols. The Z-indanol was eluted before the E-indanol. The products were recovered as oils.



Scheme 61. Photoproducts of α -(2-Ethylphenyl)acetophenone

Z-1-methyl-2-phenyl-2-indanol

$^1\text{H NMR}(\text{CDCl}_3)$: δ 1.16 (d, $J=7.0$ Hz, 3H, CH_3), 3.05, 3.40 (AB quartet, $J=16.3$ Hz, 2H, CH_2), 3.48 (q, $J=7.0$ Hz, 1H, CH), 7.15-7.3 (m, 5H, Ar), 7.36 (t, $J=7.0$ Hz, 2H, Ar), 7.60 (d, $J=7.0$ Hz, 2H, Ar)

$^1\text{H NMR}(\text{Toluene-}d_8)$: δ 1.02 (d, $J=7.2$ Hz, 3H, CH_3), 2.8, 3.20 (AB quartet, $J=16.3$ Hz, 2H, CH_2), 3.22 (q, $J=7.2$ Hz, 1H, CH), 6.9-7.2 (m, 7H, Ar), 7.40 (d, $J=7.0$ Hz, 2H, Ar)

$^{13}\text{C NMR}(\text{CDCl}_3)$: δ 10.3, 49.3, 50.4, 85.4, 121.7, 124.8, 125.4, 126.9, 127.0, 127.1, 128.2, 140.0, 144.1, 145.0

$\text{IR}(\text{CCl}_4)$: 3600, 1175, 1043

E-1-methyl-2-phenyl-2-indanol

$^1\text{H NMR}(\text{CDCl}_3)$: δ 0.73 (d, $J=7.0$ Hz, 3H, CH_3), 3.1, 3.70 (2H, AB quartet, $J=16.0$ Hz, 2H, CH_2), 3.23 (q, $J=7.0$ Hz, 1H, CH), 7.21 (m, 4H, Ar), 7.29 (m, 1H, Ar), 7.34 (t, $J=6.6$ Hz, 2H, Ar), 7.45 (d, $J=6.56$ Hz, 2H, Ar)

$^1\text{H NMR}(\text{Toluene-}d_8)$: δ 0.69 (d, $J=7.5$ Hz, 3H, CH_3), 2.65, 3.40 (AB quartet, $J=15.9$ Hz, 2H, CH_2), 3.0 (q, $J=7.5$ Hz, 1H, CH), 6.9-7.2 (m, 9H, Ar)

$^{13}\text{C NMR}(\text{CDCl}_3)$: δ 17.6, 44.6, 52.4, 86.1, 124.3, 124.9, 126.2, 126.9, 127.0, 127.3, 128.1, 140.1, 140.2, 146.7

$\text{IR}(\text{CCl}_4)$: 3605, 1165, 1050

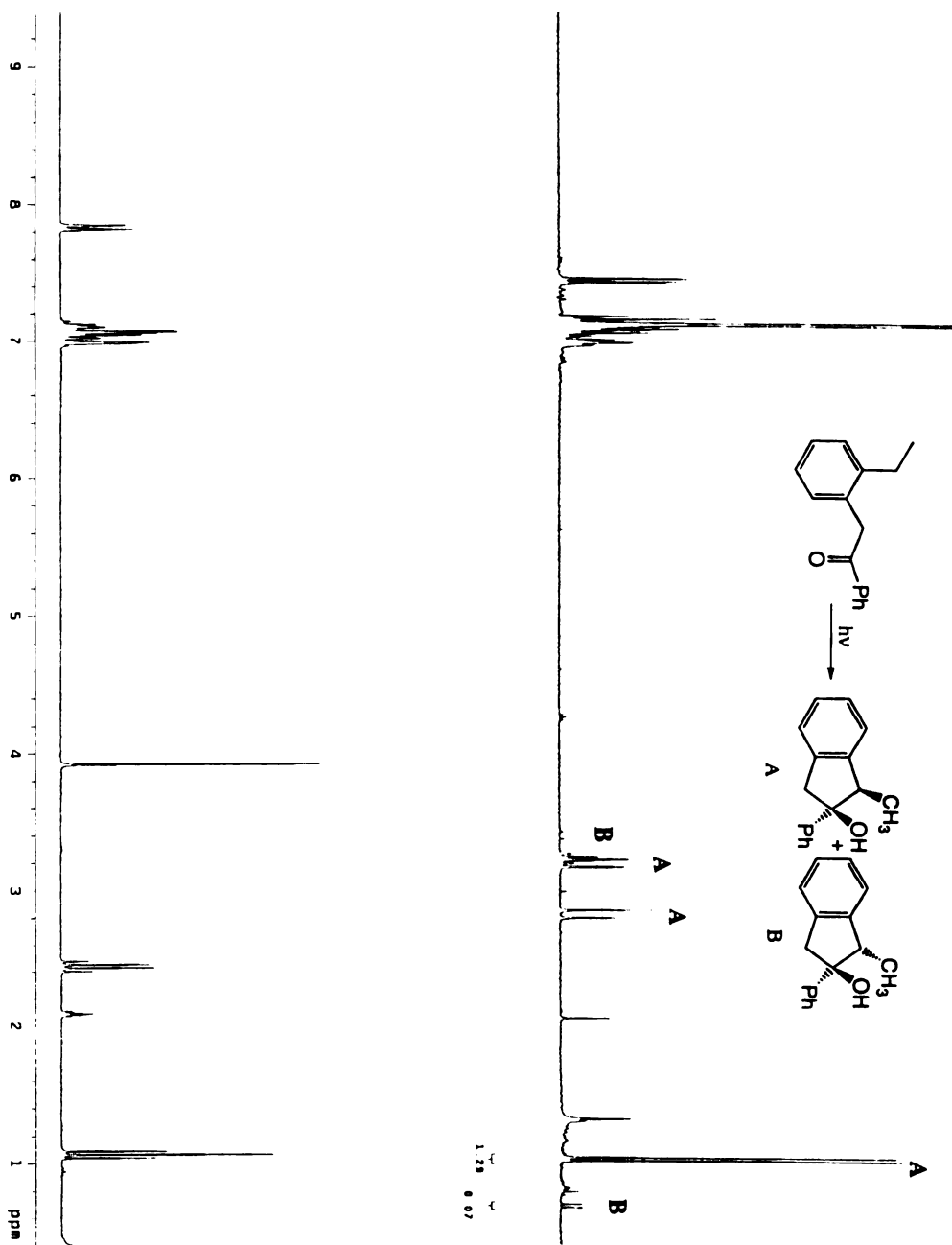
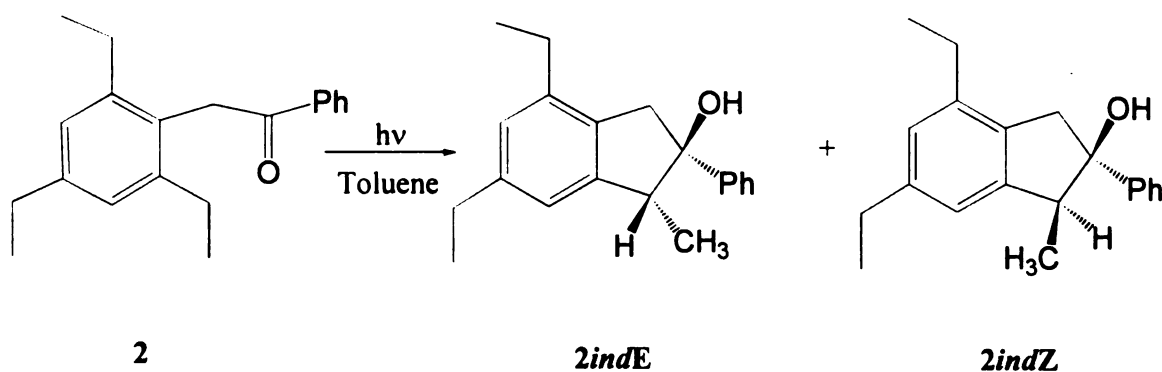


Figure 34. ^1H NMR of α -(2-Ethylphenyl)acetophenone Before and After Irradiation in Toluene ($\lambda > 290$ nm)

Products from α -(2,4,6-Triethylphenyl)acetophenone

α -(2,4,6-Triethylphenyl)acetophenone (0.002 g) in 0.8 mL of deuterated benzene was irradiated until starting material could not be observed by NMR. The signals corresponding to two isomeric indanols were detected in the NMR spectrum of the mixture. The effect of temperature on product ratios was investigated by conducting the photochemistry in acetone/ethanol, ice-water and silicon oil (110°C) baths. Solid state irradiation was performed by packing a melting point capillary with the compound and irradiating it through Pyrex-filtered uv light for three hours. The diastereomeric ratio of the products was determined by NMR integration of the methyl doublet peaks corresponding to each isomer. Large scale irradiation using 0.35 g of α -(2,4,6-triethylphenyl)acetophenone in 150 mL of toluene was performed until 100% conversion (GC). Solvent was removed to leave a yellow oil which was separated by PTLC using 5% ethyl acetate in hexane to separate the two isomers. The Z-isomer was eluted before the E-isomer. The products were recovered as oils.



Scheme 62. Photoproducts of α -(2,4,6-Triethylphenyl)acetophenone

Z-1-methyl-4,6-diethyl-2-phenyl-2-indanol

¹H NMR(CDCl₃): δ 1.25 (t, J=7.5 Hz, 3H, CH₃CH₂), 1.25 (d, J=7.5 Hz, 3H, CH₃CH), 1.32 (3H, t, J= 7.5 Hz, 3H, CH₃CH₂), 2.1 (s, 1H, OH), 2.6 (q, J=7.5 Hz, 2H, CH₂CH₃), 2.7 (q, J=7.5 Hz, 2H, CH₂CH₃), 3.2, 3.43 (AB quartet, J= 18 Hz, 2H, CH₂), 3.6 (q, J=7.5 Hz, 1H, CHCH₃), 6.95 (s, 1H, Ar), 6.98 (s, 1H, Ar), 7.3 (1H, t, J=6.7 Hz, 1H, Ar), 7.45 (2H, dd, J= 6.7, 7.0 Hz, 2H, Ar), 7.68 (d, J= 7.0 Hz, 2H, Ar)

¹H NMR(Toluene-d₈): δ 1.12 (d, J=6.9 Hz, 3H, CH₃), 1.15 (t, J=7.8 Hz, 3H, CH₃), 1.23 (t, J=7.8 Hz, 3H, CH₃), 1.4 (s, 1H, OH), 2.45 (q, J=7.8 Hz, 2H, CH₂), 2.59 (q, J=7.8 Hz, 2H, CH₂), 2.88, 3.13 (AB quartet, J=16.2 Hz, 2H, CH₂COH), 3.30 (q, J=7.8 Hz, 1H, CHCH₃), 6.84 (s, 1H, Ar), 6.87 (s, 1H, Ar), 7.11 (t, J= 6.6 Hz, 1H, Ar), 7.21 (dd, J=6.6, 7.2 Hz, 2H, Ar), 7.5 (d, J=7.2 Hz, 2H, Ar)

¹³C NMR(CDCl₃): δ 10.08, 14.21, 15.64, 26.01, 28.62, 47.16, 50.08, 84.88, 120.34, 125.01, 125.70, 126.48, 127.76, 135.05, 139.81, 143.36, 144.04, 144.79

IR(CCl₄): 3592, 2966.9, 2934.1, 2874.2, 1240.4, 1174.8, 991.54, 935.59, 871.94, 700.25

E-1-methyl-4,6-diethyl-2-phenyl-2-indanol

¹H NMR(CDCl₃): δ 0.79 (d, J=7.2 Hz, 3H, CH₃CH), 1.20 (t, J=7.5 Hz, 3H, CH₃CH₂), 1.25 (t, J=7.5 Hz, 3H, CH₃CH₂), 2.0 (broad s, 1H, OH), 2.62 (q, J=7.5 Hz, 2H, CH₂CH₃), 2.63 (q, J=7.5 Hz, 2H, CH₂CH₃), 3.12, 3.65 (AB quartet, J=18 Hz, 2H, CH₂), 3.39 (q, J= 7.2 Hz, 1H, CHCH₃), 6.90 (s, 1H, Ar), 6.92 (s, 1H, Ar), 7.25-7.5 (m, 5H, Ar)

¹H NMR(Toluene-d₈): δ 0.78 (d, J=6.9 Hz, 3H, CH₃CH), 1.15 (t, J=7.5 Hz, 3H, CH₃CH₂), 1.23 (t, J=7.5 Hz, 3H, CH₃CH₂), 1.4 (broad s, 1H, OH), 2.44 (q, J=7.5 Hz, 2H,

CH₂CH₃), 2.59 (q, J=7.5 Hz, 2H, CH₂CH₃), peaks between 3.0-7.5 overlapped with those from the major isomer.

¹³C NMR(CDCl₃): δ 14.52, 15.82, 17.84, 26.48, 28.87, 42.53, 52.55, 85.98, 121.30, 125.35, 125.89, 126.17, 127.26, 128.09, 135.18, 140.02, 143.30, 146.80

IR(CCl₄): 3472, 2968.8, 2930.24, 2872.37, 1277, 1211.4, 1066.8, 881.58, 746.55, 700.25

Products from α-(o-Tolyl)propiophenone (3)

α-(o-Tolyl)propiophenone (0.002 g) in 0.8 mL of deuterated benzene was irradiated until starting material could not be observed by NMR. The signals corresponding to several products were detected in the NMR spectrum of the mixture. These products were identified as two isomeric 2-phenyl-2-indanols, two isomeric diarylethanes, β-tolylpropiophenone and benzaldehyde. The effect of temperature on product ratios was investigated by conducting photochemistry in dry ice-ethanol, ice-water and silicon oil (110°C) baths. The diastereomeric ratio of indanols was determined by NMR integration of the methyl doublet signals corresponding to each isomer. Large scale irradiation using 0.3 g of α-(o-tolyl)propiophenone in 150 mL of methanol was performed until 100% conversion by NMR. The products were separated by PTLC using 5% ethyl acetate in hexane as eluent and characterized. Two additional products which were identified as two isomeric 1-phenyl-2-tolyl-1-propanols were also recovered. The order of elution was as follows: diarylethenes followed by β-tolylpropiophenone, the Z-indanol, the E-indanol and photoreduction products. The products were recovered as oils.

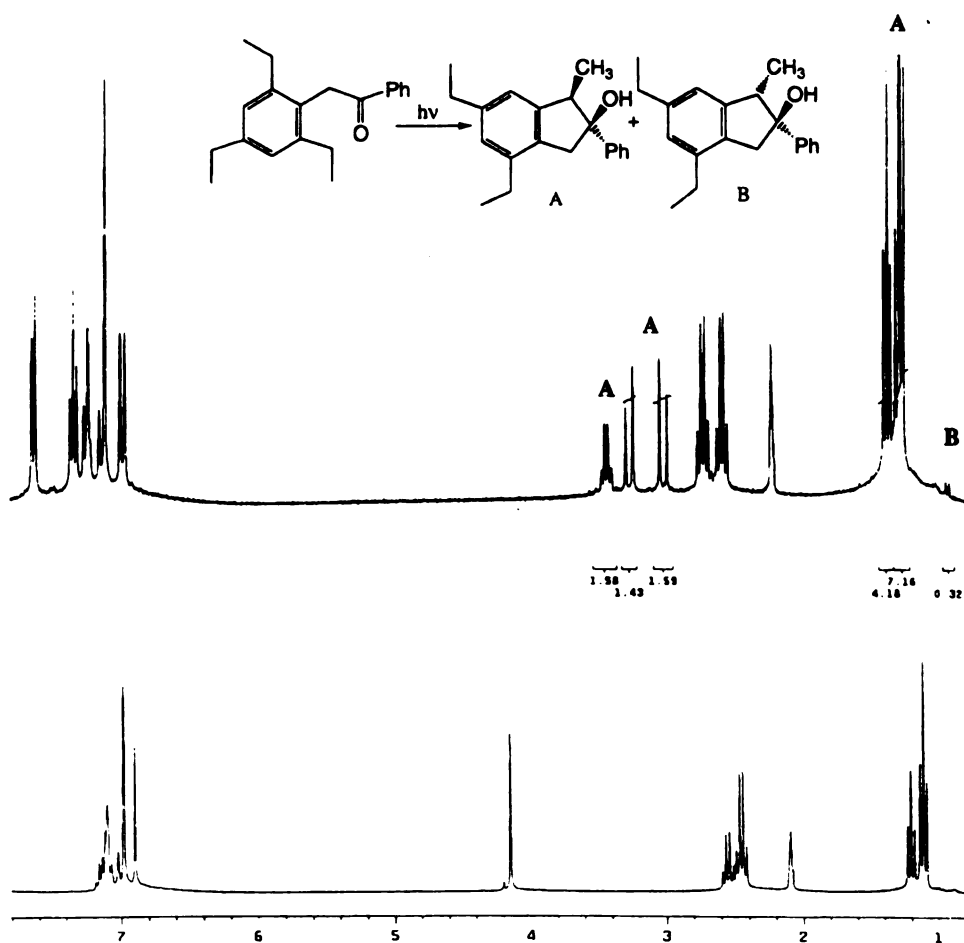


Figure 35. ^1H NMR Spectra of α -(2,4,6-Triethylphenyl)acetophenone Before and After Irradiation in Toluene ($\lambda > 290$ nm)

IR(CCl₄): 3605, 1165, 1050

(R,R) and (S,S)-1-Phenyl-2-tolyl-1-propanol

¹H NMR(CDCl₃): δ 0.95 (d, J=7.0 Hz, 3H, CH₃CH), 2.15 (s, 3H, CH₃Ar), 3.25 (dq, J=7.0, 6.7 Hz, 1H, CHCH₃), 4.47 (d, J=6.7 Hz, 1H, CHOH), 7.0-7.3 (m, 9H, Ar)

(R,S) and (S,R)-1-Phenyl-2-tolyl-1-propanol

¹H NMR(CDCl₃): δ 1.30 (d, J=7.0 Hz, 3H, CH₃CH), 1.92 (s, 3H, CH₃Ar), 3.25 (dq, J=7.0, 6.7 Hz, 1H, CHCH₃), 4.47 (d, J=6.7 Hz, 1H, CHOH), 7.0-7.3 (m, 9H, Ar)

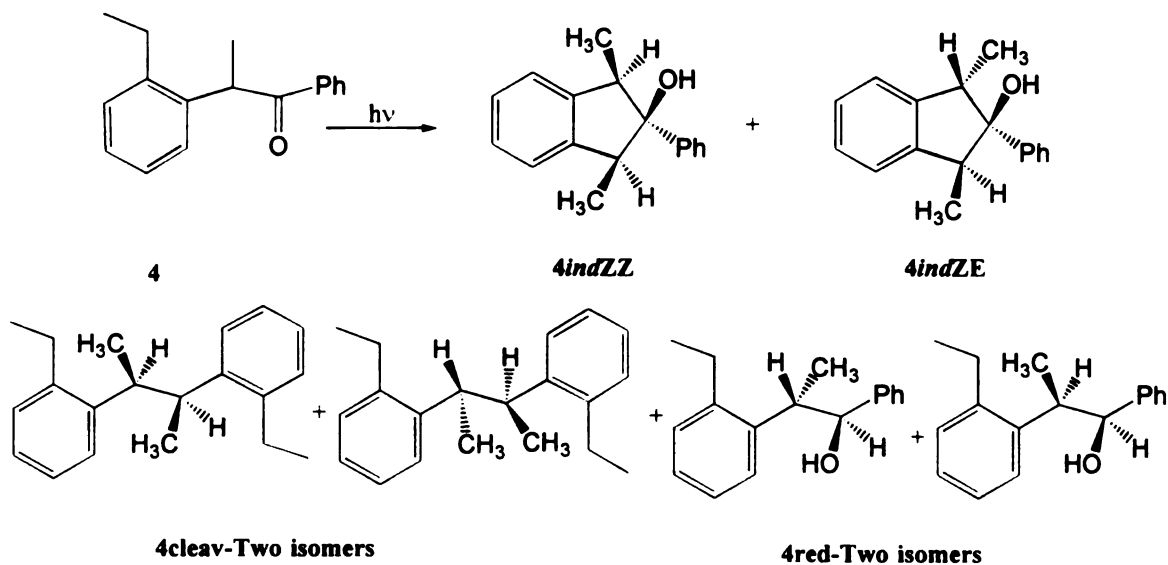
1,2-Ditolylbutanes

¹H NMR(CDCl₃): δ 1.0 (d, J=7.0 Hz, 6H, 2CH₃CH), 1.20 (d, J=7.0 Hz, 6H, 2CH₃CH), 2.0 (s, 6H, 2CH₃Ar), 2.2 (s, 6H, 2CH₃Ar), 3.15 (m, 4H, CHCH₃), 6.8-7.3 (m, 16H, Ar)

Products from α-(2-Ethylphenyl)-β,β,β-trideuteropropiophenone and/or α-(2-Ethylphenyl)propiofenone (4, 4d₃)

α-(2-Ethylphenyl)-β,β,β-trideuteropropiophenone (0.003 g) in 0.8 mL of deuterated benzene was irradiated until no trace of starting material could be observed by NMR. A mixture of several products including two isomeric indanols, two isomeric diphenylethanes, and benzaldehyde were detected, by their signals, upon analysis of the NMR spectrum of the photolysis mixture. The effect of temperature and phase on product ratios was also investigated by conducting the photochemistry in acetone/ethanol, ice-water and silicon oil (110°C) baths and in solid. The diastereomeric ratio of indanols was

determined by NMR integration of the methyl doublet signals corresponding to each isomer. Large scale irradiation using 0.25 g of α -(2-ethylphenyl)- β,β,β -trideutero propiophenone in 100 mL of benzene was performed. Solvent was evaporated to leave a colorless oil which was chromatographed by preparative scale tlc using 3% ethyl acetate in hexane solution. The order of elution was as follows: diarylethenes, the Z-indanol, the E-indanol and photoreduction products. The indanols and photoreduction products were recovered as oils.



Scheme 64. Photoproducts of α -(2-Ethylphenyl)- β,β,β -trideuteropropiophenone

Z-1-Methyl-Z-3-trideuteromethyl-2-phenyl-2-indanol

$^1\text{H NMR}(\text{CDCl}_3)$: δ 1.19 (d, $J=7.0$ Hz, 3H, CH_3CH), 1.52 (broad s, 1H, OH), 3.50 (s, 1H, CHCD_3), 3.50 (q, $J=7.0$ Hz, 1H, CHCH_3), 7.18 (dd, $J=0.7, 4.5$ Hz, 1H, Ar), 7.20 (broad, 1H, Ar), 7.25-7.27 (m, 2H, Ar), 7.29 (t, $J=7.7$ Hz, 1H, Ar), 7.38 (dd, $J=7.7, 7.1$ Hz, 2H, Ar), 7.60 (d, $J=7.1$ Hz, 2H, Ar)

^1H NMR(Toluene- d_8): δ 0.92 (d, $J=7.2\text{Hz}$, 3H, CH_3CH), 3.12 (s, 1H, CHCD_3), 3.12 (q, $J=7.2\text{ Hz}$, 1H, CHCH_3), 7.0-7.6 (m, 9H, Ar)

^2H NMR(CCl_4): δ 1.29 (s, 3D)

^{13}C NMR(CDCl_3): δ 9.90, 9.91 (septet), 50.05, 88.23, 123.35, 125.7, 126.9, 127.16, 128.1, 144.3

IR(CCl_4): 3588, 2966, 2932, 2224, 1489, 1176.7, 1055, 985.8, 951, 912.4, 871.9, 746.5

(Z,Z)-1,3-Dimethyl-2-phenyl-2-indanol

^1H NMR(CDCl_3): δ 1.19 (d, $J=7.0\text{ Hz}$, 6H, $2\text{CH}_3\text{CH}$), 1.52 (broad s, 1H, OH), 3.50 (q, $J=7.0\text{ Hz}$, 2H, 2CHCH_3), 7.18 (dd, $J=0.7, 4.5\text{ Hz}$, 1H, Ar), 7.20 (broad, 1H, Ar), 7.25-7.27 (m, 2H, Ar), 7.29 (t, $J=7.7\text{ Hz}$, 1H, Ar), 7.38 (dd, $J=7.7, 7.1\text{ Hz}$, 2H, Ar), 7.60 (d, $J=7.1\text{ Hz}$, 2H, Ar)

^1H NMR(Toluene- d_8): δ 0.92 (d, $J=7.2\text{Hz}$, 6H, $2\text{CH}_3\text{CH}$), 3.12 (q, $J=7.2\text{ Hz}$, 2H, 2CHCH_3), 7.0-7.6 (m, 9H, Ar)

^{13}C NMR(CDCl_3): δ 9.90, 9.91, 50.05, 88.23, 123.35, 125.7, 126.9, 127.16, 128.1, 144.3

IR(CCl_4): 3588, 2966, 2932, 1489, 1176.7, 1055, 985.8, 951, 912.4, 871.9, 746.5, 700.25

E-1-methyl-Z-3-trideuteromethyl-2-phenyl-2-indanol

^1H NMR(CDCl_3): δ 0.74 (d, $J=7.35\text{ Hz}$, 3H, CH_3CH), 1.65 (broad s, 1H, OH), 3.28 (q, $J=7.40\text{ Hz}$, 1H, CHCH_3), 3.90 (s, 1H, CHCD_3), 7.20-7.28 (m, 4H, Ar), 7.32 (t, $J=7.2\text{ Hz}$, 1H, Ar), 7.37 (dd, $J=7.35, 7.2\text{ Hz}$, 2H, Ar), 7.52 (d, $J=7.35\text{ Hz}$, 2H, Ar)

$^1\text{H NMR}$ (Toluene- d_8): δ 0.55 (d, $J=7.5\text{Hz}$, 3H, CH_3CH), 2.95 (q, $J=7.5\text{ Hz}$, 1H, CHCH_3), 3.43 (s, 1H, CHCD_3), 7.0-7.6 (m, 9H, Ar)

$^2\text{H NMR}$ (CCl_4): δ 1.4 (s, 3D)

$^{13}\text{C NMR}$ (CDCl_3): δ 11.1 (septet), 18.3, 43.3, 52.5, 79.9, 123.9, 124.4, 126.0, 126.58, 127.1, 127.3, 127.9, 128.2, 128.3, 128.7

IR(CCl_4): 3470, 2966.9, 2932.2, 2874, 2229.9, 1223, 1062, 970, 870, 740.7

(E,Z)-1,3-Dimethyl-2-phenyl-2-indanol

$^1\text{H NMR}$ (CDCl_3): δ 0.74 (d, $J=7.4\text{ Hz}$, 3H, CH_3CH), 1.34 (d, $J=7.3\text{ Hz}$, 3H, CH_3CH), 1.65 (broad s, 1H, OH), 3.28 (q, $J=7.40\text{ Hz}$, 1H, CHCH_3), 3.90 (q, $J=7.3\text{ Hz}$, 1H, CHCH_3), 7.20-7.28 (m, 4H, Ar), 7.32 (t, $J=7.2\text{ Hz}$, 1H, Ar), 7.37 (dd, $J=7.35, 7.2\text{ Hz}$, 2H, Ar), 7.52 (d, $J=7.35\text{ Hz}$, 2H, Ar)

$^1\text{H NMR}$ (Toluene- d_8): δ 0.55 (d, $J=7.5\text{Hz}$, 3H, CH_3CH), 1.1 (d, $J=7.4\text{ Hz}$, 3H, CH_3CH), 2.95 (q, $J=7.5\text{ Hz}$, 1H, CHCH_3), 3.43 (q, $J=7.4\text{ Hz}$, 1H, CHCH_3), 7.0-7.6 (m, 9H, Ar)

$^{13}\text{C NMR}$ (CDCl_3): δ 11.1, 18.3, 43.3, 52.5, 79.9, 123.9, 124.4, 126.0, 126.58, 127.1, 127.3, 127.9, 128.2, 128.3, 128.7

IR(CCl_4): 3470, 2966.9, 2932.2, 2874, 1223, 1062, 970, 870, 740.7

(R,R) and (S,S)-2,3-di(ethylphenyl)butane

$^1\text{H NMR}$ (CDCl_3): δ 1.09 (t, $J=7.48\text{ Hz}$, 3H, CH_3CH_2), 1.27 (3H, t, $J=7.54\text{ Hz}$, 3H, CH_3CH_2), 2.36 (dq, $J=7.42, 14.56\text{ Hz}$, 1H, CH_2CH_3), 2.60 (dq, $J=7.47, 14.56\text{ Hz}$, 1H, CH_2CH_3), 2.72 (1H, dq, $J=7.49, 14.49\text{ Hz}$, 1H, CH_2CH_3), 2.84 (dq, $J=7.41, 14.56\text{ Hz}$, 1H,

CH₂CH₃), 3.20 (s, 1H, CHCD₃), 3.26 (s, 1H, CHCD₃), 6.96 (1H, dt, J=2.19, 7.7 Hz, 1H, Ar), 6.98 (dt, J=1.38, 7.5 Hz, 1H, Ar), 7.05 (dt, J=2.19, 7.7 Hz, 1H, Ar), 7.15 (dt, J=1.37, 7.7 Hz, 1H, Ar), 7.19 (dt, J=2.14, 7.7 Hz, 1H, Ar), 7.23 (broad d, J=7.7 Hz, 1H, Ar), 7.25 (dt, J=1.98, 7.5 Hz, 1H, Ar), 7.34 (broad d, J=7.41 Hz, 1H, Ar)

¹³C NMR(CDCl₃): δ 15.5, 15.89, 20.84, 21.33, 25.54, 26.33, 39.84, 40.34, 125.45, 125.7, 125.8, 126.27, 126.51, 128.15, 128.68, 140.5, 141.99, 144.46, 144.51

(R,S) and (S,R)-2,3-di(ethylphenyl)butane

¹H NMR(CDCl₃): δ 1.05 (t, J=7.60 Hz, 6H, 2 CH₃CH₂), 2.34 (dq, J=7.63, 14.35 Hz, 2H, CH₂CH₃), 2.58 (dq, J=7.69, 14.56 Hz, 2H, CH₂CH₃), 3.25 (broad s, 2H, 2CHCD₃), 6.94 (dt, J=2.19, 7.5 Hz, 2H, Ar), 6.96 (dt, J=1.35, 7.5 Hz, 2H, Ar), 7.03 (dt, J=2.19, 7.5 Hz, 2H, Ar), 7.21 (broad d, J=7.42 Hz, 2H, Ar)

¹³C NMR(CDCl₃): δ 15.5, 20.84, 25.54, 39.83, 125.43, 126.50, 128.15

1-Phenyl-2-(2'-ethylphenyl)-3,3,3-trideutero-1-propanol (one isomer)

¹H NMR(CDCl₃): δ 1.10 (t, J= 7.6 Hz, 3H, CH₃CH₂), 2.5 (AB quartet of q, J=7.6 Hz, J=15 Hz, 2H, CH₂CH₃), 3.35 (d, 1H, CHCD₃), 4.8 (d, 2H, CHOH), 7.1-7.5 (m, 9H, Ar)

1-Phenyl-2-(2'-ethylphenyl)-3,3,3-trideutero-1-propanol (second isomer)

¹H NMR(CDCl₃): δ 1.25 (t, J= 7.6 Hz, 3H, CH₃CH₂), 2.7 (AB quartet of q, J=7.6, 15 Hz, 2H, CH₂CH₃), 3.35 (d, 1H, CHCD₃), 4.7 (d, 2H, CHOH), 7.1-7.5 (m, 9H, Ar)

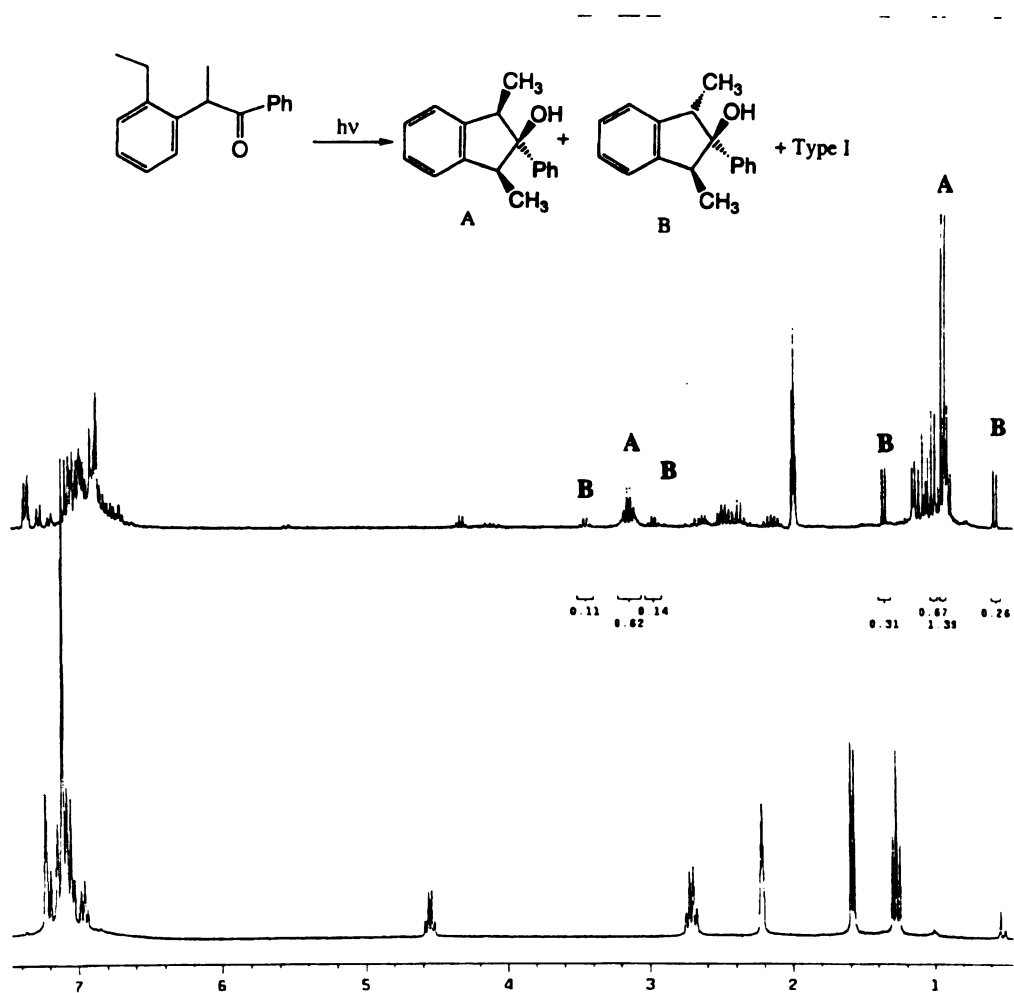
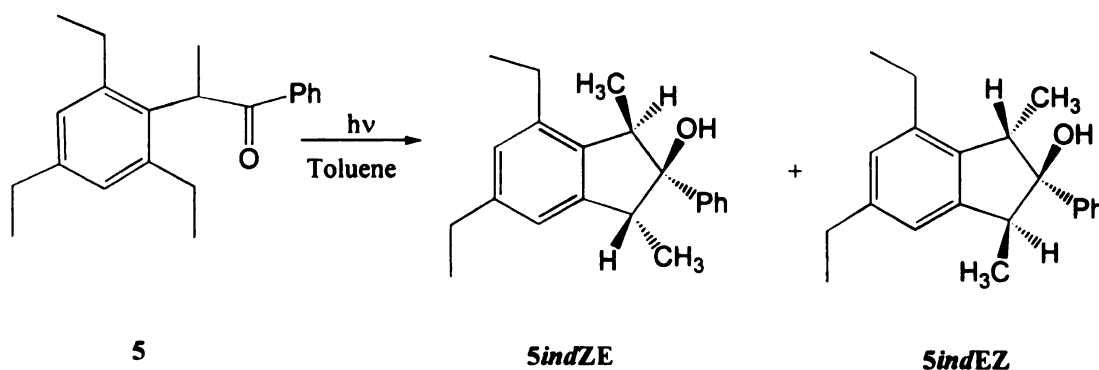


Figure 36. ^1H NMR Spectra of α -(2-Ethylphenyl)propiophenone Before and After Irradiation in Toluene ($\lambda > 290$ nm)

Products from α -(2,4,6-Triethylphenyl)- β,β,β -trideuteropropiophenone and/or α -(2,4,6-Triethylphenyl)propiophenone (5, 5d₃)

α -(2,4,6-Triethylphenyl)- β,β,β -trideuteropropiophenone (0.005 g) in 0.8 mL of deuterated benzene was irradiated until no trace of starting material could be observed by NMR. The signals for two isomeric indanols were detected upon analysis of the NMR spectrum of the photolysis mixture. In our investigation we separated the products from both the deuterated and fully protanated species. The effect of temperature and phase on product ratios was also investigated by conducting the photochemistry in acetone/ethanol, ice-water and silicon oil (110°C) baths and in solid. The diastereomeric ratio of indanols was determined by NMR integration of methyl doublet signals corresponding to each isomer. In order to separate the two indanols, large scale irradiation using 0.30 g of α -(2,4,6-triethylphenyl)- β,β,β -trideuteropropiophenone in 100 mL of benzene was performed. Solvent was evaporated to leave a yellow oil which was chromatographed by PTLC 7% ethyl acetate in hexane solution. The plate had to be diluted several times to separate the two isomers (oils). The ZE-isomer was the top fraction eluted.



Scheme 65. Photoproducts of α -(2,4,6-Triethylphenyl) β,β,β -trideutero propiophenone

4,6-Diethyl-Z-1-trideuteromethyl-E-3-methyl-2-phenyl-2-indanol

¹H NMR(CDCl₃): δ 0.86 (d, J=7.14 Hz, 3H, CH₃CH), 1.24 (t, J=7.8 Hz, 3H, CH₃CH₂), 1.29 (t, J=7.8 Hz, 3H, CH₃CH₂), 2.0 (broad s, 1H, OH), 2.6 (q, J=7.8 Hz, 2H, CH₂CH₃), 2.7 (dq, J=7.8, 14.5 Hz, 2H, CH₂CH₃), 3.45 (q, J=7.1 Hz, 1H, CHCH₃), 3.6 (broad s, 1H, CHCD₃), 6.74 (s, 1H, Ar), 6.90 (s, 1H, Ar), 7.15-7.3 (m, 5H, Ar)

¹H NMR(Toluene-d₈): δ 0.92 (d, J=7.2 Hz, 3H, CH₃CH), 1.16-1.3 (m, 6H), 2.0 (broad s, 1H, OH), 2.5 (dq, J=7.2, 14.4 Hz, 2H, CH₂CH₃), 2.6 (q, J=7.5 Hz, 2H, CH₂CH₃), 3.20 (q, J=7.1 Hz, 1H, CHCH₃), 3.34 (broad s, 1H, CHCD₃), 6.8-7.3 (m, 7H, Ar)

²H NMR(CCl₄): δ 1.48 (s, 3D)

¹³C NMR(CDCl₃): δ 13.62, 14.4 (septet), 14.77, 15.22, 24.84, 28.42, 46.29, 48.80, 86.20, 120.22, 125.42, 126.05, 126.42, 127.38, 138.45, 140.95, 142.90, 144.10, 144.44

IR(CCl₄): 3470.2, 3061.4, 2966.9, 2932.2, 2874.3, 2230, 1280.9, 1062.9, 970.3, 870, 806.4, 740.7

4,6-Diethyl-Z,E-1,3-dimethyl-2-phenyl-2-indanol

¹H NMR(CDCl₃): δ 0.86 (d, J=7.14 Hz, 3H, CH₃CH), 1.24 (t, J=7.8 Hz, 3H, CH₃CH₂), 1.29 (t, J=7.8 Hz, 3H, CH₃CH₂), 1.47 (d, J=7.2 Hz, 3H, CH₃CH), 2.0 (broad s, 1H, OH), 2.6 (q, J=7.8 Hz, 2H, CH₂CH₃), 2.7 (dq, J=7.8, 14.5 Hz, 2H, CH₂CH₃), 3.45 (q, J=7.1 Hz, 1H, CHCH₃), 3.6 (q, J=7.2, 1H, CHCH₃), 6.74 (s, 1H, Ar), 6.90 (s, 1H, Ar), 7.15-7.3 (m, 5H, Ar)

^1H NMR(Toluene- d_8): δ 0.92 (d, $J=7.2$ Hz, 3H, CH_3CH), 1.16-1.3 (m, 9H), 2.0 (broad s, 1H, OH), 2.5 (dq, $J=7.2, 14.4$ Hz, 2H, CH_2CH_3), 2.6 (q, $J=7.5$ Hz, 2H, CH_2CH_3), 3.20 (q, $J=7.1$ Hz, 1H, CHCH_3), 3.34 (q, $J=7.2$ Hz, 1H, CHCH_3), 6.8-7.3 (m, 7H, Ar)

^{13}C NMR(CDCl_3): δ 13.62, 14.4, 14.77, 15.22, 24.84, 28.42, 46.29, 48.80, 86.20, 120.22, 125.42, 126.05, 126.42, 127.38, 138.45, 140.95, 142.90, 144.10, 144.44

IR(CCl_4): 3470.2, 3061.4, 2966.9, 2932.2, 2874.3, 1280.9, 1062.9, 970.3, 870, 806.4, 740.7

4,6-Diethyl-E-1-trideuteromethyl-Z-3-methyl--2-phenyl-2-indanol

^1H NMR(CDCl_3): δ 1.291 (t, $J=7.56$ Hz, 3H, CH_3CH_2), 1.294 (t, $J=7.56$ Hz, 3H, CH_3CH_2), 1.36 (d, $J=7.0$ Hz, 3H, CH_3CH), 2.0 (broad s, 1H, OH), 2.6 (dq, $J=7.56, 14.3$ Hz, 2H, CH_2CH_3), 2.7 (q, $J=7.8$ Hz, 2H, CH_2CH_3), 3.30 (broad s, 1H, CHCD_3), 3.95 (q, $J=7.0$ Hz, 1H, CHCH_3), 6.92 (s, 2H, Ar), 7.30 (t, $J=7.3$ Hz, 1H, Ar), 7.40 (2H, dd, $J=7.3, 7.5$ Hz, 2H, Ar), 7.6 (d, $J=7.5$ Hz, 2H, Ar)

^1H NMR(Toluene- d_8): δ 1.32 (d, $J=7.2$ Hz, 3H, CH_3CH), 1.16-1.3 (m, 6H), 2.0 (broad s, 1H, OH), 2.52 (dq, $J=7.2, 14.4$ Hz, 2H, CH_2CH_3), 2.61 (q, $J=7.5$ Hz, 2H, CH_2CH_3), 3.32 (broad s, 1H, CHCD_3), 3.71 (q, $J=7.1$ Hz, 1H, CHCH_3), 6.8-7.3 (m, 7H, Ar)

^2H NMR(CCl_4): δ 0.816 (s, 3D)

^{13}C NMR(CDCl_3): δ 10.58, 15.28, 15.72, 17.20 (septet), 24.95, 28.95, 42.20, 50.65, 87.92, 121.04, 126.08, 126.70, 127.26, 128.24, 139.92, 141.20, 141.73, 143.42, 143.84

IR(CCl_4): 3572, 3061.4, 3030.6, 2966.9, 2932.2, 2230, 1282.8, 1033.9, 987.6, 951, 871.9,

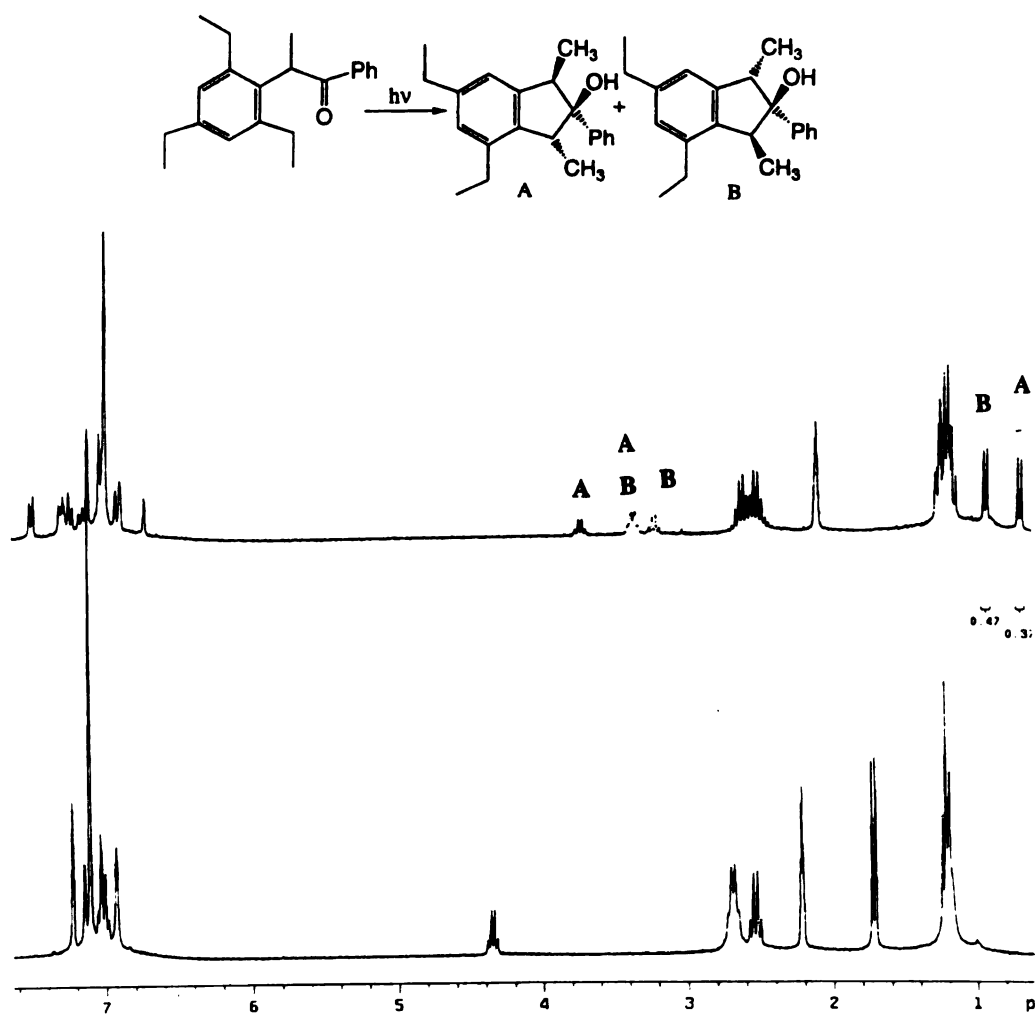


Figure 37. ¹H NMR Spectra of α -(2,4,6-Triethylphenyl)propiophenone Before and After Irradiation in Toluene ($\lambda > 290$ nm)

4,6-Diethyl-E,Z-1,3-dimethyl-2-phenyl-2-indanol

¹H NMR(CDCl₃): δ 0.82 (d, J=7.0 Hz, 3H, CH₃CH), 1.291 (t, J=7.56 Hz, 3H, CH₃CH₂), 1.294 (t, J=7.56 Hz, 3H, CH₃CH₂), 1.36 (d, J=7.0 Hz, 3H, CH₃CH), 2.0 (broad s, 1H, OH), 2.6 (dq, J=7.56, 14.3 Hz, 2H, CH₂CH₃), 2.7 (q, J=7.8 Hz, 2H, CH₂CH₃), 3.30 (q, J=7.0 Hz, 1H, CHCH₃), 3.95 (q, J=7.0 Hz, 1H, CHCH₃), 6.92 (s, 2H, Ar), 7.30 (t, J=7.3 Hz, 1H, Ar), 7.40 (2H, dd, J=7.3, 7.5 Hz, 2H, Ar), 7.6 (d, J=7.5 Hz, 2H, Ar)

¹H NMR(Toluene-d₈): δ 0.8 (d, J=7.1 Hz, 3H, CH₃CH), 1.16-1.3 (m, 9H), 2.0 (broad s, 1H, OH), 2.52 (dq, J=7.2, 14.4 Hz, 2H, CH₂CH₃), 2.61 (q, J=7.5 Hz, 2H, CH₂CH₃), 3.32 (q, J=7.1 Hz, 1H, CHCH₃), 3.71 (q, J=7.1 Hz, 1H, CHCH₃), 6.8-7.3 (m, 7H, Ar)

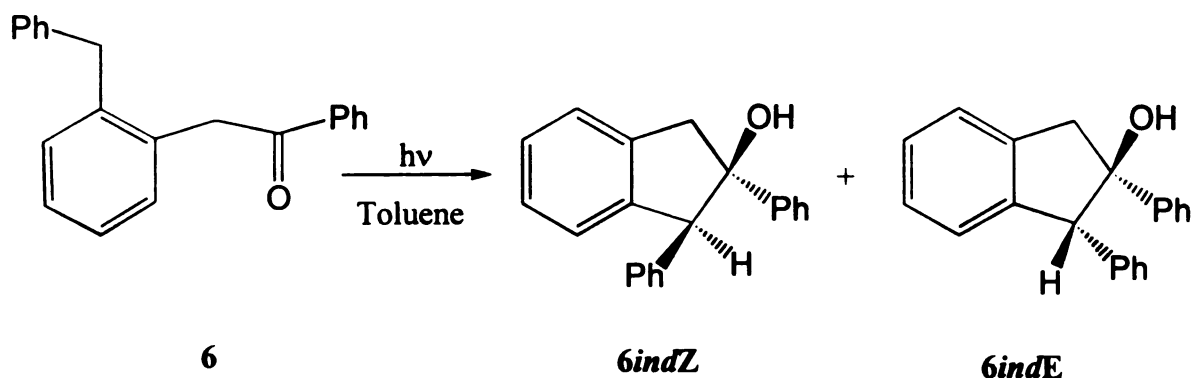
¹³C NMR(CDCl₃): δ 10.58, 15.28, 15.72, 17.20, 24.95, 28.95, 42.20, 50.65, 87.92, 121.04, 126.08, 126.70, 127.26, 128.24, 139.92, 141.20, 141.73, 143.42, 143.84

IR(CCl₄): 3572, 3061.4, 3030.6, 2966.9, 2932.2, 1033.9, 987.6, 951, 871.9, 787

Products from α-(2-Benzylphenyl)acetophenone (6)

α-(2-Benzylphenyl)acetophenone (0.003 g) in 0.8 mL of deuterated benzene was irradiated until no trace of starting material could be detected by NMR. The signals for two isomeric indanols in a 1:1 ratio were detected. NOe experiments were performed on isolated indanols to correctly assign their stereochemical arrangement. The effect of temperature and phase on product ratios was also investigated by conducting the photochemistry in acetone/ethanol, ice-water and silicon oil (110°C) baths and in solid. The diastereomeric ratio of indanols was determined by NMR integration of the methylene (AB quartet) signals corresponding to each isomer. Large scale irradiation (0.4

g in 100 mL benzene) was performed and the two indanols were separated by preparative scale tlc using 5% ethyl acetate in hexane solution. The Z-indanol was the first eluted isomer.



Scheme 66. Photoproducts of α -(2-Benzylphenyl)acetophenone

Z-1,2-diphenyl-2-indanol

$^1\text{H NMR}(\text{CDCl}_3)$: δ 1.85 (s, 1H, OH), 3.4, 3.65 (AB quartet, $J=16.5$ Hz, 2H, CH_2), 4.95 (s, 1H, CHPh), 7.05 (dd, $J=7.38, 2.97$ Hz, 2H, Ar), 7.12 (d, $J=7.41$ Hz, 1H, Ar), 7.2-7.45 (m, 9H, Ar), 7.53 (d, $J=7.38$ Hz, 2H, Ar)

$^1\text{H NMR}(\text{Toluene-}d_8)$: δ 1.85 (s, 1H, OH), 3.22, 3.33 (AB quartet, $J=16.2$ Hz, 2H, CH_2), 4.64 (s, 1H, CHPh), 7.00-7.6 (m, 14H, Ar)

$^{13}\text{C NMR}(\text{CDCl}_3)$: δ 48.93, 63.92, 84.99, 124.85, 125.36, 125.49, 126.84, 127.46, 127.64, 128.04, 128.48, 129.97, 136.15, 141.71, 142.74, 145.18

$\text{IR}(\text{CCl}_4)$: 3557, 3030.6, 1495, 1452.6, 1286.7, 1053.3, 702.18

Noe (CDCl_3): irradiation of the peak at δ 1.85 (OH) enhanced peaks at 3.4 ppm (2%), and 7.0-7.6 ppm (25%)

Irradiation of the peak at δ 4.95 ppm (methine) enhanced peaks at 3.4 ppm (2.5%), 3.65 ppm (2.1%), 7.05, 7.12 ppm (27%), 7.2-7.45 ppm (18.6%), and 7.53 ppm (3.0%)

Irradiation of the peak at δ 3.65 ppm enhanced peaks at 3.4 ppm (37%), 4.95 ppm (1.3%), and 7.0-7.4 ppm (32%)

Irradiation of the peak at δ 3.4 ppm enhanced peaks at 1.85 ppm (3.8%), 3.65 ppm (22%), and 7.0-7.6 ppm (16%)

E-1,2-diphenyl-2-indanol

$^1\text{H NMR}(\text{CDCl}_3)$: δ 2.45 (broad s, 1H, OH), 3.30, 3.85 (AB quartet, $J=16$ Hz, 2H, CH_2), 4.61 (s, 1H, CHPh), 6.61 (dd, $J=7.86, 1.92$ Hz, 2H, Ar), 6.90-7.10 (m, 8H, Ar), 7.13 (1H, d, $J=7.71$ Hz), 7.25 (t, $J=7.14$ Hz, 1H, Ar), 7.34 (t, $J=7.14$ Hz, 1H, Ar), 7.43 (d, $J=7.2$ Hz, 1H, Ar)

$^1\text{H NMR}(\text{Toluene-}d_8)$: δ 1.85 (s, 1H, OH), 2.94, 3.53 (AB quartet, $J=16.2$ Hz, 2H, CH_2), 4.45 (s, 1H, CHPh), 6.8-7.6 (m, 14H, Ar)

$^{13}\text{C NMR}(\text{CDCl}_3)$: δ 46.0, 65.18, 87.3, 124.6, 125.96, 126.0, 126.3, 126.87, 127.2, 127.4, 127.6, 128.9, 139.6, 141.5, 142.64, 144.0

IR(CCl_4): 3560, 3030.5, 1495, 1286, 702.3

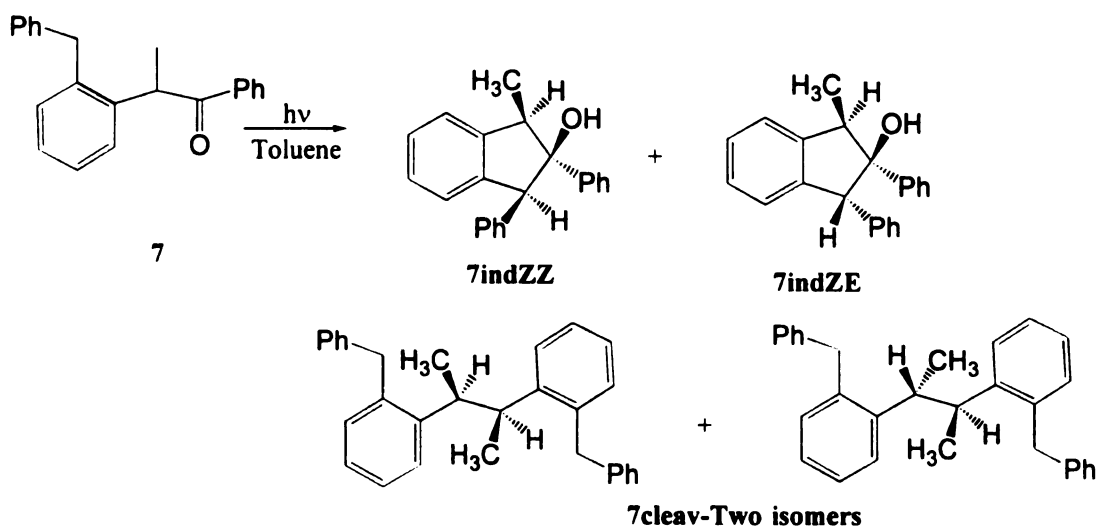
Noe (CDCl_3): irradiation of the peak at δ 2.45 ppm (OH) enhanced peaks at 3.3 ppm (1%), and 4.61 (2.1%)

Irradiation of the peak at δ 4.61 ppm (methine) enhanced peaks at 2.45 ppm (5.5%), 6.60 ppm (12%), and 6.9-7.1 ppm (14.5%)

Irradiation of the peak at δ 6.60 ppm enhanced peaks at 3.3 ppm (3%), 4.61 ppm (7.75%), and 6.9-7.14 ppm (24%).

Products from α -(2-Benzylphenyl)propiophenone (7)

α -(2-Benzylphenyl)propiophenone (0.005 g) in 0.8 mL of deuterated benzene was irradiated until no trace of starting material could be observed by NMR. The signals for two isomeric indanols and two diarylethanes were detected upon analysis of the NMR spectrum of the photolysis mixture. The diastereomeric ratio of indanols was determined by NMR integration of methyl doublet signals corresponding to each isomer. Products were separated by performing large scale irradiation using 0.30 g of α -(2-benzylphenyl)propiophenone in 100 mL of benzene. Solvent was evaporated to leave a yellow oil which was chromatographed by PTLC using 3% ethyl acetate in hexane solution. The diarylbutanes moved with the solvent line and had a r_f value of nearly 1.0, the indanols had an r_f value of nearly 0.4 with the ZZ-indanol having a slightly higher value. The indanols were recovered as oils.



Scheme 67. Photoproducts of α -(2-Benzylphenyl)propiophenone

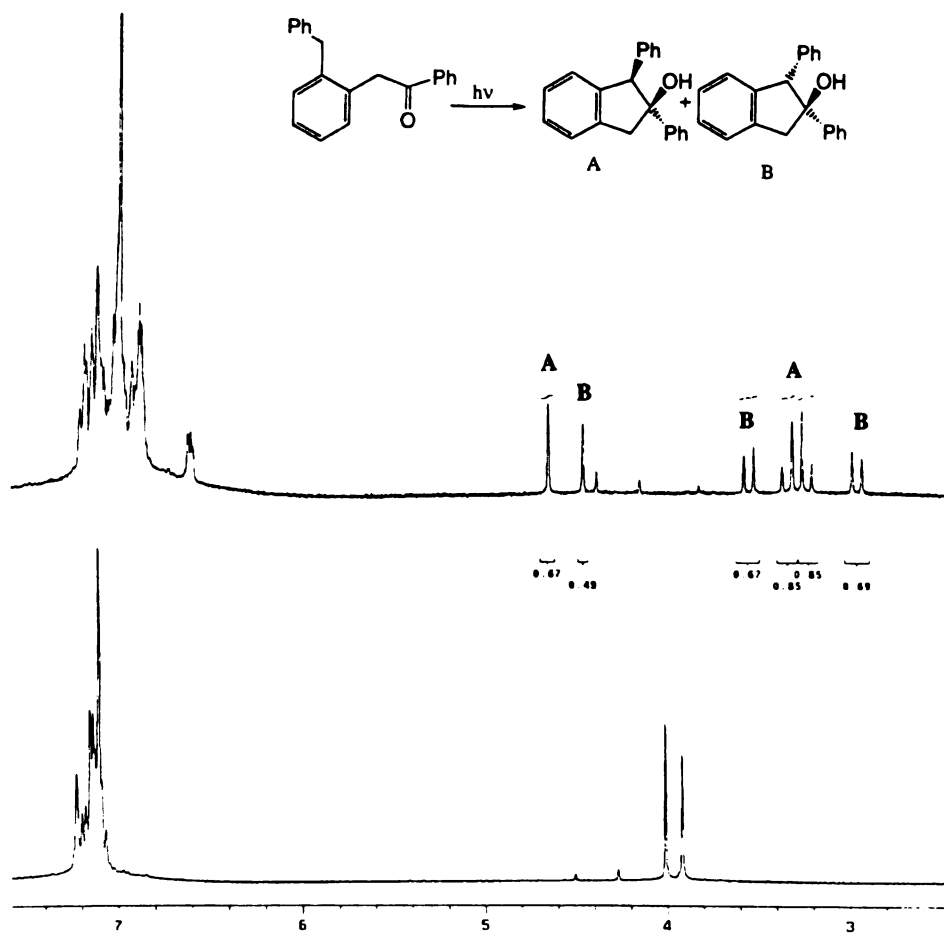


Figure 38. ^1H NMR Spectra of α -(2-Benzylphenyl)acetophenone Before and After Irradiation in Toluene ($\lambda > 290$ nm)

Z-1-methyl-3 (E),2-diphenyl -2-indanol

¹H NMR(CDCl₃): δ 1.30 (d, J= 6.72 Hz, 3H, CH₃CH), 2.20 (broad s, 1H, OH), 3.95 (q, J=6.72 Hz, 1H, CHCH₃), 4.50 (s, 1H, CHPh), 6.50 (dd, J=7.7, 1.9 Hz, 2H, Ar), 6.9-7.3 (10H, m, Ar), 7.4 (d, J=7.0 Hz, 2H, Ar)

¹³C NMR(CDCl₃): δ 10.9, 44.8, 64.8, 88.8, 123.9, 126, 126.2, 126.3, 126.9, 127.5, 127.6, 127.7, 128.1, 128.8, 139.9, 141.2, 143.4, 145.8

IR(CCl₄): 3570, 3065.3, 3028.6, 2963, 2932.2, 1475.9, 1275.1, 1076.4, 1032, 951, 873.8, 785.1, 729.2, 702.18

Z-1-methyl-3 (Z),2-diphenyl-2-indanol

¹H NMR(CDCl₃): δ 1.25 (d, J= 6.72 Hz, 3H, CH₃CH), 1.60 (broad s, 1H, OH), 3.66 (q, J=6.72 Hz, 1H, CHCH₃), 4.95 (s, 1H, CHPh), 7.0 (dd, J=7.4, 3.0 Hz, 2H, Ar), 7.10 (d, J= 7.4 Hz, 1H, Ar), 7.2-7.4 (m, 9H, Ar), 7.5 (d, J= 6.9 Hz, 2H, Ar)

¹³C NMR(CDCl₃): δ 10.2, 50.6, 62.8, 87.8, 123.3, 125.2, 125.8, 126.8, 126.9, 127.5, 128, 128.4, 130, 136, 141.8, 143.4, 145.9

IR(CCl₄): 3584, 3065.3, 2966.9, 2928.3, 1495, 1176.7, 1076.4, 972.3, 873.9, 729.2, 698.3

2R(S),3R(S)-Di(2'-benzylphenyl)butane

¹H NMR(CDCl₃): δ 0.6 (d, J= 6.72 Hz, 6H, 2CH₃CH), 3.10 (broad, 2H, 2CHCH₃), 4.0 (AB quartet, J= 15.8 Hz, 4H, 2CH₂Ph), 6.8-7.3 (m, 18H, Ar)

¹³C NMR(CDCl₃): δ 20.7, 38.7, 40.4, 125.6, 125.8, 126.4, 126.9, 128.8, 130.1, 138.3, 141.1, 145.4

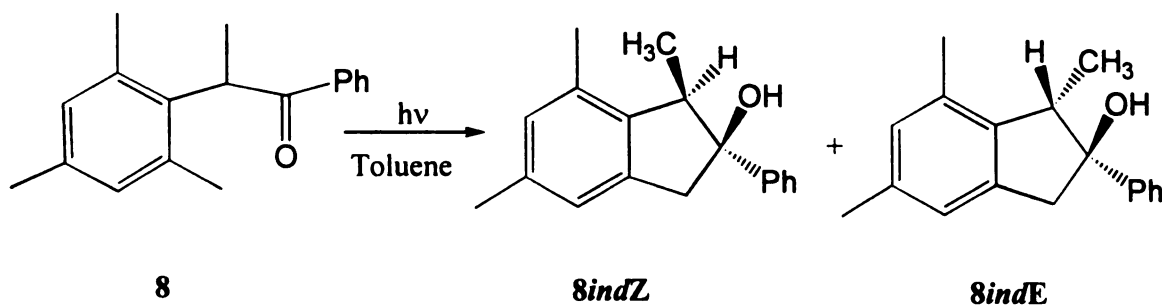
2R(S),3S(R)-Di(2'-benzylphenyl)butane

^1H NMR(CDCl_3): δ 1.10 (d, $J= 6.72$ Hz, 6H, $2\text{CH}_3\text{CH}$), 3.20 (broad, 2H, 2CHCH_3), 3.7 (AB quartet, $J= 15.8$ Hz, 4H, $2\text{CH}_2\text{Ph}$), 6.8-7.3 (m, 18H, Ar)

^{13}C NMR(CDCl_3): δ 20.5, 38.7, 39.6, 125.4, 125.9, 126.3, 126.8, 128.7, 130.7, 137.5, 141.2, 145.3

Products from α -Mesitylpropiophenone (8)

α -Mesitylpropiophenone (0.002 g) in 0.8 mL of deuterated benzene was irradiated until no trace of starting material could be observed by NMR. The signals for two isomeric indanols were detected upon analysis of the NMR spectrum of the photolysis mixture. In our investigation, photochemistry was conducted at various temperatures to ascertain the effect of temperature on product ratios. The diastereomeric ratio of indanols was determined by NMR integration of the methyl doublet signals corresponding to each isomer. In order to separate the two indanols, large scale irradiation using 0.25 g of α -mesitylpropiophenone in 100 mL of benzene was performed. Solvent was evaporated to leave a colorless oil which was chromatographed by PTLC using 3% ethyl acetate in hexane solution. The *Z*-isomer was the first compound eluted.



Scheme 68. Photoproducts from α -Mesitylpropiophenone

Z-1,5,7-Trimethyl-2-phenyl-2-indanol

$^1\text{H NMR}(\text{CDCl}_3)$: δ 1.36 (d, $J=7.0$ Hz, 3H, CH_3CH), 2.10 (broad s, 1H, OH), 2.35 (s, 3H, CH_3Ar), 2.37 (s, 3H, CH_3Ar), 3.35 (AB quartet, $J=15.6$ Hz, 2H, CH_2), 3.55 (q, $J=7.0$ Hz, 1H, CHCH_3), 6.90 (s, 1H, Ar), 6.95 (s, 1H, Ar), 7.10 (t, $J=6.8$ Hz, 1H, Ar), 7.25 (2H, dd, $J=6.8, 7.0$ Hz, 2H, Ar), 7.53 (d, $J=7.0$ Hz, 2H, Ar)

$^1\text{H NMR}(\text{Toluene-}d_8)$: δ 1.15 (d, $J=7.2$ Hz, 3H, CH_3CH), 1.7 (broad s, 1H, OH), 2.06 (s, 3H, CH_3Ar), 2.15 (s, 3H, CH_3Ar), 3.05, 3.12 (AB quartet, $J=15.9$ Hz, 2H, CH_2), 3.23 (q, $J=7.2$ Hz, 1H, CHCH_3), 6.90-7.5 (m, 7H, Ar)

$^{13}\text{C NMR}(\text{CDCl}_3)$: δ 13.18, 18.77, 20.80, 47.42, 49.48, 83.55, 122.47, 124.76, 126.46, 127.74, 129.37, 133.5, 136.26, 139.72, 140.65, 146.52

$\text{IR}(\text{CCl}_4)$: 3602, 2976, 2939, 1455, 1374, 1248.9, 1036, 845.5, 700.25

E-1,5,7-Trimethyl-2-phenyl-2-indanol

$^1\text{H NMR}(\text{CDCl}_3)$: δ 0.70 (d, $J=7.0$ Hz, 3H, CH_3CH), 2.0 (1H, broad s, 1H, OH), 2.99 (s, 3H, CH_3Ar), 2.31 (s, 3H, CH_3Ar), 3.0, 3.85 (AB quartet, $J=15.4$ Hz, 2H, CH_2), 3.35 (q, $J=7.0$ Hz, 1H, CHCH_3), 6.85 (s, 1H, Ar), 7.0 (s, 1H, Ar), 7.30 (t, $J=6.9$ Hz, 1H, Ar), 7.40 (dd, $J=6.9, 7.1$ Hz, 2H, Ar), 7.58 (d, $J=7.1$ Hz, 2H, Ar)

$^1\text{H NMR}(\text{Toluene-}d_8)$: δ 0.62 (d, $J=7.2$ Hz, 3H, CH_3CH), 1.7 (broad s, 1H, OH), 2.09 (s, 3H, CH_3Ar), 2.21 (s, 3H, CH_3Ar), 2.63, 3.58 (AB quartet, $J=15.9$ Hz, 2H, CH_2), 3.18 (q, $J=7.2$ Hz, 1H, CHCH_3), 6.90-7.5 (m, 7H, Ar)

$\text{IR}(\text{CCl}_4)$: 3462, 3061.4, 2968.8, 1448, 1240.3, 912.4, 848.8, 700.25

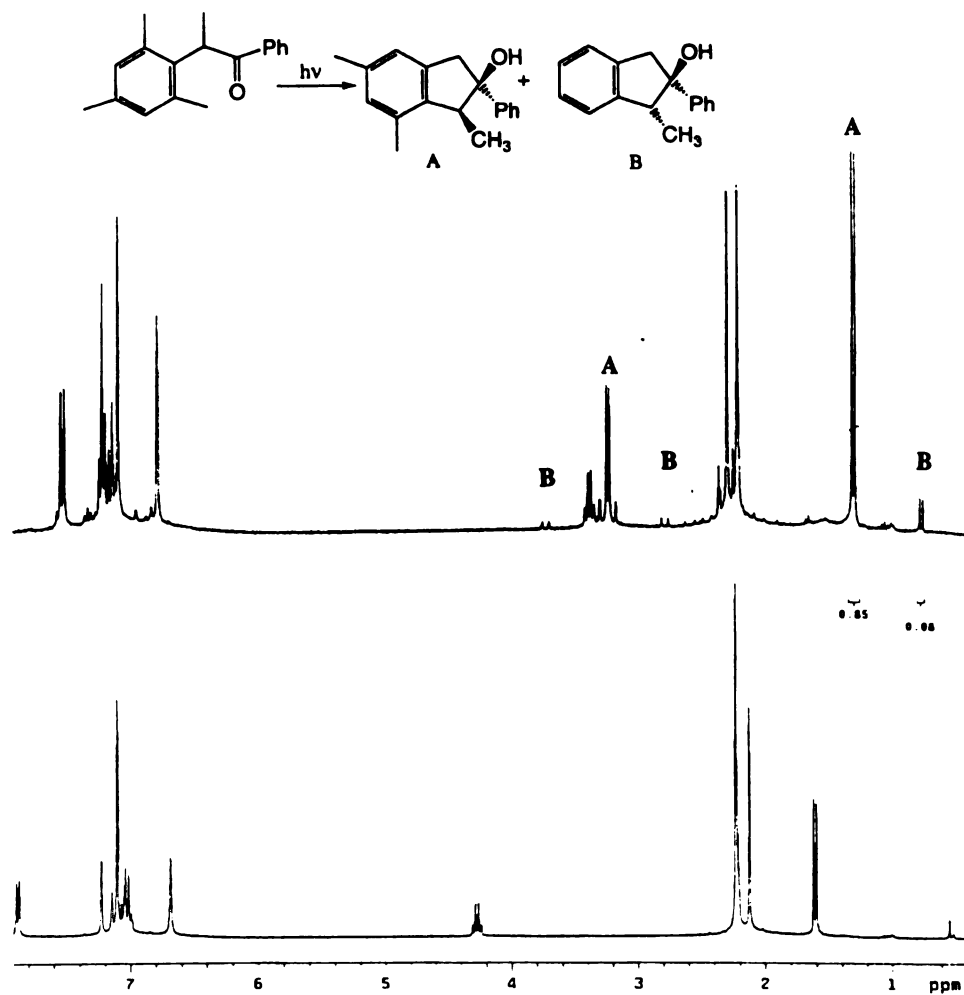
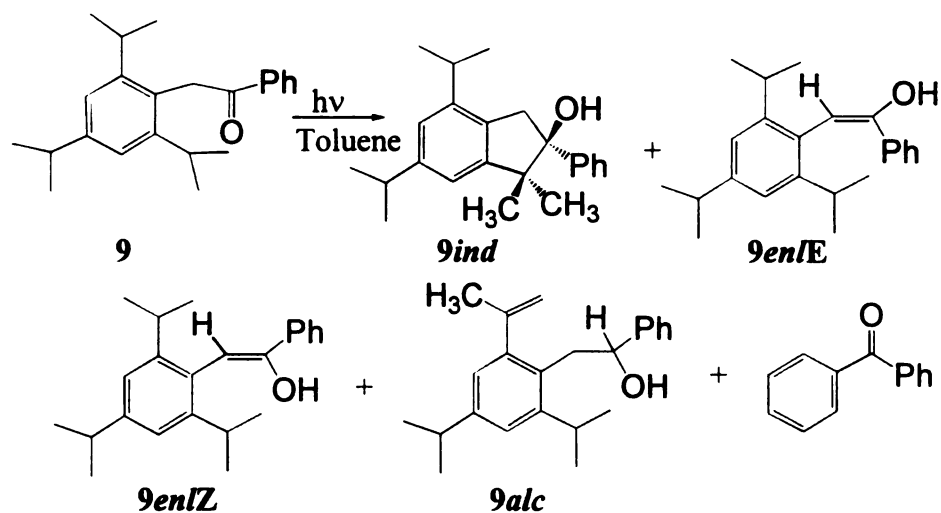


Figure 39. ^1H NMR Spectra of α -Mesitylpropiophenone Before and After Irradiation in Toluene ($\lambda > 290$ nm)

Products from α -(2,4,6-Triisopropylphenyl)acetophenone (9)

α -(2,4,6-Triisopropylphenyl)propiofenone (0.005 g) in 0.8 mL of deuterated benzene was irradiated through Pyrex filter. The signals for two products, an enol and an indanol, were detected upon analysis of the NMR spectrum of the photolysis mixture. The effect of temperature and phase on product ratios was also investigated by conducting the photochemistry in acetone/ethanol, ice-water and silicon oil (110°C) baths and in solid. A small amount of the other disproportionation product, 1-phenyl-2-(2-(2-propenyl)-4,6-diisopropylphenyl)ethanol, was observed at 24°C and 90°C irradiations. The enol indanol ratio was determined by NMR integration of the vinylic singlet signals of the enols and the upfield methyl singlet signal of the indanol. In order to separate the products, large scale irradiation using 0.40 g of α -(2,4,6-triisopropylphenyl) propiofenone in 100 mL of benzene was performed. Solvent was evaporated to leave a yellow solid which was separated by PTLC using 3% ethyl acetate in hexane solution.



Scheme 69. Photoproducts of α -(2,4,6-Triisopropylphenyl)acetophenone

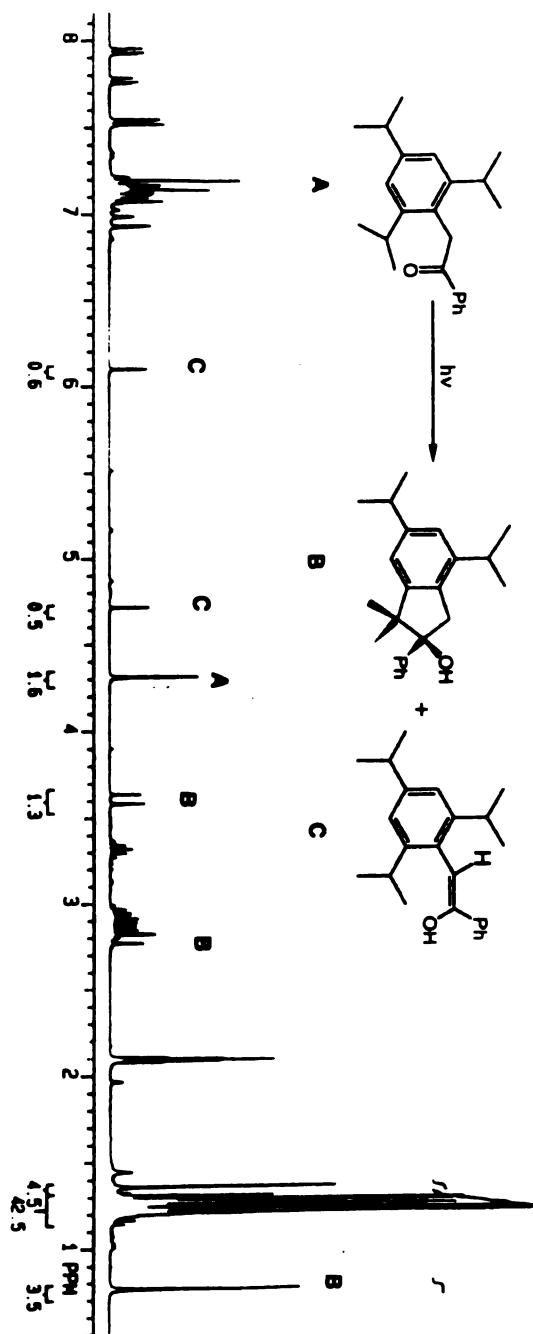


Figure 40. ^1H NMR of α -(2,4,6-Triisopropylphenyl)acetophenone After Irradiation in Toluene ($\lambda > 290\text{nm}$)

4,6-Diisopropyl-1,1-dimethyl-2-phenyl-2-indanol

$^1\text{H NMR}(\text{CDCl}_3)$: δ 0.78 (s, 3H, CH_3), 1.29 (d, $J=7.3$ Hz, 12H, 2 $(\text{CH}_3)_2\text{CH}$), 1.36 (s, 3H, CH_3), 2.14 (broad s, 1H, OH), 2.92 (septet, $J= 7.2$ Hz, 2H, $2\text{CH}(\text{CH}_3)_2$), 3.08, 3.81 (AB quartet, $J= 16.1$ Hz, 2H, CH_2), 6.90 (s, 1H, Ar), 7.0 (s, 1H, Ar), 7.24-7.40 (m, 3H, Ar), 7.60 (d, $J= 7$ Hz, 2H, Ar)

$^1\text{H NMR}(\text{Toluene-}d_8)$: δ 0.75 (s, 3H, CH_3), 1.20 (d, $J=7.2$ Hz, 6H, 2 $(\text{CH}_3)_2\text{CH}$), 1.30 (d, $J=7.2$ Hz, 12H, 2 $(\text{CH}_3)_2\text{CH}$), 1.35 (s, 3H, CH_3), 2.80, 3.60 (AB quartet, $J= 16.1$ Hz, 2H, CH_2), 2.85 (septet, $J= 7.2$ Hz, 1H, $\text{CH}(\text{CH}_3)_2$), 3.30 (septet, $J= 7.2$ Hz, 2H, $2\text{CH}(\text{CH}_3)_2$), 6.90 (s, 1H, Ar), 7.1 (s, 2H, Ar), 7.1-7.3 (m, 3H, Ar), 7.5 (d, $J= 7$ Hz, 2H, Ar)

$^{13}\text{C NMR}(\text{CDCl}_3)$: δ 19.6, 22.9, 23.1, 24.2, 24.3, 28.1, 31.0, 34.4, 42.2, 51.6, 87.2, 118.4, 121.6, 126.6, 127.1, 127.7, 133.6, 141.8, 144.8, 148.4, 150.3

IR(neat): 3420, 3080, 2850, 1494, 1384, 876.8 cm^{-1}

(Z)-1-Phenyl-2-(2,4,6-triisopropylphenyl)ethenol

$^1\text{H NMR}(\text{Toluene-}d_8)$: δ 1.20 (d, $J=7.2$ Hz, 6H, 2 $(\text{CH}_3)_2\text{CH}$), 1.30 (d, $J=7.2$ Hz, 12H, 2 $(\text{CH}_3)_2\text{CH}$), 2.85 (septet, $J= 7.2$ Hz, 1H, $\text{CH}(\text{CH}_3)_2$), 3.30 (septet, $J= 7.2$ Hz, 2H, $2\text{CH}(\text{CH}_3)_2$), 4.75 (broad s, 1H, OH), 6.1 (s, 1H, Vinyl), 7.0-7.2 (m, 3H, Ar), 7.2 (s, 2H, Ar), 7.8 (d, $J= 7$ Hz, 2H, Ar)

$^1\text{H NMR}(\text{Methanol-}d_4)$: δ 1.16 (d, $J= 7.2$ Hz, 6H, $(\text{CH}_3)_2\text{CH}$), 1.18 (d, $J= 7.2$ Hz, 6H, $(\text{CH}_3)_2\text{CH}$), 1.24 (d, $J= 7.2$ Hz, 6H, $(\text{CH}_3)_2\text{CH}$), 2.85 (septet, $J= 7.2$ Hz, 2H, $2\text{CH}(\text{CH}_3)_2$), 3.27 (septet, $J= 7.2$ Hz, 1H, $\text{CH}(\text{CH}_3)_2$), 5.91 (s, 1H, vinylic), 7.0 (s, 1H, Ar), 7.2-7.4 (m, 5H, Ar), 7.70 (d, $J= 7$ Hz, 2H, Ar)

(E)-1-Phenyl-2-(2,4,6-triisopropylphenyl)ethenol

¹H NMR(Toluene-d₈): δ 1.10 (d, J=7.2 Hz, 6H, 2 (CH₃)₂CH), 1.18 (d, J=7.2 Hz, 12H, 2 (CH₃)₂CH), 2.85 (septet, J= 7.2 Hz, 1H, CH(CH₃)₂), 3.30 (septet, J= 7.2 Hz, 2H, 2CH(CH₃)₂), 4.75 (broad s, 1H, OH), 6.4 (s, 1H, Vinyl), 7.0 (s, 2H, Ar), 7.1-7.2 (m, 3H, Ar), 7.7 (d, J= 7 Hz, 2H, Ar)

¹H NMR(Methanol-d₄): δ 0.88 (d, J= 7.2 Hz, 6H, (CH₃)₂CH), 1.08 (d, J= 7.2 Hz, 6H, (CH₃)₂CH), 1.2 (d, J= 7.2 Hz, 6H, (CH₃)₂CH), 2.85 (septet, J= 7.2 Hz, 2H, 2CH(CH₃)₂), 3.27 (septet, J= 7.2 Hz, 1H, CH(CH₃)₂), 5.88 (s, 1H, vinylic), 6.90 (s, 1H, Ar), 7.2-7.4 (m, 5H, Ar), 7.65 (d, J= 7 Hz, 2H, Ar)

1-Phenyl-2-(2-(2-propenyl)-4,6-diisopropylphenyl)ethanol

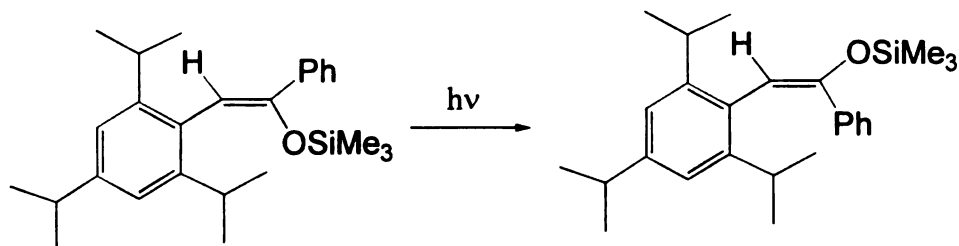
¹H NMR(Toluene-d₈): δ 1.15 (d, J=7.2 Hz, 3H, (CH₃)₂CH), 1.25 (d, J=7.2 Hz, 3H, (CH₃)₂CH), 1.3 (6H, t, J=7.2 Hz, 6H, (CH₃)₂CH), 1.6 (broad s, 1H, OH), 1.95 (s, 3H, allylic CH₃), 2.85 (septet, J= 7.2 Hz, 1H, CH(CH₃)₂), 3.1, 3.24 (2H, AB quartet of d, J= 8.4, 2.7, 5.4 Hz, 2H, CH₂), 3.45 (septet, J= 7.2 Hz, 1H, CH(CH₃)₂), 4.79 (1H, dd, J= 2.7, 5.4 Hz, 1H, CHOH), 4.85 (d, J= 1.5 Hz, 1H, vinylic), 5.15 (d, J= 1.5 Hz, 1H, vinylic), 6.95 (s, 1H, Ar), 7.05 (s, 1H, Ar), 7.1-7.2 (m, 3H, Ar), 7.3 (2H, d, J= 7 Hz, 2H, Ar)

IR(CCl₄): 3582.3, 2964, 2931.2, 1464.2, 1384.1, 1167, 1055.2, 901.8, 808.3, 738.8

Products from 1-Trimethylsiloxy-1-phenyl-2-(2',4',6'-triisopropylphenyl)ethene

Photochemical conversion of enol to indanol was checked by synthesis and irradiation of trimethylsilyl enol ether of α-(2,4,6-triisopropylphenyl)acetophenone. The

Z-enol ether was synthesized by treatment of ketone with KH and trimethylsilyl chloride. Irradiation of this enol ether in benzene resulted in formation of the E-isomer but no indanol or ketone.



Scheme 70. Photochemistry of Trimethylsilylenol Ether of 9

Z-1-Trimethylsiloxy-1-phenyl-2-(2',4',6'-triisopropylphenyl)ethene

$^1\text{H NMR}(\text{C}_6\text{D}_6)$: δ -0.1 (s, 9H, $\text{Si}(\text{CH}_3)_3$), 1.3-1.5 (broad, 18H, 3 $(\text{CH}_3)_2\text{CH}$), 2.85 (septet, $J=7.1$ Hz, 1H, $\text{CH}(\text{CH}_3)_2$), 3.5 (septet, $J=7.2$ Hz, 2H, 2 $\text{CH}(\text{CH}_3)_2$), 6.5 (s, 1H, vinylic), 7.0-7.2 (m, 5H, Ar), 7.7 (d, $J=6.9$ Hz, 2H, Ar)

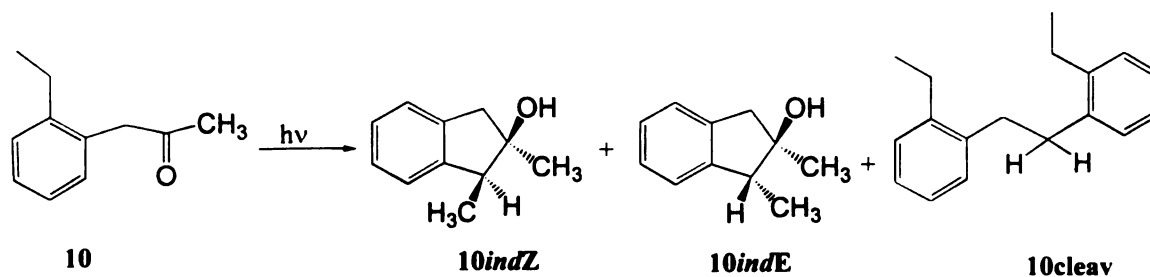
$^{13}\text{C NMR}(\text{CDCl}_3)$: δ 0.13, 24.21, 29.74, 30.55, 34.41, 107.28, 120.24, 125.43, 127.76, 128.24, 129.93, 147.28, 147.61, 149.33

E-1-Trimethylsiloxy-1-phenyl-2-(2',4',6'-triisopropylphenyl)ethene

$^1\text{H NMR}(\text{C}_6\text{D}_6)$: δ 0.0 (s, 9H, $\text{Si}(\text{CH}_3)_3$), 1.3-1.5 (broad, 18H, 3 $(\text{CH}_3)_2\text{CH}$), 2.85 (septet, $J=7.1$ Hz, 1H, $\text{CH}(\text{CH}_3)_2$), 3.5 (septet, $J=7.2$ Hz, 2H, 2 $\text{CH}(\text{CH}_3)_2$), 6.7 (s, 1H, vinylic), 7.0-7.2 (m, 5H, Ar), 7.5 (d, $J=6.9$ Hz, 2H, Ar)

Products from α -(2-Ethylphenyl)acetone (10)

α -(2-Ethylphenyl)acetone (0.002 g) in 0.8 mL of deuterated benzene was irradiated until starting material could not be observed by NMR. The signals for three products were detected in the NMR spectrum of the mixture. These products included two isomeric indanols and a diarylethane. The effect of temperature and phase on product ratios was also investigated by conducting the photochemistry in acetone/ethanol, ice-water and silicon oil (110°C) baths and in solid. The product ratios were determined by NMR integration of the methyl doublet signals of the indanols and the methylene singlet signal of the diarylethane. The structural assignments of the indanols was accomplished by performing shift and nOe experiments. Addition of Rondeau's reagent to 0.01 M solution of each indanol in CDCl₃, caused an upfield shift of all proton signals. However, the methine signal in the minor isomer moved upfield twice as much as the methyl signal, while the upfield shifts of both methyl and methine signals in the major isomer were comparable. Furthermore, irradiation of the methine signal in the minor isomer caused an enhancement of the OH signal. These data strongly suggest that the minor isomer has an E-stereochemistry. Large scale irradiation using 0.20 g of α -(2-ethylphenyl)acetone in 150 mL of toluene was performed until 100% conversion (GC). Solvent was removed to leave a yellow oil which was chromatographed by PTLC using 3% ethyl acetate in hexane to separate the products. The Z-indanol was the first eluted isomer. The indanols were recovered as oils.



Scheme 71. Photoproducts of α -(2-Ethylphenyl)acetone

Z-1,2-Dimethyl-2-indanol

$^1\text{H NMR}(\text{CDCl}_3)$: δ 1.28 (d, $J=7.1$ Hz, 3H, CH_3CH), 1.45 (s, 3H, CH_3), 2.93 (Half of an AB quartet, $J=16$ Hz, 1H, CH_2), 2.97 (q, $J=7.1$ Hz, 1H, CHCH_3), 3.02 (Half of an AB quartet, $J=16$ Hz, 1H, CH_2), 7.13-7.23 (m, 4H, Ar)

$^1\text{H NMR}(\text{C}_6\text{D}_6)$: δ 1.12 (d, $J=7.2$ Hz, 3H, CH_3CH), 1.2 (s, 3H, CH_3), 1.6 (s, 1H, OH), 2.65 (q, $J=7.2$ Hz, 1H, CHCH_3), 2.7 (AB quartet, $J=15.94$ Hz, 2H, CH_2), 7.0-7.15 (m, 4H, Ar)

$^1\text{H NMR}(\text{Toluene-}d_8)$: δ 1.11 (d, $J=7.2$ Hz, 3H, CH_3CH), 1.18 (s, 3H, CH_3), 1.6 (s, 1H, OH), 2.65 (q, $J=7.2$ Hz, 1H, CHCH_3), 2.7 (AB quartet, $J=15.94$ Hz, 2H, CH_2), 7.0-7.15 (m, 4H, Ar)

$^{13}\text{C NMR}(\text{C}_6\text{D}_6)$: δ 14.5, 25.4, 47.7, 49.3, 81.1, 124, 125.1, 126.8, 126.9, 141.2, 146.9

IR(CCl_4): 3580.4, 3072.9, 3024.7, 2966.9, 2934.1, 1460.3, 1246.2, 1157.4, 1072.6, 951, 775.4, 763.9, 740.7

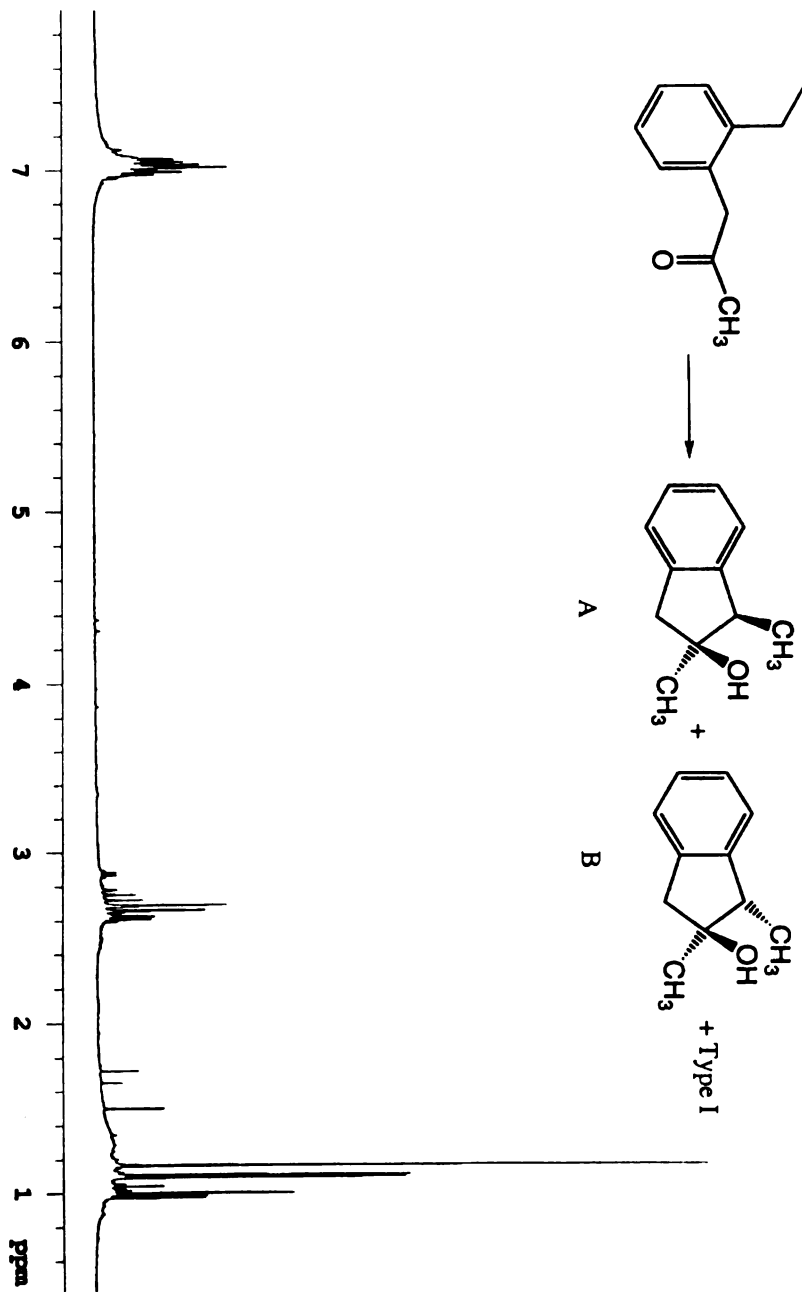


Figure 41. ¹H NMR of the Indanol Mixture from α-(2-Ethylphenyl)acetone in Benzene

E-1,2-Dimethyl-2-indanol

$^1\text{H NMR}(\text{C}_6\text{D}_6)$: δ 1.0 (d, $J=7.2$ Hz, 3H, CH_3CH), 1.02 (s, 3H, CH_3), 2.73 (AB quartet, $J=15.5$ Hz, 2H, CH_2), 2.88 (q, $J=7.2$ Hz, 1H, CHCH_3), 7.0 (dd, $J=2.4, 2.3$ Hz, 1H, Ar), 7.03 (d, $J=1.4$ Hz, 1H, Ar), 7.05 (d, $J=2.4$ Hz, 1H, Ar), 7.09 (dd, $J=2.3, 1.4$ Hz, 1H, Ar)

$^1\text{H NMR}(\text{Toluene-}d_8)$: δ 1.0 (d, $J=7.2$ Hz, 3H, CH_3CH), 0.99 (s, 3H, CH_3), 2.73 (AB quartet, $J=15.5$ Hz, 2H, CH_2), 2.88 (q, $J=7.2$ Hz, 1H, CHCH_3), 7.0 (dd, $J=2.4, 2.3$ Hz, 1H, Ar), 7.03 (d, $J=1.4$ Hz, 1H, Ar), 7.05 (d, $J=2.4$ Hz, 1H, Ar), 7.09 (dd, $J=2.3, 1.4$ Hz, 1H, Ar)

$^1\text{H NMR}(\text{CDCl}_3)$: δ 1.19 (d, $J=7.3$ Hz, 3H, CH_3CH), 1.30 (s, 3H, CH_3), 2.96 (collapsed AB quartet, 2H, CH_2), 3.05 (q, $J=7.2$ Hz, 1H, CHCH_3), 7.0-7.3 (m, 4H)

$^{13}\text{C NMR}(\text{C}_6\text{D}_6)$: δ 14.4, 22.6, 47.4, 50.9, 82.0, 123.9, 124.9, 126.8, 126.9, 127.9, 147.0

IR(CCl_4): 3431.8, 3072.9, 3024.9, 2964.7, 2932.2, 1255.8, 1145.8, 1032, 987.7, 927.9, 763.9, 740.7

Shift Reagent Experiments:

Addition of Rondeau's reagent, tris(6,6,7,7,8,8,8-heptafluoro-2,2-dimethyl-3,5-octandionato) praseodymium, to 0.01 M solution of each indanol in CDCl_3 , caused the following upfield shifts:

Z-1,2-Dimethyl-2-indanol: methyl doublet signal at 1.30 ppm moved to 1.01 ppm, methyl singlet signal at 1.47 ppm moved to 1.06 ppm, methine quartet signal at 2.97 ppm moved to 2.68 ppm, and the AB quartet signals at 2.95 and 3.04 ppm moved to 2.54 and 2.74 ppm.

E-1,2-Dimethyl-2-indanol: methyl doublet signal at 1.18 ppm moved to 1.13 ppm, methyl singlet signal at 1.27 ppm moved to 1.20 ppm, methine quartet signal at 3.05 ppm move to 2.96 ppm, and the AB quartet signal at 2.96 ppm moved to 2.98 and 2.86 ppm.

Addition of tris(2,2,6,6-tetramethyl-3,5-heptandionato)europium reagent to the mixture of indanols in CDCl_3 caused the following downfield shifts:

Z-1,2-Dimethyl-2-indanol: methyl doublet signal at 1.30 ppm moved to 1.33 ppm, methyl singlet signal at 1.47 ppm moved to 1.52 ppm. The other peaks could not be identified due to peak broadening.

E-1,2-Dimethyl-2-indanol: methyl doublet signal at 1.19 ppm moved to 1.23 ppm, methyl singlet signal at 1.27 ppm moved to 1.34 ppm. The other peaks could not be identified due to peak broadening.

NOe Experiments:

Z-1,2-Dimethyl-2-indanol: Irradiation of the signal at 1.30 ppm (CDCl_3) caused the following enhancements: 2.96-3.05 ppm (3%), 7.1-7.3 ppm (3.1%)

Irradiation of the signal at 1.47 ppm caused the following enhancements: 2.96-3.05 ppm (4%), 7.1-7.3 ppm (1.6%)

E-1,2-Dimethyl-2-indanol: Irradiation of the signal at 2.73 ppm (C_6D_6) caused the following enhancements: 1.0-1.05 ppm (1.0%), 1.6 ppm (0.4%), 6.9-7.1 ppm (1.7 %)

Irradiation of the signal at 2.88 ppm caused the following enhancements: 1.0-1.05 (0.8%), 1.6ppm (0.6%), 6.9-7.1 ppm (2%)

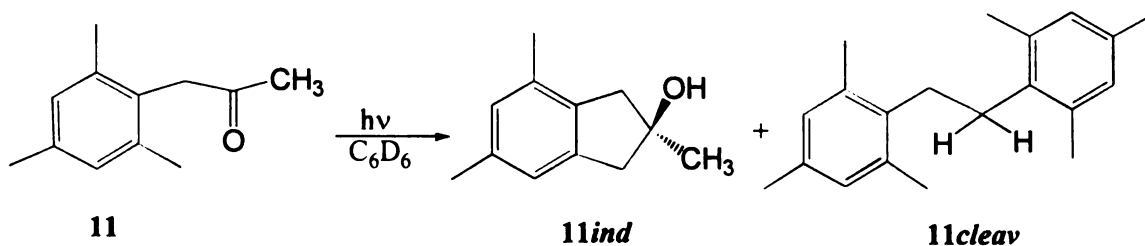
1,2-Di(2'-ethylphenyl)ethane

$^1\text{H NMR}(\text{CDCl}_3)$: δ 1.22 (t, $J=7.5$ Hz, 6H, $2\text{CH}_3\text{CH}_2$), 2.67 (q, $J=7.6$ Hz, 4H, $2\text{CH}_2\text{CH}_3$), 2.8 (s, 4H, 2CH_2), 7.1-7.2 (m, 8H, Ar)

$^{13}\text{C NMR}(\text{CDCl}_3)$: δ 15.4, 25.5, 34.3, 125.9, 126.3, 128.5, 129.1

Products from α -Mesitylacetone (11)

α -Mesitylacetone (0.002 g) in deuterated benzene was irradiated until starting material could not be observed by NMR. Two products were detected in the NMR spectrum of the mixture and were identified as an indanol and a diarylethane. The effect of temperature and phase on product ratios was also investigated by conducting the photochemistry in acetone/ethanol and silicon oil (110°C) baths and in solid. Product ratios were determined by NMR integration of the methylene signals of the indanol (AB quartet) and the diarylethane (singlet). Large scale irradiation using 0.20 g of α -mesitylacetone in 100 mL of benzene was performed until 100% conversion by GC. Solvent was removed to leave a yellow oil which was chromatographed by PTLC using 3% ethyl acetate in hexane to separate the products. The indanol was eluted after the diarylethane and was recovered as an oil.



Scheme 72. Photoproducts of α -Mesitylacetone

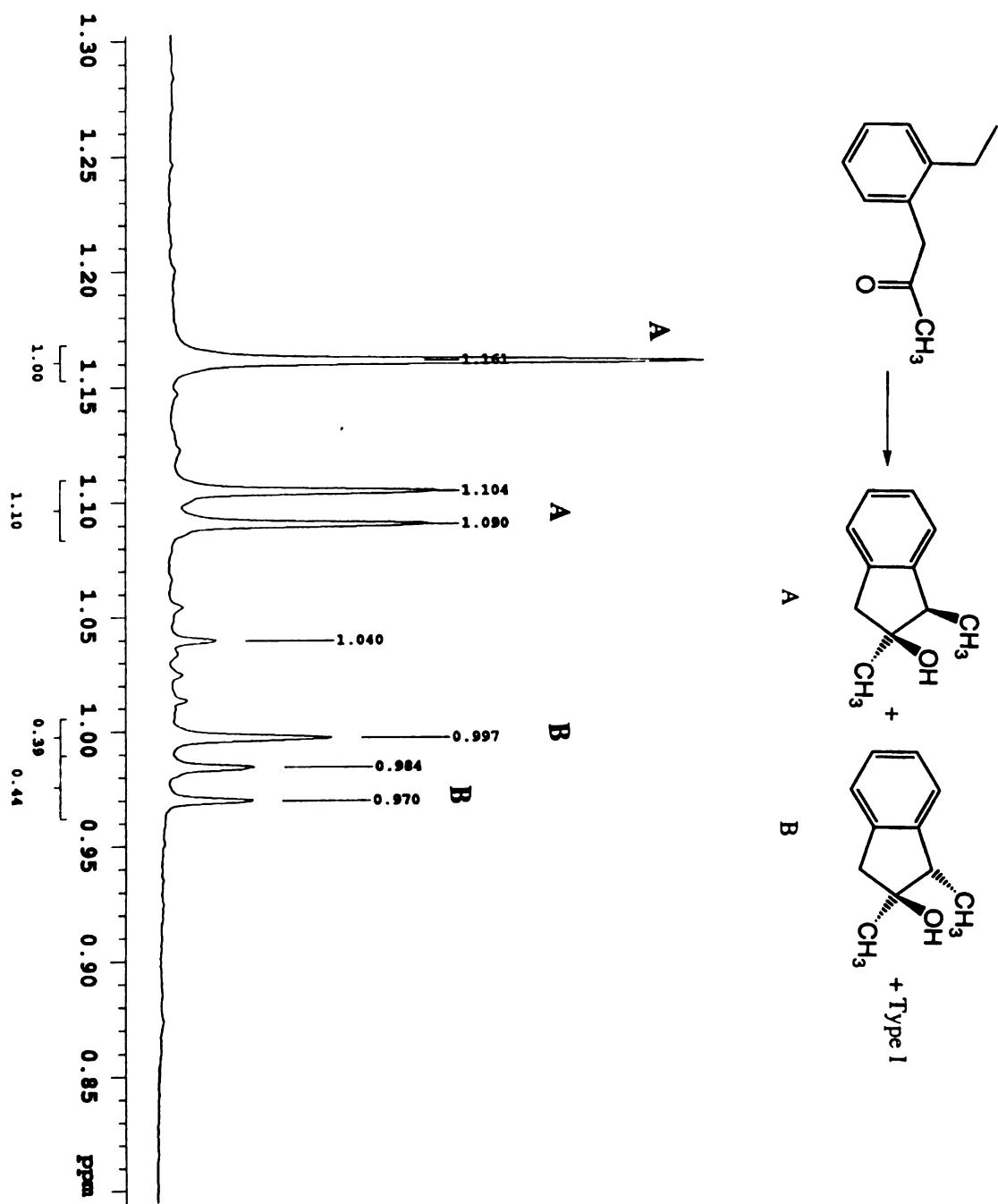


Figure 42. ^1H NMR of the Methyl Region of the Indanol Mixture from α -(2-Ethylphenyl)-acetone in Benzene

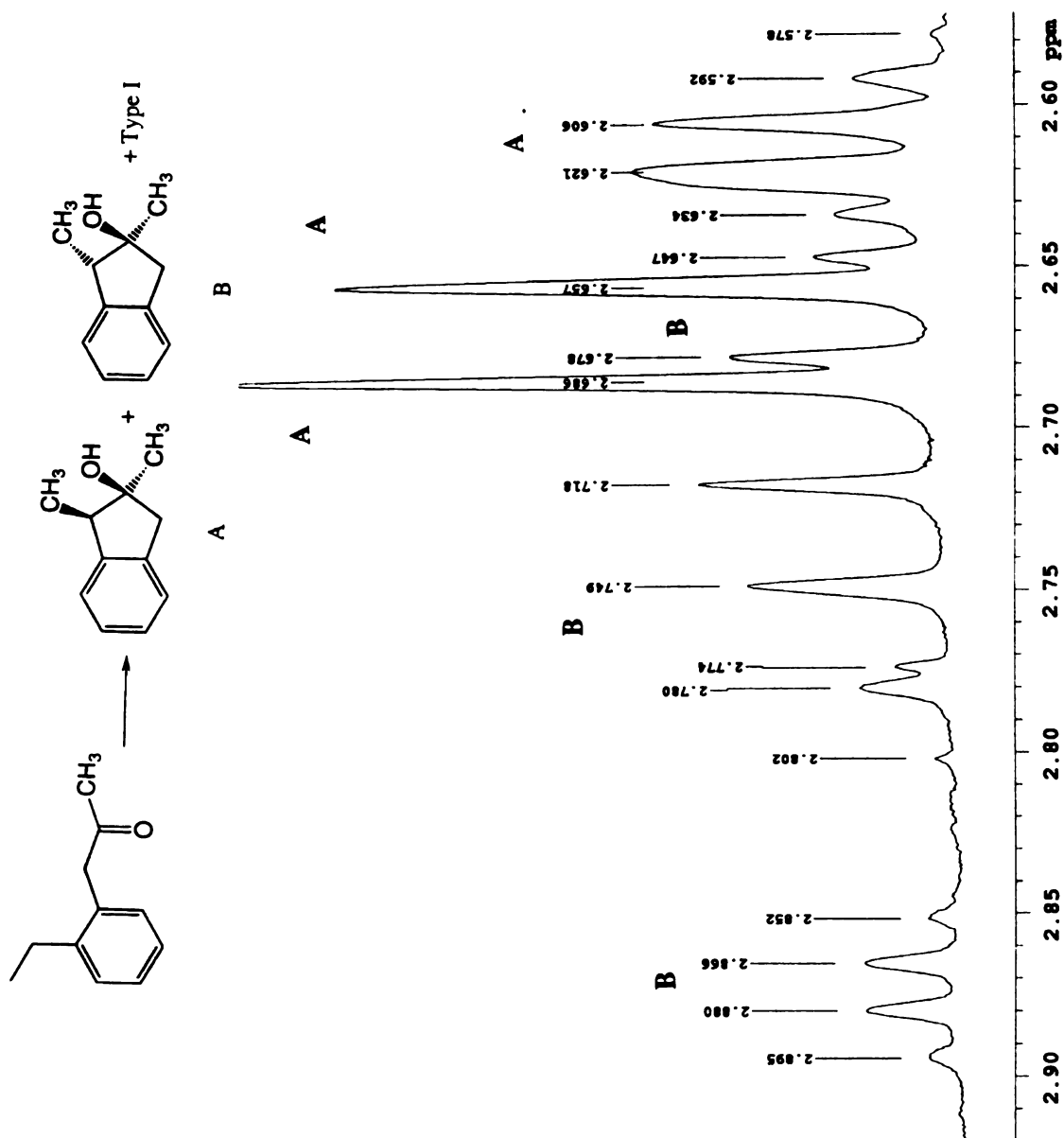


Figure 43. ^1H NMR of the Methylene Region of the Indanol Mixture from α -(2-Ethylphenyl)acetone in Benzene

2,4,6-Trimethyl-2-indanol

$^1\text{H NMR}(\text{C}_6\text{D}_6)$: δ 1.30 (s, 3H, CH_3), 2.05 (s, 3H, CH_3Ar), 2.20 (s, 3H, CH_3Ar), 2.65 (AB quartet, $J=16.6$ Hz, 2H, CH_2), 2.80 (AB quartet, $J=16.5$ Hz, 2H, CH_2), 6.72 (s, 1H, Ar), 6.73 (s, 1H, Ar)

$^1\text{H NMR}(\text{CDCl}_3)$: δ 1.63 (s, 3H, CH_3), 2.13 (s, 3H, CH_3Ar), 2.33 (s, 3H, CH_3Ar), 3.0 (Half of an AB quartet, $J=16.6$ Hz, 1H, CH_2), 3.1 (Half of an AB quartet, $J=16.5$ Hz, 1H, CH_2), 3.25 (Half of an AB quartet, $J=16.6$ Hz, 1H, CH_2), 3.35 (Half of an AB quartet, $J=16.5$ Hz, 1H, CH_2), 6.79 (s, 1H, Ar), 6.81 (s, 1H, Ar)

$^{13}\text{C NMR}(\text{C}_6\text{D}_6)$: δ 19.0, 21.3, 28.0, 47.0, 48.9, 79.3, 123.3, 128.5, 133.7, 136.1, 137.9, 141.9

IR(CCl_4): 3443, 2968.8, 2926.4, 1469.9, 1448.7, 1230.7, 1076.4, 895, 873.8, 850.7, 702.2

1,2-Dimesitylethane

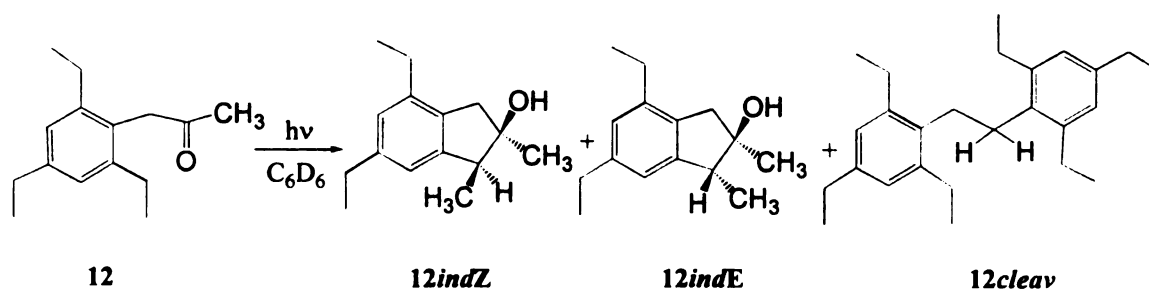
$^1\text{H NMR}(\text{CDCl}_3)$: δ 2.3 (s, 6H, 2CH_3), 2.4 (12H, s, 4 CH_3), 2.8 (s, 4H, 2CH_2), 6.9 (s, 4H, Ar)

$^{13}\text{C NMR}(\text{CDCl}_3)$: δ 20.1, 20.8, 28.9, 129.1, 135.2, 135.7, 136.3

Products from α -(2,4,6-Triethylphenyl)acetone (12)

α -(2,4,6-Triethylphenyl)acetone (0.004 g) in deuterated toluene was irradiated until starting material could not be observed by NMR. The signals for several products were detected in the NMR spectrum of the mixture. These products included two isomeric indanols and a diarylethane. The peaks for the two isomeric indanols overlap

and separation is difficult. The Z-stereochemistry for the major indanol was based on the comparison of the peaks to that of the Z-indanol of α -(2-ethylphenyl)acetone. Product ratios were determined by NMR integration of methyl doublet signals of indanols and the methylene singlet signal of the diarylethane. Large scale irradiation using 0.30 g of α -(2,4,6-triethylphenyl)acetone in 100 mL of benzene was performed until 100% conversion by GC. Solvent was removed to leave a yellow oil which was chromatographed by PTLC using 5% ethyl acetate in hexane to separate the products. The indanols had a lower r_f value than the diarylethane which had moved with the solvent line.



Scheme 73. Photoproducts of α -(2,4,6-Triethylphenyl)acetone

4,6-Diethyl-1 (Z),2-dimethyl-2-indanol

$^1\text{H NMR}(\text{C}_6\text{D}_6)$: δ 1.12 (t, $J = 7.5$ Hz, 3H, CH_3CH_2), 1.19 (d, $J = 7$ Hz, 3H, CH_3CH), 1.20 (t, $J = 7.5$ Hz, 3H, CH_3CH_2), 1.26 (s, 3H, CH_3), 2.44 (q, $J = 7.5$ Hz, 2H, CH_2CH_3), 2.56 (q, $J = 7.5$ Hz, 2H, $\text{C CH}_2\text{H}_3$), 2.62 (Half of AB quartet, $J = 16$ Hz, 1H, CH_2), 2.72 (1H, q, $J = 7.5$ Hz, 1H, CHCH_3), 2.74 (Half of AB quartet, $J = 16$ Hz, 1H, CH_2), 6.85 (s, 2H, Ar)

$^{13}\text{C NMR}(\text{C}_6\text{D}_6)$: δ 11.6, 14.9, 16.5, 25.4, 26.8, 29.4, 45.6, 49.3, 80.9, 121.1, 125.9, 143.3, 146.9

IR(CCl₄): 3440, 2968, 2930, 1470, 1076.4, 895, 704.2

4,6-Diethyl-1 (E),2-dimethyl-2-indanol

¹H NMR(C₆D₆): δ 1.11 (d, J= 7.5 Hz, 3H, CH₃CH), 1.13 (s, 3H, CH₃), 1.15 (t, J=7.5 Hz, 3H, CH₃CH₂), 1.20 (t, J=7.5 Hz, 3H, CH₃CH₂), 2.43 (AB quartet, J= 14 Hz, 2H, CH₂), 2.48 (q, J= 7.5 Hz, 2H, CH₂CH₃), 2.56 (q, J= 7.5 Hz, 1H, CHCH₃), 2.62 (q, J= 7.5 Hz, 2H, CH₂CH₃), 6.81 (s, 1H, Ar), 7.05 (s, 1H, Ar)

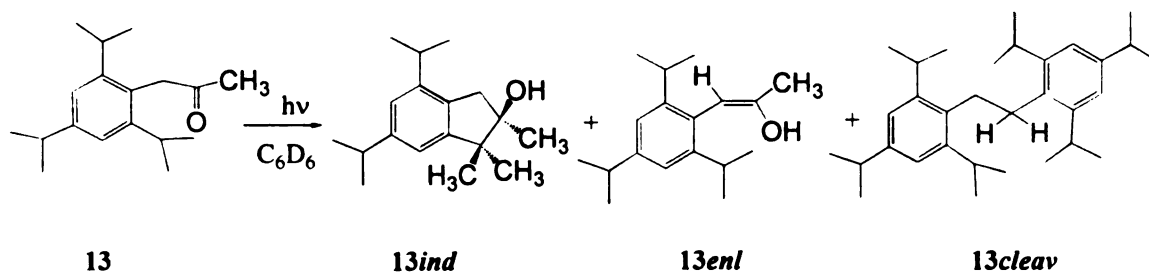
1,2-Di(2,4,6-triethylphenyl)ethane

¹H NMR(C₆D₆): δ 1.15 (t, J= 7.5 Hz, 12H, 4CH₃CH₂), 1.2 (t, J= 7.5 Hz, 6H, 2CH₃CH₂), 2.5 (q, J= 7.5 Hz, 4H, CH₂CH₃), 2.7 (q, J= 7.5 Hz, 8H, 2CH₂CH₃), 2.85 (s, 4H, Ar), 6.9 (s, 4H, Ar)

Products from α-(2,4,6-Triisopropylphenyl)acetone (13)

α-(2,4,6-Triisopropylphenyl)acetone (0.005 g) in deuterated benzene was irradiated. The signals for three products were detected in the NMR spectrum of the mixture. One of these products, the enol, disappears as the irradiation time (percent conversion) increases. The signals for two products were detected at 100% conversion in the NMR spectrum of the photolysis mixture. These products included an indanol and a diarylethane. The indanol/diarylethane ratio was determined by NMR integration of the methyl singlet signal of the indanol and the methylene singlet signal of the diarylethane. Large scale irradiation using 0.30 g of α-(2,4,6-triisopropylphenyl)acetone in 100 mL of toluene was performed until 100% conversion (GC). Solvent was removed to leave a

yellow oil which was chromatographed by preparative scale tlc using hexane to separate the products. The indanol was the second fraction eluted and was recovered as an oil.



Scheme 74. Photoproducts of α -(2,4,6-Triisopropylphenyl)acetone

4,6-Diisopropyl-1,1,2-trimethyl-2-indanol

$^1\text{H NMR}(\text{CDCl}_3)$: δ 1.10 (s, 3H, CH_3), 1.25 (6H, t, $J = 6.84$ Hz, 6H, $(\text{CH}_3)_2\text{CH}$), 1.27 (d, $J = 6.84$ Hz, 6H, $(\text{CH}_3)_2\text{CH}$), 1.30 (s, 3H, CH_3), 1.36 (s, 3H, CH_3), 1.8 (broad s, 1H, OH), 2.8-3.0 (m, 2H, $2\text{CH}(\text{CH}_3)_2$), 2.95, 2.99 (AB quartet, $J = 16$ Hz, 2H, CH_2), 6.88 (d, $J = 1.59$ Hz, 1H, Ar), 6.95 (d, $J = 1.59$ Hz, 1H, Ar)

$^{13}\text{C NMR}(\text{CDCl}_3)$: δ 19.9, 20.6, 22.6, 23.9, 26.1, 30.6, 33.9, 43.4, 49.4, 83.1, 117.8, 120.9, 133.6, 144.2, 147.7, 150.6

IR(CCl_4): 3448, 2966, 2930, 1448.7, 1076, 802.4

(Z)-1-Methyl-2-(2,4,6-triisopropylphenyl)ethenol

$^1\text{H NMR}(\text{C}_6\text{D}_6)$: δ 1.1-1.3 (d, $J = 6.84$ Hz, 18H, 3 $(\text{CH}_3)_2\text{CH}$), 1.8 (s, 3H, allylic CH_3), 2.7-3.0 (3H, septet, $J = 6.84$ Hz, 3H, 3 $\text{CH}(\text{CH}_3)_2$), 4.4 (broad s, 1H, OH), 5.2 (s, 1H, vinylic CH), 6.9 (s, 1H, Ar), 7.05 (s, 1H, Ar)

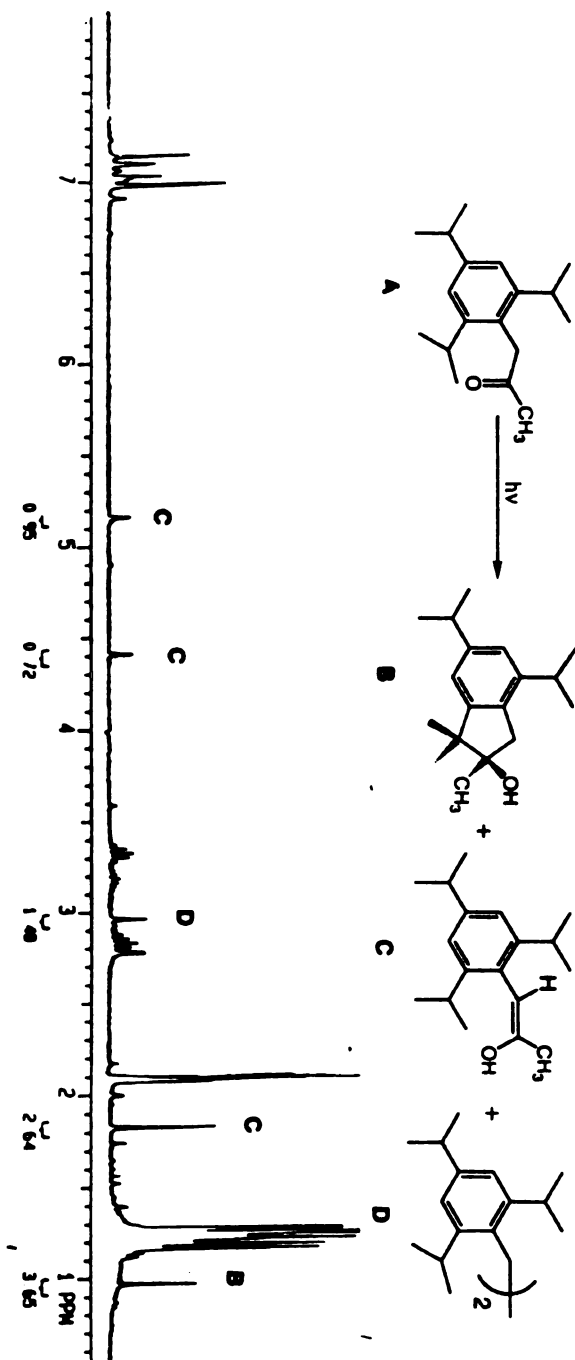


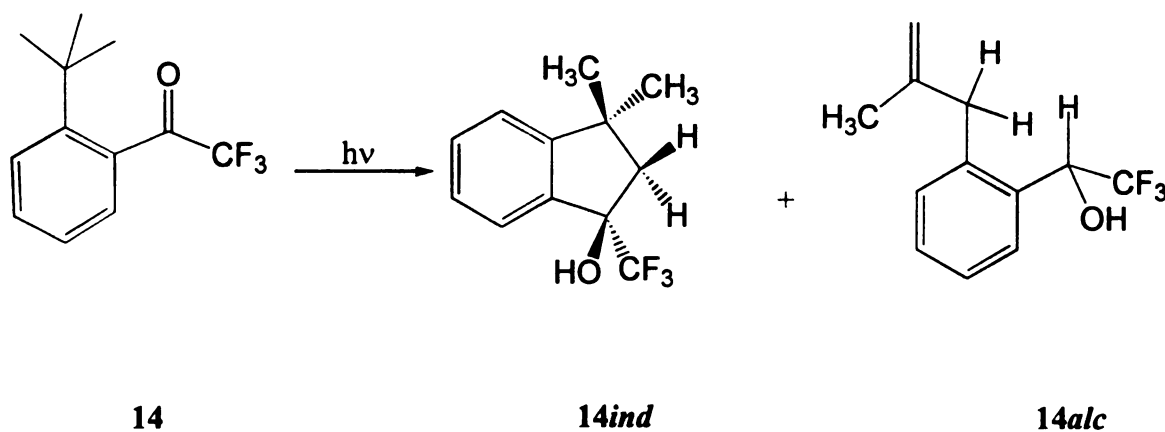
Figure 44. ^1H NMR of α -(2,4,6-Triisopropylphenyl)acetone after Irradiation in Toluene ($\lambda > 290$ nm, $T = 297$ K)

1,2-Di(2,4,6-triisopropylphenyl)ethane

^1H NMR(CDCl_3): δ 1.20 (d, $J=6.84$ Hz, 24H, 4 $(\text{CH}_3)_2\text{CH}$), 1.24 (d, $J=6.84$ Hz, 12H, 2 $(\text{CH}_3)_2\text{CH}$), 2.90 (s, 4H, 2 CH_2), 3.25 (septet, $J=6.84$ Hz, 6H, 6 $\text{CH}(\text{CH}_3)_2$), 6.98 (s, 4H, Ar)

Products from *o*-tert-Butyltrifluoroacetophenone (14)

o-tert-Butyltrifluoroacetophenone (0.003 g) in 0.8 mL of deuterated benzene was irradiated until no trace of starting material could be observed by NMR. The signals for two products were detected upon analysis of the NMR spectrum of the photolysis mixture. The products were identified to be an unsaturated alcohol and an indanol. The product ratios were determined by NMR integration of the methyl singlet signal of the alcohol and indanol. Products were separated by performing large scale irradiation using 0.30 g of *o*-tert-Butyltrifluoroacetophenone in 100 mL of benzene. Solvent was evaporated to leave a yellow oil which was chromatographed by PTLC using 30% ethyl acetate in hexane solution. The indanol eluted before the unsaturated alcohol.



Scheme 75. Photoproducts of *o*-tert-Butyltrifluoroacetophenone

1-{2'-(3-(2"-Methyl)propargyl)phenyl}trifluoromethylethanol

$^1\text{H NMR}(\text{CDCl}_3)$: δ 1.8 (s, 3H, allylic CH_3), 2.42 (d, $J= 4.88$ Hz, 1H, OH), 3.40 (AB quartet, $J= 16.5$ Hz, 2H, CH_2), 4.5 (dq, $J=1.4, 0.83$ Hz, 1H, vinylic CH), 4.88 (dq, $J=1.4, 1.5$ Hz, 1H, vinylic CH), 5.3 (dq, $J= 4.8, 6.7$ Hz, 1H, CHOH), 7.2 (m, 1H, Ar), 7.35 (m, 2H, Ar), 7.65 (m, 1H, Ar)

$^{13}\text{C NMR}(\text{CDCl}_3)$: δ 22.3, 41.6, 69 (q, $J= 34$ Hz), 112.5, 124.5 (q, $J=290$ Hz), 127, 127.4, 129, 131, 133, 138, 144.8

$^{19}\text{F NMR}(\text{CDCl}_3)$: δ -2.0 (d, $J= 6.7$ Hz, 3F, CF_3) reference: ethyl trifuroacetate

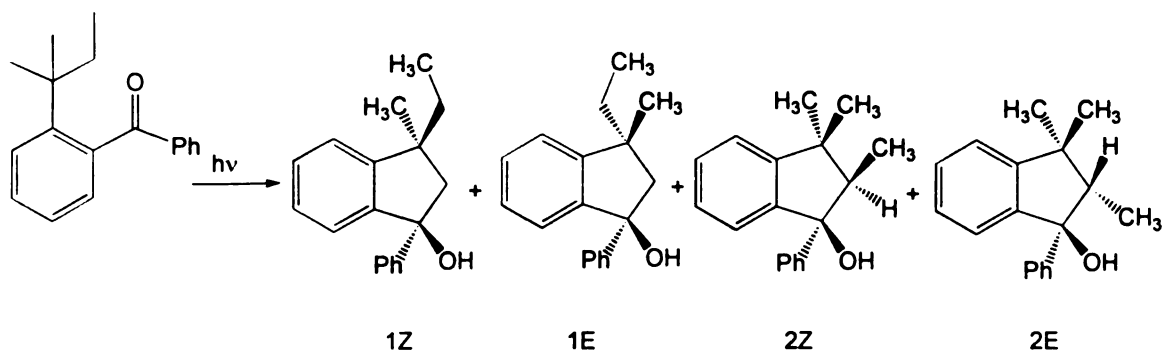
IR(CCl_4): 3618.9, 2937.9, 1453.5, 1272.2, 1169.1, 1132.4, 1061.9, 898.9, 803.4, 701.2

3,3-Dimethyl-1-trifluoromethyl-1-indanol

$^1\text{H NMR}(\text{CDCl}_3)$: δ 1.37 (s, 3H, CH_3), 1.42 (s, 3H, CH_3), 2.20 (1H, q and half of an AB quartet, $J=1.16, 14.4$ Hz, 1H, CH_2), 2.45 (half of an AB quartet, $J= 14.2$ Hz, 1H, CH_2), 7.0 (m, 1H, Ar), 7.35 (m, 2H, Ar), 7.55 (d, 1H, Ar)

Products from o-tert-Amylbenzophenone

o-tert-Amylbenzophenone 0.4 g in 100 mL of benzene was irradiated until no trace of starting material could be observed by GC. The signals for two pairs of isomeric indanols were detected upon analysis of the NMR spectrum of the photolysis mixture. The products were separated by liquid chromatography using 5% ethyl acetate in hexane. NOe experiments were performed to determine the stereochemistry of the isomers.



Scheme 76. Photoproducts of *o*-tert-Amylbenzophenone

(E)-2,3,3-Trimethyl-1-phenyl-1-indanol

$^1\text{H NMR}(\text{CDCl}_3)$: δ 0.82 (d, $J = 7.3$ Hz, 3H, CH_3CH), 0.89 (s, 3H, CH_3), 1.36 (s, 3H, CH_3), 2.41 (q, $J = 7.3$ Hz, 1H, CHCH_3), 7.09 (m, 2H, Ar), 7.2-7.5 (m, 7H, Ar)

Noe(CDCl_3): Irradiation at δ 0.82 ppm produced the following enhancements δ 1.36 ppm (2.5%), δ 2.4 ppm (2.5%), δ 7.2-7.5 ppm (3.8%)

(Z)-2,3,3-Trimethyl-1-phenyl-1-indanol

$^1\text{H NMR}(\text{CDCl}_3)$: δ 1.01 (d, $J = 7.3$ Hz, 3H, CH_3CH), 1.30 (s, 3H, CH_3), 1.39 (s, 3H, CH_3), 2.22 (q, $J = 7.3$ Hz, 1H, CHCH_3), 6.98 (d, 1H, Ar), 7.2-7.5 (m, 8H, Ar)

Noe(CDCl_3): Irradiation at δ 1.01 ppm produced the following enhancements δ 2.22 ppm (4.5%), and δ 1.39 ppm (2.5%)

(E)-3-Methyl-3-ethyl-1-phenyl-1-indanol

$^1\text{H NMR}(\text{CDCl}_3)$: δ 0.96 (t, $J = 7.4$ Hz, 3H, CH_3CH_2), 1.27 (s, 3H, CH_3), 1.80 (q, $J = 7.4$ Hz, 2H, CH_2CH_3), 2.29-2.56 (AB quartet, $J = 14.1$ Hz, 2H, CH_2), 7.07 (d, 1H, Ar), 7.2-7.5 (m, 8H, Ar)

Noe(CDCl₃): Irradiation at δ 1.27 ppm produced the following enhancements δ 1.80 ppm (1.7%), and δ 2.29 ppm (1.9%), and δ 7.07 ppm (2.9%)

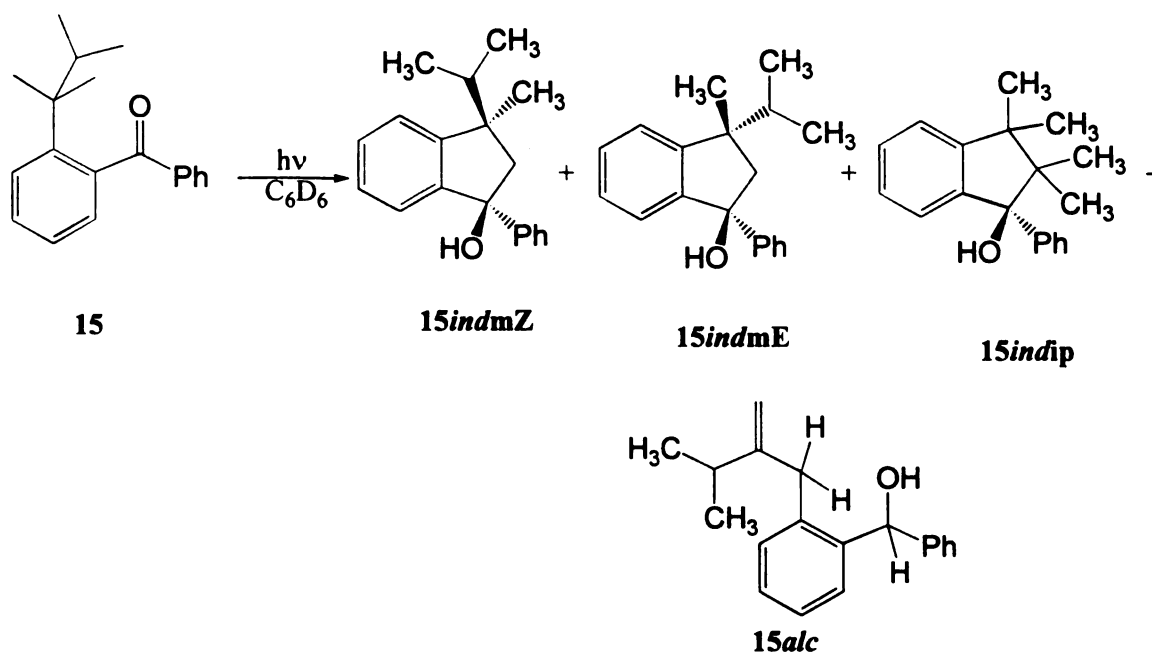
(Z)- 3-Methyl-3-ethyl-1-phenyl-1-indanol

¹H NMR(CDCl₃): δ 0.81 (t, J= 7.4 Hz, 3H, CH₃CH₂), 1.42 (s, 3H, CH₃), 1.58-1.72 (m, 2H), 2.26-2.45 (AB quartet, J= 14.1 Hz, 2H, CH₂), 7.01 (d, 1H, Ar), 7.2-7.5 (m, 8H, Ar)

Noe(CDCl₃): Irradiation at δ 1.42 ppm produced the following enhancements δ 2.26 ppm (0.8%), and δ 2.56 ppm (0.9%), and δ 7.0 ppm (0.8%).

Products from 2'-(2,3-Dimethyl-2-butyl)benzophenone (15)

2'-(2,3-Dimethyl-2-butyl)benzophenone (0.004 g) in 0.8 mL of deuterated benzene was irradiated until no trace of starting material could be observed by NMR. The signals for four isomeric products were detected upon analysis of the NMR spectrum of the photolysis mixture. The products were identified as indanols and an unsaturated alcohol. The product ratios were determined by NMR integration of the methyl singlet signals of indanols and the isopropyl doublet signal of the alcohol. The effect of temperature and phase on product ratios was also investigated by conducting the photochemistry in acetone/ethanol, ice-water and silicon oil (110°C) baths and in solid. The products were difficult to isolate because of a rapid dehydration on silica gel. The spectroscopic data given are from the NMR mixtures of photoproducts in benzene.



Scheme 77. Photoproducts of 2-(2'-(2',3'-Dimethyl)butyl)benzophenone

Z-3-Isopropyl-3-methyl-1-phenyl-1-indanol

$^1\text{H NMR}(\text{C}_6\text{D}_6)$: δ 0.62 (d, $J = 6.84$ Hz, 3H, $(\text{CH}_3)_2\text{CH}$), 0.78 (d, $J = 6.84$ Hz, 3H, $(\text{CH}_3)_2\text{CH}$), 1.40 (s, 3H, CH_3), 1.91 (septet, $J = 6.8$ Hz, 1H, $\text{CH}(\text{CH}_3)_2$), 2.05 (Half of an AB quartet, $J = 14.1$ Hz, 1H, CH_2), 2.38 (Half of an AB quartet, $J = 14.1$ Hz, 1H, CH_2), 6.8-7.2 (m, 7H, Ar), 7.5 (d, $J = 6.9$ Hz, 2H, Ar)

E-3-Isopropyl-3-methyl-1-phenyl-1-indanol

$^1\text{H NMR}(\text{C}_6\text{D}_6)$: δ 0.76 (d, $J = 6.81$ Hz, 3H, $(\text{CH}_3)_2\text{CH}$), 0.85 (d, $J = 6.78$ Hz, 3H, $(\text{CH}_3)_2\text{CH}$), 1.10 (s, 3H, CH_3), 1.91 (septet, $J = 6.8$ Hz, 1H, $\text{CH}(\text{CH}_3)_2$), 2.08 (Half of an AB quartet, $J = 14.5$ Hz, 1H, CH_2), 2.58 (Half of an AB quartet, $J = 14.5$ Hz, 1H, CH_2), 6.8-7.2 (m, 7H, Ar), 7.4 (d, $J = 6.9$ Hz, 2H, Ar)

3,3,4,4-tetramethyl-1-phenyl-1-indanol

$^1\text{H NMR}(\text{C}_6\text{D}_6)$: δ 1.11 (s, 3H, CH_3), 1.16 (s, 3H, CH_3), 1.18 (s, 3H, CH_3), 1.45 (s, 3H, CH_3), 6.8-7.3 (m, 9H, Ar)

1-{2'-[3-(2"-Isopropyl)propargyl]phenyl}benzyl alcohol

$^1\text{H NMR}(\text{C}_6\text{D}_6)$: δ 0.92 (d, $J=6.96$ Hz, 3H, $(\text{CH}_3)_2\text{CH}$), 0.95 (d, $J=6.85$ Hz, 3H, $(\text{CH}_3)_2\text{CH}$), 1.91 (septet, $J=6.8$ Hz, 1H, $\text{CH}(\text{CH}_3)_2$), 3.26 (Collapsed AB quartet, $J=1.14$ Hz, 2H, CH_2), 4.47 (dd, $J=1.53$ Hz, 1H, vinylic CH), 4.84 (m, 1H, vinylic CH), 5.92 (s, 1H, CHOH), 6.8-7.2 (m, 7H, Ar), 7.4 (d, $J=6.9$ Hz, 2H, Ar)

3-Isopropyl-3-methyl-1-phenylindene

$^1\text{H NMR}(\text{C}_6\text{D}_6)$: δ 0.64 (d, $J=6.75$ Hz, 3H, $(\text{CH}_3)_2\text{CH}$), 0.94 (d, $J=6.81$ Hz, 3H, $(\text{CH}_3)_2\text{CH}$), 1.25 (s, 3H, CH_3), 1.97 (septet, $J=6.8$ Hz, 1H, $\text{CH}(\text{CH}_3)_2$), 6.22 (s, 1H, vinylic CH), 7.15-7.30 (m, 6H, Ar), 7.5 (m, 1H, Ar), 7.5 (d, $J=6.8$ Hz, 2H, Ar)

D. Quantitative Measurements***1. Semiempirical and Molecular Mechanics Calculations***

All calculations were performed on a 7100/80 Power Macintosh computer equipped with the Cache program. MOPAC, a version of MOPAC6 written by James J. P. Stewart¹¹², was used for semiempirical calculations. The calculations were generally done by creating a structural input which was minimized first by molecular mechanics and then by semiempirical calculations at AM1 level of theory. The purpose of this procedure was to provide MOPAC with a better input structure.

Global minimizations (semiempirical-AM1) with dihedral drivers around bonds a and b were performed on the minimized structures to obtain the conformations of other minima.

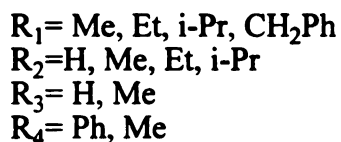
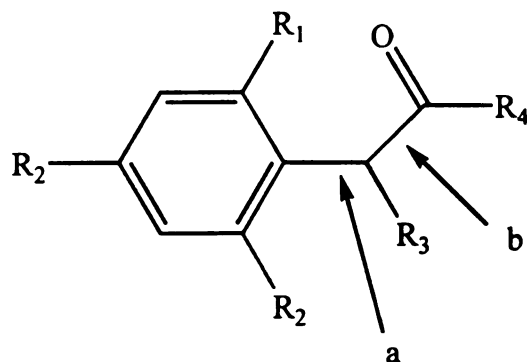


Figure 45

For $R_1 = \text{Et}$ and CH_2Ph only conformations with the methyl and phenyl trans to the hemipinacol radical moiety were considered, since the syn isomer was found to lie 4 kcal/mole above the trans. The lowest energy rotational maps for interconversion of various minima were constructed by locating the lowest energy path between the minima in the global minimization maps, minimizing the geometries in the path (semiempirical-AM1) and plotting the energies. The details of global minimizations for all compounds studied are listed in Tables 28 and 29. Tables 30-38 contain energies from double dihedral minimizations about bonds a and b (Figure 45), calculated by MOPAC, for several compounds.

Table 28. Details of Global Minimizations for Compounds 1-9

Compound	State	Calculation	Level	# of Drivers ^a	Increments	Key Words ^b
1	Ground	Semiempirical	AM1	2	36°, 36°	NOANCI GEO-OK
1	Triplet Br.	Semiempirical	AM1-UHF	2	10°, 10°	//
2	Ground	Mechanics	MM2	2	36°, 36°	//
2	Triplet Br.	Semiempirical	AM1-UHF	2	20°, 20°	//
3	Triplet Br.	Semiempirical	AM1-UHF	2	24°, 24°	//
4	Ground	Semiempirical	AM1	2	10°, 10°	//
4	Triplet Br.	Semiempirical	AM1-UHF	2	36°, 36°	//
5	Ground	Semiempirical	AM1	2	15°, 15°	//
5	Triplet Br.	Semiempirical	AM1-UHF	2	30°, 30°	//
6	Ground	Semiempirical	AM1	2	36°, 36°	//
6	Triplet Br.	Semiempirical	AM1-UHF	2	15°, 15°	//
7	Ground	Mechanics	MM2	2	36°, 36°	//
8	Ground	Semiempirical	AM1	2	36°, 10°	//
8	Triplet Br.	Semiempirical	AM1-UHF	2	22°, 22°	//
9	Triplet Br.	Semiempirical	AM1-UHF	2	15°, 15°	//

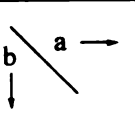
a) Dihedral rotations about bonds a and b, respectively. b) NOANCI= no analytical configuration interaction was used, GEO-OK= will allow the calculation to continue if a high energy (non convergent) geometry is reached.

Table 29. Details of Global Minimizations for Compounds 10-15

Compound	State	Calculation	Level	# of Drivers ^a	Increments	Key Words ^b
10	Ground	Semiempirical	AM1	2	16°, 16°	NOANCI GEO-OK
10	Triplet Br.	Semiempirical	AM1-UHF	2	30°, 30°	//
11	Ground	Mechanics	MM2	2	36°, 36°	//
12	Ground	Mechanics	MM2	2	36°, 36°	//
12	Triplet Br.	Semiempirical	AM1-UHF	2	36°, 36°	//
13	Triplet Br.	Semiempirical	AM1-UHF	2	15°, 30°	//
14	Ground	Mechanics	MM2	1	10°	//
15	Ground	Semiempirical	AM1-UHF	1	36°	//

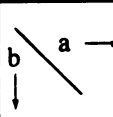
a) Dihedral rotations about bonds a and b, respectively. b) NOANCI= no analytical configuration interaction was used, GEO-OK= will allow the calculation to continue if a high energy (non convergent) geometry is reached.

Table 30. Grid of Energies (kcal/mole) for The Ground State Optimization of α -(2-Ethylphenyl)acetophenone

	0°	36°	72°	108°	144°	180°	216°	252°	288°	324°	360°
0°	2.79	3.32	2.66	3.36	6.01	6.9	5.4	2.54	2.35	2.67	1.75
36°	1.4	2.04	2.03	1.13	4.4	7.31	6.48	2.14	1.62	2.71	1.44
72°	2.94	3.89	2.9	2.76	6.74	8.94	8.37	4.98	3.02	2.69	2.20
108°	2.53	2.88	2.44	3.03	6.27	8.08	7.39	4.59	2.51	2.88	2.52
144°	5.67	4.81	5.53	5.74	8	12.62	14.38	8.78	4.77	6.31	5.66
180°	5.56	6.94	6.98	8.22	12.83	17.55	12.32	6.71	6.53	7.13	6.84
216°	3.66	5.11	3.92	6.89	14.47	12.13	7.84	3.88	4.45	3.84	3.67
252°	1.89	2.13	2.07	5.14	7.53	8.53	5.74	2.49	1.65	2.31	1.90
288°	2.44	2.94	3.11	2.09	5.86	7.94	7.1	2.58	2.53	3.61	2.45
324°	3.02	4.18	4.24	3.87	7.54	8.76	5.88	2.8	3.62	3.56	3.03
360°	3.02	3.07	1.91	2.63	5.26	6.9	5.38	2.56	1.89	2.33	1.75

AM1 NOMM MULLIK BONDS NOINTER PRECISE DENOUT ISOTOPE NODIIS
 NOANCI GEO-OK, oetpap.sm, Optimized search (grid) TOTAL CPU TIME IN FLEPO
 : 89056.987

Table 31. Grid of Energies (kcal/mole) for Global Minimization of The Triplet Biradical of α -(2,4,6-Triethylphenyl)acetophenone

	0°	30°	60°	90°	120°	150°	180°	210°	240°	270°	300°	330°	360°
0°	19.35	13.7	10.98	12.1	18.43	28.69	29.16	20.17	13.5	10.73	12.44	17.36	24.72
30°	9.71	8.18	8.85	13.37	22.22	22.28	17.12	12.42	9.5	10.64	18.93	14.3	9.83
60°	5.95	6.25	7.17	11.83	17.83	13.64	11.14	9.41	8.67	10.31	15.08	7.47	5.94
90°	5.42	5.35	6.25	12.63	10.11	9.71	10.08	13.78	12.86	10.67	5.9	5.22	5.25
120°	6.78	9.35	11.63	11.27	8.1	9.77	12.76	16.92	20.25	20.17	17.62	6.65	6.61
150°	11.79	16.94	17.49	11.35	10.37	13.99	33.52	28.03	19.34	14.37	9.64	9.06	11.65
180°	18.1	23.15	13.47	11.19	12.81	18.77	25.72	29.84	12.87	11.46	12.01	15.31	20.21
210°	13.96	11.51	11.12	13.92	20.14	22.81	17.71	12.12	8.71	10.96	14.64	21.14	24.37
240°	9.91	8.89	8.71	11.33	15.96	15.22	11.64	8.43	7.73	9.34	11.89	12.24	9.79
270°	8.25	8.25	9.69	11.59	11.24	10.84	9.72	9.69	10.54	9.43	9.31	8.7	8.21
300°	9.06	11.17	10.89	8.26	7.81	8.57	10.6	12.77	15.75	17.81	9.5	9.3	9.43
330°	12.4	16.22	13.6	9.34	8.53	11.09	17.25	22.35	22.37	14.98	11.32	11.32	13.6
360°	17.84	19.76	13.49	9.76	11.32	16.75	24.15	29.94	16.23	11.89	11.82	13.97	17.86

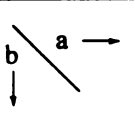
UHF TRIPLET AM1 NOMM MULLIK BONDS NOINTER DENOUT ISOTOPE
 NOANCI, GEO-OK, tetpap.br, Optimized search (grid), TOTAL CPU TIME IN FLEPO
 : 63458.344

Table 32. Grid of Energies (kcal/mole) for Global Minimization of The Triplet Biradical of α -(2-Tolyl)propiofenone

$\begin{array}{l} \backslash \\ a \\ \downarrow \\ b \end{array}$	0°	24°	48°	72°	96°	120°	144°	168°	192°	216°	240°	264°	288°	312°	336°	360°
0°	35.05	41.78	33.1	32.41	32.52	29.43	32.73	37.53	41.28	34.04	29.4	27.24	26.58	27.19	29.82	35.04
24°	32.87	31.48	30.04	28.38	27.91	29.27	36.07	33.87	30.96	28.15	26.56	25.41	25.8	27.5	30.12	29.83
48°	32.21	31.52	30.17	28.82	29.54	29.87	32.22	38.16	35.86	27.76	26.17	25.91	26.8	27.76	28.37	28.55
72°	33.04	31.88	30.58	30.08	31.16	31.08	30.45	30.03	31.09	30.01	28.46	26.65	26.51	27.06	27.87	28.55
96°	32.46	32.45	31.26	28.85	27.07	27.54	28.9	30.37	32.45	32.75	31.35	29.06	27.17	27.31	27.75	28.66
120°	34.86	35.21	34.08	30.93	27.32	26.45	27.08	29.53	32.57	38.57	35.65	31.83	28.86	28.02	28.72	29.97
144°	39.63	38.81	41.88	34.21	29.93	28.74	30.21	34.04	38.95	43.3	40.83	35.56	31.72	30.53	31.33	33.8
168°	46.41	41.71	37.03	33.68	31.56	32.06	35.02	51.09	47.96	42.17	36.07	32.86	31.67	32.31	34.81	39
192°	39.67	36.24	33.84	32.56	32.75	35.54	39.65	45.41	50.43	34.67	31.63	30.32	32.27	34.75	38.23	42.85
216°	32.47	32.88	32.97	33.71	34.76	41.84	39.65	36.78	33.41	29.75	28	27.98	30.6	34.6	33.79	32.49
240°	29.75	31.01	31.42	31.93	32.34	35	37.77	38.09	36.76	27.71	26.38	27.26	28.58	30.55	30.39	29.61
264°	34.13	33.2	34.24	33.39	33.53	33.31	32.78	34.01	32.8	32.07	30.4	29.03	28.6	29.68	30.08	30.77
288°	36.24	36.59	34.55	32.47	31.31	31.76	33.04	34.44	33.83	34.78	35.8	35.87	30.82	31.62	31.98	33.2
312°	39.04	39.58	37.43	33.73	31.47	31.33	32.53	34.6	36.8	39.86	36.43	33.42	32.49	33.23	33.68	35.26
336°	43.77	43.03	43.4	39.87	30.58	30.76	32.56	36.57	40.56	44.42	35.67	32.3	31.91	31.96	32.92	36.39
360°	37.09	34.43	32.01	30.3	28.48	29.19	31.51	35.85	36.99	32.58	29.1	28.16	28.16	28.93	31.78	35.32

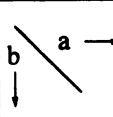
UHF TRIPLET AM1 NOMM MULLIK BONDS NOINTER DENOUT ISOTOPE
 NOANCI, GEO-OK, otolpp.br, Optimized search (grid), TOTAL CPU TIME IN FLEPO
 : 53680.500

Table 33. Grid of Energies (kcal/mole) for Global Minimization of The Triplet Biradical of α -(2-Ethylphenyl)propiophenone

	0°	36°	72°	108°	144°	180°	216°	252°	288°	324°	360°
0°	29.23	24.02	22.74	22.91	22.9	30	24.43	18.35	16.62	18.91	29.31
36°	22.62	19.57	18.66	19.71	26.35	22.82	19.03	15.9	16.47	23.63	19.72
72°	17.76	19.89	20.7	20.66	23.09	23.23	21.64	18.23	17.44	16.64	17.23
108°	21.99	23.81	22.06	18.43	18.17	26.78	28.39	23.73	17.11	15.40	16.89
144°	22.02	34.78	28.83	20.61	21.52	28.37	38.29	29.64	20.56	18.33	22.0
180°	34.28	25.93	23.64	23.57	29.3	38.89	30.55	22.21	20.89	22.37	32.54
216°	23.73	21.27	22.75	28.39	36.5	27.13	21.05	18.2	23.85	27.95	21.35
252°	21.29	20.32	27.03	27.97	24.99	21.83	19.72	17.94	20.28	18.60	17.71
288°	24.82	26.59	25.15	24.31	23.42	24.66	26.58	28.43	20.28	19.44	21.34
324°	32.69	37.11	27.14	23.57	25.02	29.32	35.17	26.89	22.66	22.01	26.24
360°	29.24	24.07	22.94	22.92	23.03	29.91	24.34	18.71	16.72	18.8	29.4

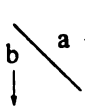
UHF TRIPLET AM1 NOMM MULLIK BONDS NOINTER DENOUT ISOTOPE
 NOANCI, GEO-OK, oethylphenpph.br2, Optimized search (grid), TOTAL CPU TIME
 IN FLEPO : 34510.688

Table 34. Grid of Energies (kcal/mole) for Global Minimization of The Triplet Biradical of α -(2,4,6-Triethylphenyl)propiophenone

	0°	30°	60°	90°	120°	150°	180°	210°	240°	270°	300°	330°	360°
0°	22.31	34.49	17.39	15.23	17.41	23.88	32.96	28.28	18.88	13.67	13.44	17.5	24.33
30°	13.7	13.67	13.65	15.52	20.05	22.05	16.78	11.52	7.91	9.9	15.27	23.57	20.28
60°	11.35	12.57	13.04	14.36	17.88	20.4	12.29	9.33	7.75	8.92	12.48	12.02	10.83
90°	15.11	15.47	16.09	14.46	12.75	12.76	13.9	15.35	14.39	11.69	10.92	10.62	12.19
120°	21.68	24.25	20.57	15.36	13.62	14.05	17.98	22.58	25.76	25.67	15.22	15.2	17.14
150°	21.17	29.54	23.32	16.91	14.93	17.75	24.47	33.96	28.58	21.09	17.02	17.18	21.31
180°	22.84	28.75	22.13	20.13	15.41	21.41	28.32	33.84	24.95	17.01	15.21	17.74	22.92
210°	13.49	13.21	13.42	15.25	18.8	21	16.48	11.19	7.74	8.44	14.43	19.57	25.45
240°	9.95	11.34	11.37	12.23	15.83	18.2	18.03	9.01	7.37	9.24	13.3	11.41	9.84
270°	11.68	15.08	15.4	13.91	12.82	12.38	12.78	15.82	14.45	12.2	11.85	10.67	11.15
300°	15.04	19.72	20.27	19.21	12.91	13.07	16.12	19.97	24.2	17.87	13.9	13.91	15.12
330°	24.02	32.09	24.36	18.78	16.91	20.3	26.98	38.33	29.45	22.87	19.94	20.11	24.21
360°	36.07	21.86	19.75	17.28	15.51	21.38	29.84	24.63	17.14	12.63	12.82	16.36	22.91

UHF TRIPLET AM1 NOMM MULLIK BONDS NOINTER DENOUT ISOTOPE
 GEO-OK, tetpph.br, Optimized search (grid), TOTAL CPU TIME IN FLEPO :
 74793.797

Table 35. Grid of Energies (kcal/mole) for Global Minimization of The Triplet Biradical of α -Mesitylpropiophenone

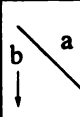
	0°	24°	48°	72°	96°	120°	144°	168°	192°	216°	240°	264°	288°	312°	336°	360°
0°	25.87	25.97	27.29	29.7	34.63	39.35	35.92	32.09	27.95	24.07	22.21	23.04	25.57	30.29	36.44	27.96
24°	26.67	27.23	28.04	29.32	34.81	32.43	29.7	27.51	24.96	22.85	22.14	22.96	25.45	27.71	26.53	25.95
48°	26.85	26.97	27.17	27.9	29.66	27.91	26.74	25.73	25.06	24.11	23.97	24.97	25.78	25.37	24.91	24.89
72°	30.19	29.89	29.37	27.37	26	26.41	27.53	29.66	30.61	29.82	28.01	25.54	24.21	24.41	25.08	26.28
96°	35.13	33.18	30.48	27.18	26.24	26.24	28.06	30.72	33.67	36.16	37.05	30.59	27.98	27.25	27.7	29.63
120°	40.55	37.19	32.93	29.04	28.04	28.46	31.8	36.26	40.78	41.85	37.64	33.22	30.38	29.31	30.84	33.14
144°	43.83	38.5	32.85	28.88	28.34	30.33	34.83	40.06	44.94	44.97	38.79	33.28	30.76	30.12	31.71	36.15
168°	33.57	31.27	29.69	28.34	37.38	41.71	43.1	39.98	35.38	30.64	27.79	27.65	27.98	29.78	33.17	38.55
192°	28.57	27.36	28.1	29.17	32.67	36.28	41.32	45.66	27.7	24.33	23.31	24.08	27.16	30.36	31.29	29.09
216°	26.2	26.46	26.98	28.19	33.25	31.82	29.31	26.39	23.6	21.36	21.03	22.21	24.9	27	25.97	25.1
240°	25.54	25.92	26.28	26.82	29.56	31.14	31.77	30.65	23.56	23.05	22.36	23.8	25.23	25.03	25.4	24.33
264°	28.37	29.42	27.98	27.44	27.26	27.05	27.23	27.12	28.48	29.3	26.89	24.73	24.62	24.42	24.89	25.59
288°	34.63	32.16	29.43	27.04	26.19	27.4	29.02	31.44	31.03	33.72	35.92	29.23	27.25	26.71	27.23	28.05
312°	41.45	38.12	32.93	28.9	27.9	28.56	31.4	35.27	39.61	45.25	39.33	34.09	31.63	29.86	30.38	32.75
336°	45.39	40.12	35.78	32.87	32.67	34.91	39.84	46.1	52.73	45.17	37.33	31.72	29.9	29.99	31.46	35.54
360°	34.2	30.38	27.96	27.39	29.62	32.99	38.78	45.91	39.63	33.11	28.36	25.85	26.02	28.4	32.08	36.91

UHF TRIPLET AM1 NOMM MULLIK BONDS NOINTER DENOUT ISOTOPE

NOANCI GEO-OK, mespph.br, Optimized search (grid), TOTAL CPU TIME IN FLEPO

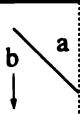
: 70180.500

Table 36. Grid of Energies (kcal/mole) for Global Minimization of The Triplet Biradical of α -(2-Ethylphenyl)acetone

	0°	30°	60°	90°	120°	150°	180°	210°	240°	270°	300°	330°	360°
0°	-6.08	-9.62	-10.68	-11.47	-11.43	-7.72	-1.06	5.84	-11.51	-11.49	-10.69	-9.66	-6.09
30°	-10.49	-11.37	-10.9	-11.99	2.82	-1.28	-5.97	-9.65	-11.63	-11.73	-9.89	-6.54	-10.61
60°	-12	-11.49	-10.83	-11.76	-7.98	-0.51	-7.49	-8.89	-10.8	-11.5	-9.08	-10.15	-12.08
90°	-11.46	-10.67	-10.19	-10.86	-8.87	-7.8	-7.23	-4.97	-9.14	-10.95	-9.91	-11.14	-11.86
120°	-10.4	-8.42	-9.47	-10.66	-10.6	-8.57	-5.57	-0.45	-7.86	-10.34	-9.89	-10.61	-10.4
150°	-7.52	-6.49	-9.21	-10.36	-10.03	-6.88	4.96	-0.84	-8.12	-10.3	-9.41	-9.52	-7.49
180°	-6.03	-7.71	-9.36	-10.39	-9.46	-3.79	3.55	6.95	-9.21	-10.33	-9.41	-7.73	-6.05
210°	-7.49	-9.54	-9.7	-10.17	-8.16	5.25	-0.6	-6.95	-10.46	-10.36	-8.98	-6.6	-7.53
240°	-10.52	-10.48	-9.87	-10.45	-7.86	-1.56	1.63	-8.59	-10.47	-10.44	-9.3	-8.44	-10.52
270°	-11.8	-11	-10.22	-10.92	-9.04	-5.86	-7.27	-7.54	-8.77	-10.77	-9.66	-10.64	-11.61
300°	-11.99	-10.19	-9.16	-11.67	-10.83	-8.93	-7.53	-5.62	-3.62	-11.75	-10.78	-11.45	-12.04
330°	-9.19	-8.02	-8.73	-9.12	-9.03	-6.57	-3.07	-2.99	-10.13	-11.93	-10.69	-11.52	-10.6
360°	-7.28	-7.96	-8.26	-8.8	-8.23	-4.56	0.81	4.79	-8.25	-8.66	-8.18	-8.14	-6.92

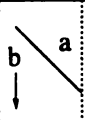
UHF TRIPLET AM1 NOMM MULLIK BONDS NOINTER DENOUT ISOTOPE
 NOANCI GEO-OK, oetphacetone.br2, Optimized search (grid), TOTAL CPU TIME IN
 FLEPO : 17316.492

Table 37. Grid of Energies (kcal/mole) for Global Minimization of The Singlet Biradical of α -(2-Ethylphenyl)acetone

	0°	30°	60°	90°	120°	150°	180°	210°	240°	270°	300°	330°	360°
0°	84.75	80.21	74.28	69.84	69.59	83.53	51.6	56.39	74.57	100.04	143.77	123.75	130.76
30°	83.73	92.96	109.3	107.29	108.21	96.28	113.29	86.86	77.56	78.54	87.65	111.12	107.14
60°	84.84	82.12	77.17	83.49	97.35	127.45	105.15	99.79	94.44	91.99	85.78	88.07	84.53
90°	87.05	85.14	80.65	77.18	75.48	83.91	87.53	87.86	97.67	97.43	85.36	87.8	86.3
120°	87.56	89.01	85.75	80.54	81.42	78.39	89.63	99.53	110.11	112.63	102.11	93.76	88.37
150°	96.63	94.05	84.07	89.93	102.76	108.62	105.88	147.2	121.69	88.6	86.18	89.06	95.13
180°	95.34	92.36	86.14	79.26	85.8	99.38	107.6	123.11	133.15	119.12	94.12	93.93	93.32
210°	105.77	95.69	94	104.8	115.46	118.36	92.43	102.12	79.9	81.16	86.16	87.91	95.35
240°	88.58	88.05	86.28	90.04	84.66	113.9	140.77	96.78	90.46	90.92	84.59	90.04	87.51
270°	92.73	94.96	99.74	99.58	91.79	82.07	84.8	80.67	70.65	74.12	81.95	84.65	84.93
300°	97.15	96.1	89.73	90.5	92.73	93.01	94.19	80.51	71.51	78	82.75	83.55	88.73
330°	96.13	97.2	88.89	89.17	104.09	148.62	129.76	96.37	71.62	75.57	78.77	81.82	88.06
360°	94.8	87.56	81.07	77.98	89.53	109.86	94.75	84.2	77.14	77.29	80.06	93.46	109.97

EXCITED SINGLET AM1 NOMM MULLIK BONDS NOINTER DENOUT NOANCI
 GEO-OK, oetphacetone.br, Optimized search (grid), TOTAL CPU TIME IN FLEPO :
 54177.381

Table 38. Grid of Energies (kcal/mole) for Global Minimization of The Triplet Biradical of α -(2,4,6-Triisopropylphenyl)acetone

	0°	30°	60°	90°	120°	150°	180°	210°	240°	270°	300°	330°	360°
-90°	-25.42	-27.17	-27.2	-24.75	-20.51	-19.57	-26.96	-28.86	-28.33	-26.21	-21.45	-22.32	-25.22
-60°	-26.82	-27.68	-27.84	-24.19	-24.59	-27	-28.55	-29.28	-28.8	-26.97	-23.43	-24.52	-26.97
-30°	-27.34	-27.62	-27.57	-26.95	-26.18	-28.51	-28.75	-28.97	-28.33	-27.38	-25.93	-26.46	-27.25
0°	-26.66	-27.09	-26.92	-27.34	-27.69	-28.52	-28.17	-28.68	-28.84	-27.73	-27.09	-26.69	-26.95
30°	-26.49	-26.15	-25.97	-26.91	-27.68	-27.9	-27.53	-27.99	-27.71	-27.97	-26.84	-26.52	-26.46
60°	-26.01	-23.61	-23.88	-25.68	-26.28	-27.1	-26.99	-26.19	-24.66	-25.46	-25.46	-26.34	-25.88
90°	-24.42	-22.26	-20.07	-23.49	-25.14	-26.37	-25.47	-23.46	-22.09	-22.57	-24.26	-25.46	-24.29

UHF TRIPLET AM1 RESTART NOMM MULLIK BONDS NOINTER DENOUT
 NOANCI GEO-OK, tippacetone.br, Optimized search (grid), TOTAL CPU TIME IN
 FLEPO : 81761.701

2. Quantum Yield Measurements

Quantum yields for product formation were measured by irradiating solutions of desired precursor parallel to 0.1 M valerophenone samples in sealed, degassed tubes.

Quantum yields were calculated from the following equation,

$$\Phi = [P] / I$$

where [P] is the concentration of photoproducts and I is the intensity of light absorbed by samples.

The intensity of light, I, was determined by 0.10 M valerophenone actinometer irradiated parallel with the samples to be analyzed. The irradiation was stopped after less than 10% conversion and the valerophenone sample was analyzed for presence of acetophenone. Acetophenone's concentration was, then, determined from Equation 6:

$$[AP] = R_f \times [Std] \times A_{AP} / A_{Std}$$

Equation 6

where [AP] is the concentration of acetophenone, R_f is the instrument response factor for acetophenone, A_{AP} is the integrated area for acetophenone, [Std] is the concentration of standard, and A_{Std} is the integrated area for the internal standard. The intensity of the light, I, can then be calculated using the acetophenone concentration based on $\Phi_{AP} = 0.33$, thus,

$$I = [AP] / 0.33$$

The concentration of photoproduct, [P], can be calculated using Equation 7.

$$[P] = R_{f(P)} \times [Std] \times A_p / A_{Std}$$

Equation 7

Where $R_{f(P)}$ is the instrument response factor for the product and A_p is the integrated area for the photoproduct. The instrumental response factors for photoproducts were obtained using Equation 8:

$$R_{f(P)} = ([P]/[Std]) \times (A_{Std} / A_P)$$

Equation 8

In cases where the photoproducts are difficult to isolate or unstable to analyze, the response factors can be calculated using Equation 9:

$$R.F. = \{ \# \text{ of Carbons} + 1/2 (\# \text{ of C-O bonds})_{Std} / \{ \# \text{ of Carbons} + 1/2 (\# \text{ of C-O bonds}) \}_P$$

Equation 9

3. Quenching Studies

Stern-Volmer quenching studies were performed by irradiating sealed degassed tubes containing the precursor and various amounts of quencher. The quenching is assumed to be diffusion-controlled with a rate constant of $6 \times 10^9 \text{ M}^{-1} \text{ s}^{-1}$.³⁰ The experimental results measure the quenching of triplet to biradical. Thus in order to translate this into triplet lifetime, it must be assumed that the predominant mode of triplet relaxation is its conversion to the biradical. The results of these experiments are summarized below.

Quantum Yield Measurement for α -(2-Ethylphenyl)acetophenone in Benzene

GC analysis: 1400 Varian GC

DB-225 Megabore column

Initial column temp.: 100°C

Initial col. hold time: 2 min.

Final col. temp.: 160°C

Rate: 6°C/min., Hold time: 2 min.

Table 39. Product Quantum Yields of α -(2-Ethylphenyl)acetophenone in Benzene

Photoproduct	A(product)	A(std.)	Concentration	Φ
Indanols	9.81939	29.23396	0.0015	0.47
Indanols	9.72419	29.94644	0.0014	0.46
Indanols	10.86830	29.26621	0.0016	0.50
Indanols	9.93122	29.79142	0.0015	0.47
Indanols	10.00819	29.49707	0.0015	0.48
Indanols	9.70557	29.39158	0.0015	0.46
Indanols	9.72804	29.24990	0.0015	0.47

[Ketone]= 0.0239 M, [VP]= 0.1456 M, [C₂₀]= 0.00328 M, λ = 313 nm $R_f^{\text{Indanols}}=1.36$, $R_f^{\text{AP}}=2.90$, Irradiation Time=2 hrs., Source= Mercury Arc Lamp

Quantum Yield Measurement for α -(2,4,6-Triethylphenyl)acetophenone in Benzene

GC analysis: 1400 Varian GC

DB-225 Megabore column

Initial column temp.: 100°C

Initial col. hold time: 2 min.

Final col. temp.: 172°C

Rate: 8°C/min., Hold time: 5 min

Table 40. Product Quantum Yields of α -(2,4,6-Triethylphenyl)acetophenone in Benzene

Photoproduct	A(product)	A(std.)	Concentration	Φ
Indanols	7.26507	23.16086	0.00149	0.47
Indanols	7.45212	23.74302	0.00149	0.47
Indanols	7.22500	22.81123	0.00151	0.48
Indanols	7.20434	22.42082	0.00153	0.48
Indanols	7.51868	22.80132	0.00157	0.50
Indanols	7.09332	23.35354	0.00145	0.46
Indanols	7.38268	21.62746	0.00163	0.51
Indanols	7.26572	23.24797	0.00149	0.48

[Ketone]= 0.0307 M, [VP]= 0.1456 M, [C₂₀]= 0.00328 M, λ = 313 nm $R_f^{\text{Indanols}}=1.45$, $R_f^{\text{AP}}=2.90$, Irradiation Time=2 hrs., Source= Mercury Arc Lamp

Quantum Yield Measurement for α -(2-Benzylphenyl)acetophenone in Benzene

GC analysis: 1400 Varian GC

DB-225 Megabore column

Initial column temp.: 130°C

Initial col. hold time: 2 min.

Final col. temp.: 210°C

Rate: 20°C/min., Hold time: 5 min

Table 41. Product Quantum Yields of α -(2-Benzylphenyl)acetophenone in Benzene

Photoproduct	A(product)	A(std.)	Concentration	Φ
Indanols	3.55851	18.36751	0.00057	0.41
Indanols	3.72227	19.22229	0.00057	0.41
Indanols	3.69135	19.28770	0.00056	0.41
Indanols	3.48125	19.31330	0.00053	0.38
Indanols	3.56177	18.25970	0.00057	0.41
Indanols	3.57529	19.49070	0.00054	0.39
Indanols	3.55951	19.35477	0.00054	0.39
Indanols	4.11391	22.20100	0.00055	0.40

[Ketone]= 0.0195 M, [VP]= 0.03 M, [C₂₀]= 0.00328 M, λ = 313 nm $R_f^{\text{Indanols}}=1.34$, $R_f^{\text{AP}}=2.90$, Irradiation Time=2 hrs., Source= Mercury Arc Lamp

Quantum Yield Measurement for α -(2-Ethylphenyl)propiophenone in Benzene

GC analysis: 1400 Varian GC

DB-225 Megabore column

Initial column temp.: 100°C

Initial col. hold time: 5 min.

Final col. temp.: 195°C

Rate: 8 °C/min., Hold time: 5 min

Table 42. Product Quantum Yields of α -(2-Ethylphenyl)propiophenone in Benzene

Photoproduct	A(product)	A(std.)	Concentration	Φ
Indanols	2.44339	11.27331	0.00029	0.061
Indanols	2.41312	10.37372	0.00031	0.066
Indanols	2.33439	9.97659	0.00032	0.066
Indanols	2.38892	9.97659	0.00033	0.068
2,3-Diarylbutanes	2.56981	11.27331	0.00029	0.061
2,3-Diarylbutanes	2.28177	10.37372	0.00028	0.059
2,3-Diarylbutanes	2.28231	9.97651	0.00030	0.62
Benzaldehyde ^a	1.57951	4.53267	0.00190	0.43
Benzaldehyde ^a	1.53167	4.44051	0.00188	0.42
Benzaldehyde ^a	1.60169	4.41437	0.00198	0.44

a) Quantum yield determined in presence of thiol, $\lambda=313$ nm

[Ketone]= 0.0216 M, [VP]= 0.118 M, [C17]= 0.0015 M, Source= Mercury Arc Lamp

 $R_f^{\text{Indanols}}=0.89$, $R_f^{2,3\text{-Diarylethanes}}=0.85$, $R_f^{\text{Benzaldehyde}}=4.1$, $R_f^{\text{AP}}=3.0$, Irradiation Time=6 hrs.

Quantum Yield Measurement for α -(2,4,6-Triethylphenyl)propiophenone in Benzene

GC analysis: 1400 Varian GC

DB-225 Megabore column

Initial column temp.: 100°C

Initial col. hold time: 5 min.

Final col. temp.: 195°C

Rate: 8 °C/min., Hold time: 5 min

Table 43. Product Quantum Yields of α -(2,4,6-Triethylphenyl)propiophenone in Benzene

Photoproduct	A(product)	A(std.)	Concentration	Φ
Z,E-Indanol	1.62441	17.58086	0.00025	0.16319
Z,E-Indanol	1.60987	18.18207	0.00024	0.15605
Z,E-Indanol	1.56916	17.44271	0.00024	0.15865
Z,E-Indanol	1.54773	17.98575	0.00023	0.15215
Z,E-Indanol	1.52696	18.03058	0.00023	0.15215
E,Z-Indanol	1.37224	18.14674	0.00021	0.13329
E,Z-Indanol	1.31834	18.03058	0.00020	0.12874
E,Z-Indanol	1.26739	17.83340	0.00019	0.12549
E,Z-Indanol	1.40440	17.44271	0.00022	0.14174
E,Z-Indanol	1.46234	17.5886	0.00023	0.14629

[Ketone]= 0.0202 M, [VP]= 0.118 M, [C₂₀]= 0.0033 M, Source= Mercury Arc Lamp

$R_f^{\text{Indanols}}=1.24$, $R_f^{\text{AP}}=3.0$, Irradiation Time=6 hrs., $\lambda=313$ nm

Quantum Yield Measurement for α -(2-Ethylphenyl)acetone in Benzene

GC analysis: 1400 Varian GC

DB-225 Megabore column

Initial column temp.: 105°C

Initial col. hold time: 5 min.

Final col. temp.: 185°C

Rate: 6 °C/min., Hold time: 1 min.

Table 44. Product Quantum Yields of α -(2-Ethylphenyl)acetone in Benzene

Photoproduct	A(product)	A(std.)	Concentration	Φ
Indanols	3.46544	45.64795	0.00048	0.01268
Indanols	3.43325	45.21899	0.00048	0.01268
Indanols	3.46251	43.69783	0.00050	0.01285
Indanols	3.33783	44.11101	0.00048	0.01228
Indanols	3.26094	43.41493	0.00047	0.01285
Diarylethane	6.69141	45.64795	0.00057	0.01495
Diarylethane	6.25961	45.21899	0.00053	0.01405
Diarylethane	7.01283	43.69783	0.00062	0.01601
Diarylethane	7.09688	44.11101	0.00062	0.01596
Diarylethane	6.62436	43.41493	0.00059	0.01504

[Ketone]= 0.0196 M, [VP]= 0.052 M, [C20]= 0.00351 M

 $R_f^{\text{Indanols}}=1.8$, $R_f^{2,3\text{-Diarylethanes}}=1.1$, $R_f^{\text{AP}}=2.9$, Irradiation Time=20 hrs, $\lambda=313$ nm,

Source= Mercury Arc Lamp

Quantum Yield Measurement for α -Mesitylacetone in Benzene

GC analysis: 1400 Varian GC

DB-225 Megabore column

Initial column temp.: 100°C

Initial col. hold time: 1 min.

Final col. temp.: 195°C

Rate: 8 °C/min., Hold time: 10 min.

Table 45. Product Quantum Yields of α -Mesitylacetone in Benzene

Photoproduct	A(product)	A(std.)	Concentration	Φ
Indanol	15.16800	22.35858	0.00238	0.08686
Indanol	15.51011	22.34461	0.00243	0.08868
Indanol	15.74424	22.88781	0.00241	0.08795
Indanol	15.97379	22.52081	0.0249	0.09087
Dimesitylethane	9.48040	22.35858	0.00149	0.05438
Dimesitylethane	9.69382	22.34461	0.00152	0.05547
Dimesitylethane	9.84015	22.88781	0.00150	0.05474
Dimesitylethane	9.98362	22.52081	0.00155	0.05657
Dimesitylethane	9.83397	22.38118	0.00154	0.05620
Dimesitylethane	9.80945	22.37678	0.00154	0.05620

[Ketone]= 0.049 M, [VP]= 0.052 M, [C₂₀]= 0.00351 M, Source= Mercury Arc Lamp $R_f^{\text{Indanols}}=1.7$, $R_f^{2,3\text{-Diarylethanes}}=1.0$, $R_f^{\text{AP}}=2.9$, Irradiation Time=20 hrs, $\lambda=313$ nm

Quantum Yield Measurement for α -(2,4,6-Triethylphenyl)acetone in Benzene

NMR analysis: Gemini 300 MHz

Table 46. Product Quantum Yields of α -(2,4,6-Triethylphenyl)acetone in Benzene

Photoproduct	A(product)	A(std.)	Concentration	Φ
Indanol	4.9	62.4	0.0039	0.039
Indanol	4.3	64.5	0.0033	0.033
Indanol	5.2	64.5	0.0040	0.040
Diarylethane	2.3	62.4	0.0018	0.018
Diarylethane	2.3	64.5	0.0018	0.0018
Diarylethane	2.6	64.5	0.002	0.02

[Ketone]= 0.032 M, [VP]= 0.156 M, [Methyl benzoate]= 0.05 M

Irradiation Time=20 hrs, λ =313 nm

Irradiation Source= Mercury Arc Lamp

Quantum Yield Measurement for α -(2,4,6-Triisopropylphenyl)acetophenone in Benzene

GC analysis: 3400 Varian GC

DB-1 Megabore column

Initial column temp.: 65°C

Initial col. hold time: 5 min.

Final col. temp.: 225°C

Rate: 10 °C/min., Hold time: 22 min.

Table 47. Product Quantum Yields of α -(2,4,6-Triisopropylphenyl)acetophenone in Benzene

λ (nm)	%Conversion	[Enol]	$\Phi_{\text{enol}}^{\text{a}}$	[Indanol]	$\Phi_{\text{indanol}}^{\text{a,b}}$
313	6	0.0065	0.35	-	-
313	15	0.013	0.234	0.003	0.062
313	19	0.014	0.15	0.006	0.059
313	24	0.014	0.09	0.009	0.052
366	10	0.13	0.64	-	-
366	18	0.18	0.64	0.024	0.085
366	25	0.24	0.64	0.034	0.085

a) Quantum yields were measured by NMR (b) Quantum yields were measured by GC

[Ketone]= 0.0143 M (GC studies), [Ketone]= 0.0983 M (NMR studies)

[VP]= 0.024 M (GC studies), [VP]= 0.1165 M (NMR studies)

[C20]= 0.0033 M (GC studies), [Methyl benzoate]= 0.03 M (NMR studies)

$R_f^{\text{Indanol}}=1.12$, $R_f^{\text{AP}}=1.34$, Irradiation Time=4 hrs, Irradiation Source= Mercury Arc

Quantum Yield Measurement for α -(2-Benzylphenyl)propiophenone in Benzene

NMR analysis: Gemini 300 MHz

Table 48. Product Quantum Yields of α -(2-Benzylphenyl)propiophenone in Benzene

Photoproduct	A(product)	A(std.)	Concentration	Φ
Z,Z-Indanol	0.57	11.05	0.0033	0.052
Z,Z-Indanol	0.51	9.36	0.0034	0.053
Z,Z-Indanol	0.54	9.34	0.0036	0.056
Z,E-Indanol	0.54	11.05	0.0031	0.049
Z,E-Indanol	0.42	9.36	0.0029	0.045
Z,E-Indanol	0.42	9.34	0.0029	0.045

[Ketone]= 0.0113 M, [VP]= 0.166 M, [Methyl benzoate]= 0.064 M

Irradiation Time=8 hrs, λ =313 nm

Irradiation Source= Mercury Arc Lamp

Quantum Yield Measurement for α -(2,4,6-Triisopropylphenyl)acetone in Benzene

GC analysis: 1400 Varian GC

DB-225 Megabore column

Initial column temp.: 100°C

Initial col. hold time: 5 min.

Final col. temp.: 185°C

Rate: 8 °C/min., Hold time: 5 min.

Table 49. Product Quantum Yields of α -(2,4,6-Triisopropylphenyl)acetone in Benzene

Photoproduct	A(product)	A(std.)	Concentration	Φ
Indanol	2.69067	66.80157	0.0002	0.009
Indanol	2.64648	66.75248	0.0002	0.009
Indanol	2.68319	66.19910	0.0002	0.009
Diarylethane	2.03309	66.80157	0.00009	0.004
Diarylethane	1.85067	66.75248	0.00008	0.004
Diarylethane	2.06752	66.19910	0.00009	0.004.
Enol	0.15	22.5	0.0036	0.028
Enol	0.18	231	0.0042	0.032
Enol	0.15	22.3	0.0036	0.028

[Ketone] = 0.0245 m, [VP]= 0.03 M, [C₂₀]= 0.0035 M $R_f^{\text{Indanols}}=1.0$, $R_f^{2,3\text{-Diarylethanes}}=0.62$, $R_f^{\text{AP}}=2.9$, Irradiation Time=20 hrs, $\lambda=313$ nm

Irradiation Source= Mercury Arc Lamp

Quantum Yield Measurements for 2-(2'-(2',3'-Dimethyl)butyl)benzophenone

NMR analysis: Gemini 300 MHz

Table 50. Product Quantum Yields of 2-(2'-(2',3'-Dimethyl)butyl)benzophenone

Solvent	Photoproduct	A(product)	A(std.)	Concentration	Φ
Benzene	15indmZ	0.98	17.84	0.0021	0.026
Benzene	15indmZ	1.19	18.54	0.0024	0.028
Benzene	15indmE	2.17	17.84	0.0046	0.052
Benzene	15indmE	2.20	18.54	0.0045	0.052
Benzene	15indip	0.47	17.84	0.0010	0.01
Benzene	15indip	0.35	18.54	0.0008	0.009
Benzene	15alc	0.28	17.84	0.0006	0.006
Benzene	15alc	0.24	18.54	0.0005	0.005
Methanol	15indmZ	3.26	12.3	0.0037	0.116
Methanol	15indmE	3.72	12.3	0.0042	0.132
Methanol	15indip	2.98	12.3	0.0034	0.107
Methanol	15alc	1.65	12.3	0.0019	0.06

[Ketone]= 0.0145 M, [VP]= 0.131 M, [MB]= 0.04 M

Irradiation Time=8 hrs, λ =313 nm, Irradiation Source= Mercury Arc Lamp

Table 51. Quenching of the Indanol Formation in α -(2-Ethylphenyl)acetophenone with 2,5-Dimethyl-2,4-hexadiene at 313 nm in Benzene

[Q]	A(product)/A(std.)	Φ^0/Φ
0.00	0.145	1.00
0.0046	0.138	1.05
0.0092	0.135	1.07
0.0138	0.131	1.11
0.0184	0.127	1.14

[Ketone] = 0.032 M

$$k_q\tau = 8$$

Table 52. Quenching of the Indanol Formation in α -(2,4,6-Triethylphenyl)acetophenone with 2,5-Dimethyl-2,4-hexadiene at 313 nm in Benzene

[Q]	A(product)/A(std.)	Φ^0/Φ
0.00	0.094	1.00
0.0046	0.089	1.06
0.0092	0.088	1.07
0.0138	0.084	1.12

[Ketone] = 0.075 M

$$k_q\tau = 7$$

Table 53. Quenching of the Indanol Formation in α -(2-Benzylphenyl)acetophenone with 2,5-Dimethyl-2,4-hexadiene at 313 nm in Benzene

[Q]	A(product)/A(std.)	Φ^0/Φ
0.00	0.393	1.00
0.00978	0.378	1.04
0.0195	0.356	1.07
0.0293	0.348	1.10
0.0391	0.327	1.16

[Ketone] = 0.085 M

$$k_q\tau = 4$$

Table 54. Quenching of the Indanol Formation in α -(2-Ethylphenyl)propiophenone with 2,5-Dimethyl-2,4-hexadiene at 313 nm in Benzene

[Q]	A(product)/A(std.)	Φ^0/Φ
0.00	0.056	1.00
0.00978	0.0422	1.32
0.0195	0.0393	1.42
0.0293	0.035	1.60
0.0391	0.034	1.7

[Ketone] = 0.064 M

$$k_q\tau = 17.4$$

Table 55. Quenching of the Indanol Formation in α -(2,4,6-Triethylphenyl) propiophenone with 2,5-Dimethyl-2,4-hexadiene at 313 nm in Benzene

[Q]	A(product)/A(std.)	Φ^0/Φ
0.00	0.4241	1.00
0.00978	0.3876	1.06
0.0195	0.352	1.17
0.0293	0.3278	1.26
0.0391	0.3198	1.29

[Ketone] = 0.0825 M

$$k_q\tau = 8$$

Table 56. Quenching of the Indanol Formation in 2'-(2,3-Dimethyl-2-butyl)benzophenone with 2,5-Dimethyl-2,4-hexadiene at 313 nm in Benzene

[Q]	A(product)/A(std.)	Φ^0/Φ
0.00	0.0595	1.00
0.025	0.0365	1.63
0.062	0.025	2.38
0.079	0.0225	2.64

[Ketone] = 0.0051 M

$$k_q\tau = 20.8$$

Table 57. Quenching of the Diarylethane Formation in α -(2-Ethylphenyl)acetone with 2,5-Dimethyl-2,4-hexadiene at 313 nm in Benzene

[Q]	A(product)/A(std.)	Φ^0/Φ
0.00	0.333	1.00
0.0046	0.318	1.05
0.0092	0.315	1.06
0.0138	0.302	1.10

[Ketone] = 0.0075 M

$$k_q\tau = 6.7$$

Table 58. Quenching of the Diarylethane Formation in α -Mesitylacetone with 2,5-Dimethyl-2,4-hexadiene at 313 nm in Benzene

[Q]	A(product)/A(std.)	Φ^0/Φ
0.00	0.586	1.00
0.0046	0.517	1.133
0.0092	0.4795	1.222
0.0138	0.4035	1.452

[Ketone] = 0.0312 M

$$k_q\tau = 31.4$$

Table 59. Quenching of the Diarylethane Formation in α -(2,4,6-Trisopropylphenyl) acetone with 2,5-Dimethyl-2,4-hexadiene at 313 nm in Benzene

[Q]	A(product)/A(std.)	Φ^0/Φ
0.00	0.136	1.00
0.0092	0.067	2.03
0.0138	0.054	2.52
0.0184	0.046	2.96

[Ketone] = 0.006 M

$k_q t = 107.1$

References:

1. Jablonski, A. Z. *Physik*. **1935**, *94*, 38.
2. Cowen, D. O.; Drisco, R. L. "*Elements of Organic Photochemistry*", Academic Press, New York, N.Y., **1969**.
3. Turro, N. J. in "*Modern Molecular Photochemistry*", Benjamin-Cummings, Menlo Park, Ca, **1978**.
4. Halpren, A.; Ware, W. R. *J. Chem. Phys.* **1970**, *53*, 1969.
5. Almgren, M. *Mol. Photochem.* **1972**, *4*, 327.
6. a) Morris, J. M.; Williams, D. F. *Chem. Phys. Lett.* **1974**, *25*, 312.
b) El-Sayed, M. A.; Leyerle, R. *J. Chem. Phys.* **1975**, *62*, 1579.
c) Bately, M.; Kearns, D. R. *Chem. Phys. Lett.* **1968**, *2*, 423.
7. a) Matsumoto, T.; Sato, M.; Hiroyama, S. *Chem. Phys. Lett.* **1972**, *13*, 13.
b) Hansen, D. A.; Lee, K. C. *J. Chem. Phys.* **1975**, *62*, 183.
c) Anderson, R. W.; Hochstrasser, R. M.; Lutz, H.; Scott, G. W. *J. Chem. Phys.* **1974**, *61*, 2500.
8. a. Wagner, P. J.; Kochevar, I. *J. Am. Chem. Soc.* **1968**, *90*, 2232.
b. Clark, W. D.; Litt, A. D.; Steel, C. *J. Am. Chem. Soc.* **1969**, *91*, 5413.
c. Herkstroeter, W. G.; Jones, L. B.; Hammond, G. S. *J. Am. Chem. Soc.* **1966**, *88*, 4777.
9. Turro, N. J. "*Modern Molecular Photochemistry*", Benjamin-Cummings, Menlo Park, Ca. 1978.
10. Wagner, P. J. in "*Rearrangements in Ground and Excited Molecules*", Academic Press, New York, N. Y. 1980, V3, 381.
11. Wagner, P. J. *Topic in Curr. Chem.* **1976**, *66*, 1.
12. a) Yang, N. C.; McClure, D. S.; Murov, S. L.; Houser, J. J.; Dusenberry, R. *J. Am. Chem. Soc.* **1967**, *89*, 5466.
b) Yang, N. C.; Dusenberry, R. L. *J. Am. Chem. Soc.* **1968**, *90*, 5899.
13. Wagner, P. J.; Kemppainen, A. E.; Schott, H. N. *J. Am. Chem. Soc.* **1973**, *95*, 5604.
14. Wagner, P. J.; Thomas, M. J.; Harris, E. *J. Am. Chem. Soc.* **1976**, *98*, 7675.
15. Scaiano, J. C.; Leigh, W. J.; Meador, M. A.; Wagner, P. J. *J. Am. Chem. Soc.* **1985**, *107*, 5806.
16. a) Norrish, R. G. W.; Bamford, C. H. *Nature* **1936**, *138*, 1016.
b) Norrish, R. G. W.; Bamford, C. H. *Nature* **1937**, *140*, 195.
17. a) Heine, H. G.; Hartmann, W.; Kory, D. R.; Magyar, J. G.; Hoyle, C. E.; McVey, J. K.; Lewis, F. D. *J. Org. Chem.* **1974**, *39*, 691.
b) Lewis, F. D.; Hoyle, C. H.; Magyar, J. G. *J. Org. Chem.* **1975**, *40*, 488.
c) Lewis, F. D.; Magyar, J. G. *J. Am. Chem. Soc.* **1973**, *95*, 5973.
18. Zimmerman, H. E. *Adv. Photochem.* **1963**, *1*, 183.
19. Gray, P.; Williams, A. *Chem. Rev.* **1959**, *59*, 239.
20. Walling, C.; Padwa, A. *J. Am. Chem. Soc.* **1963**, *85*, 1593.
21. Lewis, F. D.; Magyar, J. G. *J. Org. Chem.* **1972**, *37*, 2102.
22. Baum, A. A. *J. Am. Chem. Soc.* **1972**, *94*, 6866.

23. Hamer, N. K. *J. Chem. Soc: Perkin 1* **1979**, 1285.
24. Padwa, A.; Au, A. *J. Am. Chem. Soc.* **1976**, *98*, 5581.
25. a) Dalton, J. C.; Dawes, K.; Turro, N. J.; Weiss, D. S.; Baltrop, J. A.; Coyle, J. D. *J. Am. Chem. Soc.* **1971**, *93*, 7213.
b) Dalton, J. C.; Pond, D. M.; Weiss, D. S.; Lewis, F. D.; Turro, N. J. *J. Am. Chem. Soc.* **1970**, *92*, 2564.
26. Yang, N. C.; Feit, E. D.; Hui, M. H.; Turro, N. J.; Dalton, J. C. *J. Am. Chem. Soc.* **1970**, *92*, 6974.
27. Heine, H. G. *Justus Liebigs Ann. Chem.* **1970**, *105*, 732.
28. Wagner, P. J. *Acc. Chem. Res.* **1971**, *4*, 168.
29. Wagner, P. J.; Park, B. S. *Org Photochem.* **1991**, *11*, 227.
30. Gilbert, A.; Baggott, J. in "Essentials of Molecular Photochemistry"; CRC Press: Boca Raton, FL, 1991; pp 287-352.
31. a) Walling, C.; Gibian, M. *J. Am. Chem. Soc.* **1965**, *87*, 3361.
b) Padawa, A. *Tetrahedron Lett.* **1964**, 3465.
32. Walling, C.; Padwa, A. *J. Am. Chem. Soc.* **1964**, *85*, 1593.
33. Wagner, P. J. *J. Am. Chem. Soc.* **1967**, *89*, 5898.
34. Wagner, P. J. *Acc. Chem. Res.* **1983**, *16*, 461.
35. Wagner, P. J.; Chen, C. P. *J. Am. Chem. Soc.* **1976**, *98*, 239.
36. a) Wagner, P. J.; Meador, M. A. *J. Am. Chem. Soc.* **1983**, *105*, 4484.
b) Wagner, P. J.; Meador, M. A. *J. Am. Chem. Soc.* **1984**, *106*, 3684.
c) Wagner, P. J.; Scaiano, J. C. *J. Am. Chem. Soc.* **1984**, *106*, 4626.
d) Wagner, P. J.; Zhou, B. *J. Am. Chem. Soc.* **1988**, *110*, 611.
e) Wagner, P. J.; Zhou, B. *Tetrahedron Lett.* **1989**, *30*, 5389.
f) Wagner, P. J.; Zhou, B. *Tetrahedron Lett.* **1990**, *31*, 2251.
g) Wagner, P. J.; Hasegawa, T.; Zhou, B. *J. Am. Chem. Soc.* **1991**, *113*, 9640.
37. Lewis, F. D.; Johnson, R. W.; Johnson, D. E. *J. Am. Chem. Soc.* **1974**, *96*, 6090.
38. a) Haag, R.; Wirz, J.; Wagner, P. J. *Hel. Chim. Acta.* **1977**, *60*, 2595.
b) Sammes, P. G. *Tetrahedron* **1976**, *32*, 405.
39. Turro, N. J.; Weiss, D. W. *J. Am. Chem. Soc.* **1968**, *90*, 2185.
40. Scheffer, J. R.; Trotter, J.; Omkaram, N.; Evans, S.; Ariel, S. *Mol. Cryst. Liq. Cryst.* **1986**, *134*, 169.
41. Scheffer, J. R.; Dzakpasu, A. A. *J. Am. Chem. Soc.* **1978**, *100*, 2163.
42. Severance, D.; Pandey, B.; Morrison, H. *J. Am. Chem. Soc.* **1987**, *109*, 3231.
43. Sugiyama, N.; Nishio, T.; Yamada, K.; Aoyama, H. *Bull. Chem. Soc. Japan* **1970**, *43*, 1879.
44. Lahav, M.; Chang, H. C.; Popovitz-Biro, R.; Leiserowitz, L. *J. Am. Chem. Soc.* **1987**, *109*, 3883.
45. Matsuura, T.; Ito, Y. *Tetrahedron Lett.* **1988**, *29*, 3087.
46. Sauers, R. R.; Scimone, A.; Shams, H. *J. Org. Chem.* **1988**, *53*, 6084.
47. Sauers, R. R.; Scaiano, J. C.; Bliss, R. A.; McGimpsey, W. G.; Casal, H. L. *J. Am. Chem. Soc.* **1986**, *108*, 8225.
48. Wagner, P. J.; Kelso, P.; Kemppainen, A. K.; Zepp, R. *J. Am. Chem. Soc.* **1972**, *94*, 7500.

49. Scheffer, J. R.; Ariel, S.; Ramamurthy, V.; Trotter, J. *J. Am. Chem. Soc.* **1983**, *105*, 6959.
50. a) Houk, K. N.; Dorigo, A. E. *J. Am. Chem. Soc.* **1987**, *109*, 2195.
b) Houk, K. N.; Dorigo, A. E.; Tucker, J. *Acc. Chem. Res.* **1990**, *23*, 107.
51. Houk, K. N.; Dorigo, A. E.; McCarrick, M. A.; Loncharich, R. J. *J. Am. Chem. Soc.* **1990**, *112*, 7508.
52. Sauers, R. R.; Krogh-Jespersen, K. *Tetrahedron Lett.* **1989**, *30*, 527.
53. Sauers, R. R.; Huang, S. U. *Tetrahedron Lett.* **1990**, *31*, 5709.
54. Wagner, P. J.; Giri, B. P.; Pabon, R.; Singh, S. B. *J. Am. Chem. Soc.* **1987**, *109*, 8104.
55. Wagner, P. J.; Meador, M. A.; Giri, B. P.; Scaiano, J. C. *J. Am. Chem. Soc.* **1985**, *107*, 1087.
56. Wagner, P. J.; Giri, B. P.; Scaiano, J. C.; Ward, D. L.; Gabe, E.; Lee, F. L. *J. Am. Chem. Soc.* **1985**, *107*, 5483.
57. Wagner, P. J.; Pabon, R.; Park, B. S.; Zand, A. R. Ward, D. L. *J. Am. Chem. Soc.* **1994**, *116*, 589.
58. Wagner, P. J.; Hasegawa, T.; Zhou, B. *J. Am. Chem. Soc.* **1991**, *113*, 9640.
59. a) Wagner, P. J.; Hammond, G. S. *J. Am. Chem. Soc.* **1965**, *87*, 4009.
b) Dougherty, T. J. *J. Am. Chem. Soc.* **1965**, *87*, 4011.
c) Coulson, D. R.; Yang, N. C. *J. Am. Chem. Soc.* **1966**, *88*, 4511.
d) Yang, N. C.; Elliott, S. P.; Kim, B. *J. Am. Chem. Soc.* **1969**, *91*, 7551.
60. Dalton, J. C.; Turro, N. J. *Annu. Rev. Phys. Chem.* **1970**, *21*, 499.
61. Yang, N. C.; Elliott, S. P. *J. Am. Chem. Soc.* **1969**, *91*, 7550.
62. Stephenson, L. M.; Cavigli, P. R.; Parlett, J. L. *J. Am. Chem. Soc.* **1971**, *93*, 1984
63. Heller, A. *Mol. Photochem.* **1969**, *1*, 257.
64. Hammond, G. S. *Advan. Photochem.* **1969**, *7*, 373.
65. Salem, L. *J. Am. Chem. Soc.* **1974**, *96*, 3482.
66. Scaiano, J. C.; Nau, W. M.; Cozens, F. L. *J. Am. Chem. Soc.* **1996**, *118*, 2275.
67. Noh, T.; Lei, X.-G.; Turro, N. J. *J. Am. Chem. Soc.* **1993**, *115*, 3105.
68. Turro, N. J.; Wan, P. *Tetrahedron Lett.* **1984**, *25*, 3655.
69. De Mayo, P.; Nakamura, N.; Tsang, P. W. K.; Wong, S. K. *J. Am. Chem. Soc.* **1982**, *104*, 6824.
70. Wagner, P. J.; Park, B. -S.; Sobczak, M.; Frey, J.; Rappoport, Z. *J. Am. Chem. Soc.* **1995**, *117*, 7619.
71. Evans, S. E.; Omkaram, N.; Scheffer, J. R.; Garcia-Garibay, M.; Trotter, J. *J. Am. Chem. Soc.* **1986**, *108*, 5648.
72. Evans, S. E.; Omkaram, N.; Scheffer, J. R.; Trotter, J. *Tetrahedron Lett.* **1985**, *26*, 5903.
73. Evans, S. E.; Omkaram, N.; Scheffer, J. R.; Trotter, J. *Tetrahedron Lett.* **1986**, *27*, 1419.
74. Scaiano, J. C. *Tetrahedron* **1982**, *38*, 819.
75. Salem, L.; Rowland, C. *Angew. Chem., Int. Ed. Engl.* **1972**, *11*, 92.
76. Michl, J. *J. Am. Chem. Soc.* **1996**, *118*, 3568.
77. Wagner, P. J.; Kochevar, I. E.; Kemppainen, A. E. *J. Am. Chem. Soc.* **1972**, *94*, 7489.
78. Small Jr., R. D.; Scaiano, J. C. *Chem. Phys. Lett.* **1978**, *59*, 246.
79. Small Jr., R. D.; Scaiano, J. C. *J. Phys. Chem.* **1977**, *81*, 828, 2126.

80. Wagner, P. J. *Acc. Chem. Res.* **1989**, *22*, 83.
81. Turro, N. J.; Buchachenko, A. L.; Tarasov, V. F. *Acc. Chem. Res.* **1995**, *28*, 69.
82. Closs, G. Forbes, M. D. E.; Piotrowiak, P.. *J. Am. Chem. Soc.* **1992**, *114*, 3285.
83. Griesbeck, A. G.; Stadtmuller, S. *J. Am. Chem. Soc.* **1991**, *113*, 6923.
84. Griesbeck, A. G.; Stadtmuller, S. *J. Am. Chem. Soc.* **1990**, *112*, 1281.
85. Hart, H.; Giguere, R. J. *J. Am. Chem. Soc.* **1983**, *105*, 7775.
86. Hart, H.; Lin, L. T. W. *Tetrahedron Lett.* **1985**, *26*, 575.
87. Wagner, P. J.; Meador, M. A.; Zhou, B.; Park, B. -S. *J. Am. Chem. Soc.* **1991**, *113*, 9630.
88. Park, B. S. Ph. D. Dissertation, 1992, Michigan State University, 157-199.
89. Pappas, S. P.; Blackwell, J. E. *Tetrahedron Lett.* **1966**, 1175.
90. Pappas, S. P.; Zehr, R. D.; Blackwell, J. E. *J. Heterocycl. Chem.* **1970**, 1215.
91. Wagner, P. J.; Meador, M. A.; Park, B. S. *J. Am. Chem. Soc.* **1990**, *112*, 5199.
92. a) Marshall; *Prager Aust. J. Chem.* **1979**, *32*, 1261.
b) Scholl, B.; Jolidon, S.; Hansen, H.-J. *Helv. Chim. Acta* **1986**, *69*, 184.
c) Morrison, H.; Giacherio, D. *J. Org. Chem.* **1982**, *47*, 1058.
93. Montgomery, M. E.; Wirth, M. J. *Anal. Chem.* **1992**, *64*, 2566.
94. Zielinski, W.; Mazik, M. *Pol. J. Chem.* **1992**, *66*, 661.
95. Scheffer, J. R. in "Organic Solid State Chemistry"; Desiraju, G. R. Ed.; Elsevier, New York, 1987; Chapter 1.
96. a) Closs, G. L. *Adv. Magn. Res.* **1975**, *7*, 1.
b) Closs, G. L.; Doubleday, C. *J. Am. Chem. Soc.* **1973**, *95*, 2735.
c) Kaptein, R.; Dekanter, F. *J. Am. Chem. Soc.* **1982**, *104*, 4759.
d) Carlacci, L.; Doubleday, C.; Furlani, T.; King, H.; Mciver, J.; *J. Am. Chem. Soc.* **1987**, *109*, 5323.
e) Carrington, A.; McLauchlan, A. *Introduction to Magnetic Resonance*, Harper and Row; New York, 1967.
97. Doubleday, C. Jr.; Turro, N. J.; Wang, J-F. *Acc. Chem. Res.* **1989**, *22*, 199.
98. Zimmt, M. B.; Doubleday, C. Jr.; Gould, I. R.; Turro, N. J. *J. Am. Chem. Soc.* **1985**, *107*, 6724.
99. Zimmt, M. B.; Doubleday, C. Jr.; Turro, N. J. *J. Am. Chem. Soc.* **1986**, *108*, 3618.
100. Biali, S. E.; Rappoport, Z. *J. Am. Chem. Soc.* **1984**, *106*, 5641.
101. Oki, M.; Iwamura, H. *Tetrahedron* **1968**, *24*, 1905.
102. Zhou, B. Ph. D. Dissertation, 1988, Michigan State University.
103. Wagner, P. J.; Meador, M. A.; Scaiano, J. C. *J. Am. Chem. Soc.* **1984**, *106*, 7988.
104. Wagner, P. J.; *J. Am. Chem. Soc.* **1967**, *89*, 2820.
105. Scheffer, J. R. *Org. Photochem* **1987**, *8*, 249.
106. Burke, S. D.; Silks, L. A.; Strickland, S. M. S. *Tetrahedron Lett.* **1988**, *29*, 2761.
107. Chandler, W. D.; Goodman, L. *J. Mol. Spectrosc.* **1970**, *35*, 232.
108. Lewis, F. D.; Johnson, R. W.; Johnson, D. E. *J. Am. Chem. Soc.* **1974**, *96*, 6090.
109. Wagner, P. J.; Kochevar, I. E.; Kemppainen, A. E. *J. Am. Chem. Soc.* **1972**, *94*, 7489.
110. Encinas, M. V.; Lissi, E. A.; Lemp, E.; Zanocco, A.; Scaiano, J. C. *J. Am. Chem. Soc.* **1983**, *105*, 1856.

111. a) Ariel, S.; Evans, S. V.; Garcia-Garibay, M.; Harkness, B. R.; Omkaram, N.; Scheffer, J. R.; Trotter, J. *J. Am. Chem. Soc.* **1989**, *111*, 5591.

b) Lewis, T. J.; Rettig, S. J.; Scheffer, J. R.; Trotter, J.; Wierko, F.; *J. Am. Chem. Soc.* **1990**, *112*, 3679.

112. a) Dewar, M. J. S.; Zoebisch, E. G.; Healy, H. F.; Stewart, J. J. P. *J. Am. Chem. Soc.* **1985**, *107*, 3902.

b) Stewart, J. J. P. *J. Comp. Chem.* **1989**, *10*, 209, and references therein.

MICHIGAN STATE UNIV. LIBRARIES



31293010500712